

Characterization of Expansive Soils in the Eastern Province of Saudi Arabia

by

Redwan Amin Hameed

A Thesis Presented to the

FACULTY OF THE COLLEGE OF GRADUATE STUDIES

KING FAHD UNIVERSITY OF PETROLEUM & MINERALS

DHAHRAN, SAUDI ARABIA

In Partial Fulfillment of the
Requirements for the Degree of

MASTER OF SCIENCE

In

CIVIL ENGINEERING

July, 1991

INFORMATION TO USERS

This manuscript has been reproduced from the microfilm master. UMI films the text directly from the original or copy submitted. Thus, some thesis and dissertation copies are in typewriter face, while others may be from any type of computer printer.

The quality of this reproduction is dependent upon the quality of the copy submitted. Broken or indistinct print, colored or poor quality illustrations and photographs, print bleedthrough, substandard margins, and improper alignment can adversely affect reproduction.

In the unlikely event that the author did not send UMI a complete manuscript and there are missing pages, these will be noted. Also, if unauthorized copyright material had to be removed, a note will indicate the deletion.

Oversize materials (e.g., maps, drawings, charts) are reproduced by sectioning the original, beginning at the upper left-hand corner and continuing from left to right in equal sections with small overlaps. Each original is also photographed in one exposure and is included in reduced form at the back of the book.

Photographs included in the original manuscript have been reproduced xerographically in this copy. Higher quality 6" x 9" black and white photographic prints are available for any photographs or illustrations appearing in this copy for an additional charge. Contact UMI directly to order.

U·M·I

University Microfilms International
A Bell & Howell Information Company
300 North Zeeb Road, Ann Arbor, MI 48106-1346 USA
313/761-4700 800/521-0600

Order Number 1354045

**Characterization of expansive soils in the eastern province of
Saudi Arabia**

Hameed, Redwan Amin, M.S.

King Fahd University of Petroleum and Minerals (Saudi Arabia), 1991

U·M·I
300 N. Zeeb Rd.
Ann Arbor, MI 48106

**CHARACTERIZATION OF EXPANSIVE SOILS IN THE
EASTERN PROVINCE OF SAUDI ARABIA**

BY

REDWAN AMIN HAMEED

A Thesis Presented to the
FACULTY OF THE COLLEGE OF GRADUATE STUDIES
KING FAHD UNIVERSITY OF PETROLEUM & MINERALS
DHAHRAN, SAUDI ARABIA

In Partial Fulfillment of the
Requirements for the Degree of

MASTER OF SCIENCE
In
CIVIL ENGINEERING

JULY, 1991

KING FAHD UNIVERSITY OF PETROLEUM & MINERALS

DHAHRAN, SAUDI ARABIA

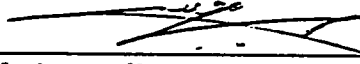
This thesis, written by

Redwan Amin Hameed

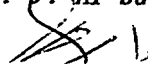
under the direction of his Thesis Advisor, and approved by his Thesis Committee, has been presented to and accepted by the Dean of the College of Graduate Studies, in partial fulfillment of the requirements for the degree of

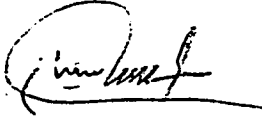
MASTER OF SCIENCE IN CIVIL ENGINEERING


Thesis Committee


Chairman (Dr. S. N. Abduljawad)


Member (Dr. G. J. Al-Sultaimani)


Member (Dr. I. A. Basunbul)


Dr. Ghazi J. Al-Sulaimani
Department Chairman


Dr. Ala H. Al-Rabeh
Dean College of Graduate Studies

Date : July, 1991.



**IN THE NAME OF GOD, MOST GRACIOUS
MOST MERCIFUL**

- * Among His signs is this: You see the earth barren and desolate; But when we send down rain to it; it is stirred to life and yields increase.

- * On no soul does God place a burden greater than it can bear. It gets every good that it earns, and it suffers every ill that it earns. "Our Lord! Condemn us not if we forget or fall into error; Our Lord! Lay not on us a burden like that which you did lay on those before us. Our Lord! lay not on us a burden greater than we have strength to bear. Blot out our sins, and grant us forgiveness. Have mercy on us. You are our Protector; Help us against those who stand against Faith".

TO
My Father, My Mother
and
My Fiancee
For their patience, moral support
and encouragement.

ACKNOWLEDGEMENT

First of all I would like to express my deepest gratitude to Almighty Allah.

I would like to thank my thesis major advisor Dr. Sahl N. Abduljauwad for his continuous guidance and helpful suggestions and advice.

My thanks are also due to other committee members Dr. G. J. Al-Sulaimani and Dr. I. A. Basunbul for their constructive comments.

The continuous help and assistance of Mr. Hasan Zakariya in the experimental part of this study is highly appreciated and acknowledged.

I would like to thank also my friend Farook Al-Shamali and my brother-in-law Ghassan Hameed for their help in preparing the thesis manuscript.

Finally, my thanks are to everyone who supported me morally during my study.

TABLE OF CONTENTS

	<i>Page</i>
Acknowledgement	v
List of Tables	x
List of Figures	xii
List of Plates	xviii
Abstract	xix
1. INTRODUCTION	
1.1 General	1
1.2 Objective of the Study	5
1.3 Methodology of the Study	6
2. LITERATURE REVIEW	
2.1 Historical Background	8
2.2 Distribution of Expansive Soils	14
2.2.1 Around The World	14
2.2.2 In Saudi Arabia	15
2.3 Origin of Expansive Soils	20
2.4 Expansive Clay Minerals	22
2.5 Cation Exchange	50
2.6 Clay Water Interaction	51
2.7 Mechanism of Swelling	35
2.8 Swell Potential	42
2.9 Swelling Pressure	43

2.10	Factors Affecting Swelling	45
2.11	Identification of Expansive Soils	54
	2.11.1 Visual Identification	54
	2.11.2 Local Experience	56
	2.11.3 Laboratory Tests	57
2.12	Protective and Remedial Measures	79
3.	METEOROLOGY & GEOLOGY OF THE STUDY AREA	
3.1	Location	87
3.2	Climate	87
	3.2.1 Temperature	89
	3.2.2 Precipitation	91
	3.2.3 Relative Humidities	91
3.3	History of the Arabian Gulf	94
3.4	Geology of the Province	97
	3.4.1 Geomorphology	99
	3.4.2 Topography	99
	3.4.3 Stratigraphy	100
4.	FIELD AND GEOTECHNICAL INVESTIGATION	
4.1	Introduction	115
4.2	Preliminary Investigation	115
4.3	Site Investigation	121
4.4	Site Description	129
	4.4.1 Qatif Housing Area	129
	4.4.2 Al-Aujam Village	151

4.4.3	<i>Al-Jesh Village</i>	131
4.4.4	<i>Umm Al-Sahek Village</i>	131
4.4.5	<i>Umm Al-Hamam Village</i>	133
4.4.6	<i>Al-Mubarraz</i>	133
4.4.7	<i>Al-Hamadiya</i>	134
4.4.8	<i>Al-Hofuf City</i>	134
5.	GEOTECHNICAL & MINERALOGICAL PROPERTIES	
5.1	Geotechnical Properties	136
5.1.1	<i>Natural Water Content and Unit Weight</i> ..	136
5.1.2	<i>Specific Gravity</i>	143
5.1.3	<i>Atterberg Limits</i>	147
5.2	Mineralogical Composition	162
6.	SWELL CHARACTERISTICS	
6.1	Introduction	172
6.2	Swell Test	172
6.3	Swell Results	175
6.4	Swell Pressure Results	205
6.5	Effect of Initial Surcharge	228
6.6	Correlation Between Geotechnical Properties and Swell Potential	231
7.	CONCLUSIONS & RECOMMENDATIONS	
7.1	Conclusions	237
7.2	Recommendations	239

REFERENCES 300

APPENDICES

*Appendix-A: Logs of boring in Al-Qatif area
and Al-Hasa area*

*Appendix-B: X-ray diffraction patterns and
mineralogical composition of some
samples*

LIST OF TABLES

<i>Table</i>		<i>Page</i>
2.1	Classification of phyllosilicates related to clay minerals	24
2.2	Swelling index values for several minerals	26
2.3	Some properties of montmorillonite	28
2.4	Atterberg values of clay minerals with various adsorbed cations.....	32
2.5	Clay potential volume change	46
2.6	Relation between swell potential and PI	61
2.7	Relation between degree of expansion and shrinkage limit	61
2.8	Relation between colloid content and degree of expansion	64
2.9	X-ray diffraction data for clay minerals and common nonclay minerals	70
2.10	Simplified X-ray analysis guide for clay minerals "Basal" (001) peak position	73
3.1	Average mean monthly temperature in degrees centigrades calculated over the years 1966-1974 ..	90
3.2	Average mean monthly and annual precipitations 1966-1974 in millimeters	92
3.3	Average mean monthly relative humidities calculated over the years 1966-1974.....	95
4.1	Location of bore holes	126
4.2	Location of test pits	128
4.3	Depth and thickness of clays in Al-Qatif Housing Area	130
4.4	Depth and thickness of clays in Al-Qatif Housing Area (Test pits).....	132

5.1	Summary of results for Al-Qatif area test pits ...	138
5.2	Summary of results for Al-Qatif area bore holes..	139
5.3	Summary of results for Al-Hasa area test pits....	140
5.4	Summary of results for Al-Hasa area bore holes..	141
5.5	Classification of Al-Qatif area samples (Test pits)	157
5.6	Classification of Al-Qatif area samples (Bore holes)	158
5.7	Classification of Al-Hasa area samples (Test pits)	159
5.8	Classification of Al-Hasa area samples (Bore holes)	160
5.9	XRD-Samples	164
5.10	Mineralogical composition of some selected samples	171
6.1	Empirical Methods for Predicting Heave	232
6.2	Comparison between experimental and calculated % swell	235

LIST OF FIGURES

<i>Figure</i>		<i>Page</i>
2.1	Distribution of expansive soils around the world .	16
2.2	Hazard map for potentially swelling soils of Arabian Peninsula.....	18
2.3	Structures of Important Clay Minerals.....	25
2.4	Triangular diagram showing approximate compositional areas for montmorillonite, palygorskite, saponite and sepiolite.....	29
2.5	Distribution of ions adjacent to an expansive clay surface according to the concept of diffuse double layers (Mitchell, 1976).....	34
2.6	Schematic representation of redistribution of ions in a truncated double layer.....	36
2.7	Schematic representation of distribution of ions in truncated and fully extended diffuse double layer.....	36
2.8	Diagrammatic sketch of thermoosmotic heaving of building on desiccated clay foundation.....	40
2.9	Effect of depth of the active zone in San Antonio	52
2.10	A check list will be a help to the technician of the suspects expansive soil in the building area, Portland Cement Association.....	58
2.11	Chart for potential expansiveness of soils.....	59
2.12a	A relationship between percentage of swell and percentage of clay sizes for experimental soils. (After Seed, Woodward and Lundgren).....	63
2.12b	Relation of volume change to colloid content, plasticity index, and shrinkage limit (air-dry to saturated condition under a load of 1 lb. per sq. in.) (after Holtz and Gibbs).....	63
2.13	Free swell related to volume change (air dry to saturated condition under a load of 1 psi).....	66

2.14	Geometry of diffraction pattern according to Bragg's Law.....	69
2.15	Schematic arrangement of an X-ray diffractometer	69
2.16	X-ray diffraction patterns of some typical clay minerals. From top to bottom, illite, Yangtse River, China, halloysite, Lawrence County, Indiana; kaolinite, Langley, South Carolina, montmorillonite, Granby, Colorado, (USBR).....	71
2.17	Schematic diagram of apparatus for differential thermal analysis	75
2.18	Schematic illustration of scanning system of the scanning electron microscope.....	78
3.1	Location map of the Study Area.....	88
3.2	Generalized geologic map of the Arabian Peninsula	98
3.3	Topographic map of the study area	101
3.4	Geological map of the study area (after Ministry of Petroleum and Minerals Resources, GM 208 A) .	102
3.5	Generalized Litho-stratigraphic sequence of the study area (after Italconsult, 1969)(208 A)	105
3.6	Distribution of the relative amount of clay minerals in the Rus and Damman Formations - Carbonate free material.....	107
4.0	Typical major house damage.....	120
4.1	Vicinity map of Al-Qatif test location.....	122
4.2	Vicinity map of Al-Hasa test location	125
5.1	Variation of unit weight with depth, BH #3 (Al-Qatif area	144
5.2	Variation of natural unit weight with depth, BH #7 (Umm Al-Sahek)	144
5.3	Variation of natural unit weight with depth, BH #7 (Umm Al-Hamam)	145

5.4	Variation of natural unit weight with depth, BH #9 (Al-Hasa)	145
5.5	Variation of natural unit weight with depth, BH #11 (Al-Hasa)	146
5.6	Variation of natural unit weight with depth, BH #12 (Al-Hasa)	146
5.7	Variation of plasticity and natural water content with depth BH #3 (Al-Qatif housing area).....	149
5.8	Variation of plasticity and natural water content with depth BH #7 (Umm Al-Sahek).....	150
5.9	Variation of plasticity and natural water content with depth BH #8 (Umm Al-Hamam)	151
5.10	Variation of plasticity and natural water content with depth BH #9 (Al-Hasa)	152
5.11	Variation of plasticity and natural water content with depth BH #11 (Al-Hasa)	153
5.12	Variation of plasticity and natural water content with depth BH #12 (Al-Hasa)	154
5.13	Plasticity Chart (Al-Qatif B.H.)	155
5.14	Plasticity Chart (Al-Hasa T.P.).....	156
5.15	Plasticity Chart for all samples	161
5.16	XR-Diffraction pattern for Sample #3, BH #11 (1.0-1 m)	166
5.17	XR-Diffraction pattern for Sample #3.....	167
5.18	XR-Diffraction pattern (enlarged scale) for Sample #3, BH #11 (1.0-1.3 m).....	169
6.1	Swelling one-dimensional odometer apparatus	173
6.2	% Swell vs Time for Al-Qatif area (Test pits)	176
6.3	% Swell vs Time BH #1, the housing area	178
6.4	% Swell vs Time BH #1.....	179

6.5	% Swell vs Time BH #2, Al-Qatif housing area....	182
6.6	% Swell vs Time BH #3, Al-Qatif housing area....	183
6.7	% Swell vs Time BH #4, Al-Jesh	184
6.8	% Swell vs Time BH #5, Al-Aujam	185
6.9	% Swell vs Time BH #6, Umm Al-Sahek	186
6.10	% Swell vs Time BH #7, Umm Al-Sahek	187
6.11	% Swell vs Time BH #8, Umm Al-Hamam	188
6.12	% Swell vs Time BH #8, Umm Al-Hamam	189
6.13	% Swell vs Time for some samples in Al-Qatif area	190
6.14	% Swell vs Time Test Pit #7, Al-Hasa	192
6.15	% Swell vs Time Test Pit #8, Al-Hasa	193
6.16	% Swell vs Time Test Pit #9, Al-Hasa	194
6.17	% Swell vs Time Test Pit #10, Al-Hasa	195
6.18	% Swell vs Time Test Pit #11, Al-Hasa	196
6.19	% Swell vs Time BH #9, Al-Hasa	198
6.20	% Swell vs Time BH #10, Al-Hasa	199
6.21	% Swell vs Time BH #11, Al-Hasa	200
6.22	% Swell vs Time BH #11, Al-Hasa	201
6.23	% Swell vs Time BH #12, Al-Hasa	202
6.24	% Swell vs Time BH #13, Al-Hasa	203
6.25	% Swell vs Time for some samples in Al-Hasa	204
6.26	% Swell vs Swell Pressure for Al-Qatif area (Test pits)	207
6.27	% Swell vs Swell Pressure BH #1 for Al-Qatif area (Test pits)	208

6.28	% Swell vs Swell Pressure BH #2 for Al-Qatif housing area	209
6.29	% Swell vs Swell Pressure BH #3 for Al-Qatif housing area	210
6.30	% Swell vs Swell Pressure BH #4 for Al-Jesh.....	211
6.31	% Swell vs Swell Pressure BH #5 for Al-Aujam ...	212
6.32	% Swell vs Swell Pressure BH #6 for Umm Al-Sahek	213
6.33	% Swell vs Swell Pressure BH #7 for Umm Al-Sahek	214
6.34	% Swell vs Swell Pressure BH #8 for Umm Al-Hamam.....	215
6.35	% Swell vs Swell Pressure for some samples in Al-Qatif area	216
6.36	% Swell vs Swell Pressure TP #7, Al-Hasa.....	217
6.37	% Swell vs Swell Pressure TP #8, Al-Hasa.....	218
6.38	% Swell vs Swell Pressure TP #9, Al-Hasa.....	219
6.39	% Swell vs Swell Pressure TP #10, Al-Hasa.....	220
6.40	% Swell vs Swell Pressure TP #11, Al-Hasa.....	221
6.41	% Swell vs Swell Pressure BH #9, Al-Hasa	222
6.42	% Swell vs Swell Pressure BH #10, Al-Hasa	223
6.43	% Swell vs Swell Pressure BH #11, Al-Hasa	224
6.44	% Swell vs Swell Pressure BH #12, Al-Hasa	225
6.45	% Swell vs Swell Pressure BH #13, Al-Hasa	226
6.46	% Swell vs Swell Pressure for some samples in Al-Hasa area	227
6.47	% Swell vs Time for Sample 2B, TP #2, (5.0 m), Al-Qatif Housing Area	229

6.48	% Swell vs Time (effect of initial surcharge Sample 2B, TP #2, depth (4.0)).....	230
6.49	Comparison between Measured and Calculated % swell	234

LIST OF PLATES

<i>Plates</i>		<i>Page</i>
4.1	Typical crack due to heaving in Al-Aujam.....	115
4.2	A diagonal crack in the brick wall in Al-Aujam...	116
4.3	Crack in the exterior wall	117
4.4	Crack in the exterior wall in Al-Qatif City.....	118
4.5	The truck-mounted drilling rig, drilling BH #1...	124

Abstract

Expansive clay soil was encountered in different areas of Saudi Arabia. This study presents the locations of this type of soil in the Eastern Province of Saudi Arabia and its characteristics.

The study showed that Al-Qatif and the villages around it, as well as Al-Hofuf and the villages around it are rich in expansive soils. Climate and geology of the area have a big influence on the formation and behavior of expansive soils. Clays in Al-Qatif area are highly plastic, possess very high swelling potential and rich in smectite, illite, dolomite and palygorskite. Al-Hasa clays are plastic, possess moderate to high swelling potential and rich in calcite, illite, palygorskite and kaolinite. A strong correlation between swelling potential and the plasticity of the clay was found and an empirical equation was developed to present this correlation. Finally, the study showed that an increase in surcharge load decreases the magnitude of percentage of swell while the swelling pressure remains almost constant.

خلاصة الرسالة

- اسم الطالب : رضوان أمين علي حميد .
عنوان الدراسة : تعيين خواص التربة المنتفخة في المنطقة الشرقية من المملكة العربية السعودية .
التخصص : هندسة مدنية .
تاريخ الشهادة : تموز يوليو ١٩٩١ م .

ووجهت التربة الطينية المنتفخة في أماكن مختلفة من المملكة العربية السعودية . وتقدم هذه الدراسة أماكن وخواص هذا النوع من التربة في المنطقة الشرقية من المملكة .

أثبتت الدراسة أن مدينة القطيف والقرى المحيطة بها إضافة إلى مدينة الهفوف والقرى المحيطة بها ، غنية بالتربة المنتفخة وإن للمناخ وجيولوجية المنطقة تأثير كبير في تكون وسلوك هذه التربة وأن التربة الطينية في منطقة القطيف عالية اللدونة ، تمتلك قابلية عالية جداً للانتفاخ ، وغنية بالسمكتايت ، والايلايت والدولومايت والباليجورسكايت . وإن تربة الأحساء الطينية لدنة ، تمتلك قابلية انتفاخ معتدلة إلى عالية ، وغنية بالكالساييت والايلايت والباليجورسكايت والكاولونايت . وقد وجد أن هناك ارتباطاً قوياً بين قابلية الانتفاخ ولدونة التربة الطينية وتم وضع علاقة تجريبية لتمثيل هذا الارتباط . أخيراً ، أظهرت الدراسة أن الزيادة في الحمل تقلل من نسبة الانتفاخ بينما يبقى ضغط الانتفاخ ثابتاً تقريباً .

درجة الماجستير في العلوم
جامعة الملك فهد للبترول والمعادن
الظهران ، المملكة العربية السعودية
التاريخ تموز يوليو ١٩٩١ م

Chapter 1

INTRODUCTION

1.1 GENERAL

Expansive soils are those that undergo volumetric changes upon wetting and drying. The moisture change can be due to natural effects such as normal seasoned effects or tree root activity, or man made effects such as garden watering, leaking underground water services, or a deficient storm water drainage system. The term expansive or swelling soils implies not only the tendency to increase in volume when water is available, but also the decrease in volume or shrink if water is removed. Soils having little or no capacity to swell will not do so under any conditions. However, soils with high swelling capacity may or may not swell; their behavior depends on the physical conditions of the material at the beginning of construction and changes of stress and moisture content to which they are subjected (40).

The swelling and shrinkage of clay soils is a very troublesome subject in the various fields of Civil Engineering. The damage caused to structures and pavements laying on swelling soils due to volume changes, swelling pressures exerted on foundations in those soils, the reduction of hydraulic conductivities due to swelling and the associated drainage problems are some examples

(45).

Whether a soil will swell or not depends on many factors. The most important one is the difference between the field moisture content at the time of construction and that which will finally be achieved under the conditions associated with the completed structure. If the final moisture content is considerably higher than the initial moisture content, and if the soil is of high swelling potential, vigorous swell may occur as evidenced by upward heaving of the soil or structure or by the development of large swelling pressures. If the final moisture content is lower than the field moisture, the soil will shrink. A second factor is the degree of compaction of the soil in a fill or the degree of over consolidation of an undisturbed natural material. Relatively, high compaction or high previous overburden pressures favor swelling as moisture becomes available. A third factor is the stress to which the material will be subjected after construction is completed. The less the imposed load, the greater the swelling (40). The quantity of smectite minerals present in the soil and the amount of exchangeable bases are also of great importance (26).

Soils with the potential to swell or shrink are found in almost all parts of the world. Expansive soils are responsible for billions of dollars worth of damage to man-made structures in the world each year. Although not as sudden as earthquake, landslide

or tornado, expansive soils cause more damages to buildings, highways and other structures than all of the other aforementioned hazards combined together (30). Jones and Holtz in 1973 stated that: "Each year, shrinking and swelling soils inflict at least \$2.3 billion in damages to houses, buildings, roads and pipelines - more than twice the damage from floods, hurricanes, tornadoes and earthquakes" (27).

Their total damage figure is divided into the following (13, 30):

Single family homes	300 million dollars
Commercial buildings	360 million dollars
Multi-story buildings	80 million dollars
Walks, drivers, parking areas	110 million dollars
Highways and streets	1140 million dollars
Underground utilities and service	100 million dollars
Air ports	40 million dollars
Urban land slides	25 million dollars
Others	100 million dollars
<hr/>	
Total	2255 million dollars

This amount was estimated by Steinberg (1980) to be 4-billion dollars (55) and by Krohn and Slossan (1980) to be 7-billion dollars (30, 43). However, in 1984 Steinberg reported that "In the United States damages caused by expansive soils probably exceeded \$10 billion in 1984" (56).

The same problem is encountered in Saudi Arabia. Expansive soil was found in different areas such as: Al Ghatt, Al Hasa, Tabouk, Tayma, Madina and Al Qatif. Major structures founded on expansive soils in these areas have been seriously affected due to heave of foundations soils.

In Tabuk, damage has been observed in numerous buildings and roads. In Tayma, 75% of the buildings in the city are damaged to varying degrees (23). In Al Mobarraz town (near Hofuf), El Sayed (20, 21) reported that due to seepage of water to bearing soil of most houses of one and two storeys of skeleton type, severe cracking was noticed a short time after their completion. The width of the cracks ranges from few millimeters to more than 15mm. Some of the doors are strongly jammed. The side-walks, which separate the exterior walls from the fence, bulge in the middle, and fences are heavily cracked. Structural damage has been also reported in numerous documented and non documented reports in Al-Qatif area. Movements of suspended ground slabs and cracks in the ground beams, in the foundation of some walls, and in the lower part of the walls were observed, due

to differential swelling (1). For instance, in one project in the Eastern Province of Saudi Arabia, 24 villas, 300 grade-slabs, sidewalks and pavements were completely demolished in 1980's due to a serious damages caused by expansion of the supporting soil. It is believed that numerous other places possessing expansive soils also exist, which are not yet located (18). One of the objectives of this study is to locate the areas of expansive soils in the Eastern Province of Saudi Arabia.

1.2 OBJECTIVE OF THE STUDY

The main objectives of this study are:

- Locate the areas of expansive clays in the Eastern Province of Saudi Arabia.
- Study the geology of the area and explain the process of formation of expansive soil.
- Determine the type and extent of structures damage in the area.
- Classify and characterize the expansive clays in the Eastern Province.
- Determine the mineralogical composition of the samples.
- Determine the swelling behavior, e.g. swelling pressure

and percentage of swell of expansive clays in this area.

- Establish a correlation between swelling potential and geotechnical properties.

1.3 METHODOLOGY OF THE STUDY

In order to achieve the stated objectives, the following sequence of tasks was carried out:

- A comprehensive literature review is conducted to get a complete picture about the properties of expansive soils and the mechanism of swelling.
- A survey of structural damages due to expansive soil in the Eastern Province area is conducted.
- The subsurface exploration is conducted by drilling bore holes and excavating test pits.
- Disturbed and undisturbed samples are collected and transported to soil mechanics lab in KFUPM.
- Soil samples are subjected to extensive tests to determine their geotechnical properties.
- Swelling tests are performed to estimate the percent of swell and swell pressure for each sample.

- Regression analysis is used to establish a correlation between the swelling potential and geotechnical properties of the expansive soil.

Chapter 2

LITERATURE REVIEW

2.1 HISTORICAL BACKGROUND

The problem of expansive soil was unknown until the early part of this century, when brick construction became widely used and cracks developing was found in the brick course. The damages were attributed to bad construction and settlement of the foundation at one corner, without recognition of the role of expansive soils (13). In 1920's it was found in San Antonio, Texas, that the surface of the ground heaved and shrank with variation in the weather. This caused serious cracking and distress to small and large structures formed of brick and concrete as well as distortion of frame structures on drilled and under-reamed shafts extending through the surface materials to the level of assumed constant soil moisture. The U. S. Bureau of Reclamation first recognized the swelling soil problem and became actively interested in the destructive effects of these soils in 1938 when considerable distress was noted in the piers and anchors of a large steel siphon in Oregon. Since that time, other structures have shown distress caused by the destructive forces of expansive soils and engineers realized the cause of damage was sometimes other than settlement. The increasingly extensive use of

concrete slab-on-ground construction after 1940, has further increased the damage to structures caused by swelling soils. A rather complete laboratory research program was initiated in order to secure basic data on these soils so that their actions could be predicted and proper design and construction measures could be adopted to provide trouble-free structures (13, 26). Shortly after World War II, in Texas, it was discovered that lime mixed with the troublesome clays seemed to stabilize the clays volumetrically. Consequently, lime as an admix, found its way into the treatment of the upper part of subgrades of highways and structures (6).

Since 1960's several international conferences on expansive soils were held. The First International Research and Engineering Conference on Expansive Soils was at the Texas A & M University in 1965. The conference presented the first formal opportunity for pooling knowledge on the problems of dealing with expansive soils. This enabled a 'state of art' appreciation to be build up on the nature and occurrence of expansive soils, their recognition and testing, prediction methods and practical techniques for building safely on such soils (61). However, the consensus of the conference was that firm conclusions could not be developed because of limited basic information available at that time (6). The Second International Research and Engineering Conference on Expansive Soils was scheduled at the Texas A & M University in 1969. Again, it was found that the conference has not gained

complete understanding of the complexities from their studies and efforts of examining the expansive clays. It is now considered that these first two conferences laid the foundation for establishing avenues of communications, whereby subsequent developments leading to the understanding of the causes and means of control of expansive clays could be achieved. The Third International Conference on Expansive Soils was held in Hifa in 1973. In this conference, it was a little disappointing that so little progress appeared to have been made in the previous years. However, remarkable advances in the treatments of expansive clays were reported at this conference that reflected appreciation of the theoretical complexities of the problems involving expansive clays. For example, papers treating the micro structure of clays, other treating control and total suctions in clays were presented. In addition, the proceedings contain reports of two different solutions for the partial correction for the foundations of small residences and for a new single storied school building of medium size. The beam-stiffened mat structure served admirably also. Post tensioned slabs were also introduced and found to be of satisfactory solution (6). The Fourth International Conference on Expansive Soils was held in Denver, Colorado in 1980. The theme of this conference was "Characterization and Treatment of Expansive Soils for Engineering Design." The purpose of the conference was to draw attention to the lack of standard characterization procedures for expansive soils and the hesitation

of many engineers to approach the expansive soils problem using sound engineering principles. Fifty two papers were presented at the conference in six categories, namely;

- Concepts in testing and analysis procedure for expansive soils
- Influence of ambient environment on behavior of expansive soils
- Treatment of expansive soils to minimize the damage caused by volume change
- Specialized design and construction procedures for foundations of structures on expansive soils
- New and Innovative Concepts for characterization and treatment of expansive soils.
- Technology transfer to enhance public awareness of the problems caused by expansive soils.

The Fifth International Conference on Expansive Soils was held in Adelaide, South Australia, in 1984. Beside these conferences, considerable activity on a world wide basis has developed. For example, the Waterways Experiment Station (U.S.A.) has conducted some extensive studies. The first effort was a report prepared by Snethen & others in 1975, entitled: "A

Review of Engineering Experiences with Expansive Clay Soils in Highway Subgrades". The second report was issued in 1976, entitled: "An Occurrence and Distribution Survey of Expansive Clays in the United States". This was a physiological classification survey to locate the principal formations in the United States which are the cause of trouble. A third report, issued in 1977, concerns "Natural Micro-Scale Mechanisms that Cause Volume Changes in Expansive Clays" (6).

Numerous authors have addressed the expansive soil problem; however, in most instances; their work has been in the form of case histories and limited to very localized areas. Some of these authors have presented solutions according to their local problems, design methods and construction procedures: Borman (1956), Jenning and Kerrich (1962), Mohan and Rao (1965), Hamilton (1965), Webb (1969), Zeitlen (1969), Lytton (1971), Richards (1973), Foss (1973), Powers and Davies (1973), Fabbri, (1975) (10).

Two interesting papers by Porter and Wooltorton draw attention to swelling clay problems. These papers were published in the proceedings of the first International Conference on Soil Mechanics and Foundation Engineering held at Harvard University in (1936). Porter reported movement observations on a 1,500 ft. long concrete pavement laid in Texas in 1931. Cracks 15cm. wide and 3.5m. deep were observed in the pavement shoulders, and

seasonal fluctuations in elevation of 12cm. at the pavement edge and 6cm. at the pavement centerline were measured. The subgrade soils at the site were reported to have a liquid limit of about 80 to 100, a plasticity index of 52 to 74, and a shrinkage limit of from 8 to 10. Wooltorton describes in detail damage to numerous building in the Mandalay District of Burma caused by vertical and horizontal soil movements. Cracks in the soil were measured at depths greater than 3.5m. About 100 damaged buildings were examined in detail. The conclusion drawn was that the damage was due to seasonal soil movement. Wooltorton drew attention to the fact that similar soils and associated foundation problems existed in India, South Africa and Sudan (62). Twenty years later, two papers were published that dealt with the identification of swelling clays, laboratory testing, and the prediction of surface heave as a function of restraining load. The first paper by Holtz and Gibbs (1954) published in the Transactions of the American Society of Civil Engineering (ASCE) and the second by McDowell published in the Proceedings of the 35th Annual Meeting of the Highway Research Board (1956). Holtz and Gibbs presented a classification of expansive clays based on the percent swell of air dried undisturbed samples when allowed to swell upon saturation in a rigid ring consolidometer. In addition to plasticity index and shrinkage limit, they suggested the use of a free swell test to identify possible troublesome soils. They also concluded that the actual degree of swelling or swelling pressure

developed depends on the initial conditions of moisture content and dry density before wetting. McDowell presented in detail his method of computing "potential vertical rise" on the basis of an assumed fixed relationship of one-third between linear swell and volumetric swell and on the basis of a family of universal curves for the relationship between volumetric swell and load upon saturation. The Proceedings of the Third International Conference on Soil Mechanics and Foundation Engineering held in Switzerland in 1953, contains eight papers by authors from seven countries dealing with the measurement of building movement, laboratory measurement of swelling pressure and soil suction, field measurement of the distribution of soil moisture, and the influence of vegetation (62). Today, books along with many hundred perhaps thousands of separate papers and reports are available dealing with expansive soils.

2.2 DISTRIBUTION OF EXPANSIVE SOILS

2.2.1 Around The World

Expansive soils are distributed all over the world. Usually the regions with the most severe problems are those with local climates that produce desiccation. Distribution of swelling soils is a result of sedimentation, geological history and local environmental conditions (23). Expansive soils have been reported

around the world above and below the Northern Tropic, Tropic of Cancer. Areas with soils developed from argillaceous rocks may exhibit some degree of swell. Worldwide rocks and sediments of Tertiary, Cretaceous, and possible Permian Ages may contain significant amount of the expansive clay minerals (51). Figure 2.1 indicates that the potentially expansive soils are confined to the semi-arid regions of the tropical and temperate climate zones. Expansive soils are in abundance where the annual evapotranspiration exceeds the precipitation. This follows the theory that in semi-arid zones, the lack of leaching has aided the formation of montmorillonite (13).

G. W. Donaldson summarized the distribution of reported instances of expansive soils around the world in 1969. The countries in which expansive soils have been reported are Argentina, Australia, Burma, Canada, Cuba, Ethiopia, Ghana, India, Iran, Mexico, Morocco, Palestine, Rhodesia, South Africa, Spain, Turkey, USA, and Venezuela. Since that time, many other nations have reported significant findings of expansive soils. Among them, China, Sudan, Cyprus, Jordan, Saudi Arabia (13), as well as Egypt, Peru and USSR.

2.2.2 In Saudi Arabia

The Arabian Peninsula is an arid area straddling the Northern Tropic and contains areas of argillaceous materials of the

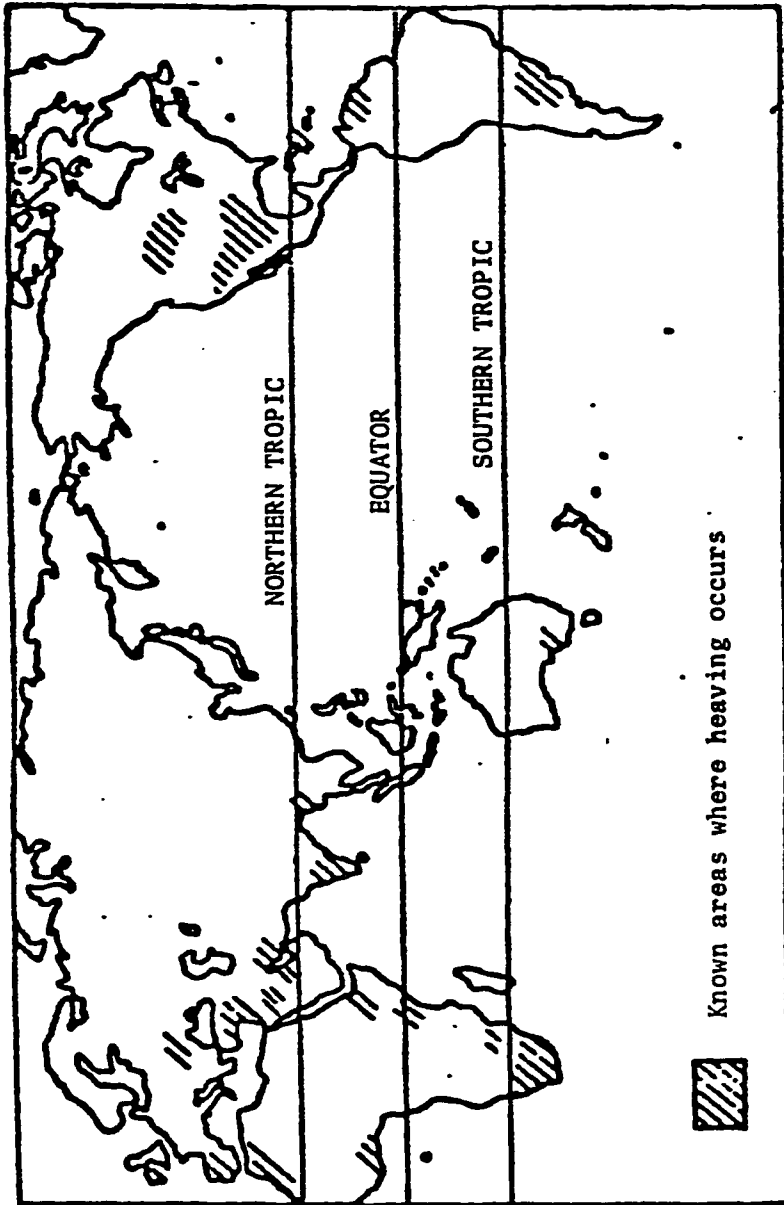


Fig. 2.1 : Distribution of Expansive Soils Around the World

Tertiary, Cretaceous and Permian Ages. A comparison of the geologic ages of known swelling soils in the arid and semi arid areas of the United States with geologic ages of suspected swelling soils in the Arabian Peninsula may yield significant information. The geology and conditions of the Arabian Peninsula along with observations and laboratory test results indicate that potential expansive soils have probability of occurring. Figure 2.2 provides an approximate guide to the suspected distribution and extent of potentially swelling soils (51). This map should be combined with new findings and local experience as it is a first order effort.

The vast area of the Kingdom of Saudi Arabia, with its complicated geological and topographical features, makes it difficult with the limited available data to locate all areas of expansive soils. However, prominent expansive soil problems are commonly observed in the development areas located in a narrow strip adjacent to the western boundary of the Arabian Shield. This swelling zone starts from the North Yemen border and extends to the north west, as shown in Fig 2.2. The expansive soil problems in the region arise primarily from the presence of outcropping shales of Tertiary age. The expansive shale zone includes three major development centers, namely Tabuk, Tayma, and AlGhatt, where extreme damage and failures have recently been reported (23). Expansive soils have also been reported in several other areas, such as, Al Madina and Al Hofuf (18,38), and Al Qatif area (1, 42). The

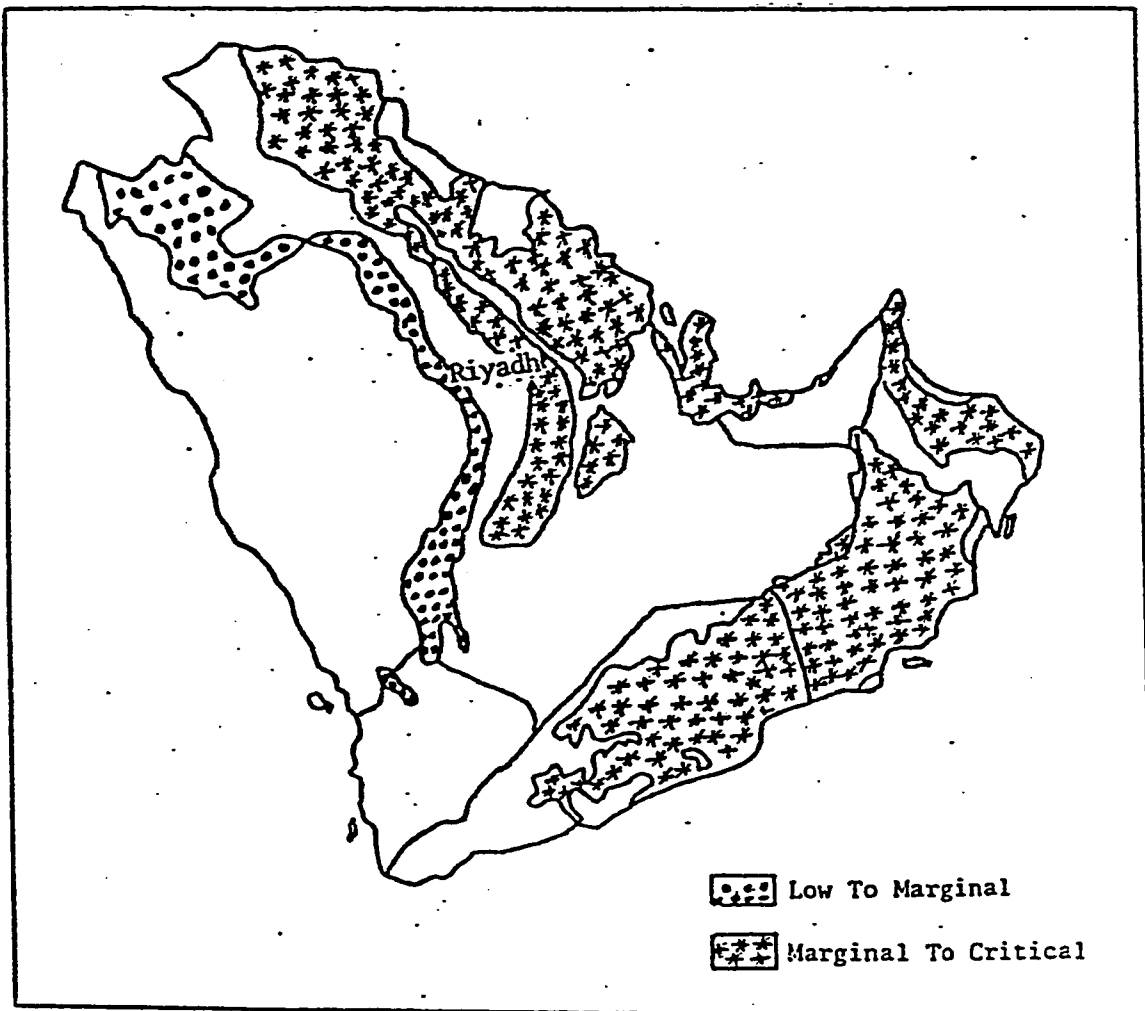


Figure (2.2) Hazard map for potentially swelling soils of Arabian Peninsula
(Slater, 1983).

subsurface soil condition in some of these regions is as follows:

- *Hofuf Region:* The ground mainly consists of brownish grey silty clay with calcareous modulus of gravel size. Hofuf Formation is classified as marl or calcareous clays and possesses swell potential. The calcareous clay of Hofuf contains appreciable amounts of silt and sand due to the presence of weathered limestone materials. Swell potential of Hofuf calcareous clays are categorized as high. The expansive nature of this formation may be due to the presence of active clay minerals as reflected by their relative high activities.

- *Madina Region:* The area is covered by a thick layer of heterogeneous fill overlying a soft to medium stiff green-white clay formation which is identified as expansive soil. This stratum contains calcareous rock fragments and sand lenses. At greater depths a hard greenish clay is encountered. Madina clay contains the highest percentage of clay fraction while the shales range from clay to silty types. Madina clays are categorized as highly expansive materials due to the fact, that particularly green clays possess major amounts of expandable montmorillonite mineral. Despite the high swell potential it is believed that swell related problems are unlikely to occur in Madina region. This is because of the fact that the substantial parts of the swell formations will be compensated by closing the shrinkage cracks.

Al Ghatt Region: The area is covered with silt, sand and gravel underlain by olivegreen shales which are part of Dhurma Formation. This formation possesses moderate swelling potential.

Tabuk Region: The upper part of Tabuk Formation consists of greenish-grey micaceous silty and clay shales and sandstone/siltstone. The swell potential of the formation vary from medium to extra high.

Tayma Region: The shales of Tayma are characterized by their high silt constituents and low plasticity and categorized as a moderately expansive material.

Al-Qatif Region: The subsurface soil consists mainly of dense to very dense calcareous clay silt with limestone fragments. Layers of hard silty clays are also present (42). Al-Qatif clays have high swelling potential and a high content of montmorillonite (1).

2.3 ORIGIN OF EXPANSIVE SOILS

The conditions which determine the clay mineralogy of the soil are composition of the parent material and degree of weathering to which the materials are subjected. Donaldson classified the parent materials that can be associated with expansive soils into basic igneous rocks and the sedimentary rocks which contain montmorillonite as a constituent. The basic igneous

rocks are relatively low in silica, generally about 45% to 52%. Rocks which are rich in metallic bases such as the pyroxenes, amphiboles, biotite and olivine fall within this category. Such rocks include the gabbros, basalts and volcanic glass. The sedimentary rocks that contain montmorillonite as a constituent include shales and claystones. Limestones and marls rich in magnesium can also weather to clay. These constituents of the shales and clay stones contain varying amounts of volcanic ash and glass which were subsequently weathered to montmorillonite. The marls and limestones in Saudi Arabia belong to this category.

The weathering processes by which clays are formed include physical, biological and chemical processes. Physical weathering processes include expansion due to unloading, crystal growth, thermal expansion and contraction, organic activity and colloidal plucking. These processes change the particle size and bulk volume of the parent material without significant change in composition. Chemical weathering causes a complete change in physical and chemical properties. The processes include hydration, hydrolysis, oxidation, carbonation and solution. The presence of water is necessary for all of these processes to occur.

Twenhofel, as quoted by Chen (13), states that the formation of expansive clays or the montmorillonite clays is favored by an alkaline environment and the absence of leaching, the presence of ferromagnesium materials in parent materials and the

presence of base. Prolonged leaching under high temperatures or tropical conditions with ferric iron parent rocks favors formation of minerals of the kaolinie group which are non expansive. The presence of potash in the parent material under these conditions results in the formation of illite (13).

2.4 EXPANSIVE CLAY MINERALS

Most clays are composed of more than one clay mineral mixed in different amounts and various ways. Their expansivity is largely influenced by in-situ soil moisture content, the types of clay minerals in predominance, certain cation exchange capacities, the cations absorbed in the clay structures and the composition of the ground water supplying the exchange cations (42).

Clay minerals may be formed by one or more of the following processes (34):

1. Crystallization from solutions.
2. Weathering of silicate minerals and rocks.
3. Diagenesis, reconstitution, and ion change.
4. Hydrothermal alterations of minerals and rocks.

The lattice structure of clay minerals is essentially the basis for their classification into four major groups, namely; 1:1,

2:1,2:1:1 and chain structures as shown in Table 2.1. Structures of some important clay minerals are shown in Fig. 2.3. groups are shown in figure 2.3. Montmorillonite is the clay mineral that causes most of the expansive soils problems. The name montmorillonite was used as a group for all clay minerals with an expanding lattice, except vermiculate, and now is used as a specified mineral name (13). The group is now called smectite rather than montmorillonite. The name montmorillonites was proposed by Damour and Salvétat (1847) and was named after Montmorillon (France). Montmorillonite has a structure very close to micas, but the bonds between the layers are weakened. Thus water in variable quantity can enter between the unit layers causing the stacking periodicity to have a variable value, in many cases, close to 14 Å. The permutation of exchangeable ions, heat treatment, and the action of polyalcohols cause this periodicity to vary between 10 to 20 Å (33).

Smectite is composed of conjoining identical units made of an alumina octahedral sheet between two silica tetrahedral sheets, Fig. 2.3. As mentioned above, the sheets are bound together rather loosely and thus unstable mineral results, especially in the presence of water. The attracted water molecules easily insert themselves between the sheets, causing swelling, Table 2.2. In such cases individual smectite flakes are enclosed within water films; thus wet smectite have a high plasticity and a low coefficient

Table 2.1: Classification of phyllosilicates related to clay minerals

Layer type	Group (x = charge per formula unit) *	Sub-group	Species **
1:1	Serpentine-kaolin ($x \sim 0$)	Serpentines Kaolins	Chrysolite, antigorite, lizardite, amesite, berthierine Kaolinite, dickite, nacrite
2:1	Talc-pyrophyllite ($x \sim 0$) Smectite ($x \sim 0.2-0.6$) Vermiculite ($x \sim 0.6-0.9$) Mica ($x \sim 1.0$) Brittle Mica ($x \sim 2.0$)	Talcs Pyrophyllites Saponites Montmorillonites Trioctahedral vermiculites Dioctahedral vermiculites Trioctahedral micas Dioctahedral micas Trioctahedral brittle micas Dioctahedral brittle micas	Talc, willemseite Pyrophyllite Saponite, hectorite, stevensite Montmorillonite, beidellite, nontronite Trioctahedral vermiculite Dioctahedral vermiculite Muscovite, paragonite, illite, phengite, celadonite, glauconite Clintonite, anandite Margarite
2:1:1	Chlorite (x variable)	Trioctahedral chlorites Dioctahedral chlorites Di, trioctahedral chlorites	Clinochlore, chamosite, nimite Donbassite Cookeite, sudoite
2:1 inverted ribbons	Sepiolite- palygorskite (x variable)	Sepiolites Palygorskites	Sepiolite, loughlinitite Palygorskite (attapulgitite)

* x refers to an $O_{10}(OH)_2$ formula unit for smectite, vermiculite, mica, and brittle mica.

** Only a few examples are given.

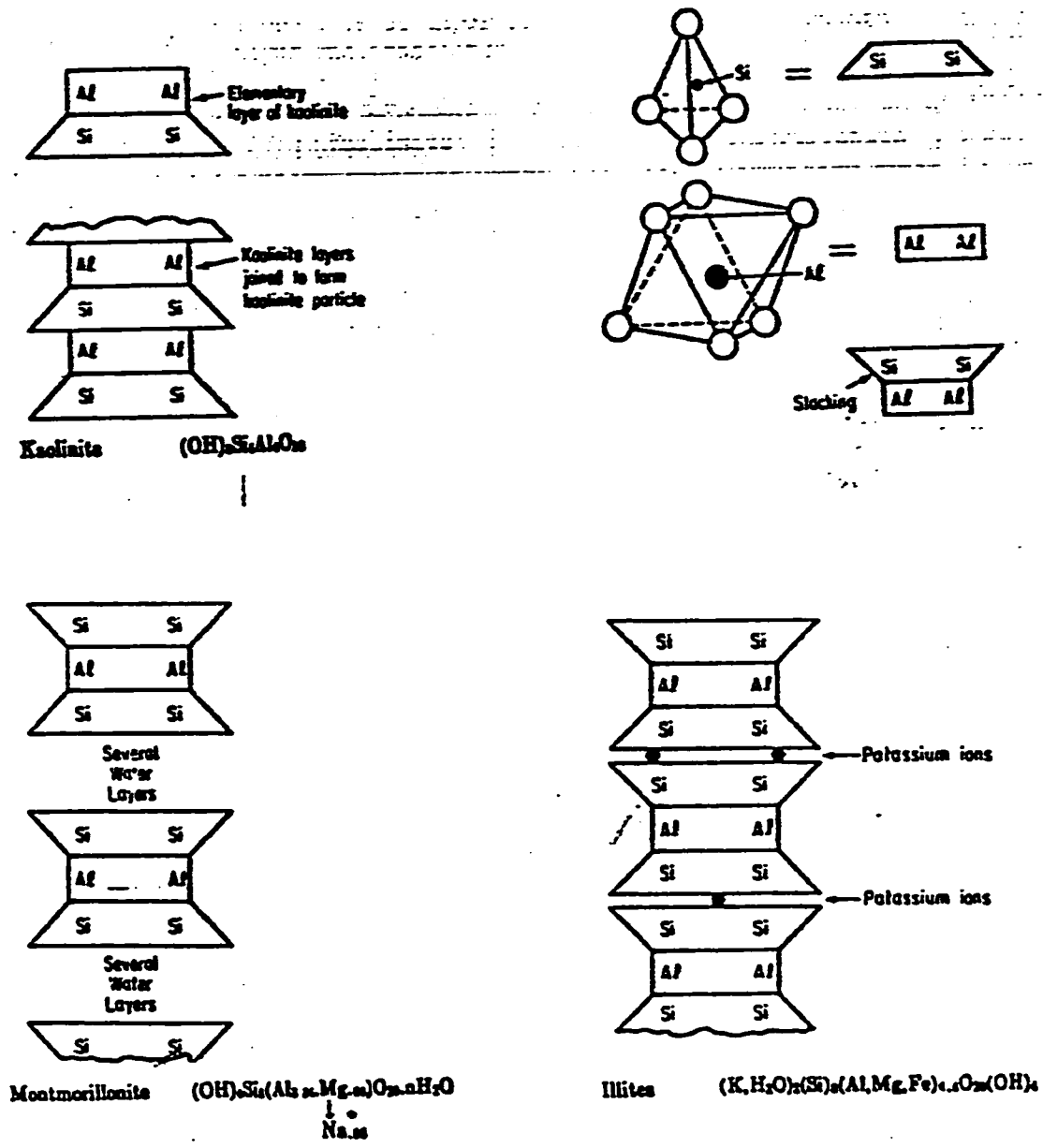


Figure (2.3), Structures of Important Clay Minerals

Table 2.2: Swelling Index Values for Several Minerals

Mineral (1)	Pore Fluid, Adsorbed Cations, Electrolyte Concentration, in Gram Equivalent Weights per Liter (2)	Void Ratio at Effective Consolidation Pressure of 100 psf (3)	Swelling Index (4)
Kaolinite	Water, sodium, 1	0.95	0.08
	Water, sodium, 1×10^{-4}	1.05	0.08
	Water, calcium, 1	0.94	0.07
	Water, calcium, 1×10^{-4}	0.98	0.07
	Ethyl alcohol	1.10	0.06
	Carbon tetrachloride	1.10	0.05
	Dry air	1.36	0.04
Illite	Water, sodium, 1	1.77	0.37
	Water, sodium, 1×10^{-2}	2.50	0.65
	Water, calcium, 1	1.51	0.28
	Water, calcium, 1×10^{-2}	1.59	0.31
	Ethyl alcohol	1.48	0.19
	Carbon tetrachloride	1.14	0.04
	Dry air	1.46	0.04
Smectite	Water, sodium, 1×10^{-1}	5.40	1.53
	Water, sodium, 5×10^{-4}	11.15	3.60
	Water, calcium, 1	1.84	0.26
	Water, calcium, 1×10^{-2}	2.18	0.34
	Ethyl alcohol	1.49	0.10
	Carbon tetrachloride	1.21	0.03
Muscovite	Water	2.19	0.42
	Carbon tetrachloride	1.98	0.35
	Dry air	2.29	0.41
Sand			0.01 to 0.03

of internal friction. When a saturated smectite is drying out, it is subjected to high shrinkage and cracking (31). Table 2.3 summarizes the properties of montmorillonite (34). Swelling of pure montmorillonite clay can affect volume changes as much as 2000 percent and generate swelling pressure in excess of 30,000 psf (30).

Tourtelot (1973), pointed out that the setting for the formation of smectite is extreme disintegration, strong hydration, and require that leaching be restricted, so that magnesium, calcium, sodium, and iron cations may accumulate in the system. Thus, the formation of smectite minerals is aided by an alkaline environment, presence of magnesium ions, and lack of leaching. Such conditions are favorable in semi-arid regions with relatively low rainfall or highly seasonal moderate rainfall, particularly where evaporation exceeds precipitation. Under these conditions, enough water is available for the alteration process, but the accumulated cations will not be removed by flush rain. It is believed that when smectite is being formed, palygorskite is dissolving and vice versa. Alteration of smectite into palygorskite under highly saline and alkaline conditions has been proposed in the soils of eastern Saudi Arabia (50). Fig. 2.4 shows the possible overlapping of the compositional fields of playgorskite and montmorillonite.

The parent minerals for the formation of smectite often consist of ferromagnesium minerals, calcic feldspars, volcanic

Table 2.3: Some properties of montmorillonite

Complete formula/ unit cell	$(\text{OH})_4 \text{Si}_8 (\text{Al}_{3.34} \text{Mg}_{0.66}) \text{O}_{20} \cdot n\text{H}_2\text{O}$ ↓ $\text{Na}_{0.66}$
Octahedral layer cations	$\text{Al}_{3.34} \text{Mg}_{0.66}$
Tetrahedral layer cations	Si_8
Isomorphous Substitution	Mg for Al Net charge always = 0.66 / unit cell
Interlayer bond	0 - 0 very weak expanding lattice
Basal spacing	9.6 Å - complete separation
Shape	Flakes Equidimensional
Size	> 10 Å X Up to 10 μ
Cation Exchange Capacity	80 - 150 meq / 100 mg
Specific gravity	2.2 - 2.7
Specific surface	50 - 120 m ² / gm } Primary 700 - 840 m ² / gm } Secondary

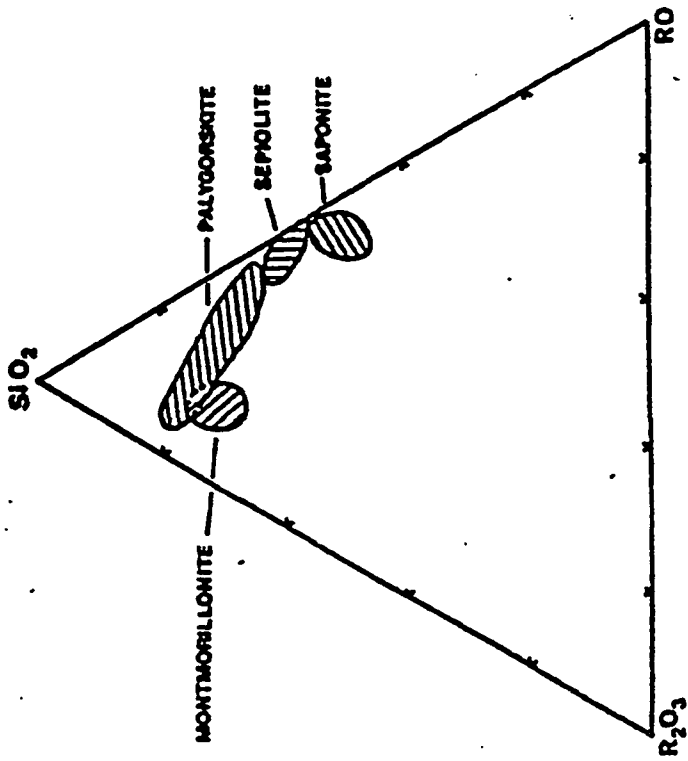


Fig. (2.4) Triangular diagram showing approximate compositional areas for montmorillonite, palygorskite, saponite and sepiolite.

glass, and many volcanic rocks. Bentonite is a clay composed of montmorillonite rich with sodium which has been formed by the chemical weathering of volcanic ash. Since commercial bentonite is white, the white calcium streaks present in stiff clays are often mistaken for bentonite. Actually, clays with an abundance of calcium seldom exhibit swelling characteristics (13).

2.5 CATION EXCHANGE

In clay minerals, the most common exchangeable cations are Ca^{++} , Mg^{++} , H^+ , K^+ , NH_4^+ , and Na^+ frequently in about that order of general relative abundance. A cation, such as Na^+ , is readily attracted from a salt solution and attached to a clay surface. However, the adsorbed Na^+ ion is not permanently attached, it can be replaced by K^+ ions if the clay is placed in a solution of potassium chloride. The process of replacement by excess cation is called cation exchange (13).

The quantity of exchangeable cations required to balance the charge deficiency of a clay is termed the cation exchange capacity (CEC) and is usually expressed in milliequivalents per 100 grams of dry clay (34). Typical ranges of (CEC) of various clay minerals are as the following: kaolinite (3-15), illite (10-40) and smectite (70-150) milliequivalents per 100 g.

Certain relationships exist between soil properties such as the Atterberg limits, the type of clay mineral, and the nature of the adsorbed ions. Table 2.4 indicates the liquid limit and plasticity index of clay minerals with various adsorbed cations (13).

Cation exchange capacity is, by itself, not an indicator of clay soil activity. When utilized with the type and amount of cations in the soil the potential for activity may be predicted. However, it is believed that swelling pressure is affected by the type and concentration of cations present in the exchange complex of the soil. As calcium concentration in both pore water and exchange complex increases swelling pressure decreases. As sodium concentration in the exchange complex increases, an increase of swelling pressure will occur. Percent of swell is directly related to the concentration of cations in the pore water. The presence of increasing amounts of sodium and calcium in the pore water of the clay soil cause more swelling to occur. Finally, as sodium concentration increase, the clay soil plasticity increases (41).

2.6 CLAY WATER INTERACTION

Interactions between soil particles, adsorbed cations, and water arise because there are unbalanced forced fields at the

Table 2.4: Atterberg values of clay minerals with various adsorbed cations

Cation	Na+		K+		Ca++		Mg++	
	Liquid limit, percent	Plasticity index, percent	Liquid limit, percent	Plasticity index, percent	Liquid limit, percent	Plasticity index, percent	Liquid limit, percent	Plasticity index, percent
Caly mineral								
Kaolinite	29	1	35	7	34	8	39	11
Illite	61	27	81	38	90	50	83	44
Montmorillonite	344	251	161	104	166	101	158	99

interfaces between the constituents (34). In the clay water system, the water within the clay is called adsorbed water; the water and ions with the clay lattice constitute the diffuse double layer (resulted from the electonegativity of the surface) (13, 36). Two forces exist in the system, the attractive and repulsive forces. The interaction of the different attracting and repulsing forces comprising the interparticle bonds is usually described by the interaction energy curve, i.e. the energy of interaction as a function of the interparticle distance (45)

In a dry clay, adsorbed cations are tightly held by the negatively charged clay surfaces. Cations in excess of those needed to neutralize the electro negativity of the clay particles and their associated anions are present as salt precipitates. When the clay is placed in water, the precipitated salts go into solution. Because the adsorbed cations are responsible for a much higher concentration near the surfaces of particles, there is a tendency for them to diffuse away in order to equalize concentrations throughout. Their freedom to do so, however, is restricted by the negative electric field originating in the particle surfaces. The escaping tendency due to diffusion and the opposing electrostatic attraction lead to a certain distribution adjacent to a clay particle in suspension as shown in figure 2.5 (34).

Bolt and Bruggenwert presented the truncated diffuse double layer. The special property of the truncated double layer

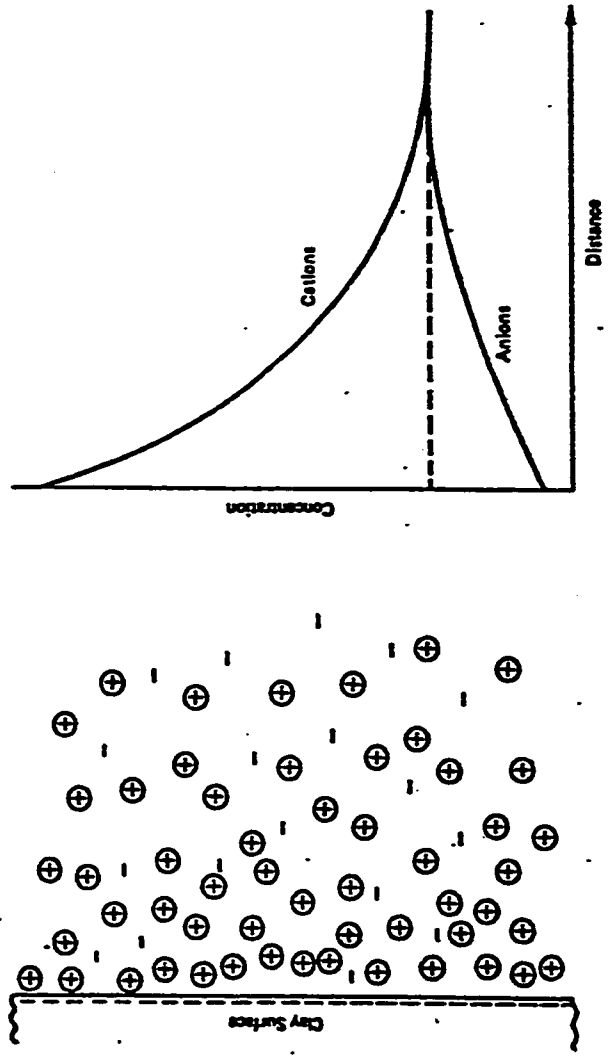


Fig. 2.5 : Distribution of Ions adjacent to an Expansive Clay Surface according to the Concept of the Diffuse Double Layer (Mitchell, 1976)

(shown in fig. 2.6) is to reabsorb moisture forcefully and to develop to an extent commensurate with the concentration of the equilibrium bulk solution. In this process, the double layer reaches a stage at which all the voids are saturated with exertion of swelling pressure for no change in void ratio. If the volume change is permitted, the double layer grows to its full extent. Fig. 2.7 schematically shows the truncated double layer due to partial saturation, the interacting double layer on saturation equilibrium under swelling pressure, and the fully extended double layer under no load (36).

2.7 MECHANISM OF SWELLING

Swelling as mentioned previously is the increase of volume of a clay soil as the water content increases. If the environment of the expansive soil has not been changed, the soil does not swell. Environmental change can consist of pressure release due to excavation, desiccation caused by temperature increase, and volume increase because of the introduction of moisture. By far the most important factor is the effect of water on expansive soils (13).

Swelling is caused by the attraction and absorption of water molecules into the expansive crystal lattice of the clay minerals. Soil shrinkage occurs when the process is reversed and

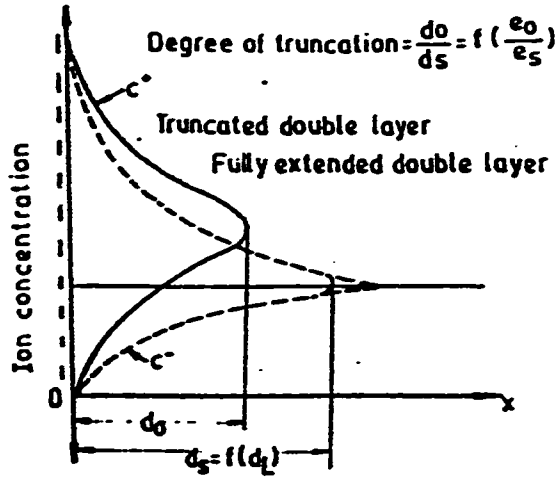


Fig. (2.6) Schematic representation of redistribution of ions in a truncated double layer.

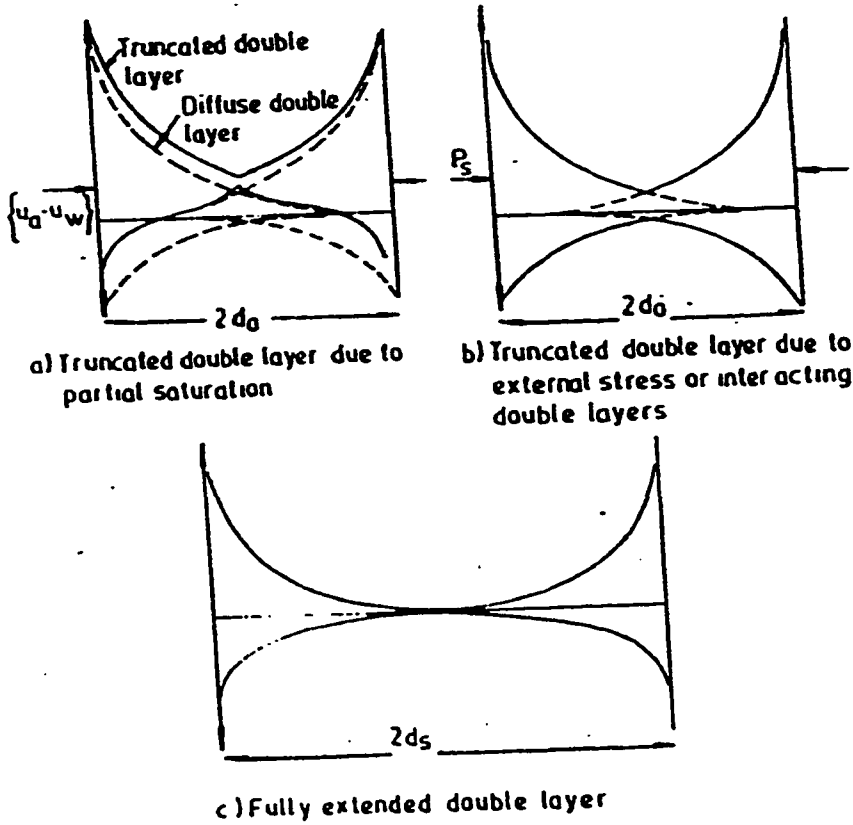


Fig. (2.7) Schematic representation of ion distribution in truncated and fully extended diffuse double layer.

the water is removed from the clay crystal lattice. The amount of water available to the clay lattice is dependent on various environmental factors. Of these, climatic conditions probably represent the most dominant element affecting expansive clays. In this respect, the most important aspect of climate is the relationship between rainfall and the rate of evapotranspiration. In areas where the seasonal climatic changes are greatest, expansive clays are very active with pronounced shrinkage and swelling quite common. Similarly, in areas where seasonal changes are less dramatic and the expansive clays are kept wet throughout the year, little or no volume change may occur within expansive clay lattice (30).

In general, the process of swelling at a continuous wetting of the clay can be represented as one consisting of two non stationary processes running together. In the first process, the water is absorbed by the pores of the soil and the negative effective tensile pressures in its skeleton are brought about as the result. In this process, the beginning of deformation of swelling and the moment its stabilization comes are taken to be respectively coincident with the beginning of percolation and the cessation of water in flow to the thickness of soil. As to the value of the volume deformation of soils which is caused by the mechanical expansion of clayey particles resulted from the thickening of the water film it directly depends upon the volume of water

participating in the process. In the second process, the water is absorbed by the mineral aggregates themselves whose density is higher than the average density of soil. In this process, the temporal rate of deformation is slower than the process of percolation and the volume of moistened soil may considerably exceed the volume of water coming to the soil when the latter is moistened. The swelling process does not always start with the moistening of the soil thickness and sufficient time elapses since the cessation of water inflow to the soil before stabilization comes (35).

During the wetting of the soil, the capillary films are automatically enlarged. Thus, the acting compression stress is relieved which permits further opening of the expandable lattice.

Swelling in clays is associated with sorption of moisture either from a liquid that comes in contact with the clay or from the ambient humid air. Water may contact the top of the clay deposit or be lifted up by suction forces from the lower strata (49). In clay, a capillary rise of more than 1000 feet is theoretically possible (13). Surface water outside a building may penetrate into its interior under continuous shallow footings. Generally, according to the rate of water affluent, the swelling will be gradual and last a long time until a limit is attained. Laboratory tests have proved that the water intake is greatest at the start of swelling process and proceeds at a decreasing rate. As the

attracted water is accumulated, swelling pressure builds up in it (31). In areas of moderate rainfall, the swelling occurs under the center of the building. There are two possible explanations for this (59):

1. A building resting directly on the surface of the ground prevents normal evaporation from beneath it, especially if its tiled floors are waxed.
2. Another explanation is the migration of water. Kraynski (13) stated that "There must be a potential gradient which can cause water migration and a continuous passage through which water transfer can take place". According to Tschebotanoff (59), moisture has a tendency to migrate from warmer to colder soil zones, a phenomenon known as thermo-osmosis. In hot climates, a building shades the soil surface area which it occupies and thereby cools the layers beneath it. The result is the migration of the water, swelling of desiccated clay and heaving of the soil surface under the building as shown in fig. 2.8. Experiments conducted at Princeton University show that a temperature differential of 1°C was at least equivalent to a hydrostatic head of three feet in its ability to cause moisture migration. The thermal gradient reaches maximum efficiency when the moisture content in the soil is near the plastic limit.

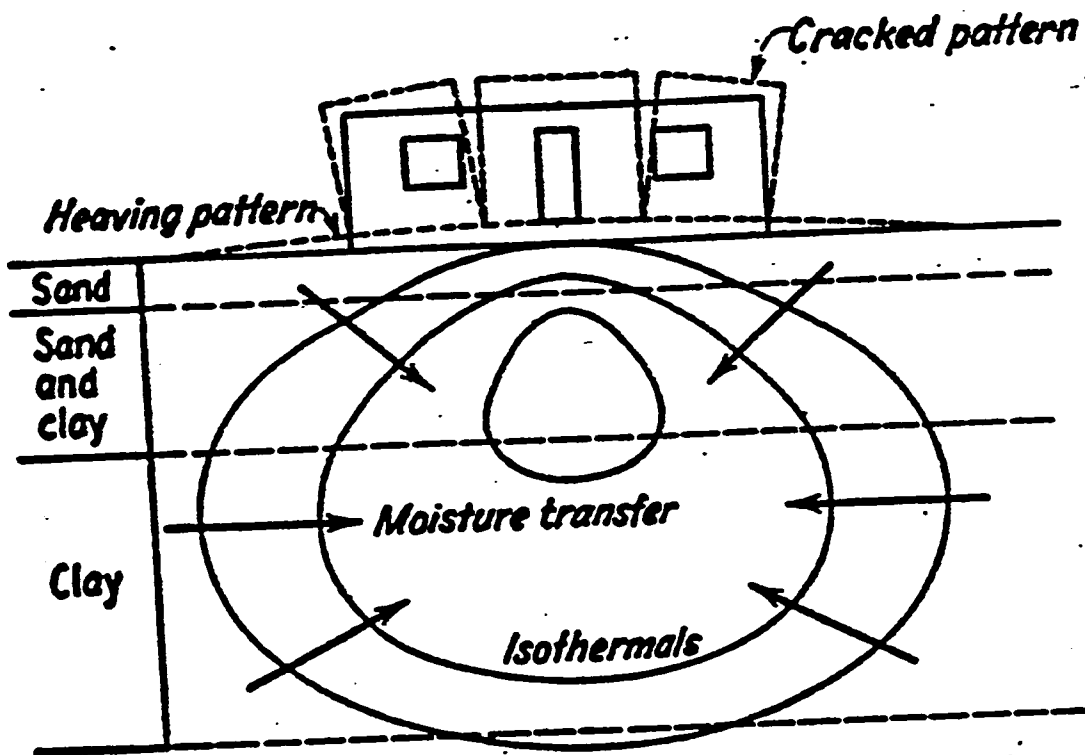


Figure (2.8) Diagrammatic sketch of thermoosmotic heaving of building on disiccated clay foundation.

Covering the ground surface around the building with plastic membranes creates a thermal gradient which may encourage water from lawn watering to transfer to the foundation soils (13). The pattern of water migration depends on the geological formations, climatic conditions, topographic features, soil types and ground water level.

Einestein and Bischoff outlined the mechanism of swelling to be a function of several phenomena. These are as follows:

1. A change in the stress state, i.e. stress relief.
2. Adsorption or absorption of water due to the differences in the concentration of saturated or partially saturated bonds.
3. Adsorption and/or absorption of water due to the stress changes of phenomena (1).
4. Stress changes due to adsorption and/or absorption of water of phenomena (2).
5. Time dependent reduction of shear strength.

It is important at this point to mention that the mechanism of swelling is still not fully understood, and researches are continuous in order to get a clearer and complete picture of this mechanism.

2.8 SWELL POTENTIAL

Although the swelling phenomenon has been known for many years, neither a definite method of measuring the swelling potential of clay nor a clear definition of swell potential has been established (13). For example, in one of the published methods the swell potential is defined as the swell (percent on a deformation basis) of an undisturbed specimen from an air dried to a saturated condition under 1 psi surcharge. In another method, it is defined as the swell (percent on a deformation basis) of a remolded specimen at optimum moisture content and maximum dry density under 650 psf (4.5 psi) surcharge (53). In 1962, Seed defined swelling as the percentage swell of laterally confined sample on soaking under the 1-psi surcharge, after being compacted to maximum density at optimum water content in the standard AASHTO compaction test (11). The difficulty in providing a suitable yardstick for measuring swell characteristics is caused by the presence of the numerous variables involved. The basic definition of potential swell, whether it is used for the purpose of identifying and/or classifying an expansive soil or predicting the amount of anticipated volume change, should provide the best simulation of in situ conditions practical. At a minimum, the definition should specify the initial conditions of the specimen, such as, moisture content, dry density, fabric, and structure, as well as the stress conditions on the specimen, such as vertical

stress and lateral confinement conditions. With this in mind, according to Snethen (53) the definition of potential swell which satisfies the largest portion of the field simulation requirement is: potential swell is the equilibrium vertical volume change or deformation from an odometer type test (i.e., total lateral confinement), expressed as a percentage of original height of an undisturbed specimen from its natural moisture content and density to a state of saturation under an applied load equivalent to the in situ overburden pressure. The definition may be changed to reflect the final stress conditions such as applied load from the structure or the fill placement conditions.

2.9 SWELLING PRESSURE

Swelling pressure is the basic physical property of expansive soils. It can be defined, according to ASTM, as the pressure which prevents the specimen from swelling or that pressure required to return the specimen back to its original state (void ratio, height) after swelling (13). Swelling pressure is affected by the type and concentration of cations present in the exchange complex of the clay soil. As calcium concentration in both pore water and exchange complex increases, swelling pressure decreases. As sodium concentration in the exchange complex increases, an increase of swelling pressure will occur (41). According to Chen(40), the swelling pressure of a clay is

independent of the surcharge pressure, the initial moisture content, the degree of saturation and the thickness of the stratum. It depends only on initial dry density, that is the swelling pressure increases with the increase of initial dry density.

The methods of measuring swelling pressure can be either stress controlled or strain controlled (13).

Stress Controlled: For this test, the conventional odometer is used. The samples are placed in the consolidation ring trimmed to a height of 3/4 to 1 inch. The samples are subjected to a vertical pressure ranging from 500 psf to 2000 psf depending upon the expected field conditions. On the completion of consolidation water is added to the sample. When swelling of the sample has ceased, the vertical stress is increased in increments until it has been compressed to its original height. The stress required to compress the sample to its original height is commonly termed the zero volume change swelling pressure.

Strain controlled: The strain controlled method is based on the principle of controlling the strain that is developed as water is added. In this test, modification of the conventional odometer is required to allow the control of strain during testing and measurement of the resulting loads.

Porter and Nelson (13) concluded that both tests give very close results, though not exact. El-Fatih Ali (13) concluded

that the constant volume method gives results of swelling pressure that are generally smaller than those obtained from the odometer method.

2.10 FACTORS AFFECTING SWELLING

The amount of volume change that can take place depends upon several factors. Each of these factors is briefly discussed in the following:

1. Type and amount of clay: The basic mineral, its surface chemistry and the fabric of a particular clay, together with the salt concentration of the soil water, generally determines its potential for volume change or heave. For engineering purposes the type of clay is determined indirectly through standard soil tests, such as linear shrinkage (L.S) or plastic index (PI), and is often related empirically to potential heave, Table 2.5 (25).
2. Mineralogical Composition: The amount of volume change is dependent on the mineralogical composition: clay mineral type, clay mineral content and exchangeable ion. Lambe and Whitman found that swellability varies with the type of clay mineral; it decreases in the order montmorillonite, illite, attapulgite, and Kaolinite (22).

Table 2.5: Clay Potential Volume Change

Potential Volume Change	ARID TO SEMI-ARID		HUMID AREAS	
	L.S %	PI %	L.S %	PI %
Low	0 to 12	0 to 15	0 to 12	0 to 30
Moderate	5 to 12	15 to 30	12 to 18	30 to 50
High	> 12	> 30	> 18	> 50

Mitchel found that most expansive soils contain montmorillonite and vermiculate. Many investigators studied the effect of clay on swelling and agreed that the amount of swell and swelling pressure increases with the increase of clay content (34). The effect of exchangeable ion on swellability may be summarized as follows: For soils containing expansive clay minerals, the type of exchangeable ion exerts a controlling influence over the amount of expansion that takes place in the presence of water. Therefore, there is a complete agreement among researchers in considering the mineralogical identification as the primary method for classifying potentially expansive soils (22).

3. Soil Structure: The stress history of a soil also influences swell. Undisturbed or cemented expansive soils experience high resistance to deformation thereby imparting large swelling pressures. Remolding undisturbed clay reduces initial hardness at high shear strength, and preferentially aligns the flat grains normal to the compacting forces. Soils with line particles, swell more in directions normal to platelets than in directions parallel to platelets (42). De Bruyn (1957) considered that clayey soils would be potentially expansive if their larger mineral grains (e.g. quartz, feldspar, etc.) were

united by intergranular braces made up of clay particles or were surrounded by a uniform colloidal coating (14).

4. Initial Moisture Content: Field conditions and construction specifications indicate the moisture requirement of the soil. Dry soils swell more than wetter ones because of the direct relation between water content and suction pressures. When a site is sloping and well drained, rain falling on it will mostly runoff, so the clay will not wet up significantly and therefore little seasonal heave will occur. Alternatively, if a site is flat and water logged during the wetter months of the year, significant wetting up of the clay will occur, leading to substantial heave. Improvements of site drainage can therefore dramatically reduce the magnitude of seasonal heave. Excessive garden watering and fractured buried pipes are two sources of moisture (25).
5. Initial dry density: The single most important factor affecting swelling characteristics of swelling soils is density. Dense clays will swell more when they become wetted, compared with the same clay at a lower density and same initial water content (13). Laboratory testing indicates that swelling pressure of a given soil varies only with its dry density. The swelling pressure increases with the increase of initial dry density (11).

6. Climate: Potentially expansive clays will only swell and shrink if the prevailing climatic conditions lead to significant seasonal wetting and drying. In areas where seasonal climatic changes are greatest, expansive clays are very active. Similarly, in areas where the seasonal changes are less dramatic and the expansive clays are kept wet throughout the year, little or no volume change may occur within expansive clay (30). In semi arid climates, potential evapotranspiration usually exceed rainfall and the probability of heaving a substantial amount of movement around the edges of a slab-on-ground becomes greater. Thus, a design procedure must be able to provide a uniform guide for design in each climate without penalizing engineers in wetter climates for the greater uncertainties in design that occur in drier climates. Similarly, engineers in drier climates should be allowed the greater reliability that is provided by more substantial sections and reinforcing that is adequate in wet climates (63). Several models were developed to consider the changes in moisture content that occur in clay soil when the soil mass is subjected to a series of climatic events. Christiansen method, Hargreaves method and Corley method are examples of these models (15).

7. Soil Profile and depth of active zone: The thickness

and location of potentially expansive clay layers in the soil profile considerably influence the seasonal heave. If the expansive clay is overlain by a layer of non-expansive top soil, or overlies bedrock at a shallow depth, the swelling of the clay will be greatly reduced. The greatest seasonal heaves are, therefore, likely where potentially expansive clays exist from the surface to depths greater than that at which significant seasonal moisture changes normally occur. The depth of seasonal movements is related to the prevailing climatic pattern and may be altered by the soil profile. When the depth over which seasonal soil moisture changes occur is small, potentially large heaves of expansive clays, indicated by table 2.4, in the profile will not be realized (25). The depth of active zone or depth of desiccation has been defined as the thickness of the layer of soil in which a moisture deficiency exists. The depth of active zone is a transient value influenced by the soil type, soil structure topography, and climate. The depth of seasonal moisture variation may be equivalent to the depth of active zone if the material responds to changes in the climate relatively fast. However, most materials do not respond rapidly enough, so the depth of active zone is generally greater than the depth of seasonal moisture variation. As far as climate is concerned, the depth of active zone generally

reflects the past arid extremes of the climatic history. No universally applicable rules exist for establishing the depth of active zone (52). Fig 2.9 shows, as an example, the effect of a variation in the depth of active zone in San Antonio, Texas (32).

8. Surcharge: Small increases of load on a potentially expansive clay soil greatly reduce clay swell. Therefore, the application of small vertical loads near the surface will significantly reduce the clay swell and consequently the seasonal heave. Damage due to underlying clay heave is, therefore, generally associated with lightly loaded buildings, and in particular, housing and pavements (25). In the laboratory, a small surcharge load in the range of 0.35 to 1 psi has been suggested for a seating load in the swell test. Since swell is very sensitive to changes in pressure in the lower ranges of pressure (less than 1 psi), the use of low surcharge pressure may lead to erroneous test results (13). The surcharge of 1 psi appears to be most widely used. Continued use of this surcharge would seem to have considerable merit, both for better correlation of results from different sources and because it is considered to be a good physical representation of the surcharge acting on swelling soils in frequently important service conditions,

SAN ANTONIO

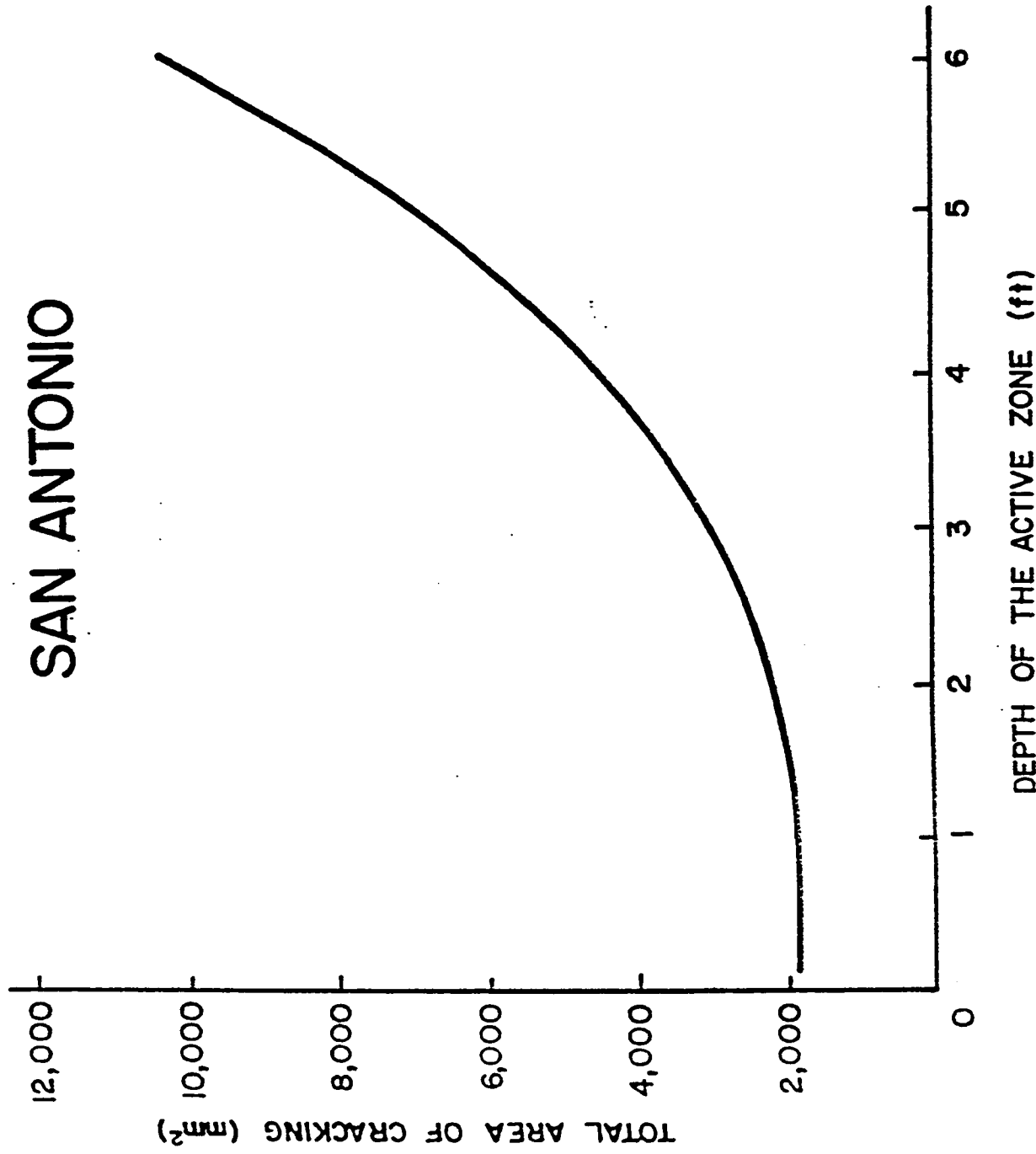


Figure (2.9) Effect of Depth of the Active Zone in San Antonio

e.g. under floor slabs and canal linings (29). However since most footing foundations can exert a pressure of about 7 psi on the soil, it is recommended that this value be used for surcharge load (13).

9. Time allowed to swell: The time required for the soil to reach its maximum swell potential may vary considerably depending on the initial dry density, permeability, and the thickness of soil layer. In testing remolded samples, generally 24 hours is sufficient to obtain 95% of the total available swell. At the same time, for undisturbed high density clay, it may require several days or even a week before complete saturation can be achieved (13)
10. Location and type of vegetation: Trees have the ability to dry clays within the zone influence of their root systems. This clay drying alters the pattern of seasonal movements by extending the drying cycle. The extent of desiccation, and finally its age. Grass alone can extend the drying cycle of some clays (25). When vegetation is removed and building floor slabs are placed on grade, the clays begin to regain moisture and swell more than clays at where such vegetation was absent. This can produce structural distress.
11. Other factors: Permeability, magnitude of horizontal

soil stresses, temperature and water properties also affect the amount of heave.

2.11 IDENTIFICATION OF EXPANSIVE SOILS

Before designing and building any construction, it is important to determine whether potentially expansive clays exist on the site of construction or not. To do so, there are several methods to identify expansive soils. Some of these methods depend on visual identification and experience, others depend on laboratory test identification or mineralogical identification.

2.11.1 Visual Identification

Site visits are useful to assess the possibility of expansive clays being present on a given site. Some indicators that can help identify expansive soils are (39):

1. Soil Clod characteristics:

- Very hard when dry.
- Glazed when cut by scraper or shovel.
- Cracks in regular pattern.
- Soft and sticky when wet.
- Leaves powdery residue after molding with hands.

2. Terrain Characteristics:

- Evidence of creep on slopes.
- Wide and deep shrinkage cracks with regular spacing.
- Gilgai structure: A mound-depression feature visible on the surface of expansive clays that have undergone weathering in a semiarid environment. Gilgai mounds tend to be more expansive than depressions due to higher mass permeability, more dispersed micro structure and lower pH. The existence of gilgai structure complicates the design of shallow foundations because of pointwise variation of swell potential across a site.

3. Existing Vegetation:

- Vegetation of a site can be indicative of the presence of expansive clays. Experience reveals that certain trees or shrubs tend to occur more frequently on soils having either high or low expansion potential. For example, in Central Texas, mesquite cover can usually be associated with expansive clays, where oak trees are associated with soils of relatively low potential expansion.

4. Climate:

- Locations prone to long dry periods followed by periods of wet weather are most susceptible to expansive clay activity. As will be discussed later in Chapter (3), the Thornthwaite Moisture Index (TMI) is a good rational means of classifying climate.

2.11.2 Local Experience

Despite the best attempts of identification, some expansive soil sites may go unidentified. Experience with behavior of structures in a given geological region may be useful in identifying potential problems. For example, water for irrigation of lawns may have different pH and solutes from those of rainfall. Such waters can be the source of free ions that stimulate a base exchange in the soil, amplifying its expansive characteristics.

Cut and fill operations in expansive clays may create foundation problems. Expansive clays become more prone to volume change when remolded and compacted, largely because of the breakup of cementation and possible production of high negative pore water pressure that may later be relieved. Thus, the same clay may vary in its expansion characteristics from one side of a site to another, depending on whether the clay is in its natural state or has been compacted. It is therefore desirable to conduct site investigations for the purpose of classifying and quantifying expansive soil behavior after rough site grading has

been accomplished.

The check list in figure 2.10 is useful to who finds what appears to be an expansive soil.

2.11.3 Laboratory tests

There are a number of laboratory tests that are useful in identifying clay soils and estimating potential swelling properties, such tests may include:

I: Atterberg Limits Tests: Plasticity index and liquid limit are useful indices for determining the swelling properties of most clays. The plasticity index, which demonstrates the magnitude of the range of moisture change possible while the soil retains a plastic condition, is related to expansion because the water in the void and clay minerals occupies space, thus causing changes in moisture content to reflect volume change. High plasticity indices are indicative of active soils (26). Plasticity indices in excess of 15 can be considered potentially expansive (17, 39). Figure 2.11 shows a plasticity chart evolved for classification of degrees of swelling (58). Relation between swelling potential of clays and plasticity index is shown in Table 2.6.

The shrinkage limit describes, indirectly, the minimum volume to which a soil will shrink upon drying and is an

SWELLING CLAY SOILS CHECKLIST

- | | YES | NO |
|---|--------------------------|--------------------------|
| 1. Have similar soils in this area been known to be expansive? | <input type="checkbox"/> | <input type="checkbox"/> |
| 2. Is there evidence of cracks in footings, walls, curbs, sidewalks or pavements in nearby construction? | <input type="checkbox"/> | <input type="checkbox"/> |
| 3. Are there shrinkage cracks in the soil in dry weather? | <input type="checkbox"/> | <input type="checkbox"/> |
| 4. Does the soil behave as a clay in wet weather? (For example: sticking to shoes and tires, "greasy" in feel between fingers, ponding water for long periods of time.) | <input type="checkbox"/> | <input type="checkbox"/> |

QUICK "FIELD TESTS"

- | | | |
|---|--------------------------|--------------------------|
| 1. Select a small lump of <i>dry</i> soil and try to break it between fingers. Is the soil strong and hard to break? | <input type="checkbox"/> | <input type="checkbox"/> |
| 2. Select a large lump of <i>dry</i> soil (about 2 to 3 lb.), raise it chest high and drop it on a hard surface (pavement). Does the soil stay in one lump, instead of breaking up into several smaller pieces? (Disregard breaking off thin edges or sharp corners.) | <input type="checkbox"/> | <input type="checkbox"/> |
| 3. Wet some soil in your hand or dish until it can be easily molded with light finger pressure. Can this soil be rolled out in the palm of your hand into a "thread" about 1/8-in. thick and more than 1 1/2-in. long? | <input type="checkbox"/> | <input type="checkbox"/> |
| 4. Mold wet soil (similar to that in point 3 above) in a ball bigger than 1-in. in diameter. Place it in the cup of your hand and strike the lower part of the hand on your knee with short strokes (2 to 3 in.) 10 to 15 times. Silty material will "bleed" water and show a wet shiny surface. Does the soil you are testing look about the same as when you started without shiny surface? | <input type="checkbox"/> | <input type="checkbox"/> |
| 5. Take a ball of wet soil (similar to that in test 4 above), drop it on a piece of smooth, dry glass plate from a height of about 18 in. Turn glass upside down (soil toward ground), slightly tilted. Tap the top of the glass plate with your fingertips. Does the soil remain stuck in the original position on the glass, instead of falling off or sliding? | <input type="checkbox"/> | <input type="checkbox"/> |

A 'yes' answer to any of the above questions may indicate a need for further testing. Report the findings to your supervisor.

PROJECT _____

LOCATION _____ DATE _____ CHECKED BY _____

REMARKS _____

Figure 2. 10 A check list will be a help to the technician if he suspects expansive soil in the building area. Portland Cement Association.

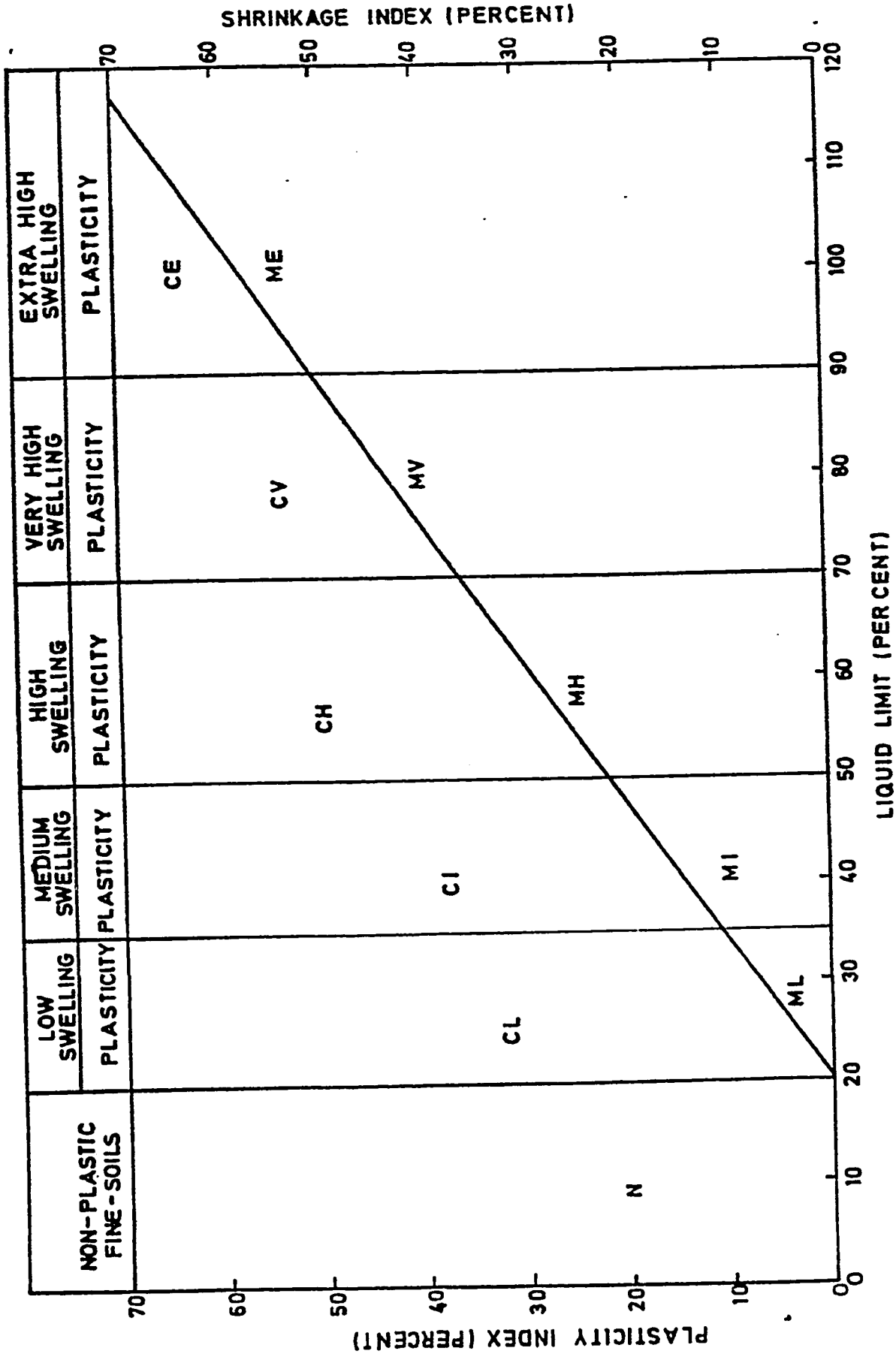


Fig. 2.1.1 Chart for potential expansiveness of soils

expression of percentage of water necessary to fill the void spaces when the soil is at minimum volume, is valuable supplemental information to the foregoing data. A low shrinkage limit would show that a soil could begin volume change at low moisture content (26). Altmeyer suggested in 1955 as a guide to the determination of potential expansiveness for various values of shrinkage limits. This is shown in table 2.7.

The evaluation shows that the most consistent indicators of potential swell are first, the liquid limit (LL) and Plasticity index (PI), second, the liquid limit (LL) and natural water content (W_n) combined; third, shrinkage limit (SL) and plasticity index (PI); and finally, the (SL) and Linear Shrinkage (53).

Since liquid limit and swelling of clays both depend on the amount of water a clay tries to imbibe, it is not surprising that they are related. In general potentially expansive clays have liquid limits about 40 (39, 17). According to Sridharan and Rao (54), the seat of swelling forces, namely, diffuse double layer repulsion, governs the index properties of montmorillonitic soils as well; hence the use of index test for predicting expansivities of montmorillonitic soils is mechanistically justified. The index properties of kaolinitic soils are not a function of diffuse

Table 2.6: Relation between swell potential and PI

Swelling Potential	Plasticity Index
Low	0 - 15
Medium	10 - 35
High	20 - 55
Very High	>35

Table 2.7: relation between degree of expansion and shrinkage limit

Degree of Expansion	% Shrinkage Limit
Critical	< 10
Marginal	10 - 12
non-critical	> 12

double layer repulsion, and hence their use in prediction of soil expansivity has no scientific basis. Comparison of classification based on index tests with those obtained from odometer results for the kaolinitic and montmorillonitic soils indicated that the index tests are better suited for estimating expansivities of montmorillonitic soils.

II: Colloid Content: The colloid content, determined from the gradation test indicates the amount of the colloidal size fraction, which is the most active part of any soil material contributing to expansion (26). For a given type of clay, the amount of swell will increase with the amount of clay present in the soil as shown in Fig. 2.12 .

Table 2.8 also shows the relation between the colloid content and degree of swell (47).

III: Free Swell Test: A simple test which provides a quick qualitative measure of expansiveness. The test consists of placing a known volume of dry soil in water and noting the swelled volume after material settles, without any surcharge to the bottom of a graduated cylinder. The difference between the final and initial volume expressed as a percentage of initial volume is the free swell value. The test is very crude and was used in the early days when refined methods of testing were not available (13). It was reported

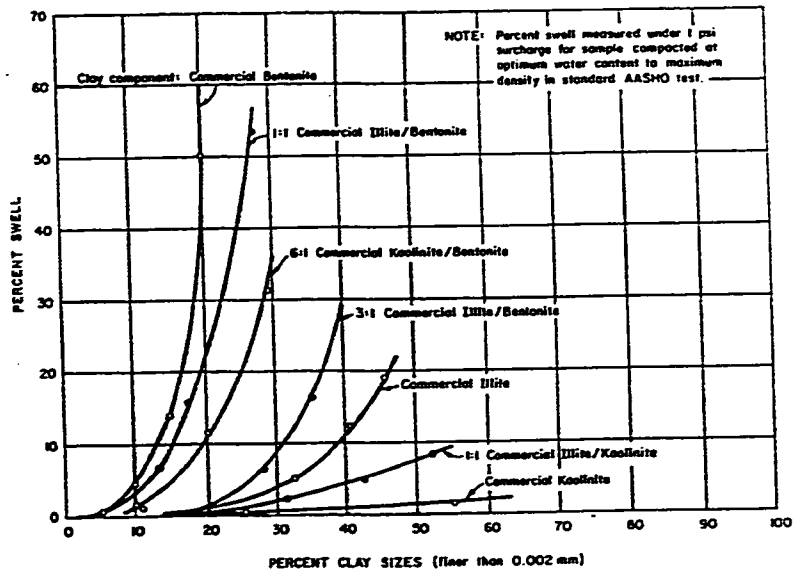


Figure 2.12A Relationship between percentage of swell and percentage of clay sizes for experimental soils. (After Seed, Woodward & Lundgren).

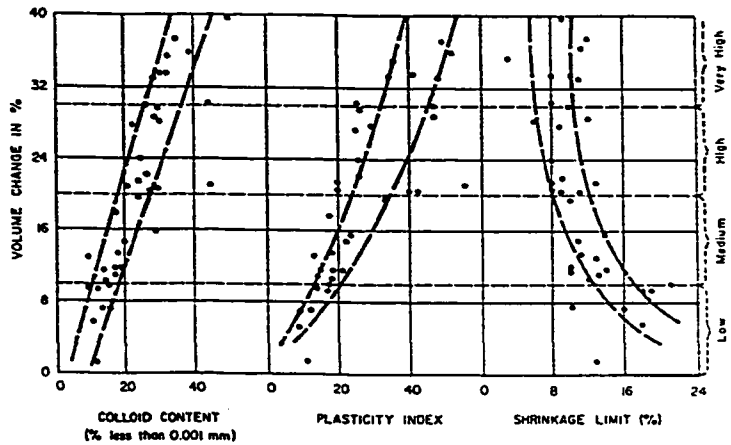


Figure 2.12B Relation of volume change to colloid content, plasticity index, and shrinkage limit (air-dry to saturated condition under a load of 1 lb. per sq. in.) (After Holtz and Gibbs)

Table 2.8: Relation of colloid content and degree of expansion.

Colloid content (% < 0.001 nm)	% Swell	Degree of expansion
> 28	> 30	very high
20 - 31	20 - 30	high
13 - 23	10 - 20	medium
< 15	< 10	low

by Holtz that soils having free swell values as low as 100% may exhibit considerable volume change when wetted under light loadings and should be viewed with caution whereas soils having free-swell values below 50% seldom exhibit appreciable volume changes, even under very light loadings (26). Free swell test provides a more reliable means of estimating relative expansivities in comparison to index properties and is applicable to both kaolinitic and montmorillonitic soils. The free swell test is not designed to provide the actual magnitude of swelling under field conditions but identifies potentially problematic soils that need be subjected to detailed investigations for design purposes (54). Fig. 2.13 shows a plot of free swell against the total expansion of undisturbed soil specimen placed in laboratory consolidometers and expanded from air dry to saturated conditions (26). It has been reported by Komornik and David (1969) that "there is a good correlation between plasticity index and free swell, and almost no correlation between shrinkage limit and free swell" (16).

IV: Mineralogical Identification: A knowledge of the mineralogy of soils is very important in order to determine whether the soil is potentially expansive or not. It is claimed by the clay mineralogist that the swelling potential of any clay can be evaluated by identification of the constituent mineral of

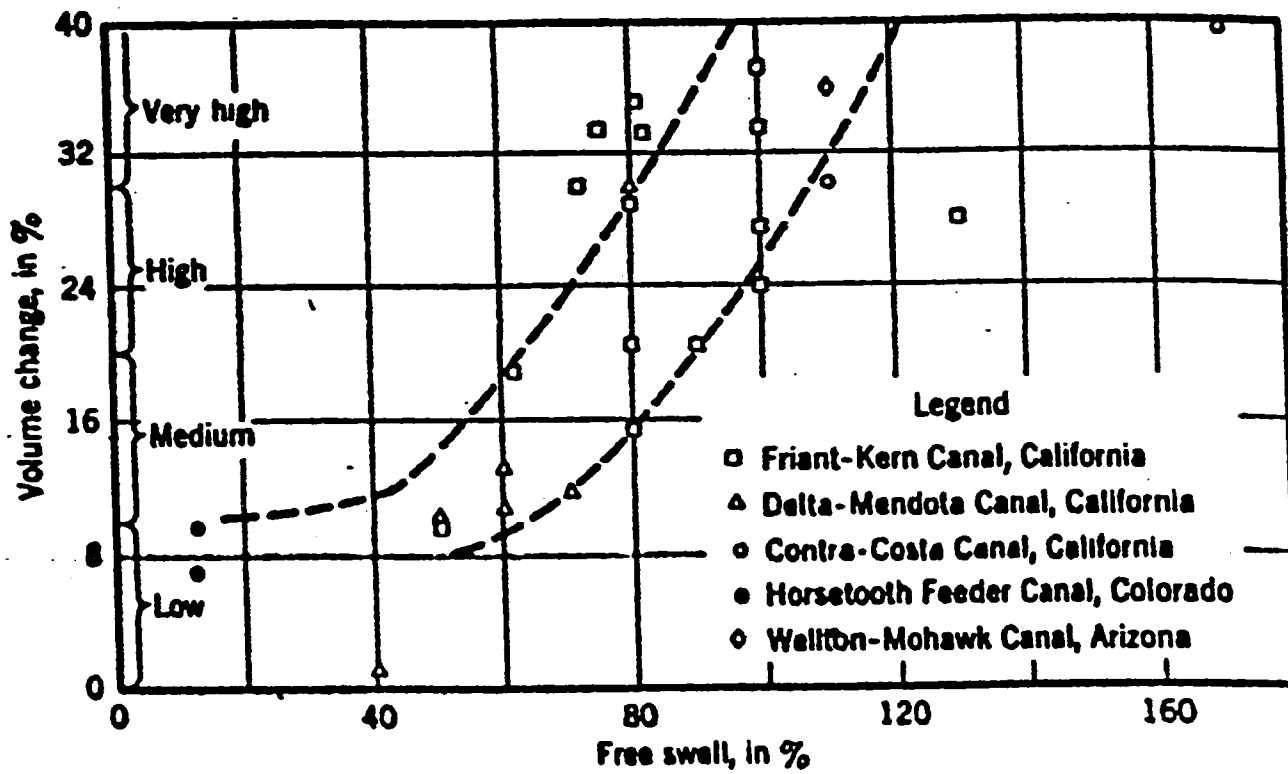


Figure (2.13), Free Swell Related to Volume Change (Air dry to Saturated condition under a load of 1 PSI)

this clay. The methods of mineralogical identification are important in a research laboratory, but are impractical and uneconomical for practicing engineers (13). The techniques which may be used for mineralogical identification are: x-ray diffraction, differential thermal analysis, microscopic examination, chemical analysis and dye adsorption.

1. X-Ray Diffraction (XRD): X-ray diffraction is the most widely used method for identification of fine grained soil minerals and the study of their crystal structure. This method consists of comparing the ratios of the intensities of diffraction lines from the different minerals with the intensities of lines from the standard substance (13).

X-rays are one of the several types of waves in the electromagnetic spectrum and have wave lengths in the range of 0.01 to 100 Å. Certain materials are able to absorb x-rays of different wave lengths so that it is possible to filter the output of an x-ray tube to give rays of only one wave length. Copper radiation, for example, which is the most frequently used type for clay mineral identification, has a wave length of 1.54 Å. When x-rays strike a crystal, they may penetrate to depth of several million layers before being absorbed. At each atomic plane a minute portion of the beam is absorbed by individual atoms that then oscillate as dipoles and radiate in all directions. Radiation in certain directions

will be in phase and can be interpreted in simplistic fashion as a wave resulting from a reflection of the incident beam. In-phase radiations emerge as a coherent beam and can be detected on film or by a radiation counting device. Figure 2.14 shows a parallel beam of x-rays of wave length striking a crystal at an angle θ to parallel atomic planes spaced at distance d . According to Bragg's law:

$$n \lambda = 2d \sin \theta$$

This law forms the basis for identification of crystals using x-ray diffraction. Since no two minerals have the same spacing interatomic planes in three dimensions the angles at which diffraction occurs are used for identification (34). Table 2.9 lists the most intense reflections for minerals commonly found in soils. Figure 2.16 shows x-ray camera patterns of illite, halloysite, kaolinite and montmorillonite, respectively. Figures B.1-B.22 in Appendix (B) show some X-ray diffraction charts.

Many of the methods used in quantitative analysis involve preparation of a calibration curve. Peak areas of intensities in the x-ray diffraction pattern of a known mixture are measured and plotted against the quantities of the respective substances in the mixtures of standard materials. Johns, Grim and Bradley (1954) suggested a

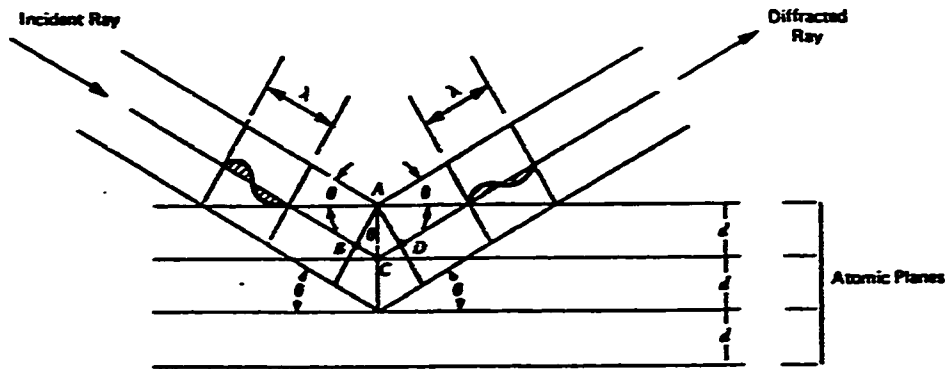


Fig.(2.14): Geometry of Diffraction Pattern according to Bragg's Law

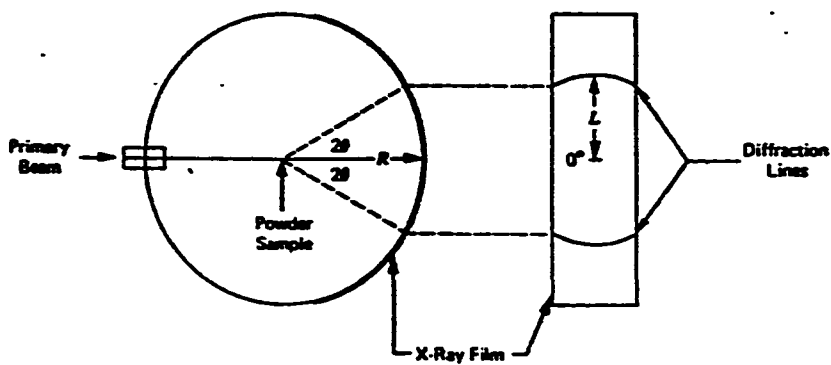


Fig.(2.15): Schematic Arrangement of an X-ray Diffractometer

Table 2.9: X-ray diffraction data for clay minerals and common non-clay minerals.

$d(\text{\AA})$	Mineral ^a	$d(\text{\AA})$	Mineral ^b
14	<i>Mont. (VS) Chl. Verm. (VS)</i>	2.93-3.00	Felds.
12	<i>Sepiolite, heated corrensitite</i>	2.89-2.90	Carb.
10	<i>Illite, Mica(S)</i>	2.86	Felds.
9.23	<i>Heated Verm.</i>	2.84	Carb. <i>Chl.</i>
7	<i>Kaol. (S); Chl.</i>	2.84-2.87	<i>Chl.</i>
6.90	<i>Chl.</i>	2.73	Carb.
6.44	Attapulgitite	2.61	Attapulgitite
6.39	Felds.	2.60	Verm., Sepiol.
4.90-5.00	10 \AA (2nd)	2.56	Illite (VS), Kaol.
4.70-4.79	<i>Chlor. (S)</i>	2.53-2.56	Chlor., Felds., Mont.
4.60	Sepiol., Verm. (S)	2.49	Kaol. (VS)
4.45-4.50	Illite (VS)	2.46	Quartz, heated Verm.
4.46	Kaol.	2.43-2.46	Chlorite
4.36	Kaol.	2.39	Verm., Illite
4.26	Quartz (S)	2.38	<i>Kaol.</i>
4.18	Kaol.	2.34	Kaol. (VS)
4.02-4.04	Felds.(S)	2.29	Kaol. (VS)
3.85-3.90	Felds.	2.28	Quartz, Sepiol.
3.82	Sepiol.	2.23	Illite, Chl.
3.78	Felds.	2.13	Quartz, Mica
3.67	Felds.	2.05-2.06	Kaol. (WK)
3.58	Carbonate, Chl.	1.99-2.00	<i>Mica, Illite(S), Kaol. Chl.</i>
3.57	<i>Kaol. (VS), Chl.</i>	1.90	Kaol.
3.54-3.56	Verm.	1.83	Carb.
3.50	Felds., Chlor.	1.82	Quartz
3.40	Carb.	1.79	Kaol.
3.34	Quartz (VS)	1.68	Quartz
3.32-3.35	<i>Illite (VS)</i>	1.66	Kaolin
3.30	Carb.	1.62	Kaolin
3.23	Attapulgitite	1.54B	Verm. (S), Quartz
3.21	Felds.	1.55	Quartz
3.20	Mica	1.58	Chl.
3.19	<i>Felds. (VS)</i>	1.53	Verm., Illite (Trioctahed)
3.05	Mont.	1.50	Ill. (S), Kaol.
3.04	Carb. (VS)	1.48-1.50	Kaol. (VS), Mont.
3.02	Felds.	1.45B	Kaol.
3.00	Heated Verm.	1.38	Quartz, Chl.
2.98	Mica (S)	1.31, 1.34, 1.36	Kaol. (B)

^a *Italics: (001) spacing.*

^b (B) = broad; (S) = strong; (VS) = very strong; (WK) = weak; Mont. = Montmorillonite; Chl. = Chlorite; Verm. = Vermiculite; Kaol. = Kaolinite; Carb. = Carbonate; Felds. = Feldspar; Sepiol. = Sepiolite.

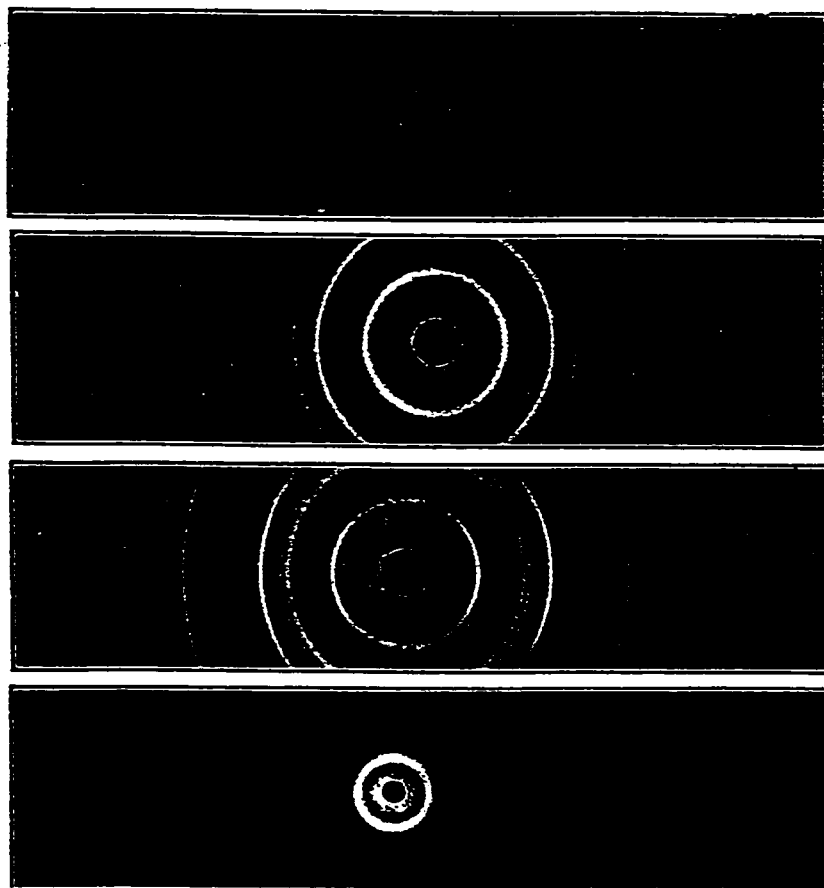


Fig. 2.16 X-ray diffraction patterns of some typical clay minerals. From top to bottom: illite, Yangtse River, China; halloysite, Lawrence County, Indiana; kaolinite, Langley, South Carolina; montmorillonite, Granby, Colorado. (USBR.)

method for quantitative estimation of clay minerals from the x-ray diffraction patterns of clay minerals. In this method, scattering from three-layer clay mineral at an angle corresponding to a 17 Å spacing was found to exceed, by a factor of approximately four, the reflected intensity of a similar material contributing to scattering at 10 Å. Thus the intensity for illite and montmorillonite cannot be compared directly. The efficiency with which a sheet-type silicate scatters along the (001) row line varies with $(\sin \theta)/\lambda$, according to a form factor function, and this renders quantitative comparisons of illite, chlorite and kaolite more difficult. However, within the range corresponding to $(\sin \theta) = 0.15$ to 0.16 or where $001 = 3.3$ to 3.5 Å, it is believed that the scattering distribution is sufficiently constant so that the 3.5 Å maximum for chlorite and kaolinite can be compared directly with the 3.3 Å reflection for illite with a peak, namely, chlorite, montmorillonite, and kaolinite (57). Table 2.10 gives a simplified x-ray analysis guide for clay minerals.

2. Differential Thermal Analysis (DTA): Differential thermal analysis when used in conjunction with x-ray diffraction and chemical analysis enables the identification of otherwise difficult materials (13). DTA also supplements the microscopic examination in identifying the finest fractions and

Table 2.10: Simplified X-ray analysis guide for clay minerals
"BASAL" (001) peak position*

Mineral	Air Dry	Glycerol treated	K ₊ -sat. & oven dried	HgCl ₂ Heated to 550 C
Kaolinite	7.2 Å	7.2 Å	7.2 Å	7.2 Å disappears
Halloysite (dehyd. form)	7.3 - 7.4 Å (broad)	7.4 Å (broad) or 10.6 Å	7.3 Å (broad)	7.3 - disappears 7.4 Å
Halloysite (hyd. form)	10 Å	10.6 Å	7.3 Å (broad)	10.0 Å disappears
Montmorillonite	11.15 Å (variable)	17.7 Å	10-12 Å	14-16 Å about 9.7 Å
Illite	10.2 Å	10.2 Å	10.2 Å	10.2 Å about 10 Å
Verniculite	12.5 Å or 14 Å	14.5 Å	10-11 Å	14 Å 10 Å (sometimes re-expands to 14 Å in air after heating)
Chlorite	14 Å	14 Å	14 Å	14 Å 13.6 - 14 Å (sometimes in- tensity reduced)

*Subject to some uncertainty depending on substitution in lattice, cation saturation, etc.

their relative abundance (26). In this method, both the sample and an inert substance are heated at a controlled rate (10 °C per minute) from room temperature to 1100 °C. The difference in temperature (ΔT) of the sample from that of the inert materials is measured as a function of either time (t) or temperature (T °C). Temperature changes in the sample occur as a result of exothermic or endothermic reactions caused by decomposition, phase change, solid phase interaction, crystallization, recrystallization, or dehydration. The temperature at which exothermic or endothermic peaks occur is used in the identification of soil minerals (38). The use of differential thermal analysis technique in identifying expansive soil is not always accurate (13). Figure 2.17 is a schematic diagram of apparatus for DTA.

3. Microscopic Examination: This technique permits direct observation of the material. Two clay may give the same x-ray pattern and the same DT curve but will show up distinct morphological characteristics under electron microscope resolution (13). This depends on the fact that all materials reflect light to different degrees and that they possess somewhat definite optical properties which can be observed precisely in polarized light. Certain stains make possible easy identification of many clay minerals. The main purpose of microscopic examination is to determine mineralogical

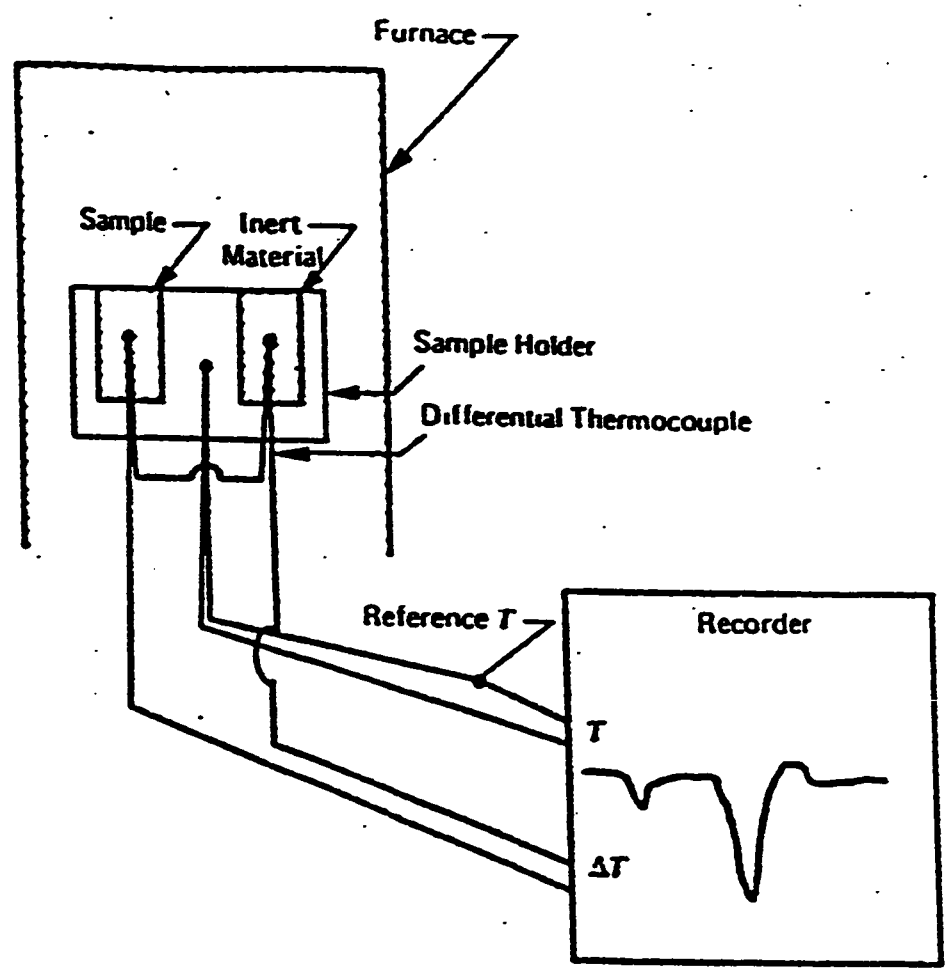


Fig. (2.17) Schematic diagram of apparatus for differential thermal analysis.

composition, texture, and internal structure (26).

The scanning electron microscope (SEM) represents a rather recent development. With this instrument, secondary electrons emitted from a sample surface form what appear to be three dimensional images. The SEM has a magnification range of x200 to x150,000 and a depth of field some 300 times greater than that of a light microscope (34).

Ravina (45) made extensive study of the mineralogical composition of expansive clays by the use of the SEM. It showed that the non-swelling clays appear as flat, relatively thick plates while montmorillonites have a crinkly, ridged, honey comb like texture. According to Ravina, it might be possible to evaluate, at least qualitatively, some properties of the clays using the degree of crinkling and interparticle bonding from scanning electron micrographs (45).

The study of soil fabric with the SEM requires an evacuated sample chamber, so we soils cannot be studied directly. The fluid which is an aqueous solution be removed from the specimen before placing it in the instrument. After drying the specimen, it is necessary to expose undisturbed surface for study by fracturing and/or peeling. It is also necessary to coat SEM sample surfaces with a conducting film to prevent surface charging and consequent loss of

resolution. Gold placed in a very thin layer (200 to 300Å) in a vacuum evaporator is often used (42). Figure 2.18 is a schematic diagram of scanning system of the SEM.

4. Chemical Analysis: Chemical analysis can be a valuable supplement to other methods such as x-ray analysis in identifying clays. In the smectite group of clay minerals, chemical analysis can be used to determine the nature of isomorphism and to show the origin and location of the change on the lattice. According to Kelley, the isomorphous character of the smectite group can probably be shown in no other way. The isomorphism involves three basic variations in the substitution: the substitution of Al for Si in tetrahedral positions in the lattice; the substitution of Fe for Al in the octahedral coordination, and the substitution of Mg for Al in the octahedral positions (13). The charge deficiency resulting from these substitutions is balanced by exchangeable cations that take up positions between the unit cell layers and on the surfaces of particles (34).

5. Dye adsorption:

Dye stuffs and other reagents which exhibit characteristic colors when absorbed by clay have been used to identify clay. When a clay sample has been pretreated with acid, the color assumed by the absorbed dye depends on the base exchange capacity of the various clay minerals

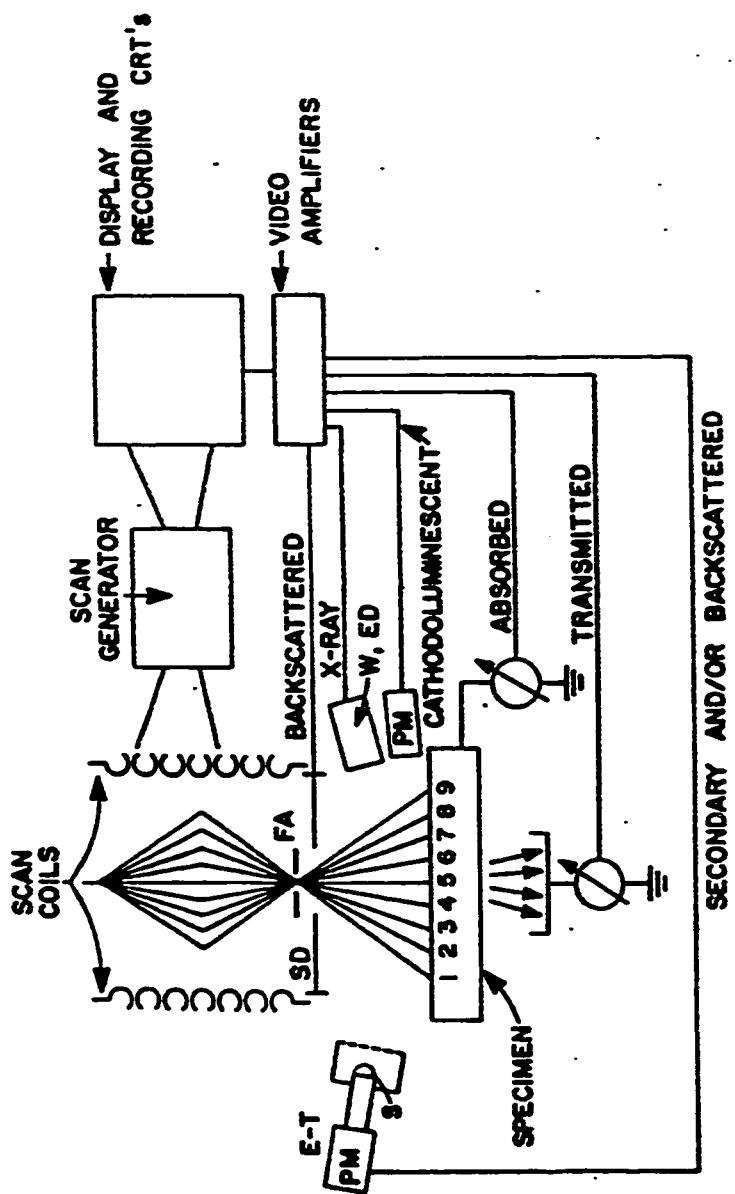


Fig. 2.18 : Schematic Illustration of Scanning System of the Scanning Electron Microscope.
 Abbreviations: FA, final aperture; SD, solid state electron detector; ET, Everhart-Thornley detector; S, scintillator; PM, photomultiplier; W, wavelength-dispersive x-ray spectrometer; ED, energy-dispersive x-ray spectrometer; CRT, cathode ray tube. Numbers 1-9 indicate successive beam positions during a scanning sequence.

present. The presence of montmorillonite can be detected if its amount is greater than about 5 to 10 percent. The relatively simple testing procedure and speed of dye staining tests compared with XRD and DTA justify wider application of the color method (13).

2.12 PROTECTIVE AND REMEDIAL MEASURES

If a soil is classified as a low swell potential, standard construction practices may be followed, However, if the soil possesses marginal or high swell potential, the following measures may be adopted:

1. *Replacement of Expansive Soil:*

If excessive swell is predicted, it may be possible to reduce the swell and arrive at a more economical foundation by removing the expansive soils lie close to the surface and replacing it with non expansive soils to a depth sufficient to provide loadings that will resist uplift (26). The pertinent requirements concerning soil replacement are the type of replacement material, the depth of replacement and the extent of the replacement (13).

Type of material:

The first requirement for the replacement soil is to be non expansive. All granular soils ranging from GW to SC in the

Unified Soil Classification System may fulfill the non expansive soil requirement (13). However, low-expansion clays are preferable to granular soils in this respect because granular soils are conducive to collecting water on the surface of expansive clays that were not excavated, either from the air or through surface seeps (39).

Depth of Replacement: The depth of selected fill should never be less than 36 inches and preferably 48 inches. The thickness of the emptied fill can be reduced if a combination of soil recompaction and soil replacement methods is used. The natural soil is scarified and recompacted for a thickness of about 2- feet, then another 2 feet of selected compacted fill placed. The combined thickness of 4-feet should be adequate to control heaving.

Extent of Replacement:

In an artificial fill situation, it is always possible for surface water to seep into the deep-seated expansive soil at the perimeter of the fill. Therefore, the larger the area of replacement, the more effective the fill.

Evaluation of Soil Replacement Measure:

Soil replacement is the best method to use in obtaining a stabilized foundation soil. Some evaluations of this method are (13):

1. The replaced nonexpansive soil can be compacted to a high degree of compaction enabling the material to support either heavily loaded slabs or footings.
2. The cost of this method is inexpensive.
3. Soil replacement provides the safest approach to slab-on-ground construction.

2. Changing the Nature of Expansive Soil:

Several means of achieving this are examined in the following, although it is difficult to assess numerically the effects of these procedures without making direct measurement on the altered clays.

Stabilization of Soil:

Chemical stabilization with the aid of lime and cement has often proved useful. A mix of about 5% lime is sufficient in most cases. Lime or cement and water are mixed with the top layer of soil and compacted. The addition of lime decreases the liquid limit, plasticity index and the swell potential of the soil (17). Lime-soil pozzolanic reaction takes place between the lime and the silicates or alumina constituents of clay to form cementing agents that provide a major increase in strength and hence retard swell forces (39). It may be possible to control expansions of montmorillonite clays by changing their exchangeable bases as, for example, changing a

sodium clay to a calcium clay.

Ponding:

Ponding is a technique to raise the water content of near-surface clays before foundations are constructed and, hence achieving most of the heave before construction. This method is time consuming and may not be effective for shallow foundation system in arid or semi arid areas (39). For a slab on ground construction, after completing ponding the ground surface must be kept moist until the slab is placed. A gravel or sand bed 4 to 6 inches thick should be placed over the subgrade prior to the ponding period. The gravel layer prevents the clay from drying and shrinkage (13).

Compaction:

Swelling of expansive soils decreases when the soil compacted to a lower density on the wet side of optimum water content. Compaction is used alone or in conjunction with replacement to control expansion and shrinkage of near surface soils. Compacted soil can be placed above moderately expansive clays to serve as a surcharge which will reduce expansion. Floor slabs and lightly loaded interior footings can then be placed on the fill. Where the total heave is expected to be > 34 mm, a slab-on-ground type of construction should not be encouraged (17, 39). The required depth of compaction depends upon the degree of expansion and the

magnitude of the imposed loads. Generally, 1 to 5 feet of compacted material will be adequate with the range of 2 to 3 feet being the most commonly used.

Installation of Moisture Barriers:

The long term effect of the differential heave can be reduced by controlling the moisture variation in the soil. This can be achieved by constructing moisture barriers around the perimeters of slab-on-grade to minimize moisture variation beneath the slab's perimeter. These moisture barriers may be constructed in trenches filled with gravel, lean concrete or impervious membranes (17). Both horizontal and vertical barriers have been used. Horizontal moisture barriers can be installed around the building in the form of membranes, rigid paving or flexible paving. The purpose of horizontal barriers is to prevent excessive intake of surface moisture. Vertical moisture barriers have been used around the perimeter of the building to cut off the source of water that may enter the underslab soils. Vertical barriers are about 1.5 m. deep by 15 cm. wide, and they are more effective than horizontal barriers in minimizing seasonal drying and shrinkage of the perimeter foundation soils, as well as maintaining long term uniform moisture conditions beneath the covered area (13).

3. Control the Direction of Expansion:

This can be achieved by allowing the soil to expand into

cavities built in the foundation, the foundation movements may be reduced to tolerable amounts. A common practice is to build "waffle" slabs so that the ribs hold the structure, the waffle voids allow soil expansion. It may be possible to build foundation walls to some depth into the ground using tiles placed such that the soil can expand laterally into the tile cavity (40).

4. Bypassing of Expansive Soil:

Generally, when total heave exceeds 8 cm., slab-on-grade foundations are not economical. In such condition expansive clays can be bypassed by using drilled piers to support structural loads. The drilled pier is installed such that an enlarged base is constructed in stable soil below the active zone. The base which should have a diameter at least 0.5 m. greater than the shaft, acts as an anchor against upward direct shear stresses generated on the shaft due to expansion of clays in the active zone (39). Drilled piers, when made with an enlarged base, are referred to as belled piers and when made without an enlarged base are referred to as a straight-shaft piers. The principle of drilled piers is to provide a relatively inexpensive way of transferring the structural loads down to stable material or to a stable zone where moisture changes are improbable. There should be no direct contact between the soil and the structure with the exception of the soils supporting the piers (13). The pier or pile shaft should be as small as possible to avoid high tension stress due to expansion

pressure and adhesion. Sometimes the pier shaft is surrounded by straw or other porous material to reduce adhesion (5).

5. Loading the Soil:

This method is used in many fills where the fill weight balances the swell pressure. This can also be used beneath buildings, either by using spread footings of high pressure intensity or excavating several feet of the clay and backfilling with granular backfill. This method may not be practical for one-story commercial buildings and residences because of small soil pressure developed (5).

6. Drainage Control:

Proper methods to drain water away from the outer wall of a building by suitable slopes and other drainage systems is useful in order to decrease the swelling of the soil (59).

7. Strengthening the Walls: The walls of some houses constructed on expansive soils were strengthened by continuous belts of reinforced concrete at the lintel, the windowsill, and the strip foundation levels. The rooms were made somewhat smaller. Some floors were found to have heaved up to 3 in. at their centers, but no cracks whatsoever developed in the reinforced walls. Therefore, provision of reinforcing belts in the walls of houses constructed on expansive soils is always advisable (59).

8. The provision of air ventilation channels under floors permits normal evaporation from beneath a building and hence inhibits swelling at its center. This method has been successfully tried in some instances (59).

Chapter 3

METEOROLOGY AND GEOLOGY OF THE STUDY AREA

3.1 LOCATION

This study is concentrated on the Eastern Province of Saudi Arabia. Eastern Province is located on the west coast of the Arabian Gulf and runs about 200 Km parallel to the coast. It is bounded on the north by latitude $26^{\circ} 50'$ N, on the east by longitude $50^{\circ} 10'$ E, on the south by latitude $25^{\circ} 22'$ N and on the west by $49^{\circ} 30'$ E, figure 3.1.

However, since the area is very large, certain locations based on extensive preinvestigation study were selected for detailed investigation. These locations are: Al-Qatif area, Al-Jesh, Umm Al-Hammam and Al-Aujam (lat. $26^{\circ} 33'$ N, long. $50^{\circ} 01'$ E), Umm Al-Sahek (lat. $26^{\circ} 38'$ N, Long. $49^{\circ} 54'$ E), and Al-Mobarraz and Al-Hofuf (lat. $25^{\circ} 22'$ N, long. $49^{\circ} 50'$) in Al-Hasa area.

3.2 CLIMATE

Local climatic conditions are major factors that affect the distribution of expansive soils (18). Moreover, they greatly affect the extent to which potentially expansive clays undergo volume

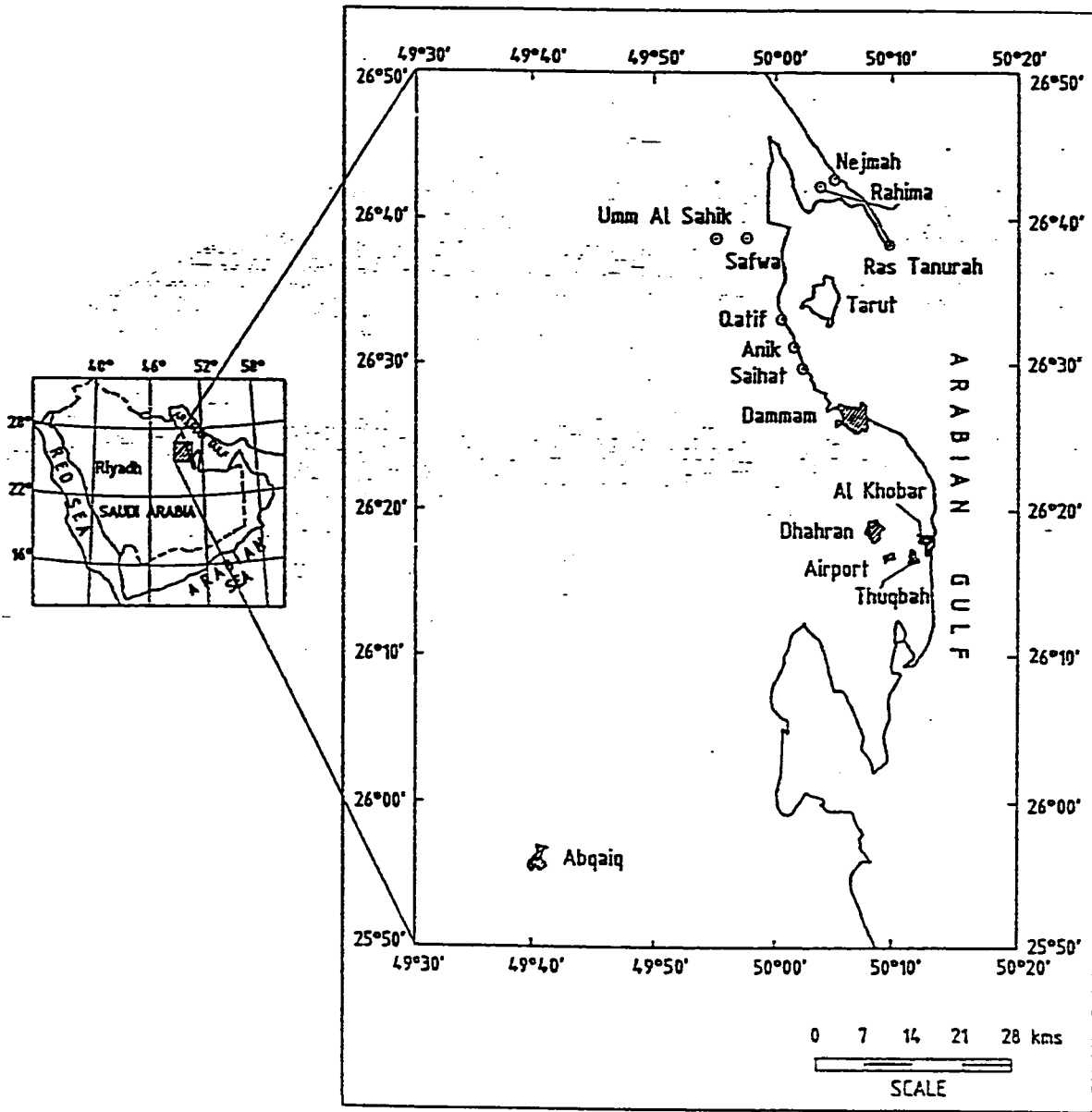


Figure 3.1 Location Map of the Study Area

change. Locations prone to long dry periods followed by periods of wet weather are most susceptible to expansive clay activity. In areas where shallow water tables do not exist, moisture conditions in the clays are controlled by moisture balance between rainfall and evaporation. One rational means of classifying climate is the Thornthwaite Moisture Index (TMI), which is defined as the difference in mean annual rainfall in inches and the amount of water in inches that would be returned to the atmosphere by evaporation from the ground surface and transpired by plants if there were an unlimited supply of water to the plants and soil. A positive TMI value indicates a net soil moisture deficit. Locations having TMI values between about +20 and -20 are most prone to experiencing difficulty with expansive clays (39). The overall climate of the Arabian Peninsula falls within Thornthwaite's "arid province" (3).

3.2.1 Temperature:

Mean monthly temperature in the shade along the Arabian Gulf range from 30.6 °C to 36.8 °C during summer months. However, in winter they range from 11 °C to 22.2 °C (1), table 3.1. The Arabian Gulf itself is the warmest sea in the world averaging 20 °C at the surface in February and 34 °C in August (7).

Table 3.1: Average mean monthly temperatures in degrees centigrades calculated over the years 1966 - 1974

Station	Jan	Feb	Mar	Apr	May	Jun	Jul	Aug	Sep	Oct	Nov	Dec
Dhahran	14	15.8	20.1	24.6	30.4	33.3	34.4	34	30.9	27.2	21.3	14.8
Abqaiq ¹	15.8	17.2	21.8	26.3	32	35.3	36.8	36.8	34.7	28.7	22.6	17.2
Dhahran ²	15.8	17	20.8	25.7	31.3	34.5	36	35.7	33.2	29	23.4	17.8
Ras Tannurah ³	16	16.5	20.3	23.6	28.6	32	33.4	33.3	30.9	27.7	22.9	17.3

1 Information from ARAMCO data from 1950 to 1970.

2 Information from ARAMCO data from 1935 to 1974.

3 Information from ARAMCO data from 1963 to 1972.

3.2.2 Precipitation:

The rainfall in the Eastern Province is scanty and sporadic. It may happen that rain falls on a certain area while it remains dry in a very close area. It is also usual for the region to go for several successive months without any rain. The annual precipitation at one area may show great differences from year to year. Dhahran, for example, has average rainfall of 72.4 mm between 1935-1974, but registered 186.9 mm in 1974 and 5.3 mm in 1946, table 3.2. Average annual rainfall at Ras Tanurah is 88 mm and at Abqiq, it is 84 mm (3). Due to rainfall variability, the value of the average annual precipitation is doubtful unless data over a considerable number of years are collected.

3.2.3 Relative Humidities:

Relative humidity is also extremely variable from place to place and from year to year. High relative humidity of 37 to 63% during summer is observed along the coast of the Eastern Province. Inland area is also characterized by high relative humidities ranging from 35 to 78% during winter and low from 13 to 47% during summer (3), table 3.3 . Climatological studies in the year 1971 at Dhahran metrological station has shown that evaporation exceeds the precipitation. A maximum monthly evaporation was 691 mm in July and a minimum of 144 mm was found in January (44).

Table(3.2), Average mean monthly and annual precipitations 1966 - 1974 in millemeters.

Station	Jan	Feb	Mar	Apr	May	Jun	Jul	Aug	Sep	Oct	Nov	Dec	Average Annual
Dhahran	10	8.3	21.6	3.1	0.6	0	0	0	0	<0.05	0.4	26.1	75.1
Abqaiq ¹	13.2	24.4	4.3	15.2	1.8	0	0	0	0	0	4.6	8.9	72.9
Dhahran ²	15.5	10.9	10.7	8.9	1.8	0	0	0	0	0	9.1	14.5	71.4
Ras Tannurah ³	23.6	13.2	9.7	10.7	3	0	0	0	0	0.5	7.9	18.8	88.1

1 Information from ARAMCO data from 1960 to 1969.

2 Information from ARAMCO data from 1935 to 1974.

3 Information from ARAMCO data from 1945 to 1974.

Table (3.3), Average mean monthly relative humidities calculated over the years 1966 - 1974.

Station	Jan	Feb	Mar	Apr	May	Jun	Jul	Aug	Sep	Oct	Nov	Dec
Dhahran	77	72	66	57	43	37	40	54	58	68	66	72
Abgaig ¹	57.6	54.4	49.5	46.3	39.5	28.4	29.5	35.1	42.6	48.7	54.5	56.7
Dhahran ²	67.5	64.6	59.7	55.3	47.6	41.3	43.9	50.2	53.4	58.2	62.7	66.8
Ras Tannurah ³	73.3	71.3	69.7	67.2	64	59.8	58.8	62.9	66.4	69.7	73	71.9

¹ Information from ARAMCO data from 1950 to 1970.

² Information from ARAMCO data from 1935 to 1974.

³ Information from ARAMCO data from 1963 to 1972.

3.3 HISTORY OF THE ARABIAN GULF

The sequence of major palaeogeographic events in the formation of the area can be summarized as follows (2):

1. In the Late Pleistocene (about 400,000 Y.B.P.), the Arabian Gulf water stood at a level of 150 meter higher than its present mean.
2. In the Latest Pleistocene (about 100,000 Y.B.P.), glaciation led to a worldwide lowering of the sea level, which caused the Arabian Gulf water to drop down to a level 120 m below its present-day mean. As a result, the Arabian Gulf basin dried up completely. This phase reached its climax at about 20,000 Y.B.P.
3. The following phase was the gradual rising of sea level and the re-infilling of the Arabian Gulf basin with water from the Indian Ocean during the post-glacial transgression. (Latest Pleistocene-earliest Holocene), between 20,000 and about 7,000 Y.B.P.
4. In the early and middle Holocene (7,000-4,000 Y.B.P.), the water level was slightly higher than today. The early middle Holocene transgression began about 7,000 Y.B.P., and continued until about 4,000 Y.B.P., when the sea level reached the position of a new, free-lying

strand bank, with minor oscillations to the present-day mean level.

5. The sea level was still oscillating between 4,000 - 1,000 Y.B.P. in minor transgressions and regressions that left their marks in the form of abraded, raised terraces (2 to 3 meters above sea level) in many coastal areas. These oscillations were accompanied by a relatively quick fall in the sea level of about 1 meter at about 3750 Y.B.P. and another drop of about 0.6 meter to the present-day level between 37,500 and 1,000 Y.B.P.
6. If this information is applied to the whole Gulf area, the water level up to 3,750 Y.B.P. would have been between 2.7 to 2.9 meters above the present day level.

According to Bush, approximately 7,000 Y.B.P., the Gulf waters transgressed over the site of the present plain, which at that time was covered by sub-aerial dunes composed of quartzose carbonate sand. The extent of this transgression varied from place to place. In the area of the southwest of Abu Dhabi Island, the maximum transgression reached a point between 5 and 6 km landward of the present low water mark approximately 4,000 Y.B.P., and a beach ridge developed at the margin of the lagoon so formed. Landward of the ridge, the dunes deflated to the level of the water table, as their source of sediment had been

submerged beneath the waters of the lagoon.

Seawards of the beach ridge, the original aeolian, quartzose carbonate sand was reworked during transgression, and then gradually buried under newly formed skeletal carbonate sand which contained considerable amounts of re-worked aeolian sand in its lower parts. It was finally covered with grey, muddy carbonate sand as the lagoonal environment became established. Deposition continued until the lagoon became very shallow and further accumulation of sediment was prevented by the action of waves and currents.

A lithified crust, cemented with high magnesium calcite, formed on the surface of the sediments in the area of non deposition (a similar crust is found on the lagoon floor at the present time). Sediments were transported by waves and currents to be deposited at the margins of the lagoons to form intertidal flats. This resulted in the lateral filling of the lagoon and the progradation of the coastline.

An apparent fall of sea level by approximately 1 m occurred between 4,000 Y.B.P. and 3,750 Y.B.P. This resulted in some of the sediments of the inner lagoon becoming intertidal instead of subtidal. The new inter tidal area was colonized by an algal mat. At first, the algal mat grew out over the lithified crust, but later it continued to grow over the sediments pushed to

the margins of the lagoons by the waves and currents. At this algal mat grew seawards it was slowly covered by sediments carried into its surface by winds and the occasional storms. About 1,000 Y.B.P., this algal mat ceased to grow and was buried by intertidal sediments but the plain continued to prograde seaward and finally a new algal mat developed and has continued to grow until the present day.

3.4 GEOLOGY OF THE PROVINCE

The Arabian Peninsula consists of two geological structural provinces, the Arabian Shield in the West and the Arabian Shelf in the East, fig. 3.2 . The Arabian Shelf forms about two thirds of the peninsula and comprises a sedimentary succession of Cambrian to Pliocene. These dip gently away from the Shield East, Southwest, Northeast and into a number of deep sedimentary basins reflecting the buried basement configuration (3, 8).

The Arabian Shelf can be divided into three zones (3):

1. An Interior Homocline boarding the shield.
2. An Interior Platform marginal to the Homocline. Sedimentary rocks in this region increase in thickness gradually eastward and may exceed 10,000 meters beneath the Arabian Gulf, and,

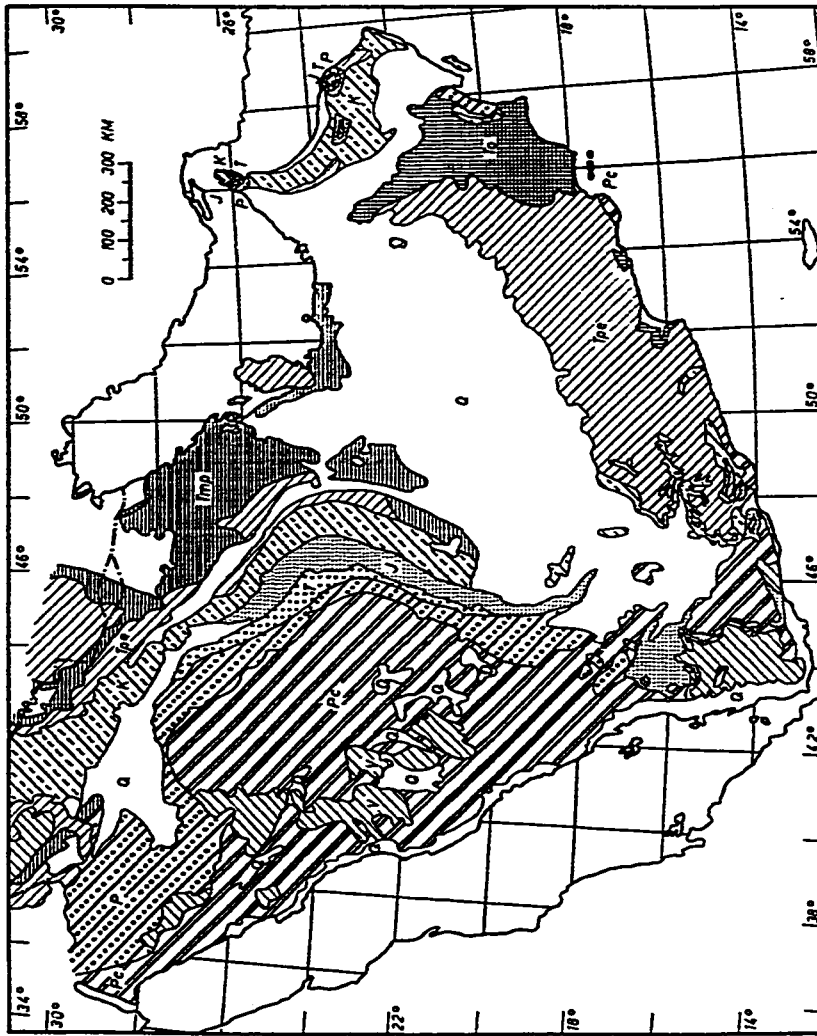


Figure (3.2) Generalized geologic map of the Arabian Peninsula

- Q EOLIAN SAND AND GRAVEL, MAINLY QUATERNARY
- V VOLCANIC ROCKS, MAINLY TERTIARY AND QUATERNARY
- Imp MIOCENE AND PLIOCENE
- O OLIGOCENE
- Ep PALEOCENE AND EOCENE
- C CRETACEOUS
- J JURASSIC
- T TRIASSIC
- P PALEOZOIC
- Pc PRECAMBRIAN BASEMENT

3. Several basins, adjacent to platform.

3.4.1 Geomorphology:

The Arabian Gulf region is a part from a rectangular depression known as Mesopotamia. The elevation of this region rises gradually inland at a rate of about one meter per kilometer (3). Sabkhas are very common in the Eastern Province and mainly close to and along shoreline. Large dunes and a wide belt of drifting sand spread from Al-Jubail and southward to Al-Hofuf. Apart from sabkhas and sand areas there are barren rock terrain developed on Eocene, Miocene and Pliocene limestones (3).

Furthermore, a marine deposit, known as the Bahr Formation and consisting of calcarenite and quartz sand interbedded with dune sand, forms low cliffs along much of the shoreline. The elevation of this formation varies between sea level and 150 meters above sea level. The Arabian Gulf coastal region west of Al-Hofuf is bounded by a prominent east-facing escarpment ranges in elevation of its base from about 150 meters to about 200 meters (3).

3.4.2 Topography

The area rises gradually from the coast of the Arabian Gulf to the edge of As-Summman Plateau where the elevation is about 300 meters. Near Al-Hofuf a steep-sided erosional butts or

jabals several tens of meters above the low lands can be seen (3), fig.3.3.

3.4.3 Stratigraphy

The eastern province of Saudi Arabia consists of several surface formations. The stratigraphic sequence of formations ranges from Paleogene to Quaternary and Recent (44). Surface Geology of the Eastern Province is shown in fig. 3.4. The Eastern Province included the following formations: Umm er Radhuma, Rus, Dammam, Hadrukh, Dam and Hofuf. (Fig. 3.5).

1. Umm er Radhuma Formation:

The rocks of the upper part of Umm er Radhuma Formation are considered to be the oldest ones in the Eastern Province of Saudi Arabia. The formation has been dated as Paleocene to Early Eocene (3). The name Umm er Radhuma came from the Umm Radmah well (lat. 28° 41' N, long. 44° 41' E) which produce water from the upper part of this formation (58). This formation is exposed only in small outcrop about a kilometer north of Dhahran (3), and it is 243.1 meters thick (58). The formation overlies the Aruma Formation and can be divided into an upper and lower units.

The upper unit consists of light gray and tan, partially dolomitized chalky limestone, with few poorly preserved fossils and

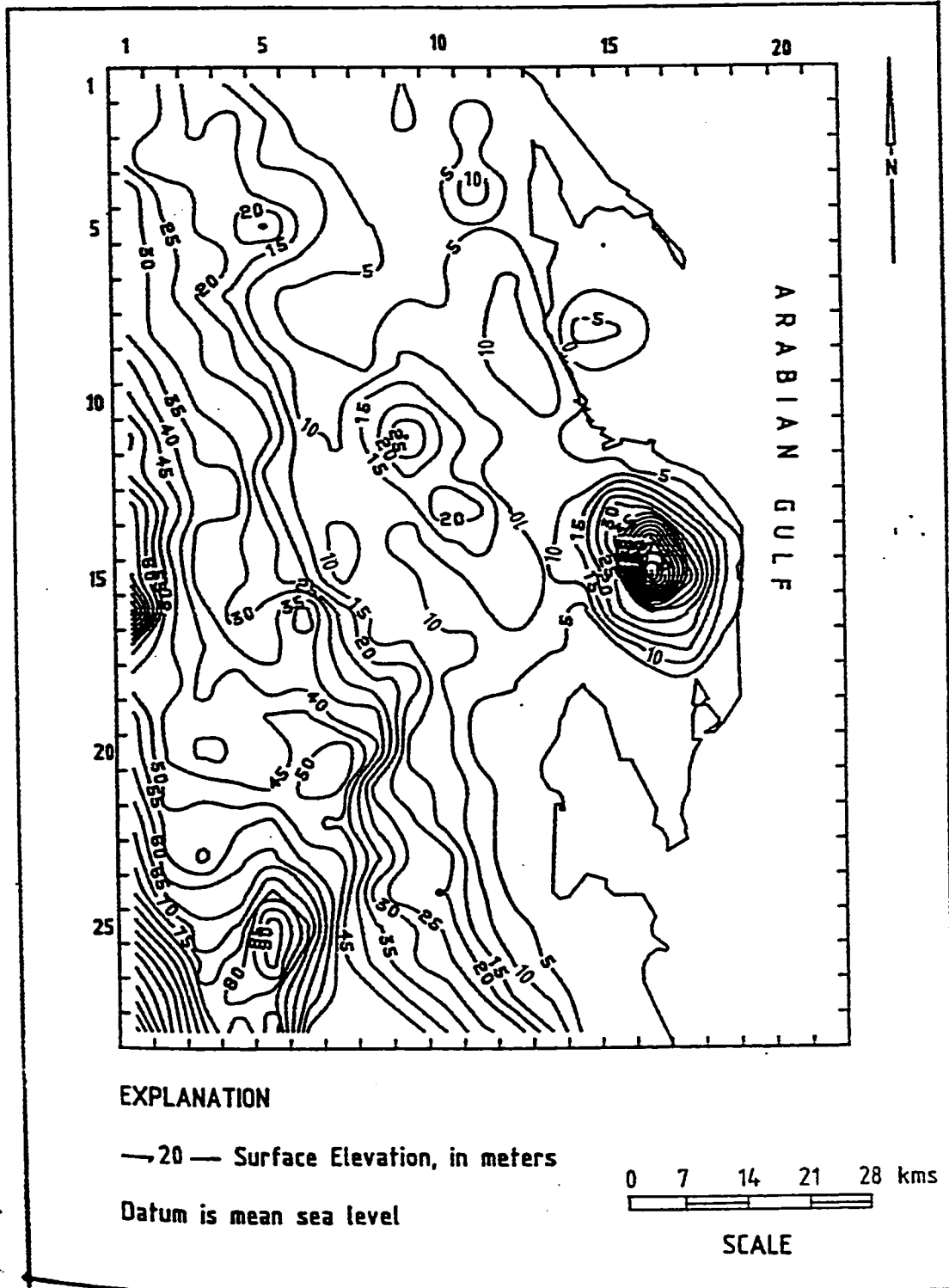
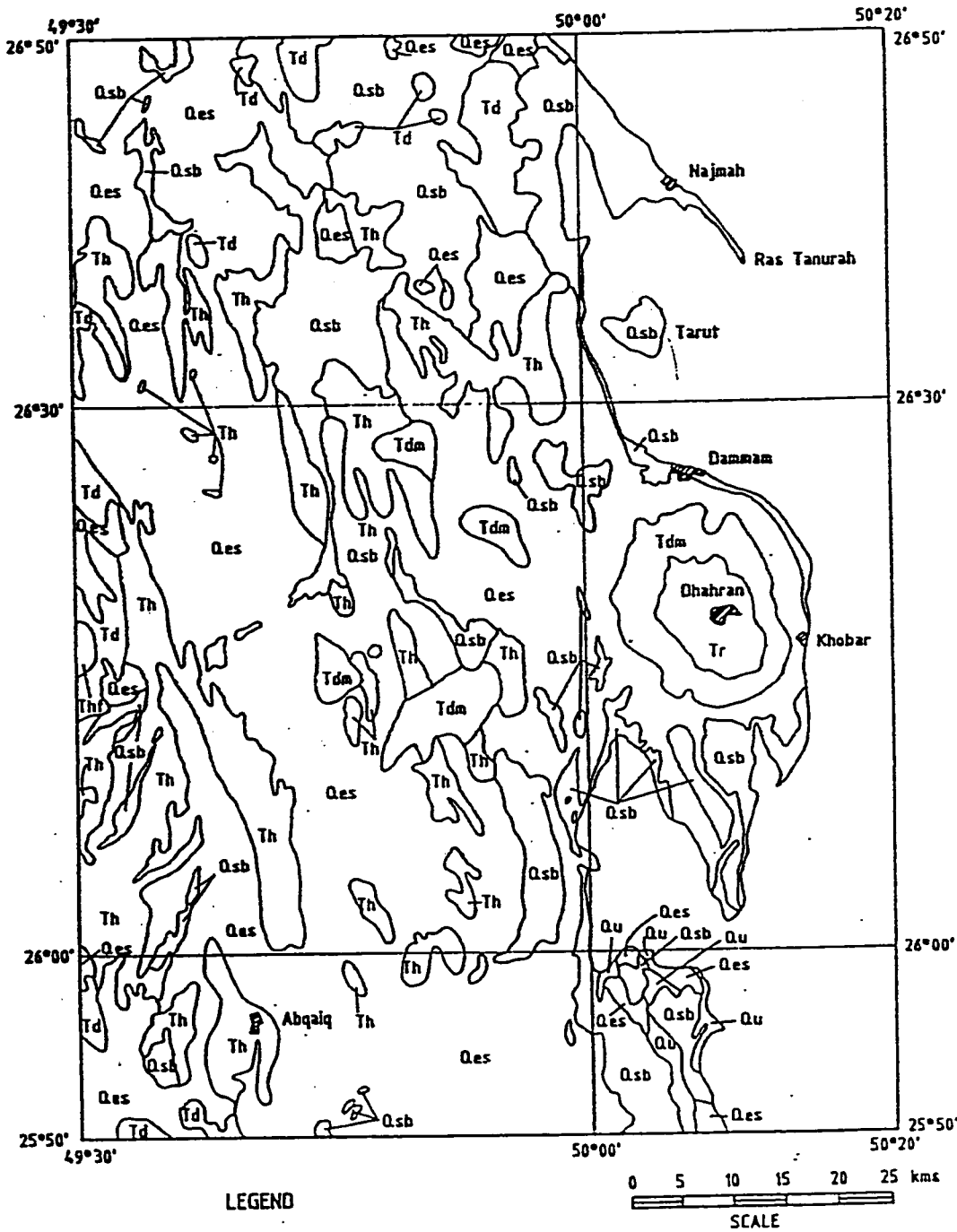


Figure (3.3), Topographic Map of the Study Area



Qes	Eolian sand	Td	Dam Formation
Qsb	Sabkha deposits	Th	Hadruk Formation
Qu	Quaternary deposits	Tdm	Dammam Formation
Thf	Hofuf Formation	Tr	Rus Formation

Figure (3.4), Geological Map of the Study Area (after Ministry of Petroleum and Mineral Resources, GM 208 A)

123

AGE	FORMATION	MEMBER	ROCK UNIT	GENERALIZED LITHOLOGIC DESCRIPTION	THICKNESS (m)	HYDROGEOLOGIC UNIT	
QUATERNARY	SURFICIAL DEPOSITS			Gravel, Sand and silt	3-30	Variable Productivity depending on recharge	
		Hufuf		Sandy marl and sandy limestone	0-95	Neogene Aquifer (LIMITED PRODUCTIVITY)	
		Dam		Sandy marls, silty clays and skeletal limestones	0-100		
Hadruk		Silty marls and shales, sandy limestones	0-90				
Tertiary	Damman	Alat	Limestone	Skeletal Detrital Limestones	0-110	Aquifer	
			Marl	Dolomitic marls with limestone intercalations (orange color)	0-35	Aquitard	
		Khobar		Skeletal, detrital, porous and friable limestones, dolomitic limestones	0-75	Aquifer	
				Limestones interbedded with shales and marls	0-20	Aquitard	
		Midra and Saifa shales		Blue and dark grey, fissile shales with gypsiferous lenses	0-20		
				Chalky limestones; anhydrite, dolomitic limestones & shales	20-110		
		Paleocene	Umm Al-Radhum		Partially dolomitized chalky limestones, detrital, skeletal limestone	average 320	Aquifer
					Varicolored limestone, subordinate dolomite and shale		Poor Aquifer
		Cretaceous	Aruma				

Figure (3.5). Generalized Litho-stratigraphic Sequence of the Study Area (after Italconsult, 1969).

thin interbeddings of gray and yellow finely crystalline dolomite (44). Tleel (3) believes that the rocks were originally slightly pelletal aphanitic limestones deposited in a shallow sea and later dolomitized. The association of gypsum and halite with palygorskite in the Umm er Radhuma shale suggests that palygorskite formed in a closed basin environment (49). The lower unit is essentially formed of fine grain, hard, compact, detrital, skeletal and at places, silicified limestone. Umm er Radhuma Formation is bounded at the bottom by the varicolored shales of the Aruma Formation and at the top by the soft chalky limestone of the Rus Formation (44).

II. Rus Formation:

The Rus Formation was first introduced by Bramkamp (1934) in an unpublished report for ARAMCO (4). The formation is exposed in the central portion of Dammam Dome, where the type section occurs on Jabal Umm Ar Ru'us (3) (lat. $26^{\circ} 19' 4''$ N, long. $50^{\circ} 6' 51''$ E) (58). The formation can be divided into three lithologic units (44, 58).

The Upper Rus: Consists of 3-4 meters of white, soft chalky, friable, porous limestone with several thin beds of colcarenite at top.

The Middle Rus: Consists of evaporite and shallow marine deposits, represented by soft, friable, cream, buff to pink chalky

limestones and gypsum lenses, geoidal quartz is present at several levels (31.8 m).

The Lower Rus: Consists of gray to buff, compact, commonly partially dolomitized limestone, with minor-beds of soft limestones that are porous as a result of leaching of small organic remains. Quartz geodes are rare in the lower part but are typical of uppermost beds (68.9 m).

The Rus Formation is presumed to fall entirely in the lower to middle Eocene (Ypresian to Lutetian), and it can be divided into two members (4). The first is the Dhahran Dolomite Member (Late Ypresian) and second is the Aqrabiyah Chalk Member (Early Lutetian). Tleel believes the depositional environment was similar to that of coastal sabkhas with occasional shallow marine transgression. Later dolomitization has destroyed much of the original texture (58). According to Cagatay Rus Formation deposited under marine conditions, more specifically under a shallow, oscillating sea level. The relative abundance of palygorskite and smectite (2-um fraction of Rus Formation) is 40-60% and 10%, respectively (9).

III. Damman Formation:

The Damman Formation was named for Damman Dome where the sequence crops out (58). The type section of Damman Formation is located in the Damman Dome along Dhahran - Al-Alat

Road, at the point where this road intersects the rim rock (lat. $26^{\circ} 19' 16''$ N, long. $50^{\circ} 4' 50''$ E) (4). Damman Formation consists mainly of carbonate rocks (limestones and dolomites), with some marly and shaly clays at its lower part. The formation lies conformably over the Rus Formation. It is bounded by the Early Lutetian Aqrabiyah Chalky limestones of the Rus at the bottom of Eocene Neogen unconformity at the top (44). The Damman Formation is considered to be of Lutetian age on the basis of both its stratigraphic position and fossil content (4). The Damman Formation has been subdivided into the following five members (3,4,44 & 58):

Midra Shale Member: Consists of 3 meters of yellowish brown, fissile, very thinly laminated shale, gray marl, or soft, impure limestone. The marly unit contains discontinuous, shaly, clayey and calcareous intercalations near its base and phosphatic clay balls as well as well-developed gypsum bands near its top. The carbonate content of the unit ranges between 45 and 60%.

Saila Shale Member: At its type locality, the Saila Member consists of 3.7 meters of dark brownish-yellow gray to off-white, impure fossiliferous calcarenitic limestone. Several beds of very pale orange, soft argillaceous limestone commonly present in the upper part of the unit. According to Cagatay (9) palygorskite averages about 60 and 40% in the clay fraction of the Midra and Saila shales, respectively. Fig. 3.6.

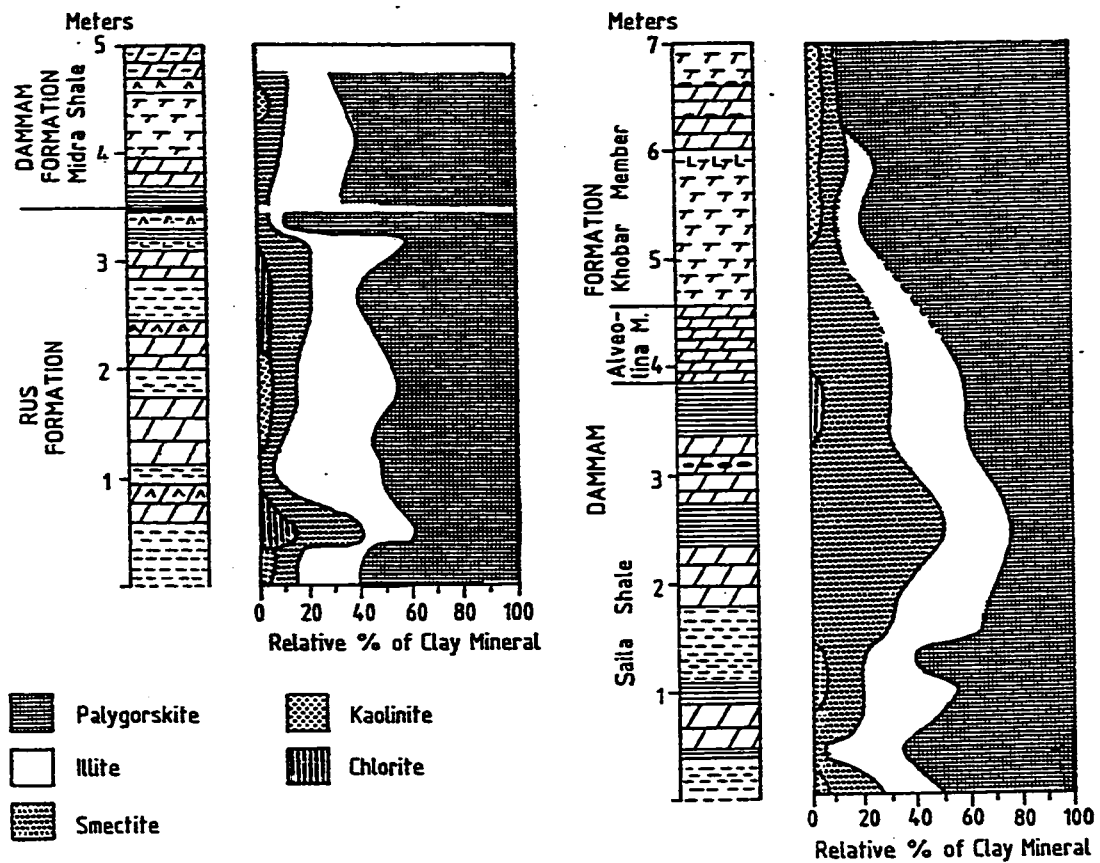


Fig. 3.6: Distribution of the relative amount of clay minerals in the Rus and Dammam formations. Carbonate-free material.

Alveoline Limestone Member: This member lies over the Midra and Saila Shales and is bounded at the bottom by blue shales of the Saila unit and at the top by white argillaceous limestones of the Khobar Member. This member consists of 1 meter of yellowish gray, microcrystalline, partially recrystallized, domomitized or rarely silicified limestone.

Khobar Member: The lower unit of the member is known as the Khobar Marl and the upper unit is known as the Khobar Dolomite. The Khobar Marl consists of 1.5 meters of light gray to tan dolomitic marl. The Khobar Dolomite (originally called Khobar Dolomite and Limestone) consists of 4 meters of off-white, partially recrystallized tight, nummulitic limestone, overlain by 1 meter of yellowish-brown, soft, marly limestone, above which is 3 meters of light brown, hard, partially recrystallized, massive, nummulitic limestone. Cagatay (9) reported that the abundance of palygorskite in the $< 2\text{-}\mu\text{m}$ fraction is high in the marls of Khobar Member.

Alat Member: Lithologically this member can also be divided into two units. The lower called Alat Marl consists of 6 meters of light colored dolomitic marl, locally argillaceous. The upper unit called Alat Limestone consists of 9 meters of slightly dolomitized, chalky, porous, cream or gray limestones.

The Dammam Formation was laid down in a turbid, open

marine environment in which shales were deposited. The sea must have clearing to permit the deposition of limestone at the base of the Saila Member (58). The pyrite in the Midra Shale Member suggests a restricted rather than open-marine environment during Midra time (3). Cagatay believes that Damman Formation was deposited under a shallow, oscillating sea level. Moreover, gypsum layers at several horizons throughout the succession suggests that the conditions were frequently hypersaline. The presence of palygorskite, along with smectite and chlorite, suggest a hot (arid to semiarid) climate with some rainy intervals (9). According to Shadfan, et al, the association of gypsum and other salts with palygorskite formed in closed-basin environments. The presence of mica and orthoclase suggests a detrital origin for these materials, probably from the igneous and metamorphic rocks of the Arabian Shield (49).

IV. Hadruk Formation:

Hadruk Formation unconformably overlies the Damman Formation (44). The Formation extends along the Gulf coast from the northern border of Saudi Arabia as far south at lat. $26^{\circ} 30' N$, and is scattered patches beyond Abqiq to about $25^{\circ} 52' N$.

The Formation is mainly non-marine, but a small area extending perhaps 60 kilometers from Al-Qatif Al-Alah has marine layers near the top of the formation (3). The formation consists of slightly silty, greenish gray fissile marls and shales and a chalky, slightly

sandy whitish limestones with lenses of gypsum and abundant chert (3,44).

V. Dam Formation:

The lower part of the Dam Formation was measured at Jabal al Lidam (lat. $26^{\circ} 21' 42''$ N, long $49^{\circ} 27' 42''$ E). The upper part of the 89.8 meters sequence was measured at Al-Umayghir (lat. $26^{\circ} 17' 15''$ N, long $49^{\circ} 30' 24''$ E.) At its type locality at Jabal Al Lidam the Dam consists mainly of pink, white and gray marl, and red, green and olive clay with minor interbeds of sandstones, chalky limestone and coquina (58). At the Damman Dome, the Dam rests unconformably on the Rus or Damman Formation at five localities. The Dam consists of an algalcoralline-molluscan reef complex in the middle of the dome but grade into molluscan-rich calcarenites and calcirudites with subordinate stromatolites and argillaceous limestones on the western flank. Powers et al (1966) presume the age of the Dam to be about Middle Miocene based on faunal evidence. Tleel believes that a Middle Miocene marine transgression covered the Damman Dome area to produce tidal flat, sheltered lagoon, and pinnacle reef environments. He reported that the transgression was gradual at first producing a tidal flat environment around the dome on which stromatolites grew (3, 58). Irtem (28) believes that the lithologic characteristic and faunal content of the oolitic grain stones indicate that these strata were deposited in a shallow subtidal to low

intertidal environment. Moreover, in the lower part of the upward deepening cycles green, buff to gray, unfossiliferous claystones and gypsiferous claystones suggest a supratidal environment. Finally, he believes that the isopachous equant calcite cementation forming a thin coating around the grains probably formed after deposition of these sediments, either during their subaerial exposure or during later burial stages (28). At Jabal Midra Al-Janubi and Jabal Midra Al-Shamali, the Dam rests on a thin 1 meter Midra shale above the Rus Formation.

VI. Hofuf Formation:

The Hofuf Formation covers large areas to the west of the Hasa oases. The formation which is the late Miocene or Early Pliocene is quite heterogeneous and consists of calcareous sand stone, variegated shale, marl and sandy clay (38) At the top locality the thickness of the formation is about 95 meters, and consists of limestones, quartz sand matrix red sandy marl, sandy limestone, light gray argillaceous sand stone (3).

VII. Quaternary and Recent:

Quaternary deposits in the area consists of recent marine terraces, raised beaches sabkhas and eolian sand (44).

Marine terraces and raised beaches are in the form of low terraces or mesas covered by sand, shells, shell fragments and

coquina limestone. They are medium cemented and porous, grayish in color (3). They correspond to the Pleistocene Age (44).

The sabkha deposits consists of silts, clays and muddy sand and chalky limestone with encrustations and interbeddings of gypsum and salt and frequently a salty surface coverings (3, 44).

Aeolian sand deposits consist of wandering dunes and loose sand sheets, generally in the form of barchans (44). These deposits cover large area. These include areas of dikakah, an irregular surface of bush and grass covered sand (3).

By comparing the geology of Eastern Province and semiarid areas of known swelling soils in the United States, one can conclude that formation of swelling soils in the study area is a result of the weathering of dolomitic limestone and marls rich in magnesium. More specifically, these soils were derived from the weathering of Permian, upper Cretaceous, and Tertiary rocks (51). Finally, Cagatay (8) reported that the poor crystallinity of smectite in Eastern Province suggests that it has a detrital origin.

Chapter 4

FIELD AND GEOTECHNICAL INVESTIGATION

4.1 INTRODUCTION

Probably, the most accurate subsoil investigation method is excavation of test pits. In a test pit, the field engineer can examine in detail the subsoil strata, stratification, layers and lenses, as well as taking samples at the desired location. However, the depth of the test pit is limited to the reach of the backhoe, generally about 15 feet. Also, when the water table is high, test pit investigation becomes useless. In locations where subsoils consist essentially of large boulders and cobbles, the use of test pit investigation is most favorable. Another possible investigation method is to drill boreholes. Probably 95% of all site investigations are conducted by drilling test holes (13).

In this study, both of the above methods were used to collect disturbed as well as undisturbed samples.

4.2 PRELIMINARY INVESTIGATION

During the preliminary investigation for suspected areas of expansive soils, numerous number of geotechnical data are reviewed to outline all possible expansive soil area in the Eastern

Province of Saudi Arabia. The data are mainly from unpublished reports developed over several years of geotechnical exploration, testing and construction experience. The reports have been provided by competent geotechnical firms working in the areas. Based on the data, a survey of damaged buildings due to expansive soils in the form of field trip was conducted in the areas having expansive soils. The following cities and villages were found to have expansive soil formations: Al-Qatif, Sayhat, Al-Aujam, Umm Al-Hamam, Anak, Al-Nabiyah, Umm Al-Sahek, Al-Jesh, Al-Hofuf and Al-Mubarraz. In part of Al Nabiyah approximately 100% of the houses are affected by expansive soils, reflecting severe cracks in structures. Plates 4.1-4.4 show examples of the damage in the study area. As can be seen in plate 4.1, a severe crack affected the exterior wall of a house in Al-Aujam. The crack is wide at the top and narrow at the bottom, which indicates that the crack is mostly a result of expansion problems. The majority of the cracks noticed in the structures of the study area are diagonal, range in width between hairline cracks and a few centimeters. The distress affects not only the bricks walls but also concrete members such as columns and beams, Plate 4.1.

The depth of the cracks differs from one case to another. In some cases the depth of the cracks is only a few millimeters, in others the interior of the house can be seen through the crack.

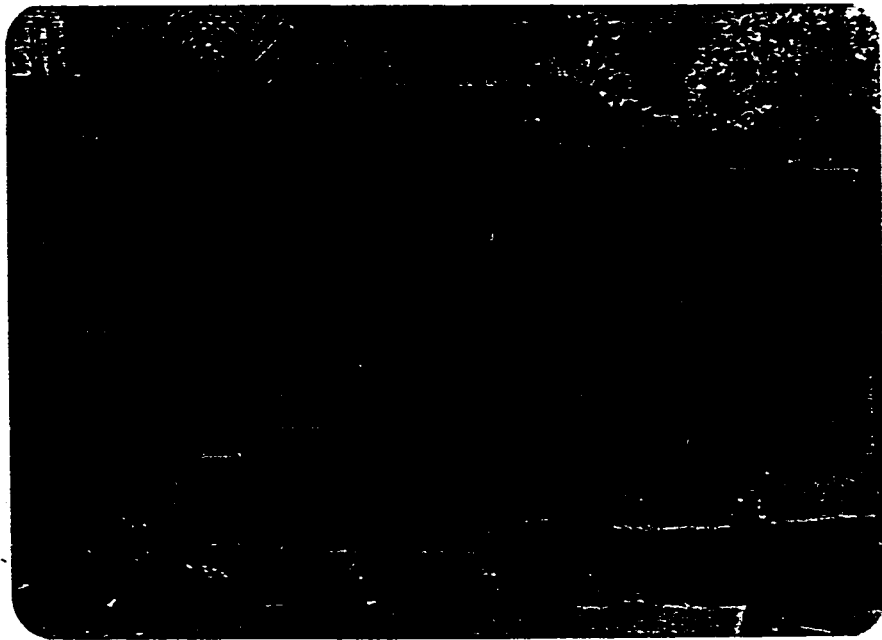


Plate (4.1), Typical Crack due to
Heaving in Al-Aujam.

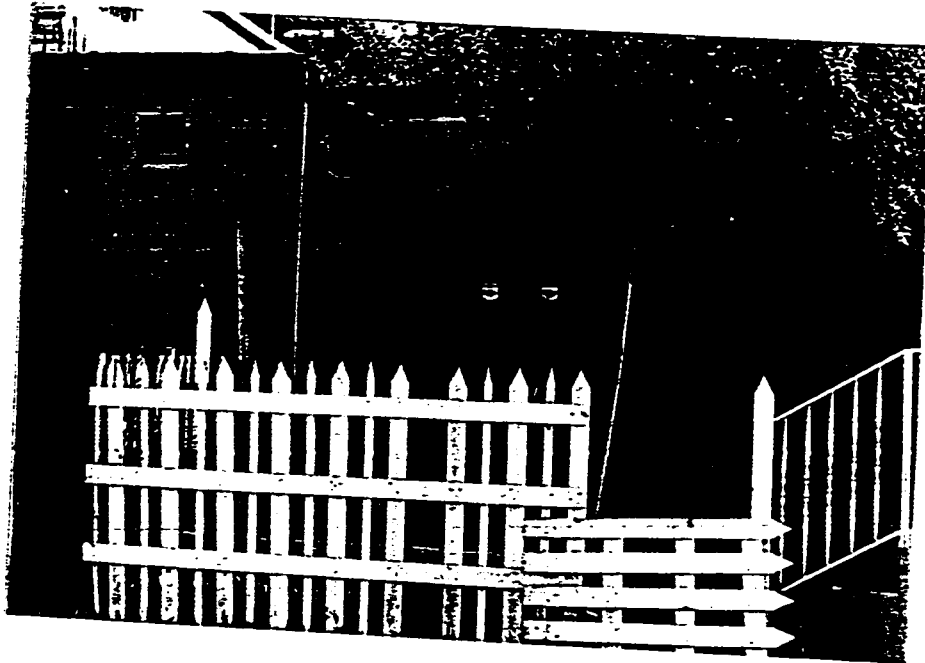


Plate (4.2), A diagonal crack in the brick wall
in Al-Aujam.

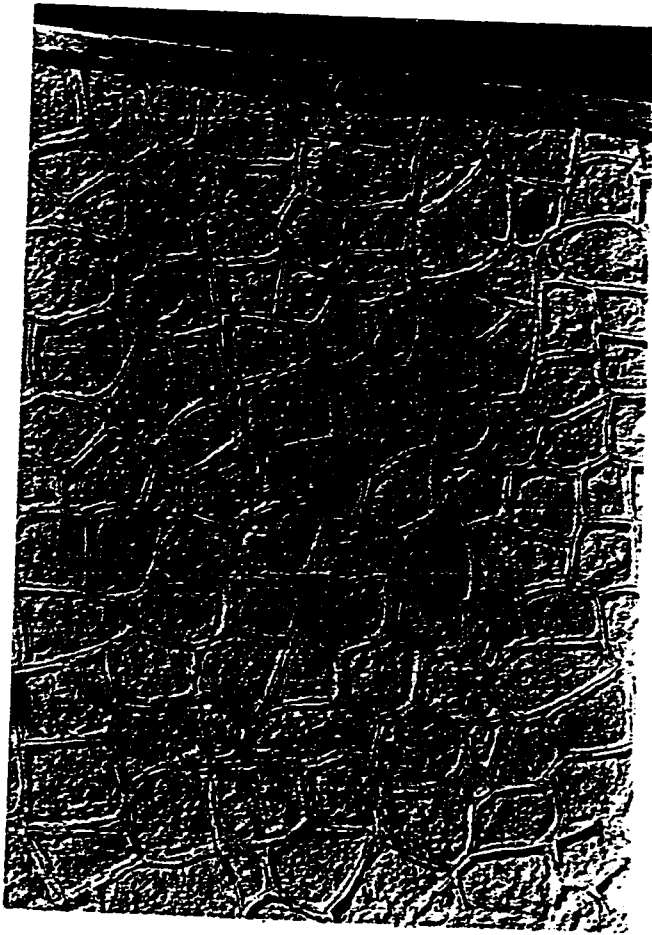


Plate (4.3), Crack in the exterior wall.

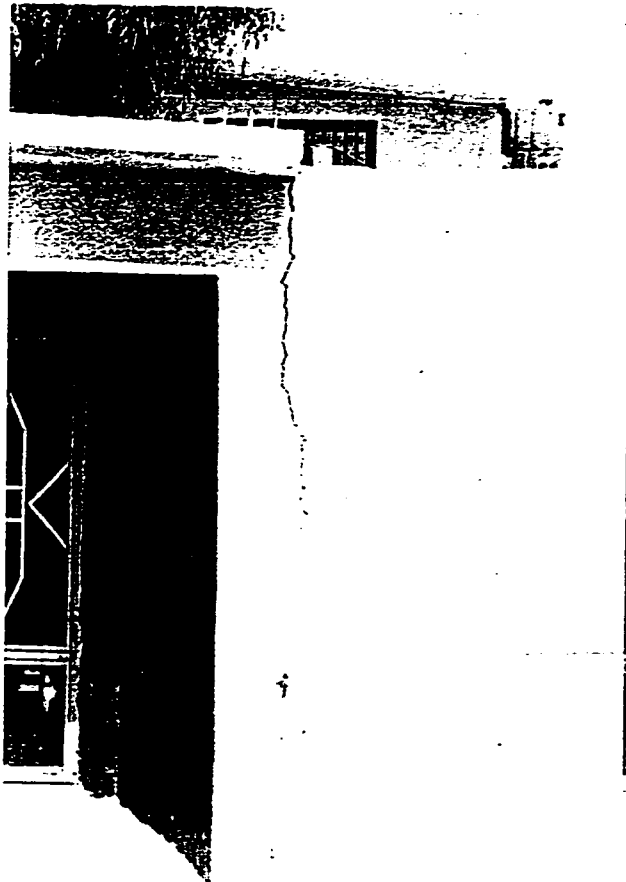


Plate (4.4), Crack in the exterior wall in
Al Qatif City.

During investigating the distress in structures the following analysis was used as a guide (13):

1. Swelling cracks are generally diagonal, wide at the top and narrow at the bottom.
2. Diagonal cracks below exterior windows or above exterior doors generally indicate footing or drilled pier foundation movement.
3. If such cracks appear only in the exterior brick course but not on the interior dry wall, the cracks can be caused by exterior patio slab heaving.
4. Hairline cracks appearing above interior doors and closets could be caused by plaster shrinkage and not necessarily foundation movement.
5. Vertical cracks below the I-beam in the basement concrete wall can be caused by the lifting of the I-beam, resulting in tension cracks.
6. Separation of the window frame from the brick course generally indicates differential heaving.
7. Drying and shrinkage of soils seldom or never cause cracking.
8. If the cracks are old and new cracks have not appeared

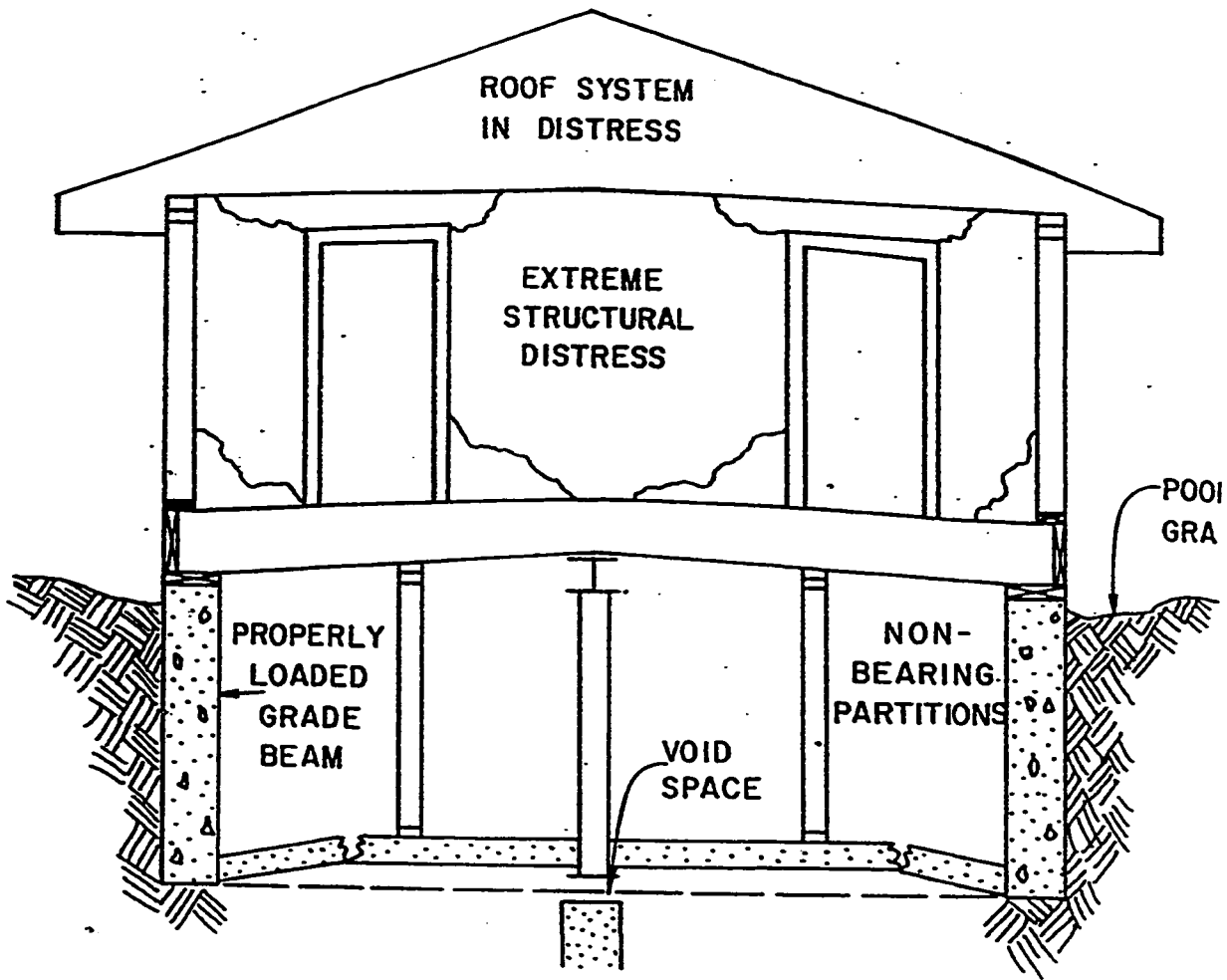


FIG. 4.0 TYPICAL MAJOR HOUSE DAMAGE

in the patched areas, this means that the foundation movement may have been stabilized.

9. It is difficult to differentiate between temperature cracks in brick walls and cracks from swelling soils.
10. While it is true that swelling soils are probably responsible for most of the cracking and movement of lightly loaded structures, other aspects of foundation movement cannot and should not be ignored.

Figure 4.0 shows typical cracks that occur due to heaving.

4.3 SITE INVESTIGATION

After the preliminary investigations, certain sites were selected for drilling and sampling.

All borings were drilled using a truck-mounted Acker Ace drilling rig, (Plate 4.5). Boreholes were advanced using mud rotary drilling technique, where a prepared solution of bentonite and water is used for maintaining borehole stability and removing cuttings from the borehole. The locations of the investigated areas are shown in Figures 4.1 and 4.2 . The detailed description of soils encountered are given on individual boring logs on Figures A.1 through A.15 in Appendix-A. Symbols and terms used on the

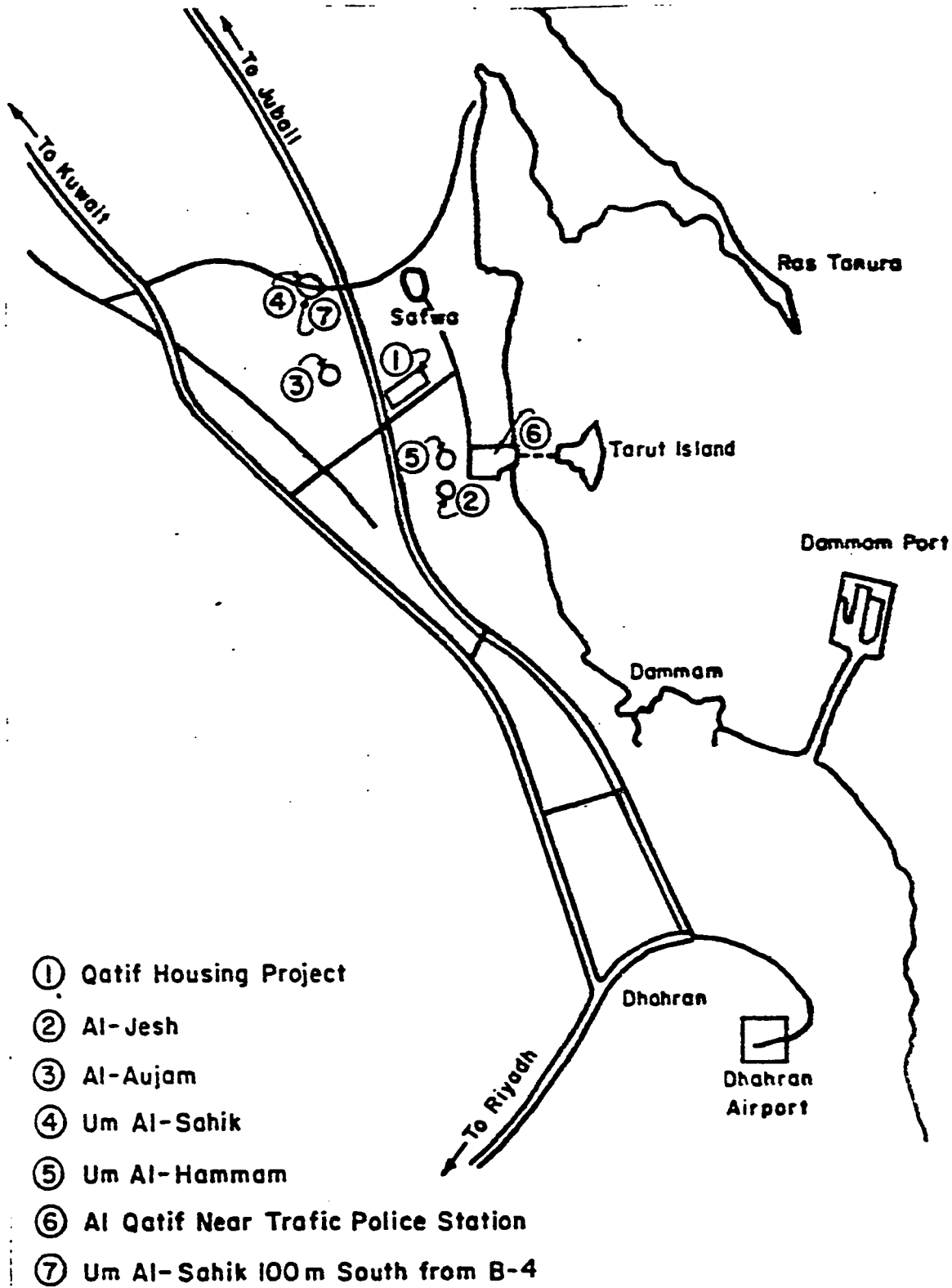


Figure (4.1), Vicinity Map of Al-Qatif Test Location.

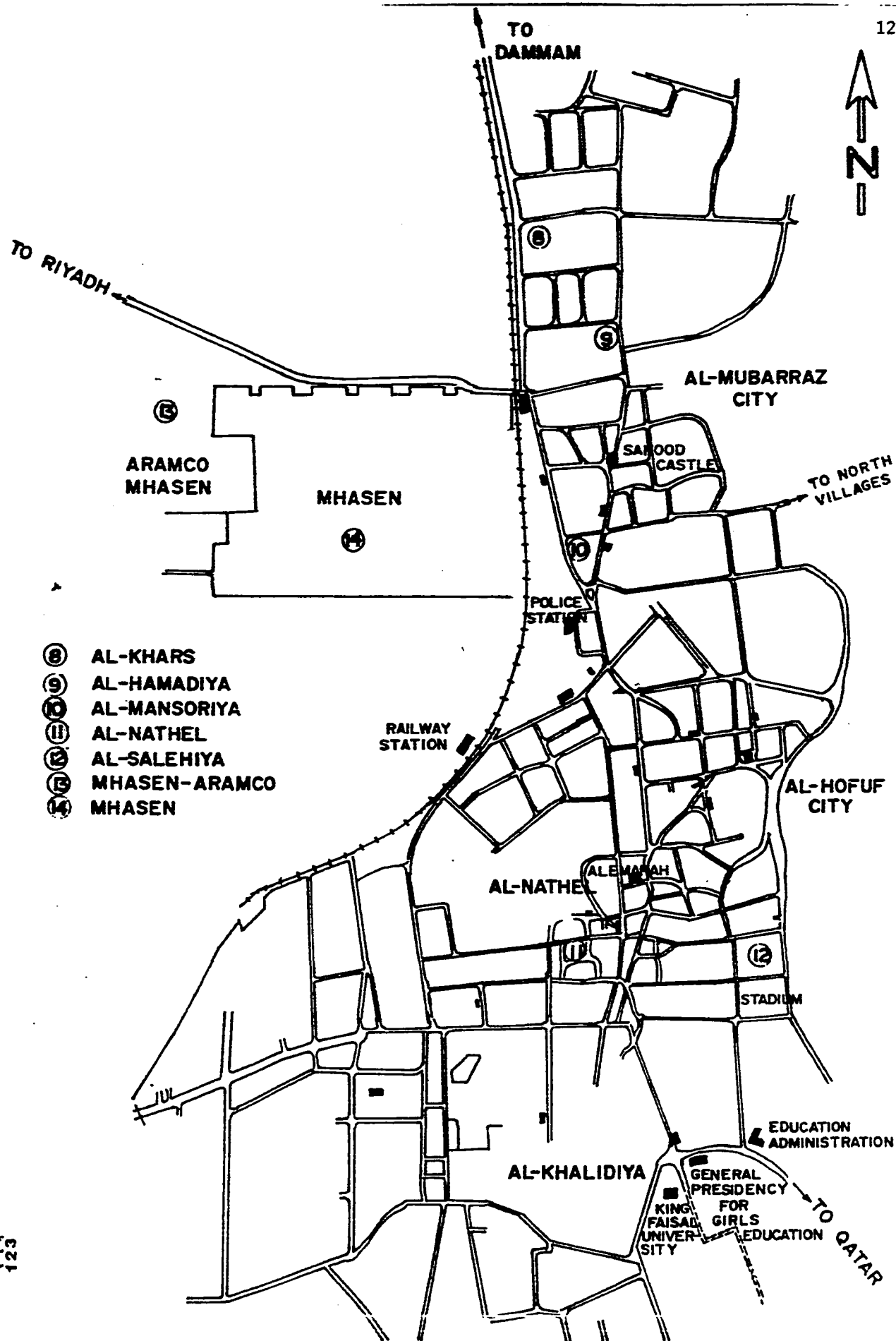


Fig. 4.2 VICINITY MAP OF AL-HASSA TEST LOCATION

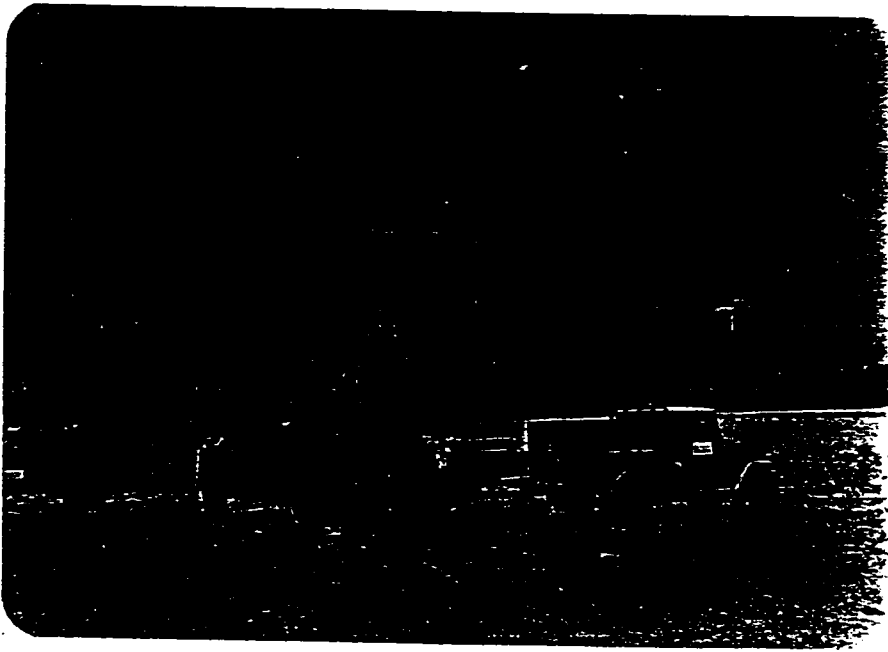


Plate (4.5), The truck-mounted drilling rig,
drilling BH # 1.

boring logs are given on Figure A.16 .

Al-Qatif Housing Area was investigated by drilling three borings designated as Borings BH-1 to BH-3. A boring each was drilled at Al-Jesh (BH-4), Al-Aujam (BH-5) and Umm-Al-Hamam (BH-8) villages. Two sites in Umm Al-Sahik village were investigated by Borings BH-6 and BH-7. Al Hasa area was investigated by drilling six borings designated as B.H-9 to B.H-14. However, no samples were recovered from bore hole #14 due to the hardness of the soil in that location. Table 4.1 gives the location of each Boring. All borings were drilled to a nominal depth of 10m. below the existing ground surface.

Samples were obtained continuously in all borings drilled for this study. Granular soils were sampled using procedures outlined in ASTM D-1587. These samples are discarded since they do not relate to the intended purposes of this investigation. Cohesive soils were sampled using either 76 mm diameter thin walled tubes or 76 mm diameter (size HX) double tube rock core barrels. The rock core barrels were used where hydraulic pushing of thin walled sampled tool failed to obtain samples of cohesive soils. All rock encountered was cored using size HX double tube rock core barrel.

All test pits were excavated using a poclain series 90 back hoe. The test pits were excavated to a nominal 5 m. depth.

Table(4.1): Location of Bore Holes

B.H #	Location		
1	Al-Qatif Housing Area	AL- QATIF AREA	
2			
3			
4	Al-Jesh		
5	Al-Aujam		
6	Umm Al-Sahek		
7	Umm Al-Sahek		
8	Umm Al-Hamam		
9	Al-Khars		AL- HASA AREA
10	Al-Mansoriya		
11	Al-Hamadiya		
12	Al-Salehiya		
13	Mahasen, near ARAMCO Hospital		
14	Al-Naathel		

The soils and rock formation based on visual identifications are presented on Figures A.17 through A.25. Four test pits, TP-1 to TP-4 were excavated at Al Qatif Housing Project area. One test pit was excavated at each of Al-Jesh and Al-Aujam villages. At two locations at Umm Al-Sahik village three test pits were excavated. Five test Pits were excavated at Al-Hasa area (TP-7 to TP-11). Table 4.2 shows the location of the test pits.

It was important to obtain high quality undisturbed samples. This was achieved by obtaining 14 block samples. The location and depth of these samples are shown on Figures A.17 through A.25. Two more block samples were obtained from Al-Hasa area from TP #10.

The block samples were obtained using the following procedure:

- At the test depth, either in the wall or floor of the test pit, a column of soil approximately 400 by 400 mm. in plan area was exposed. The depth of the column was about 450 mm.
- Using a small saw, piano wire and spatula, the exposed column was trimmed to the desired 300 by 300 mm plan area down to the total 450 mm. depth.

Table(4.2): Location of the Test Pits.

T.P #	Location	
1	Al-Qatif Housing Area	AL- QATIF AREA
2		
3		
4		
5	Al-Aujam	
6	Umm Al-Sahek	
7	Al-Mubarraz, Al-Khars	AL- HASA AREA
8	Al-Mubarraz, Al-Hamadia	
9	Hofuf, Al-Naathel	
10	Hofuf, Al-Salehiya	
11	Hofuf, Mahasen	
12	Hofuf, Mahasen near ARAMCO Hospital	

- The column was then wrapped in plastic sheet. A wooden box was then slid over the column. With the help of a shovel, the column was pried from the soil. The box was inverted and excess soil sliced off.
- The gap between the box and soil was filled with molten wax. Wax was also applied on the exposed soil. The box was sealed and transported to the laboratory for further testing and study.

4.4 SITE DESCRIPTION

The following sections describes the various sites investigated. The discussion is limited to subsurface stratigraphy. The procedure for sampling cohesive soils was also highlighted where warranted.

4.4.1 Qatif Housing Area

All borings drilled in this site encountered layers of clay. The depth and thickness of clays together with groundwater depth are summarized in table 4.3 .

Clay samples were obtained using 76mm diameter thin-walled tube. However, the base of thin-walled tubes deformed and quality and quantity of clay samples obtained were poor. Good quality samples were then obtained using 76mm. diameter

Table(4.3), Depth and thickness of clays in Al -Qatif Housing Area

Boring #	Water Depth (m)	Top of Clay Layer, m.	Thickness of Clay Layer, m.	Remarks
BH-1	5	3.5	0.5	Clay seams in limestone below 4.0 m
BH-2	-	1	0.5	Interbedded with clayey silt
		2.8	0.2	-
		5	1.8	-
BH-3	7.85	3.65	0.95	-
		4.6	2.6	Interbedded with clayey silt

size HX, double tube split core barrel using carbide bits. The clay layers occurring in test pits are summarized in Table 4.4 . One more bore hole was drilled downtown of Al-Qatif city (BH#3A). The test pit was not excavated because the boring indicated no clay. The ground water at the time of our study was 0.7m. below the existing ground surface.

4.4.2 Al Aujam Village

The boring in Al-Aujam (BH-5) indicates silty clay strata at 5.3 and 9.5m. depths below the existing ground surface. The thickness of these clay layers are 0.7m. and more than 0.5m. respectively. Based on visual inspection, no clay was encountered in TP-5. The ground water is at 1 meter below the existing ground surface.

4.4.3 Al-Jesh Village

The site at Al-Jesh was investigated by one boring BH-4 and one test pit. The ground water is at 1.1 m. depth below the existing ground surface. Since the groundwater is shallow and the clay encountered is very deep, the test pit was not excavated at this site.

4.4.4 Umm Al-Sahek Village

Two sites were investigated at Umm Al-Sahek by drilling two borings, BH-6 and BH-7, and excavating three test pits,

Table (4.4), Depth and thickness of clays in Al-Qatif Housing Area (Test Pits).

T.P #	Water Depth (m)	Top of clay layer (m)	Thickness of clay layer (m)	Remarks
TP-1	> 4.5	4.25	0.5	TP terminated in clay
TP-2	>4.5	4.5	0.25 +	_ditto_
TP-3	>4.5	3.5	0.5 +	_ditto_
TP-4	>4.5	1.2	0.2	_ditto-
		2.1	0.3 +	

TP-6, TP-6A and TP-6B.

BH-6 and TP-6 did not encounter significant clay deposits. The groundwater at BH-6 and TP-6 location is about 1 to 1.5 m. below the existing ground surface. TP-6A excavated close to TP-6 encountered a clay deposit near the surface extending from 0.1 to 0.75m. below the existing ground surface.

The second site at Umm Al-Sahek village yielded considerable clay deposits. The ground water is about 3.7m. below the existing ground surface. The clays occur to 2.1 m. depth below the existing ground surface. An interbedded clay and limestone strata also occurs between 3.45 and 7.0 m. depths. TP-6B encountered clay to the final 1.7 m depth. Three block samples from these deposits were obtained. Using a 76mm thin-walled tube, good quality undisturbed clay samples were also recovered from this site.

4.4.5 Umm Al-Hamam Village

BH-8 drilled at this site indicated the presence of clay between 7.1 m. to 8.0 m. depth. The ground water at the time of investigation was 0.6 m. deep. Test pits were not excavated at this site because the clay layer is deep and the groundwater is shallow.

4.4.6 Al-Mubarraz

Al-Mubarraz area was investigated by two test pits and three bore holes in three different areas namely: Al-Khars, Al-Hamadiya and Al-Mansoriya. Bore hole # 9 was drilled and TP # 7 was excavated in Al-Khars area, near Prince Bin Jalawi Hospital. A green red sandy clay was encountered at a depth of 1.0 m. A hard reddish brown and light green silty clay was found at 2.5 m depth with a 20 cm thickness. The water level was 3.2 m at the time of study, (Figure A.10).

4.4.7 Al-Hamadiya

Al-Hamadiya area was investigated by BH # 11 and TP # 8. The encountered clay was hard, olive green and brownish red with limestone fragments and gypsum nodules. The water level was 2.0 m deep at the time of study, (Figure A.11).

The investigation of Al-Mansoriya area was conducted through BH # 10. The clay was found at 1.0 m and 4.0 m deep. The clay is hard, light green with limestone fragments. The water level was at the time of investigation 2.5 m deep, (Figure A.12).

4.4.8 Al- Hofuf City

Three areas were investigated in Al-Hofuf city namely: Al-Naathel, Al-Salehiya and Mahasen.

Al-Naathel was investigated by excavating TP#9 and drilling BH#14. The test pit was excavated to 220 cm depth. A

very dry and stiff green to gray clay with limestone layers and fragments was found. Only disturbed samples were collected from this test pit due to the hardness of the soil and no samples could be obtained from the bore hole for the same reason, (Figure A.13).

Al-Salehiya area was investigated through TP#10 and BH#12. Two block samples were taken from TP#10, as well as other disturbed and undisturbed samples. The clay in this test pit is light green to gray, hard, sandy, silty and interbedded with gypsum. The same type of clay was found in BH#12 at 2.0 m and 5.0 m deep. The water level was at 5.0 m depth, (Figure A.14).

In Mahasen TP#11 and BH#13 were drilled near ARAMCO hospital. The clay in this area is similar to that of Al-Naathel area, i.e. very hard, brown and green silty clay with limestone fragments, (Figure A.15).

Chapter 5

GEOTECHNICAL AND MINERALOGICAL PROPERTIES

Samples collected from different sites were transported to KFUPM soil mechanics laboratory and subjected to extensive testing program, (see Figure 5.0). This chapter is devoted for the presentation of geotechnical and mineralogical properties of the samples

5.1 GEOTECHNICAL PROPERTIES

Several tests were performed in order to determine the geotechnical properties of soils. The tests and results are discussed in the following sections.

5.1.1 Natural Water Content and Unit Weight.

The natural water content (W_n) and unit weight (γ) were determined for all samples in accordance with ASTM D-2937 and ASTM D-1188, respectively. The results for all TP's and BH's samples in both Al-Qatif area and Al-Hasa area are listed in Tables 5.1 through 5.4.

Figures 5.7 to 5.12 show the variation of natural water content with depth for some bore holes. It can be seen that the

LABORATORY TESTING

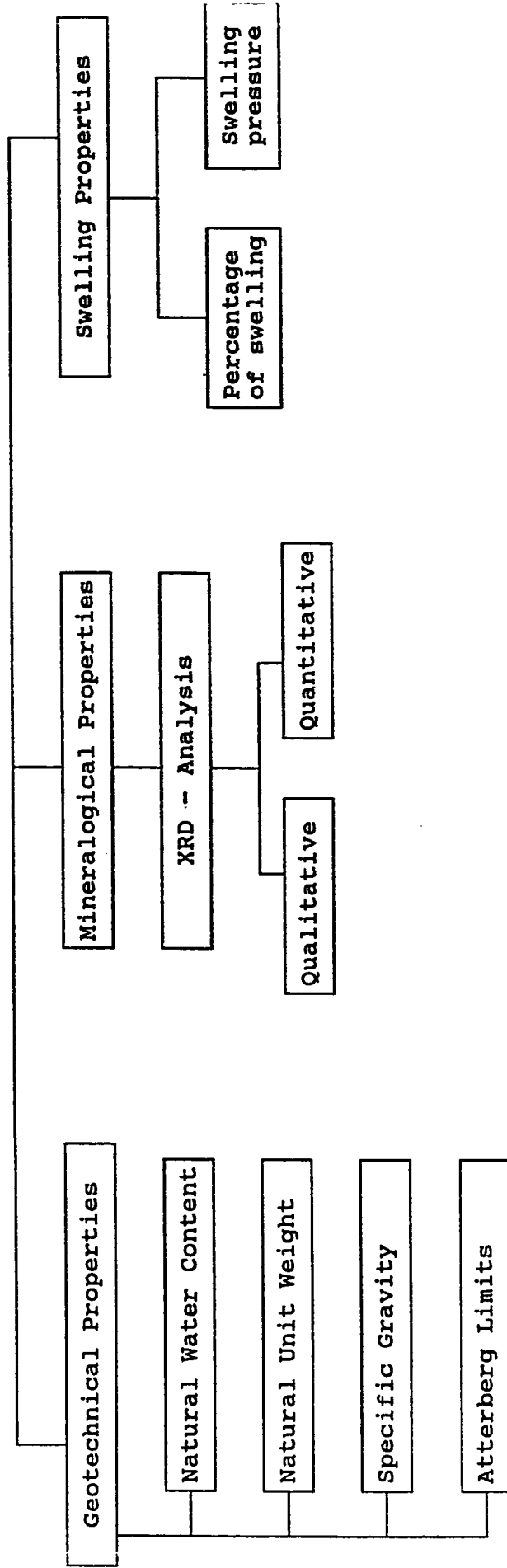


Figure 5.0: Testing Programme

Table (5.1): Summary of Results for Al-Qatif Area Test Pits

T.P.#	Sample #	Depth (m)	Location	W.C %	wet	dry	LL %	PL %	SL %	PI %	Gs	% Swell	Swell Pressure Kp/cm**2	% Passing Sieve #200
1	1-A	3.4-3.8	Housing Area	31.20	1.92	1.46	77.70	22.71	16.78	54.99	2.80	1.27	2.00	99.70
1	1-B	4.0-4.5	Housing Area	67.87	1.70	1.01	153.00	52.40	7.27	100.60	2.63	19.76	9.50	99.30
2	2-A	3.8-4.0	Housing Area	45.93	1.72	1.18	116.50	37.02	15.96	79.48	2.73	26.60	16.80	96.88
2	2-B	4	Housing Area	51.11	1.66	1.10	150.20	47.61	16.70	102.39	2.64	29.49	19.30	98.80
3	3	3.5	Housing Area	52.85	1.70	1.11	129.50	48.50	16.44	81.00	2.26	5.16	3.72	98.79
4	4	1.7	Housing Area	50.66	1.63	1.08	130.50	39.18	10.87	91.32	2.57	13.08	8.40	99.33
5	5	1.4	Al-Aujam	53.60	1.65	1.07	N0	Pla	atl	city	2.92	0.00	0.00	25.00
6	6	1.5	Jmm Al_Sahel	58.20	1.97	1.25	139.60	46.24	18.91	93.36	2.38	12.74	4.00	81.40

Table 5.2 Summary of results for Al-Qatif Area Bore Holes

Location	Bh #	Depth (m)	Water Content %	Unit Weight Dry	Liquid Limit LL %	Plastic Limit PL %	Shrinkage Limit SL %	Plasticity Index PI %	Specific Gravity Gs	% Swell	Swell pressure Kg/cm ²	
Al-Qatif Housing Area	1	3.50	39.20	1.72	74.00	30.30	23.80	43.70	2.79	9.02	3.72	
		3.80	58.20	1.07	120.00	42.60	20.60	99.40	2.69	29.02	19.15	
		4.00	55.80	1.09	150.50	38.80	9.10	111.70	2.24	16.81	5.72	
Al-Qatif Housing Area	2	4.2 S1	77.50	0.84	183.80	70.10	46.10	113.70	2.44	19.56	20.00	
		4.2 S2	55.40	1.13	97.00	36.80	13.90	60.20	2.18	0.61	0.57	
		8.50	26.20	1.58	67.20	28.60	21.10	38.60	2.72	1.02	0.34	
Al-Qatif Housing Area	3	1.8 - 2.1	22.20	1.50	80.60	30.00	20.10	50.60	2.80	14.35	5.43	
		4.0-4.15	30.60	1.49	54.80	25.10	15.10	29.70	2.50	2.10	1.43	
		4.8 - 5.0	28.40	2.15	45.10	24.20	22.30	20.90	2.82	2.00	0.86	
Al-Jesh	4	7.9 - 8.2	36.20	1.13	70.90	29.70	25.60	41.20	2.73	0.63	0.14	
		6.15	85.90	0.81	183.50	83.40	49.10	100.10	2.50	1.31	1.14	
		9.7 - 10, S1	51.10	1.26	48.60	23.20	20.70	25.40	2.89	1.72	0.29	
Al-Anjam	5	9.7 - 10, S2	21.20	1.68	36.20	19.00	18.50	17.20	2.85	0.25	0.09	
		1.35	66.50	0.88	No	plasticity					0.19	0.06
		6.6 - 6.9	55.00	1.07	85.10	45.20	18.70	39.90	2.62	2.62	1.14	
Umm-Al-Sahek	6	0.45-0.6	29.70	1.45	65.30	21.40	18.70	43.90	2.93	4.06	0.86	
		0.9-1.15	26.20	1.55	The sample is not enough						0.35	0.14
		4.5-4.7	26.70	1.56	31.80	23.00	23.30	8.80	2.74	0.24	0.06	
Umm-Al-Sahek	7	9.0-9.4	20.20	1.57	53.50	23.40	21.90	30.10	2.82	18.75	11.43	
		0.4-0.8	25.90	1.39	73.00	31.90	24.10	41.10	2.37	1.76	0.57	
		1.1-1.4	48.30	1.19	148.50	45.00	24.40	103.50	2.12	3.22	1.43	
Umm-Al-Sahek	7	4.0-4.3	27.90	2.18	58.00	25.90	31.37	32.10	2.66	1.36	0.57	
		7.5-7.6	38.10	1.91	No plasticity						0.00	0.00
		9.2-9.6	44.00	1.58	47.70	35.20	35.30	12.50	2.80	0.58	0.14	
Umm-Al-Hamam	8	0.6-0.9	26.60	1.52	30.20	17.70	19.50	12.50	2.74	0.09	0.01	
		2.3-2.6	25.30	1.62	32.70	29.50	23.20	3.20	2.66	0.03	0.01	
		4.7-4.9	24.40	1.63	53.00	24.10	20.00	28.90	2.71	0.94	0.43	
Umm-Al-Hamam	8	5.6-5.75	73.60	0.88	169.00	42.40	20.90	126.60	2.61	12.88	4.00	
		5.75-5.9	55.20	1.18	44.70	23.11	23.53	21.60	2.84	4.89	2.29	
		7.10-7.4	96.10	0.75	315.00	128.70	80.70	186.30	2.38	10.36	7.43	

Table (5.3) : Summary of Results for Al -Hasa Test Pits

T.P #	Depth (m)	W.C %	wet	dry	LL %	PL %	SL %	PI %	Gs	% Swell	Swell pressure Kg/cm**2
7	0.9	25.76	2.02	1.61	65.8	34.99	17.69	30.81	2.34	1.56	0.57
	1.1	20.36	2.05	1.7	71.3	29.7	20.81	41.6	2.89	8.4	4.29
	1.5	24.8	1.96	1.57	68	32.58	25.94	35.42	2.82	2.27	1.43
8	0.2	42.1	1.75	1.23	142	47.15	29.03	94.85	2.96	12.03	4.29
	0.8-1.1	43.26	1.77	1.23	123.8	45.06	27.12	78.74	2.83	2.7	3.72
9	1.1	21.2	1.89	1.56	74.4	32.6	16.42	41.8	2.24	14.17	13.15
	2.2	22.87	2.1	1.71	82.2	35.67	26.72	46.53	2.8	16.38	24.01
10	1.5-1.8	23.23	1.82	1.48	55	27.2	24.49	27.8	2.81	0.67	0.43
	1.8-2.1	26.24	1.88	1.49	53.1	27.79	24.53	25.31	2.86	0.27	0.14
11	2.0-2.2	20.76	2.01	1.66	61	30.05	24.32	30.95	2.85	13.11	24.298

Table (5-4): Summary of Results for Al-Hasa Area Bore Holes

BH#	Depth (m)	W.C. %	Wet	Dry	LL%	PL%	SL%	PI%	Gs	%Swoll	Swell pressure Kg/cm**2
9	2.5-2.7	19.62	2.00	1.67	75.50	29.06	21.76	46.44	2.86	2.20	3.14
	3.0-3.2	18.97	2.11	1.77	70.60	26.65	15.69	43.95	2.43	2.56	2.57
	3.5-3.7	36.04	1.82	1.34	88.00	36.71	25.92	51.29	2.76	2.93	2.86
	4-4.3	21.73	1.99	1.63	57.20	28.10	22.35	29.10	2.76	0.49	0.29
	5.0-5.3	27.02	1.88	1.48	70.10	33.29	23.03	36.81	2.76	3.27	2.57
10	6.0-6.3	32.71	1.95	1.47	77.30	38.58	27.82	38.72	2.77	1.54	2.29
	9.8-10	12.17	1.99	1.77	65.80	28.74	20.33	37.06	2.81	1.13	0.86
	0.8-1.1	17.97	2.13	1.81	60.00	29.84	24.52	30.16	2.76	2.54	2.29
	4.0-4.2	12.58	2.11	1.87	65.30	31.87	23.50	33.43	2.77	0.16	0.29
	0.3-0.6	16.49	2.08	1.79	77.00	33.18	17.61	43.82	2.44	3.98	2.00
11	1.0-1.3	29.52	1.86	1.44	90.50	33.67	22.42	56.83	2.83	7.16	4.00
	1.5-1.8	21.21	2.00	1.65	74.70	27.77	19.48	46.93	2.72	2.86	3.72
	2.5-2.8	24.42	1.79	1.44	64.60	27.33	19.20	37.27	2.77	5.39	3.14
	3.1-3.4	21.35	1.79	1.48	63.50	25.46	18.08	38.04	2.80	5.41	3.43
	3.8-4.0	19.87	1.96	1.64	65.90	27.82	17.19	38.08	2.40	2.08	3.72
12	8.3-8.5	12.71	1.66	1.47	67.30	32.67	23.51	34.63	2.76	0.00	0.00
	1.6-1.9	22.50	1.81	1.48	40.50	22.06	16.16	18.44	2.40	3.47	1.72
	2.0-2.3	18.92	1.98	1.66	52.90	27.87	26.23	25.03	2.82	1.86	1.14
	2.4-2.7	23.12	2.03	1.65	55.10	27.76	24.63	27.34	2.84	4.84	2.57
	2.7-3.0	27.41	2.09	1.64	52.00	23.98	19.59	28.02	2.79	1.99	1.00
13	3.1-3.4	26.54	1.85	1.46	70.60	33.91	26.17	36.69	2.80	4.47	2.00
	1.65-1.9	24.04	1.99	1.60	58.20	29.87	18.72	28.33	2.51	0.86	0.57
	2.0-2.25	18.90	1.91	1.61	66.80	29.00	21.40	37.80	2.81	6.28	2.00

natural water content differs greatly from one place to another and from a depth to another for the same site. Sample#2 (BH#4, 9.7-10 m), shows the minimum natural water content of 21.2% in Al-Qatif area, while the sample of depth 7.1-7.4 m (BH#8) shows the highest natural water content of 96.1%. In Al-Hasa area the lowest natural water content value of 12.1% was found in BH #9 (9.8-10 m), and the highest Wn of 43.26% was found in TP #8 (0.8-1.1 m). It can be seen that Al-Hasa samples have a lower natural water content than that of Al-Qatif area. Generally speaking, the natural water content increases as the depth increases as can be seen in Figures 5.7-5.12, and this is expected as the deeper sample is closer to or under the ground water table.

The unit weight determined using the wax method. In this method, the weight of the sample in the air is taken. Then the sample is coated by wax with known density. The weight of the waxed sample was then taken both in air and in water. The difference between weight of the sample in air and in water represents the volume of the sample. Hence the wet unit weight can be found as:

$$\gamma_{\text{wet}} = \frac{\text{Wt. of samples in air}}{\text{Volume of the sample}}$$

Consequently:

$$\gamma_{\text{dry}} = \frac{\gamma_{\text{wet}}}{(1 + W.n)}$$

The dry unit weight differs from a sample to another even for the same bore hole, however, this difference is small. In Al-Qatif area the lowest unit weight of 0.75 g/cm³ was found in a sample of BH#8 (7.1-7.4 m). The highest value of 2.15 g/cm³ was recorded for a sample at depth 4.8-5.0 m (BH #3). The lowest dry unit weight in Al-Hasa area is 1.23 g/cm³ (TP#8,0.8-1.1 m), While the highest value is 1.87 g/cm³ (BH#10, 4.0-4.2 m). Figures 5.1-5.6 show the variation of natural dry unit weight with depth for some bore holes. It is noticeable that the samples with highest natural water content has the lowest dry unit weight and vise versa.

5.1.2 Specific Gravity

The specific gravity was determined according to ASTM D-854. Briefly, the sample was put into a pycnometer partially filled with water. Air vacuum is then applied accompanied by shaking the pycnometer to remove all entrapped air. After the removal of air the pycnometer was filled with water and the weight of the pycnometer + water + sample is recorded. The sample is then transferred to a dish and dried in the oven to a constant weight. Finally, the specific gravity is calculated as follows:

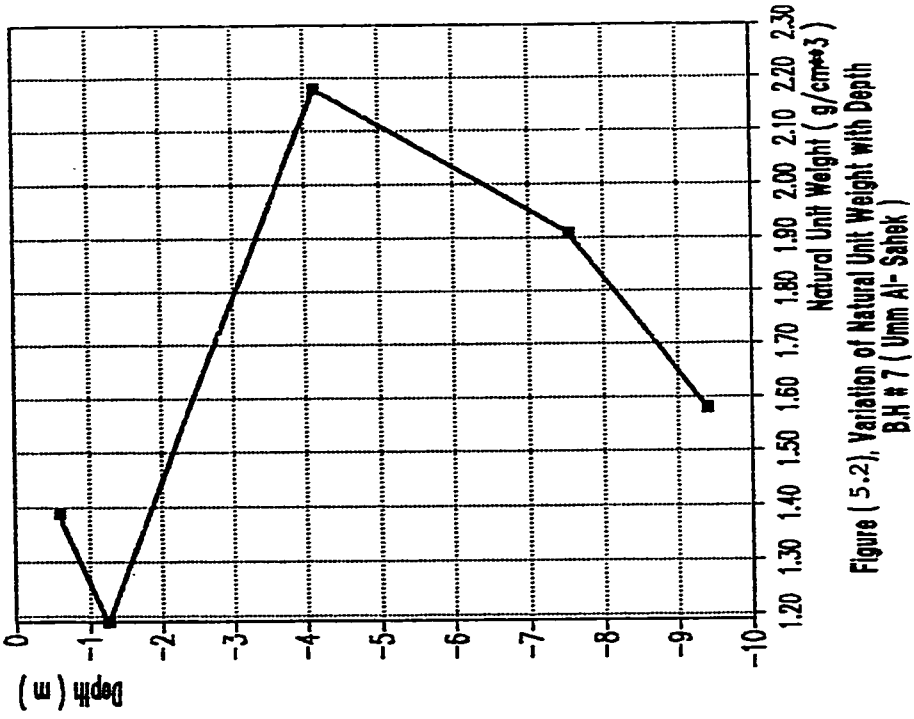


Figure (5.2), Variation of Natural Unit Weight with Depth
B.H # 7 (Umm Al- Sahak)

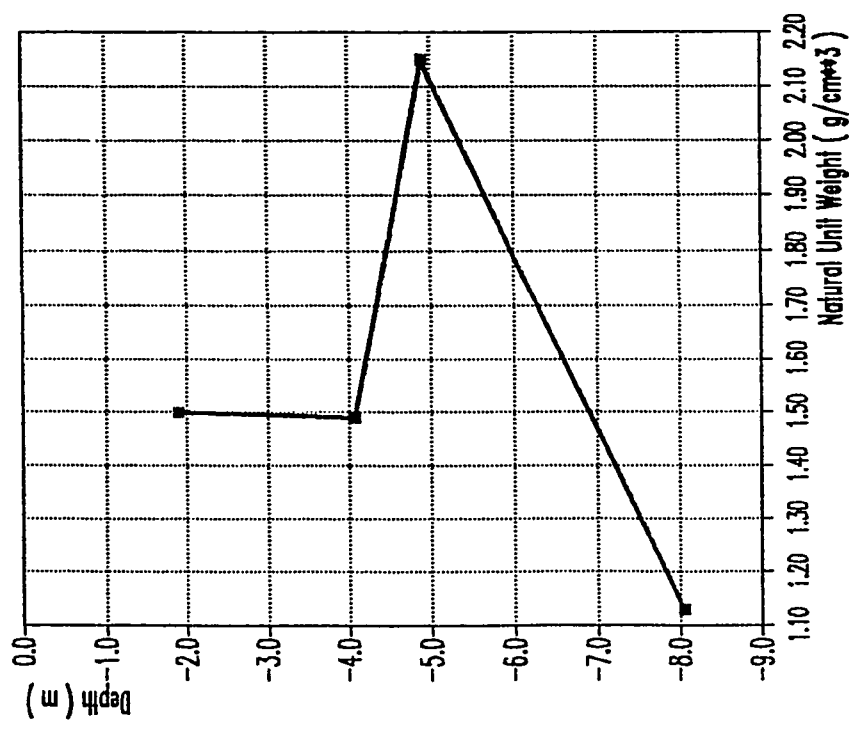


Figure (5.1), Variation of Unit Weight with depth , BH # 3 (Al-Qatiff Housing Area).

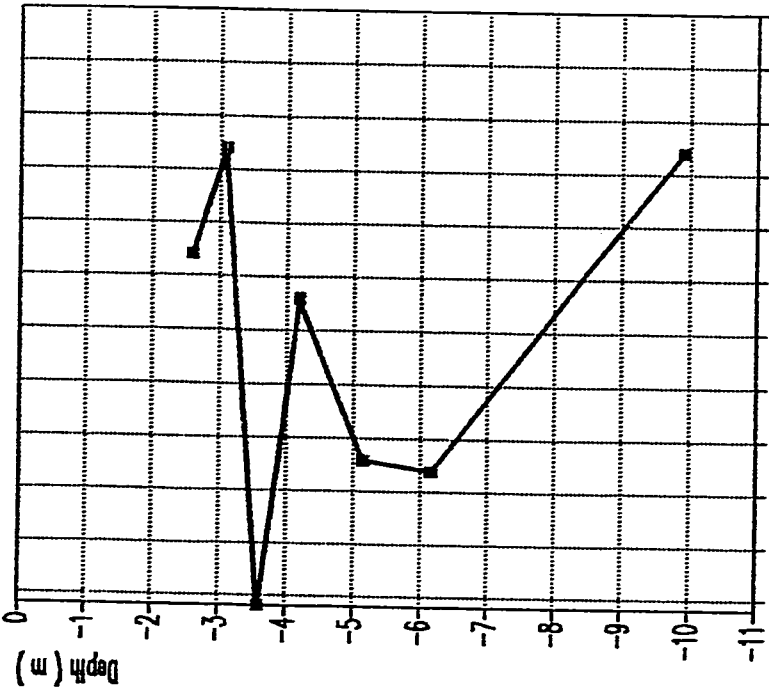


Figure (5.4), Variation of Natural Dry Unit Weight with depth
B.H # 9 (Al Hasa)

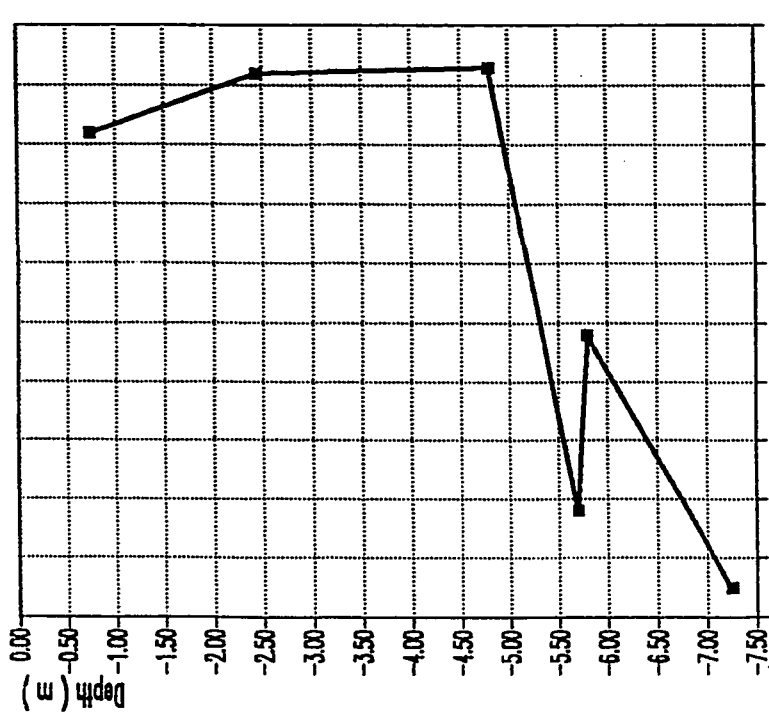


Figure (5.3), Variation of Natural Unit Weight with Depth
B.H # 8 (Umm Al-Hamam)

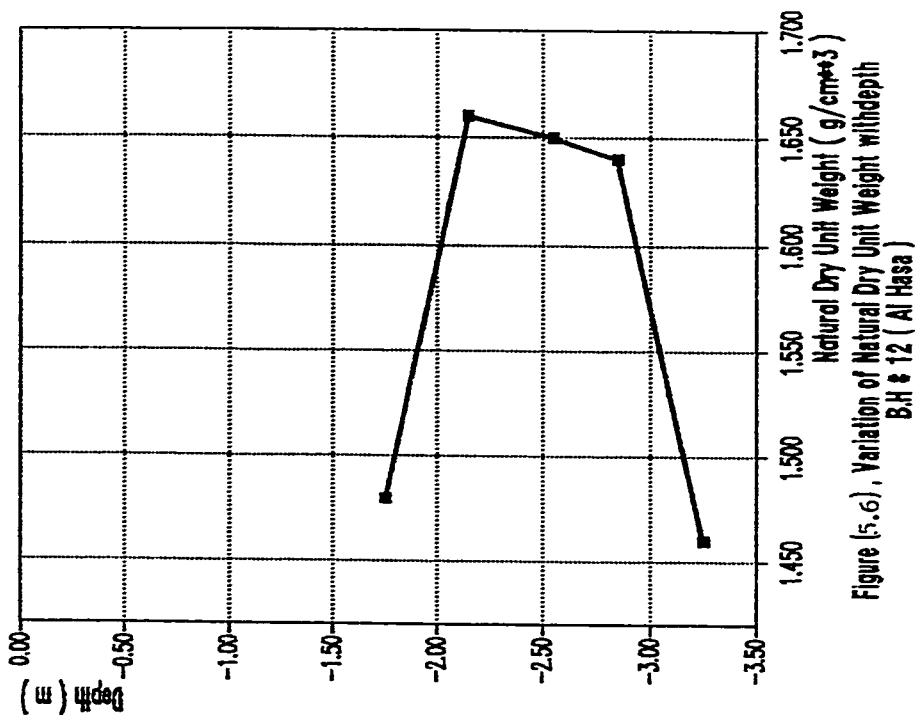


Figure (5.6), Variation of Natural Dry Unit Weight with Depth
BH # 12 (Al Hasa)

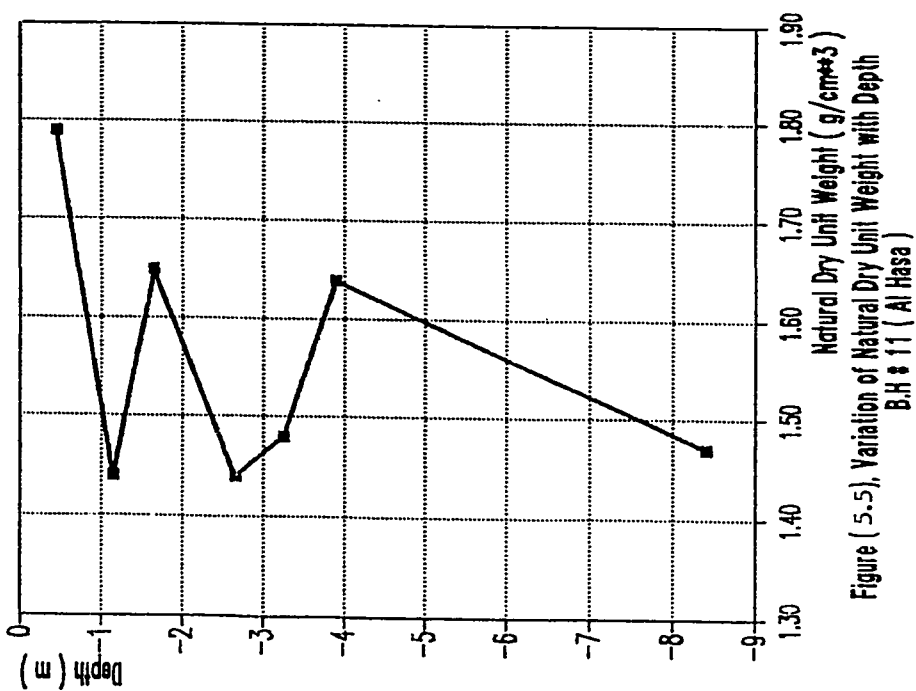


Figure (5.5), Variation of Natural Dry Unit Weight with Depth
BH # 11 (Al Hasa)

$$G_s = \frac{G_t \cdot W_s}{W_s - W_1 W_2}$$

where:

G_s = specific gravity of soil

G_t = specific gravity of water

W_s = Wt. of dry soil

W_1 = Wt. of pycnometer + sample + water

W_2 = Wt. of pycnometer + water

Tables 5.1-5.4 show specific gravity results for all samples. The specific gravity ranges between 2.12 (BH#7, 1.1-1.4 m) to 2.93 (BH #6, 0.45-0.6 m) in Al-Qatif area, and between 2.24 (TP #9, 1.1) to 2.96 (TP#8, 0.2 m) in Al-Hasa area.

5.1.3 Atterberg Limits

The liquid (LL) and plastic limits (PL) were determined according to ASTM D-4318, while the shrinkage limit (SL) was determined according to ASTM D-427. The results are presented in Tables 5.1 through 5.4.

The liquid limit was determined by Casagrand's liquid device and is defined as the percentage of moisture content at which a groove closure of 1/2 inch occurs at 25 blows. At least

six point were taken to determine the liquid limit for each sample.

The plastic limit is defined as the percentage of moisture content at which the soil crumbles when rolled into a thread of 3.18 mm in diameters. The plastic limit results presented are average of three trails for each sample.

The shrinking limit is defined as the percentage of moisture content at which the soil does not undergo further volume change with loss of moisture. Three trials were conducted for each sample to determine its shrinkage limit.

Figures 5.7-5.12 show the variation of liquid limits (LL), plastic limits (PL), shrinkage limits (SL) and natural water content (W_n) with depth for some bore holes. The results show that most of the samples are highly plastic, only few samples showed low or no plasticity. Some samples in Al-Qatif area ,such as BH #1 (4.0 m), BH #2 (4.2m, S1), BH #4 (6.15 m) and BH #8 (7.1-7.4 m) have a plasticity index larger than 100 %. The high plasticity is an indication of a high swell potential. In general, the plasticity of the samples from Al-Qatif area are higher than that of Al-Hasa. Tables 5.5-5.8 show the classification of the samples according to the U.S.C.S. based on their plasticity. Figure 5.13 shows a plasticity chart for the samples collected from the bore holes of Al-Qatif area, while Figure 5.14 shows a plasticity chart for the samples collected from Al-Hasa test pits. Figure 5.15 shows a

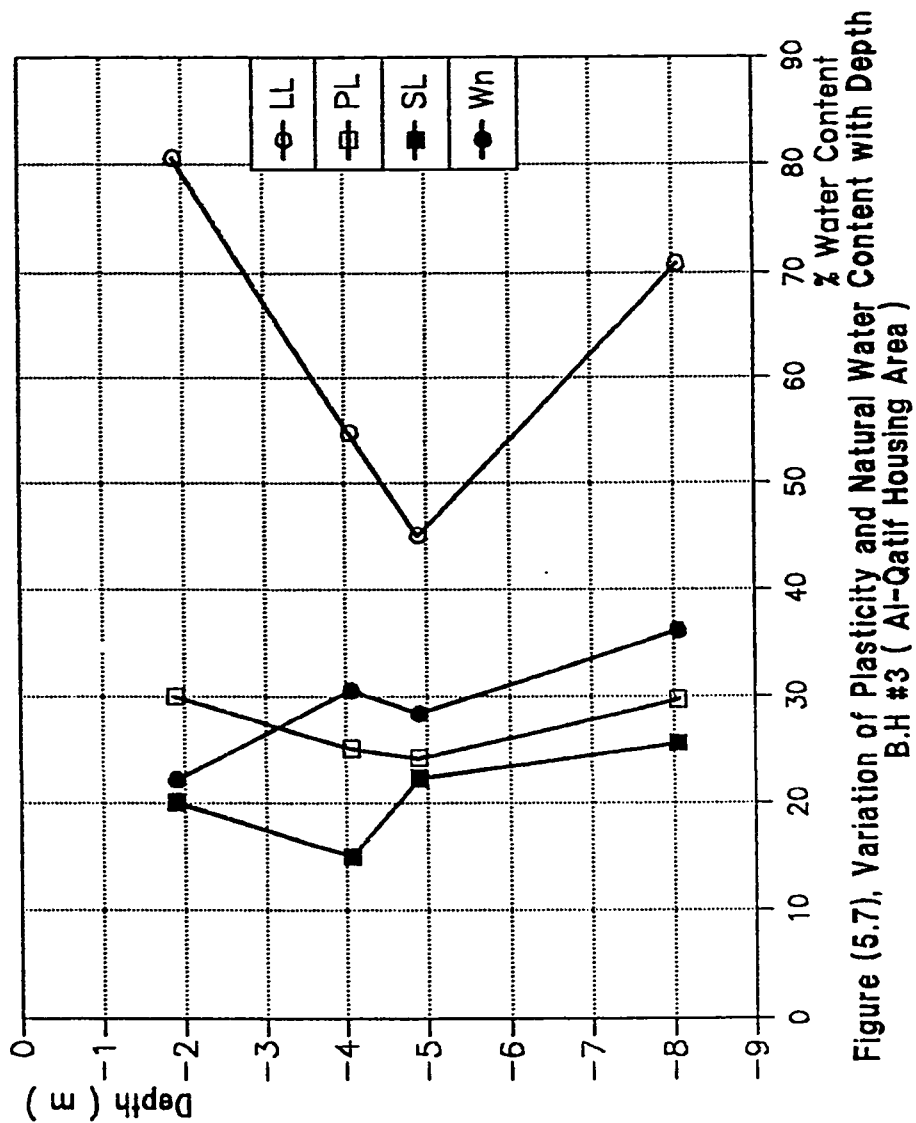


Figure (5.7), Variation of Plasticity and Natural Water Content with Depth B.H #3 (Al-Qatif Housing Area)

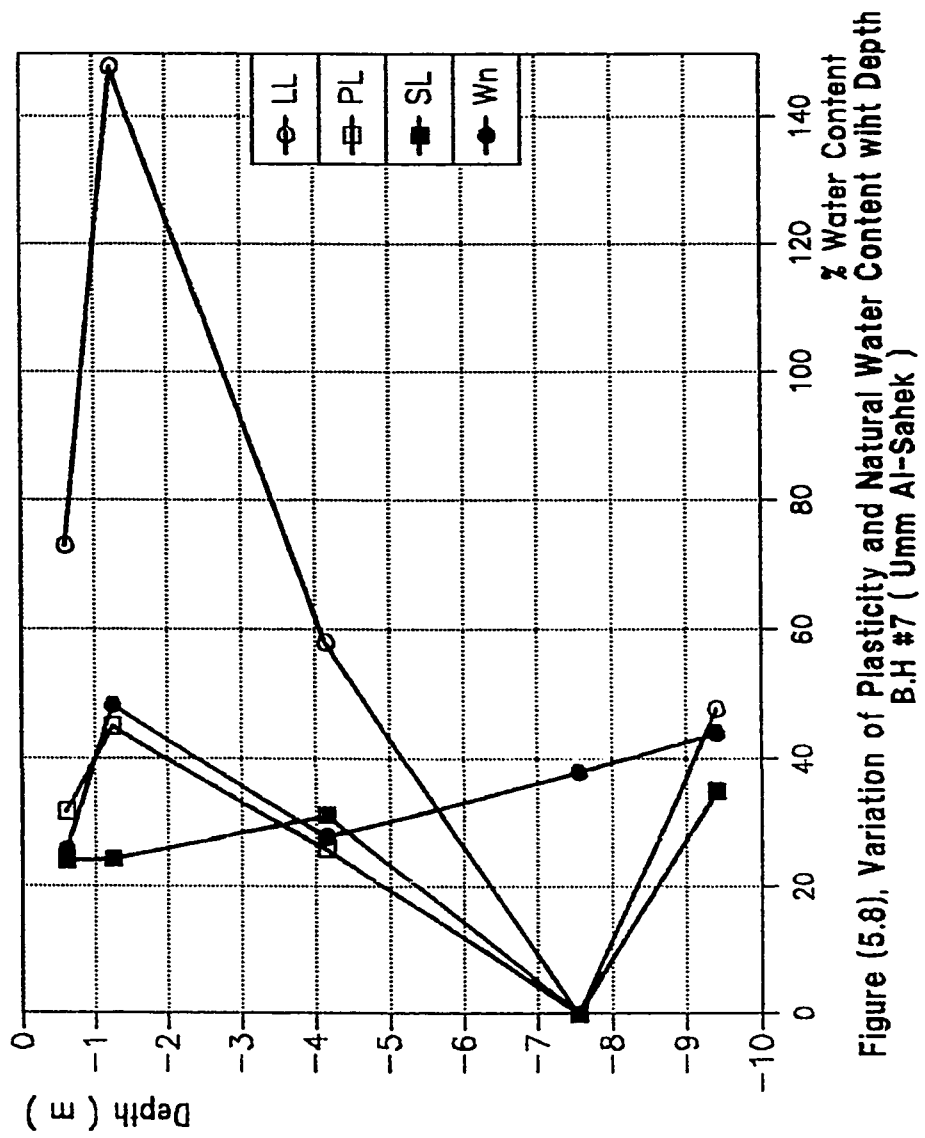


Figure (5.8), Variation of Plasticity and Natural Water Content with Depth B.H #7 (Umm Al-Sahek)

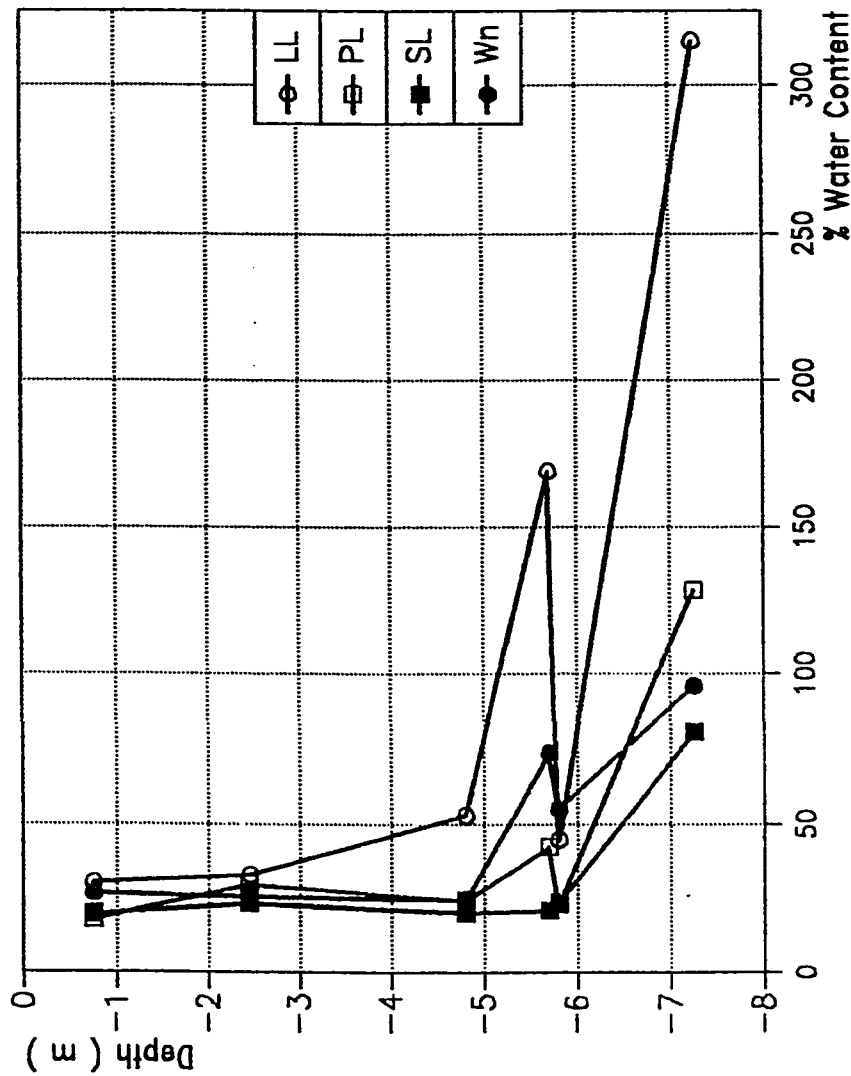


Figure (5.9). Variation of Plasticity and Natural Water content with Depth
B.H #8 (Umm Al-Hamam)

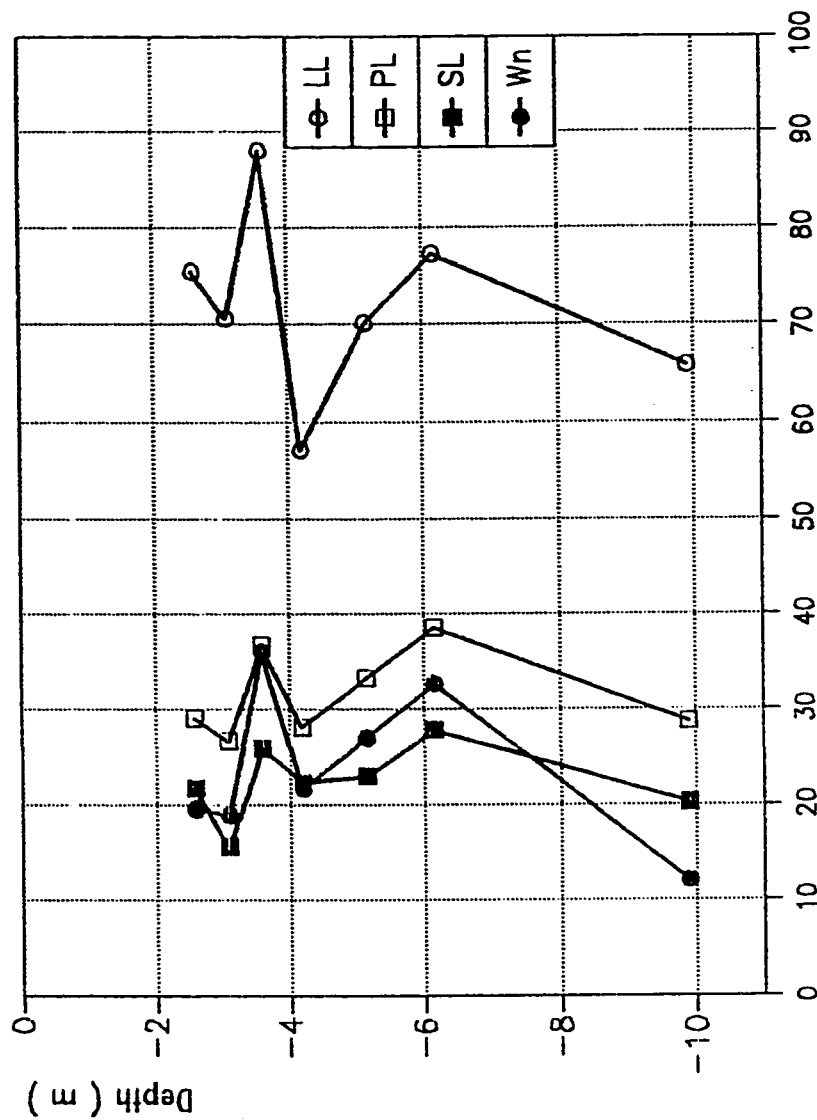


Figure (5.10), Variation of Plasticity and Natural Water Content with Depth
B.H #9 (Al-Hasa)

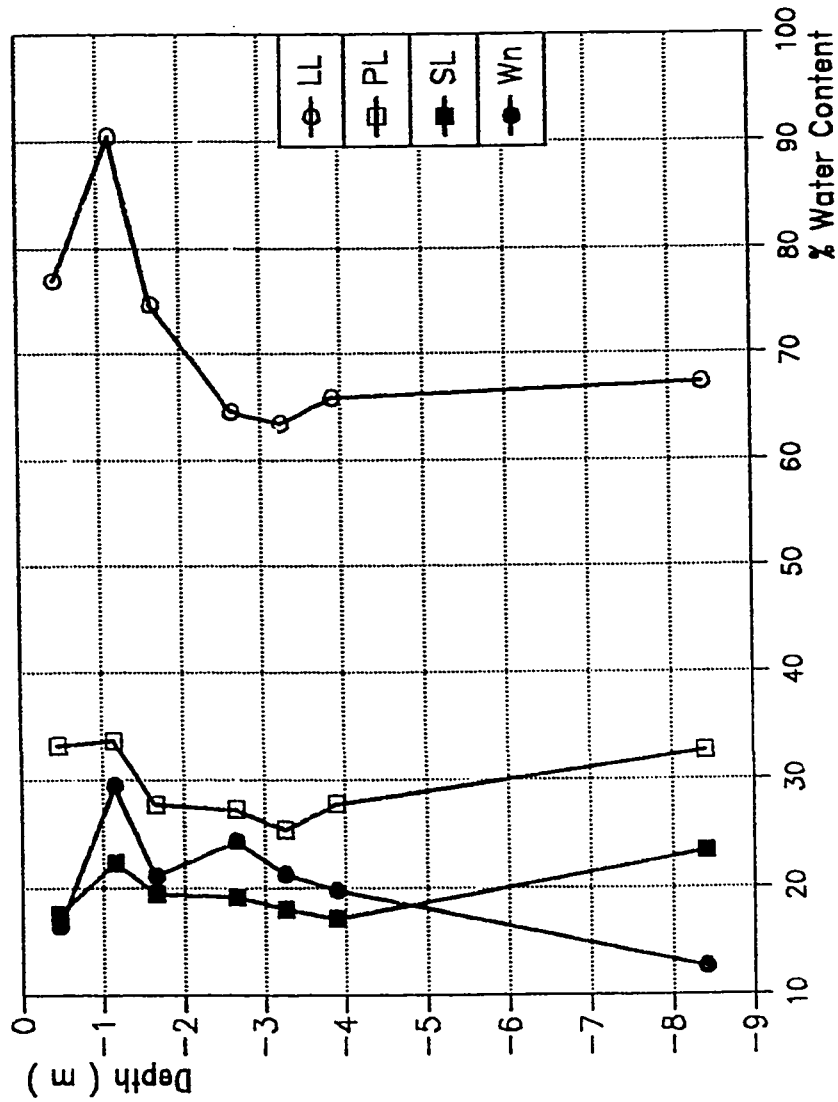


Figure (5.11), Variation of Plasticity and Natural Water Content with Depth
B.H #11 (Al-Hasa)

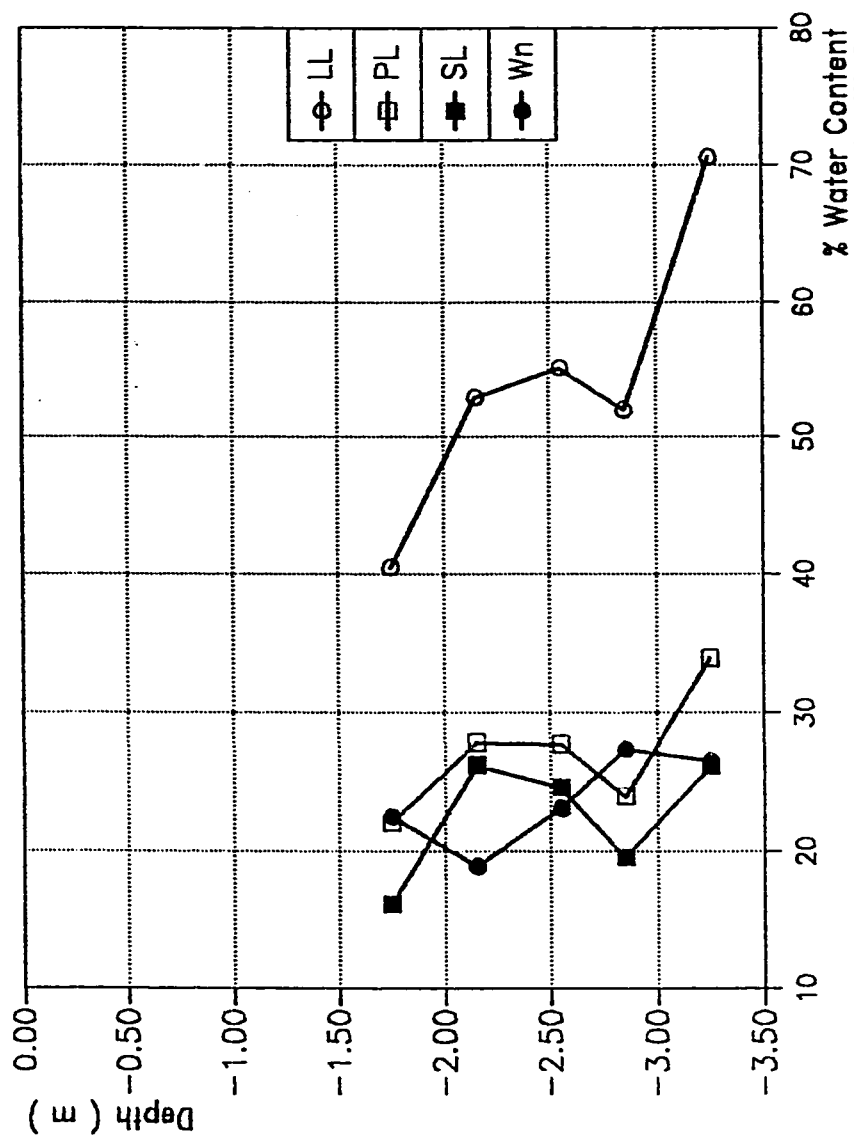


Figure (5.12), Variation of Plasticity and Natural Water Content with Depth
B.H #12 (Al-Hasa)

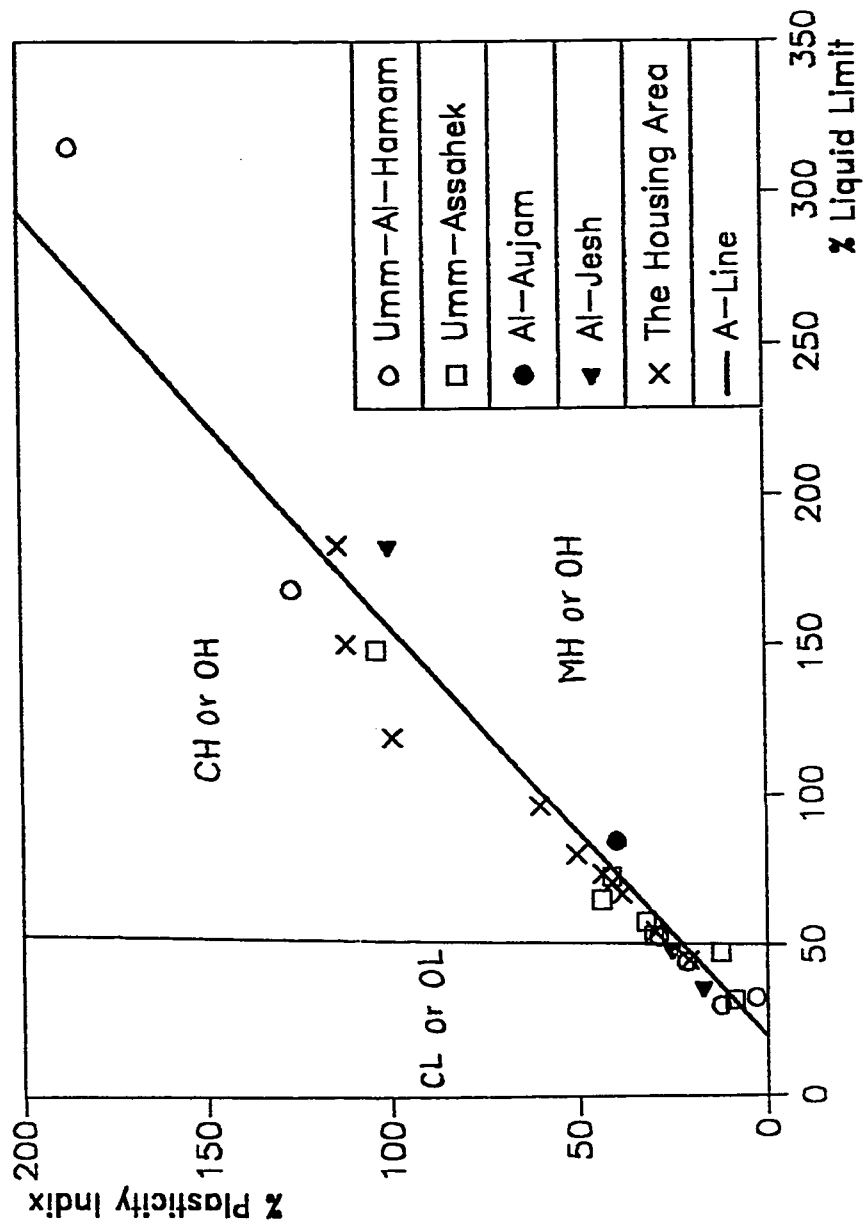


Figure (5.13) , Plasticity chart (AL Qatif B.H)

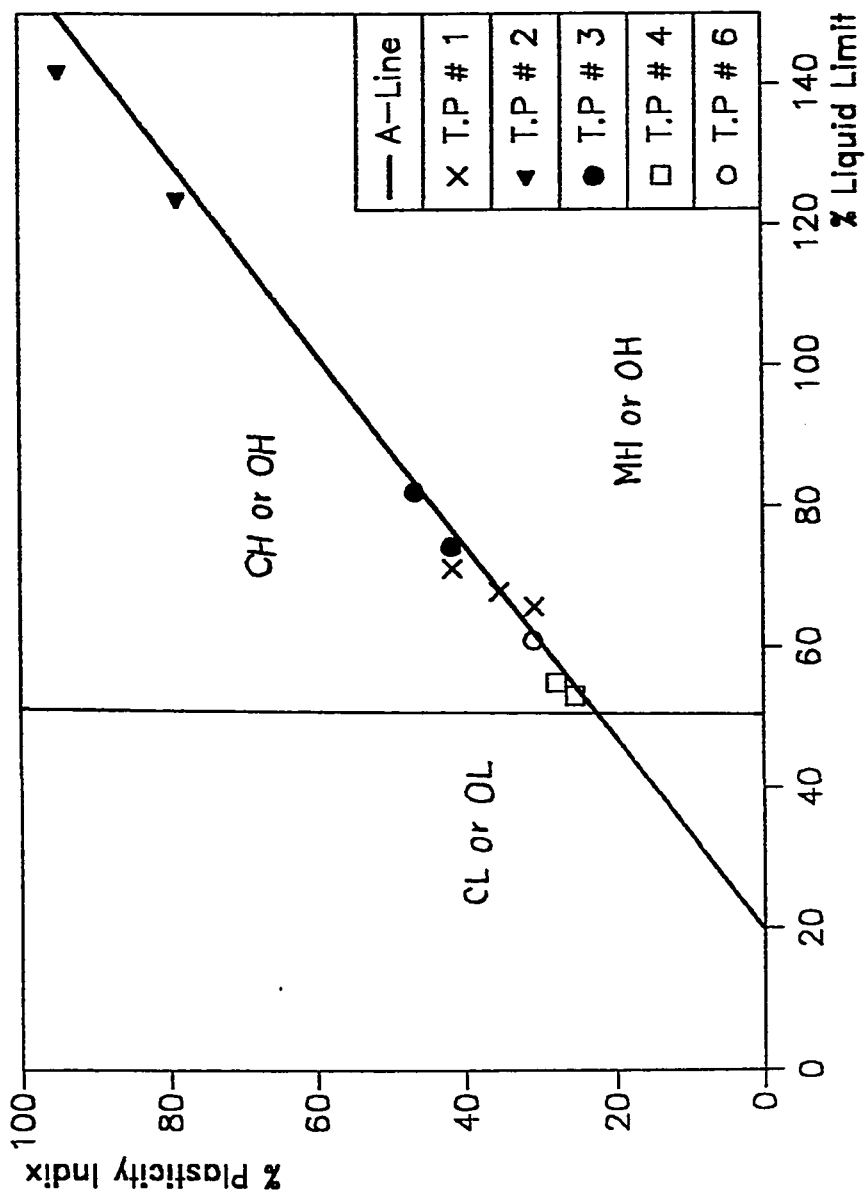


Figure (5.14) : Plasticity Chart (Al-Haso T.P)

Table 5.5: Classification of Al-Qatif Area Samples (Test Pits)

TP #	Sample	Depth	USCS*	After Darshan-murthy**	After Holtz***
1	1A	3.4-3.8	CH	V. High	V. High
1	1B	4.0-4.5	CH	Ext. High	V. High
2	2A	3.8-4.0	CH	Ext. High	V. High
2	2B	4.0	CH	Ext. High	V. High
3	3	3.5	CH	Ext. High	V. High
4	4	1.7	CH	Ext. High	V. High
5	5	1.4	--	----	----
6	6	1.5	CH	Ext. High	V. High

* Fig. 2.11

** Fig. 5.15

*** Table 2.6

Table 5.6: Classification of Al-Qatif Area Samples (Bore Holes)

BH #	Depth	USCS*	After Darshan-Murthy**	After Holtz***
1	3.5 3.8 4.0	CH CH CH	V. High Ext. High Ext. High	V. High V. High V. High
2	4.2, 51 4.2, 52 8.5	CH CH CH	Ext. High Ext. High High	V. High V. High V. High
3	1.8-2.1 4.0-4.15 4.8-5.0 7.9-8.2	CH CH CL CH	V. High High Medium Ext. High	V. High High Medium V. High
4	6.15 9.7, 10, 51 9.7, 10, 52	CH CL CL	Medium Medium Low	Medium Medium Medium
5	1.35 6.6-6.9	OH & MH	V. High	High
6	0.45-0.6 0.9-1.15 4.5-4.7 9.0-9.4	CH CL CH	High Low High	V. High Low High
7	0.4-0.8 1.1-1.4 4.0-4.3 7.5-7.6 9.2-9.6	CH CH CH ML & OL	V. High Ext. High High Medium	V. High V. High High Low
8	0.6-0.9 2.3-2.6 4.7-4.9 5.6-5.75 5.75-5.9 7.10-7.5	CL ML & OL CH CH CL CH	Low Low High Ext. High Medium Ext. High	Low Low High V. High Medium V. High

* Fig. 2.11

** Fig. 5.15

*** Table 2.6

Table 5.7: Classification of Al-Hasa Samples (Test Pits)

BH #	Depth	USCS*	After Darshan-murthy**	After Holtz***
7	0.9 1.1 1.5	OH & MH CH OH & MH	High V. High High	High V. High High
8	1.1 0.8-1.1	CH CH	Ext. High Ext. High	V. High V. High
9	1.1 2.2	CH CH	V. High V. High	V. High V. High
10	1.5-1.8 1.8-2.1	CH CH	High High	High High
11	1.8-2.1	CH	High	High

* Fig. 2.11

** Fig. 5.15

*** Table 2.6

Table 5.8: Classification of Al-Hasa Samples (Bore Holes)

BH #	Depth	USCS*	After Darshan-murthy**	After Holtz***
9	2.5-2.7	CH	V. High	V. High
	3.0-3.2	CH	V. High	V. High
	3.5-3.7	CH	V. High	V. High
	4.0-4.3	CH	High	High
	5.0-5.3	CH	V. High	High
	6.0-6.3	CH	V. High	High
	9.8-10.0	CH	High	High
10	0.8-1.1	CH	High	High
	4.0-4.2	CH	High	High
11	0.3-0.6	CH	V. High	V. High
	1.0-1.3	CH	Ext. High	V. High
	1.5-1.8	CH	V. High	V. High
	2.5-2.8	CH	High	High
	3.1-3.4	CH	High	High
	3.8-4.0	CH	High	High
	8.3-8.5	CH	High	High
12	2.6-1.9	CL	Medium	Medium
	2.0-2.3	CH	High	Medium
	2.4-2.7	CH	High	Medium
	2.7-3.0	CH	High	Medium
	3.1-3.4	OH & MH	V. High	High
13	1.6-1.9	CH	High	High
	2.0-2.25	CH	High	High

* Fig. 2.11

** Fig. 5.15

*** Table 2.6

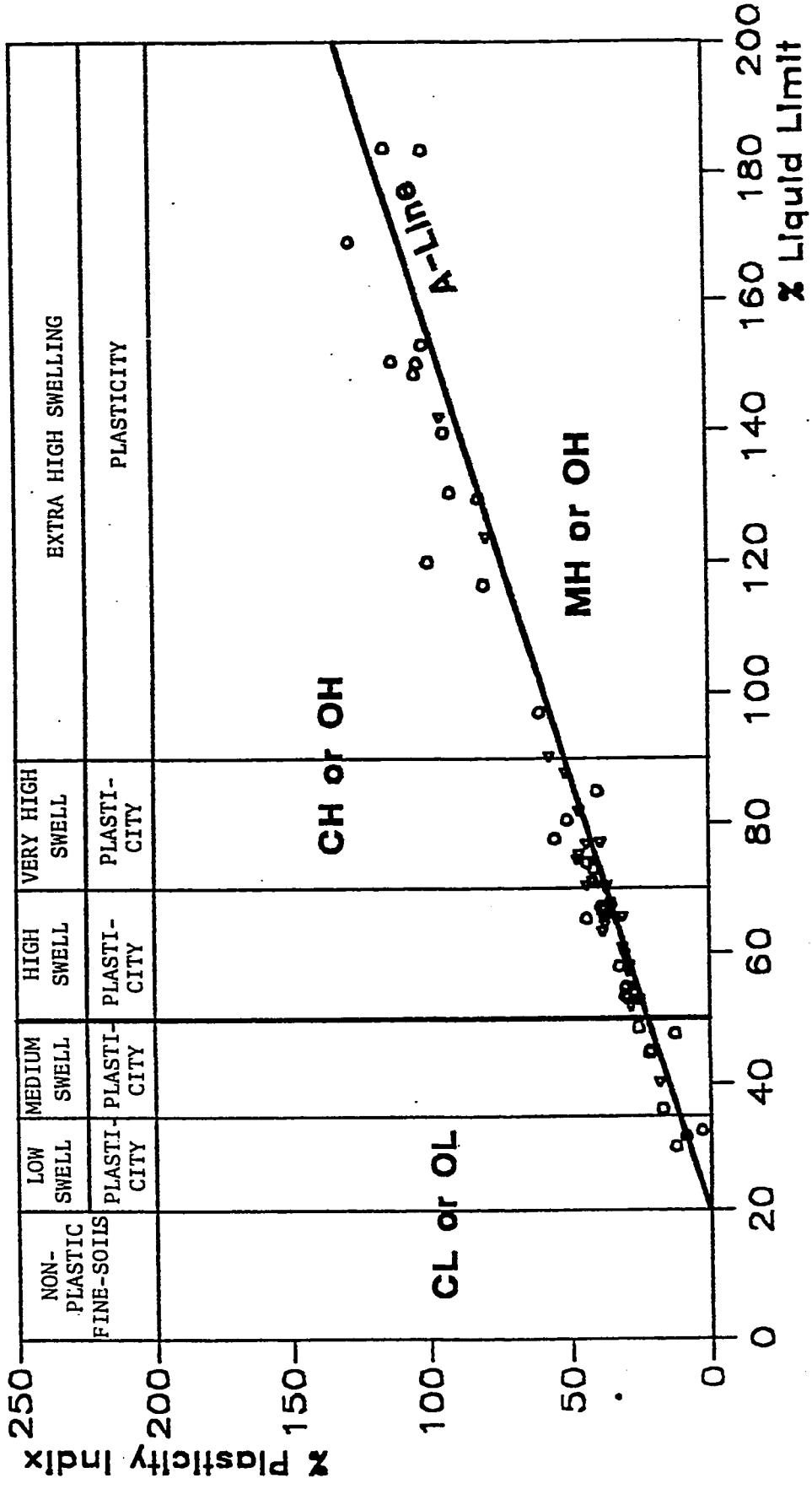


Figure (5.15), Chart for Potential Expansiveness of all Samples

plasticity chart for all the samples collected from both Al-Hasa and Al-Qatif areas. The Results show that most of the samples can be classified as CH, which means, as can be seen in tables 5.5-5.8, an expected high swell potential. As will be seen in chapter #6, the plasticity of the sample is the most important geotechnical property that determines the swellability. More specifically, liquid limit and plasticity index are good indicators of the swell potential. In fact, Seed as well as other investigators have demonstrated that plasticity index alone can be used as a preliminary indication of the swelling characteristics of most clays. It is not surprising that the liquid limit and the swelling of of clays are related, since they both depend on the amount of water a clay tries to imbibe. The results of this study show that the shrinkage limit is not a suitable index for determining the swellability of the clay in the study area. It is worth noting that for the samples under study the plasticity index can be calculated from the liquid limit value according to the following equation :

$$PI = LL / 1.7$$

The results obtained using this equation are very close to the measured values.

5.2 MINERALOGICAL COMPOSITION

Mineralogical identification is very necessary in order to

get a clear picture of the mineralogical composition of the samples under study. X-Ray diffraction analysis was conducted for eleven samples.

The samples were mechanically disaggregated and ground by hand in a porcelain mortar pestle to a powder form. Samples were sent to the R.I at KFUPM for testing. Table 5.9 shows the location of each sample. The diffraction patterns, shown on Figures B.1 to B.22 in Appendix-B, were matched with the standard patterns prepared by the Joint Committee of Powder Diffraction Data Service (JCPDS). Using this method the different clay and non-clay minerals present were identified qualitatively. The quantitative analysis was performed by comparing the ratios of the intensities of different lines or peak areas from the different minerals with that from the standard substance, as presented in tables B.1 to B.11 in Appendix B. In this method, the height of the most intense peak of the non-clay mineral in the sample is compared to that of the standard substance. However, for clay minerals the peak areas under the diffraction curve are compared with the corresponding standard intensity. The mineralogical composition of sample #3 (B.H #11, Depth: 1.0-1.3 m) is presented here as an example to illustrate the procedure used to determine the percentage of each mineral in the sample.

- Qualitative Analysis

Table (5.9), XRD-Samples

Sample #	Source	Depth (m)
1	B.H # 9	2.5-2.7
2	B.H # 13	2.0-2.25
3	B.H # 11	1.0-1.3
4	B.H # 12	2.4-2.7
5	T.P # 7	1.1
6	TP # 9	2.2
7	TP # 11	2.0-2.2
8	B.H # 1	3.8
9	B.H # 3	1.8-2.1
10	B.H # 6	0.45-0.6
11	B.H # 8	5.6-5.75

The qualitative analysis is performed by matching the diffraction pattern shown in Figure 5.16 with the standard patterns as the ones shown in Figure 5.17 for quartz, calcite and kaolinite. The type of mineral is marked over the corresponding peak as shown in Figure 5.16. The qualitative analysis for this sample shows that it contains : quartz (Q), calcite (C), palygorskite (P), illite (I), kaolinite (K), smectite (S) and sepiolite (St). The next step is to determine the percentage of each mineral in the sample.

- Quantitative Analysis

* From Figure 5.16, the height of the peak at $2\theta = 26.7^\circ$ measured from the peak to the background is 2333.3 according to the given scale. The standard intensity for quartz is 10935. Then,

$$\% \text{ Quartz} = (2333.3/10935)*100 = 21.34$$

* For calcite, Figure 5.17 is used since the peak at $2\theta = 29.4^\circ$ is not complete in Figure 5.16. The intensity of the peak is 6066.7 . The standard intensity for calcite is 8226. Then,

$$\% \text{ Calcite} = (6066.7/8226)*100 = 73.75$$

* Palygorskite: The area between the lines of $2\theta = 7.5^\circ$ and $2\theta = 8.5^\circ$ and the diffraction spectrum is used to find the

SAMPLE: ABJ File: ABJ3.RD 15-JUN-91 16:04

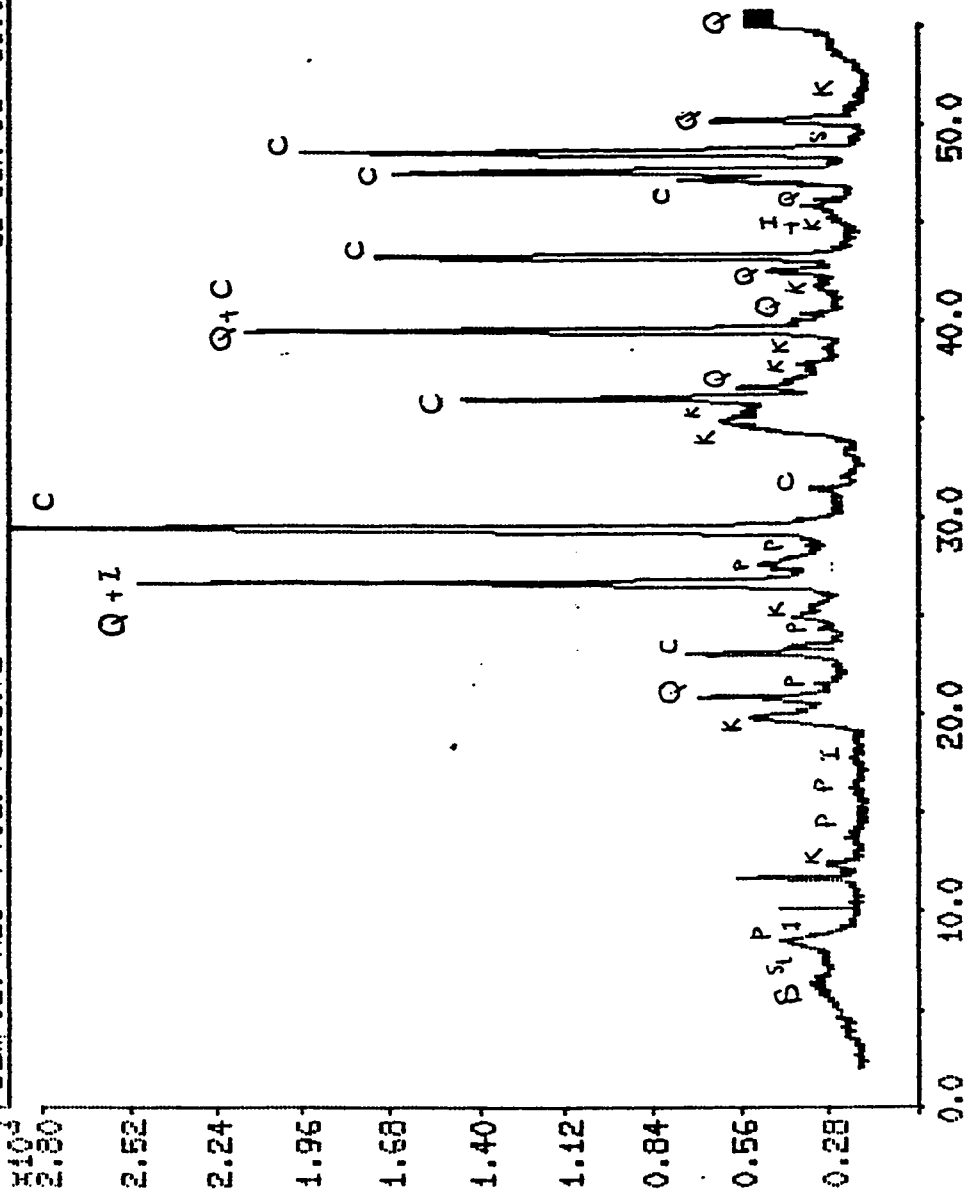


Fig. 5.16 XR-Diffraction Pattern for Sample # 3, BH # 11 (1.0-1.3 m)

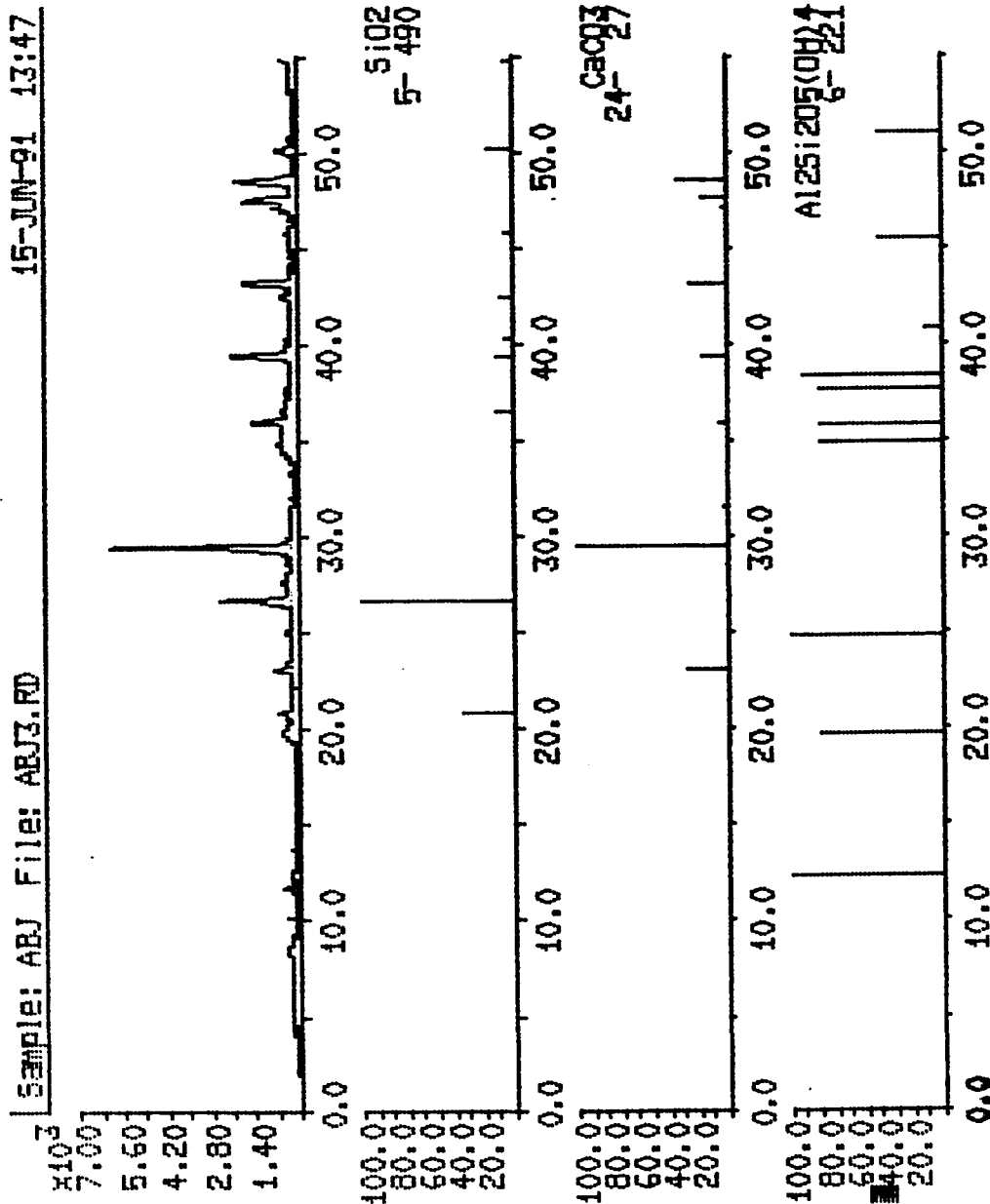


Fig. 5.17 XR-Diffraction Pattern for Sample # 3

palygorskite percentage. The area, shown in Figure 5.18, is 83.48 units according to the given scale. The standard area for palygorskite is 517 (see Table B.3). Then,

$$\% \text{ Palygorskite} = (83.48/517)*100 = 16.15$$

* Illite : Area under the XRD pattern and $2\theta = 8.5^\circ$ and $2\theta = 9.0^\circ$ is 55.65, Figure 5.18. The standard area for illite is 87.5. Then,

$$\% \text{ Illite} = (55.65 / 87.5) * 100 = 63.6$$

* Kaolinite : Area between $2\theta = 11.5^\circ$ and $2\theta = 12.5^\circ$ is 41.74. Standard area for kaolinite is 570. Then,

$$\% \text{ Kaolinite} = (41.74 / 570) * 100 = 7.3$$

* Smectite : Area between $2\theta = 4.0^\circ$ and $2\theta = 7.5^\circ$ is 211.5. Standard area for smectite is 1210. Then,

$$\% \text{ Smectite} = (211.5 / 1210) * 100 = 17.48$$

* Sepiolite : Area between $2\theta = 6.5^\circ$ and $2\theta = 7.5^\circ$ is 86.26. Standard area for sepiolite is 820. Then,

$$\% \text{ Sepiolite} = (86.26 / 820) * 100 = 10.52$$

The determined percentages are then normalized as shown in table B.3 in Appendix B.

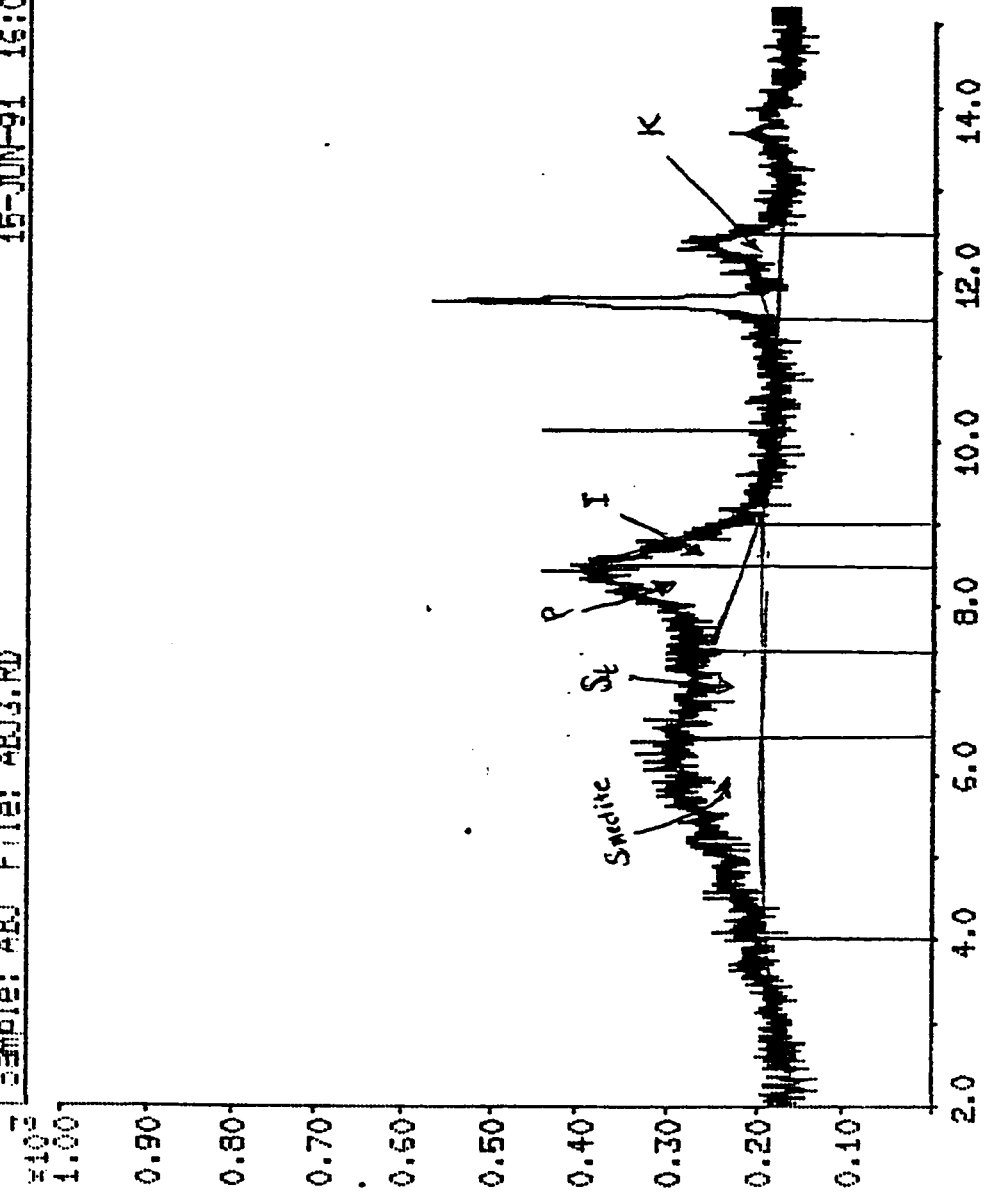


Fig. 5.18 XR-Diffraction Pattern (enlarged scale) for Sample # 3, BH # 11 (1.0-1.3 m)

The quantitative analysis results for other samples are tabulated in tables B.1 to B.11.

As can be seen from table 5.10 and Figures B.1 to B.22, the samples are mixtures of clay and non-clay minerals. All Samples contain quartz, palygorskite and smectite. Most of the samples contain calcite, sepiolite, kaolinite and illite. Sample #4 (BH#12) is rich in illite (47%), and contains Na-type smectite. Sample #8 (BH #1) from Al-Qatif Housing area contains talc and 30% of Ca-type montmorillonite. Sample #9 (BH#3) is also from Al-Qatif Housing area and its mineralogical composition is similar to that of sample#8, however, this sample is rich in dolomite (32%) and smectite percentage is 25%. Sample#10 (BH #6) is from Umm Al-Sahek area and is characterized by the presence of gypsum (11%) as well as dolomite (48%). Sample #11 consists mainly of illite (39%), smectite (39%) and palygorskite (11%). The presence of smectite in all samples points that the clay of this area must have a swelling nature. The effect of the mineralogical composition on the percentage of swelling will be discussed in the following chapter.

Table(5.10): Mineralogical Composition of Some Selected Samples.

Sample #	Location	B.H/ TP #	Depth	Mineral Type (% Composition)
1	Al-Khars, Al- Hasa	BH # 9	2.5 - 2.7	C(50), Q(10), P(8) K(5), I(19), S(7)
2	Mahasen- ARAMCO Al-Hasa	BH # 13	2.0 - 2.225	C(34), Q(16), P(8), K(3), I(31), S(4), St(4)
3	Al-Hamadiya	BH # 11	1.0 - 1.3	C(35), Q(10), P(8), K(3), I(30), S(8), St(5)
4	Al-Salehiya	BH # 12	2.4 - 2.7	C(19), Q(19), P(4), K(4), I(47), D(1), S(6)
5	Ai-Khars, Al-Hasa	TP # 7	1.1	C(39), Q(11), P(10), K(11), I(19), S(6), St(4)
6	Al-Naathel, Al-Hasa	TP # 9	2.2	C(61), Q(24), P(6), K(3), S(6)
7	Mahasen- ARAMCO Al-Hasa	TP # 11	2.0 - 2.2	C(27), Q(19), P(10), K(5), I(32), S(4), St(3)
8	Housing Area	BH # 1	3.8	Q(9), P(9), S(30), St(12), T, I(40)
9	Housing Area	BH # 3	1.8 - 2.1	Q(7), K(<1), S(25), St(10), P(4), D(32), I
10	Umm Al-Sahek	BH # 6	0.45 - 0.6	Q(4), K(<1), P(2), S(13), G(11), D(48), I(22)
11	Umm Al-Hamam	BH # 8	5.6 - 5.75	C(<1), Q(10), P(11) D(<1), S(39), I(39)

(C) Calcite, (Q) Quartz, (P) Palygorskite, (K) Kaolinite, (I) Illite, (D) Dolomite,
(St) Sepiolite, (S) Smectite, (G) Gypsum, (T) Talc.

Chapter 6

SWELL CHARACTERISTICS

6.1 INTRODUCTION

Once a potentially expansive soil has been identified and a qualitative indication of the potential swell has been made, quantitative characterization of the expansive soil is necessary to determine the amount of volume change. Techniques available for quantitative characterization of expansive soils fall into three categories, namely, odometer tests, soil suction tests, and empirical methodology (52). This study involves the use of the first and the third of the aforementioned categories.

6.2 SWELL TEST

The most important laboratory test on expansive soils is the swell test. The test was conducted on a standard one-dimensional consolidation test apparatus similar to that used in most soil laboratories for consolidation studies. This apparatus, is called an odometer and is shown in figure 6.1.

The swell test was conducted on both remolded and undisturbed samples. Undisturbed samples were taken from test pits blocks or bore holes tubes. Paraffin wax was removed by a sharp

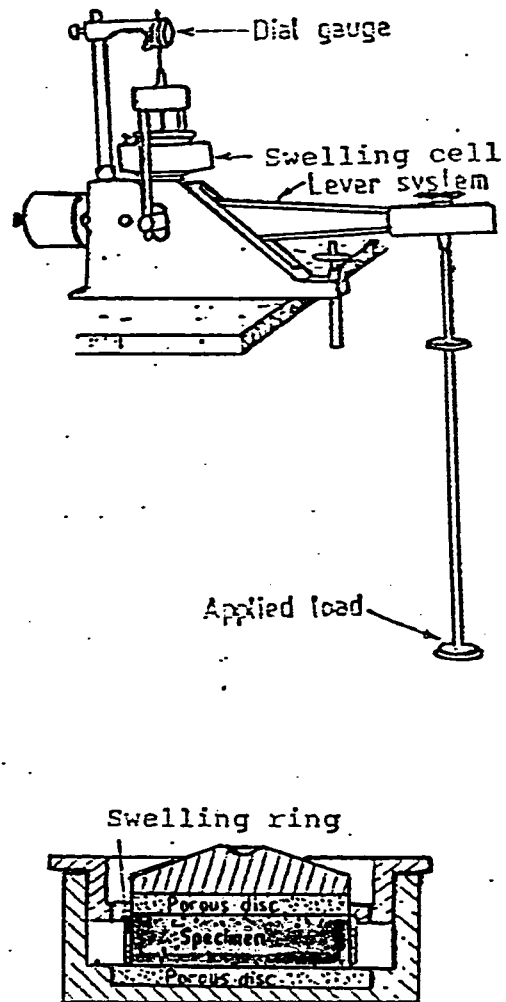


Figure 6.1 Swelling one-dimensional odometer apparatus.

edged knife. After confirming the layering system, the consolidometer ring was pushed down slowly to get a sample with a minimum degree of disturbance. Since most of the samples were quite wet due to high natural moisture content, it was easy to get undisturbed samples just by pushing the ring with hands. extra soil was removed from the top of the ring, getting a sample equal to the height of the ring. The sample enclosed in 6.9 cm X 1.9 cm brass ring was placed in the odometer between two porous stones and two paper filters. The sample was then subjected to a surcharge of 1 psi until a constant change in the height of the sample was recorded. Distilled water was then introduced into the odometer and the sample was flooded both from the top and bottom of the ring. The increase in the height of the sample was recorded by a portable data logger (TDS-300) at programmed intervals until a constant maximum reading was attained. Percentage of swell is calculated according to:

$$\text{Percentage of Swell} = \frac{\text{change in height}}{\text{Original height}} \times 100 \quad (1)$$

A small load was then added and kept until a constant reading was reached, and the processes continued until the sample returned to its original height. The swell pressure was then calculated as follows :

$$\text{Swell pressure} = \frac{(\text{Total load needed for restoring initial height}), (\text{kg})}{(\text{Area of the sample}) (\text{cm}^2)} \quad (2)$$

For the remolded samples, the sample was prepared by compressing a certain weight of the soil in the ring such that the unit weight of the specimen is equal to the natural unit weight of the soil. The swell test was then run in the same way as the undisturbed sample.

6.3 SWELL RESULTS

The percentage of swell for all samples is shown in tables 5.1 to 5.4. The percentage of swell was plotted vs. time to present the volume change of each sample after the addition of water. Figures 6.2 to 6.13 show the swell percentage vs. time for samples collected from Al-Qatif area, while Al-Hasa samples curves are shown in figures 6.14 to 6.25.

As can be observed from table 5.1 & 5.2 and Figs. 6.2 - 6.13 a high percentage of swell was exhibited by most of the samples from Al-Qatif Housing Area. Figure 6.2 shows the results of % swell for the samples collected from the test pits of Al-Qatif area. This figure shows that sample 2B (TP#2, 4.0 m), has recorded 29.49 % swell which is the highest value recorded of all the samples tested. The high percentage of swell in this sample is attributed to its very high plasticity (PI = 150.2 %). The natural water content of this sample is close to its plastic limit, which is

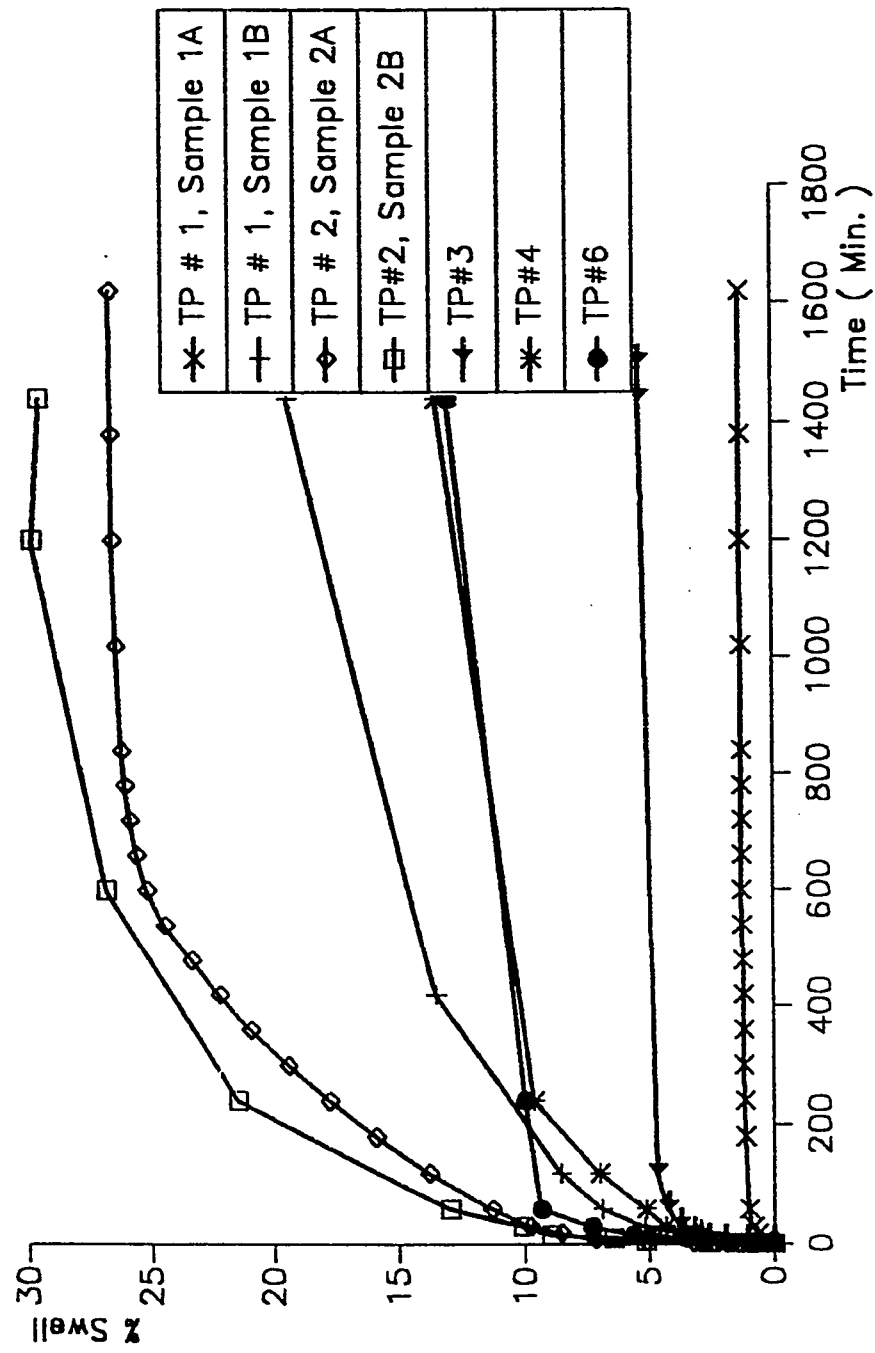


Figure (6.2) : % Swell vs Time For Al- Qatlif Area(Test Pits).

considered a critical percentage of water content. Moreover, the mineralogical composition of Al-Qatif Housing area clays indicates, as can be seen in table 5.10 and figures 5.29 & 5.30, that the clay is rich with smectite (>25%) which is the most expansive clay mineral. This sample is classified in table 5.5, based on its plasticity characteristics, as a highly expansive sample. This indicates that the plasticity is a useful index to identify the swell potential of the clay. Sample #5 (TP#5, 1.4 m) from Al-Aujam recorded zero swell potential and this was expected as it is non-plastic. Excluding this sample, other samples are considered to have high to very high swell potential. Sample # 1A (TP #1, 3.4 -3.8 m) has the lowest plasticity (PI = 77.7 %) compared to other samples shown in figure 6.2 and consequently it has the lowest percentage of swell (1.27 %).

Most of samples from Al-Qatif bore holes were undisturbed or with a minimum degree of disturbance. Thirty samples from eight bore holes were tested and the percentage of swell are presented in table 5.2 as well as Figs. 6.3 - 6.13. A maximum percentage of swell 29 % was recorded for a sample from BH#1 and at depth 3.8 m in Al-Qatif Housing area, (Fig. 6.3). This sample has a high plasticity (PI = 99.4%) and very rich with smectite (30%) as shown in table 5.19. Figure 6.4 shows the results for the same samples from BH #1 on a semi-log. scale. As can be noted in this figure the process of swelling with time can be divided into three

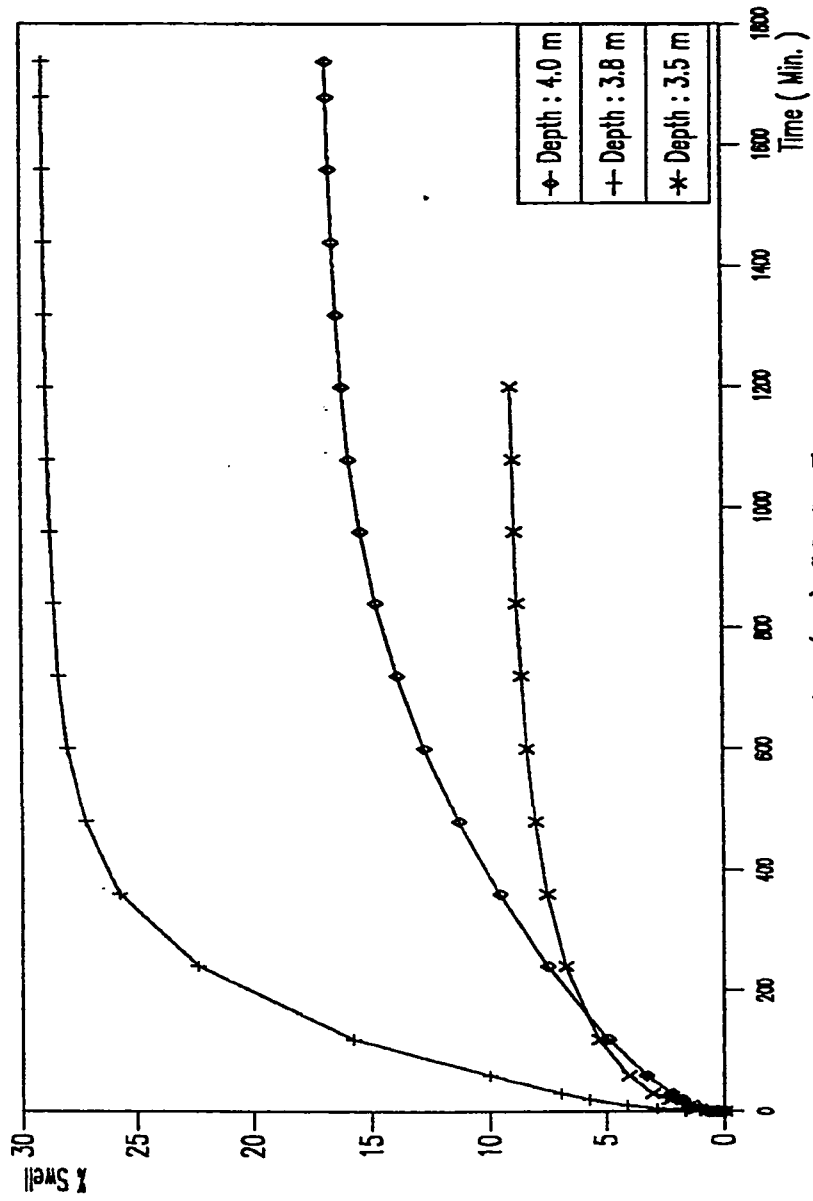


Figure (6.3) : % Swell vs Time
Bore Hole # 1, The housing area

123

174

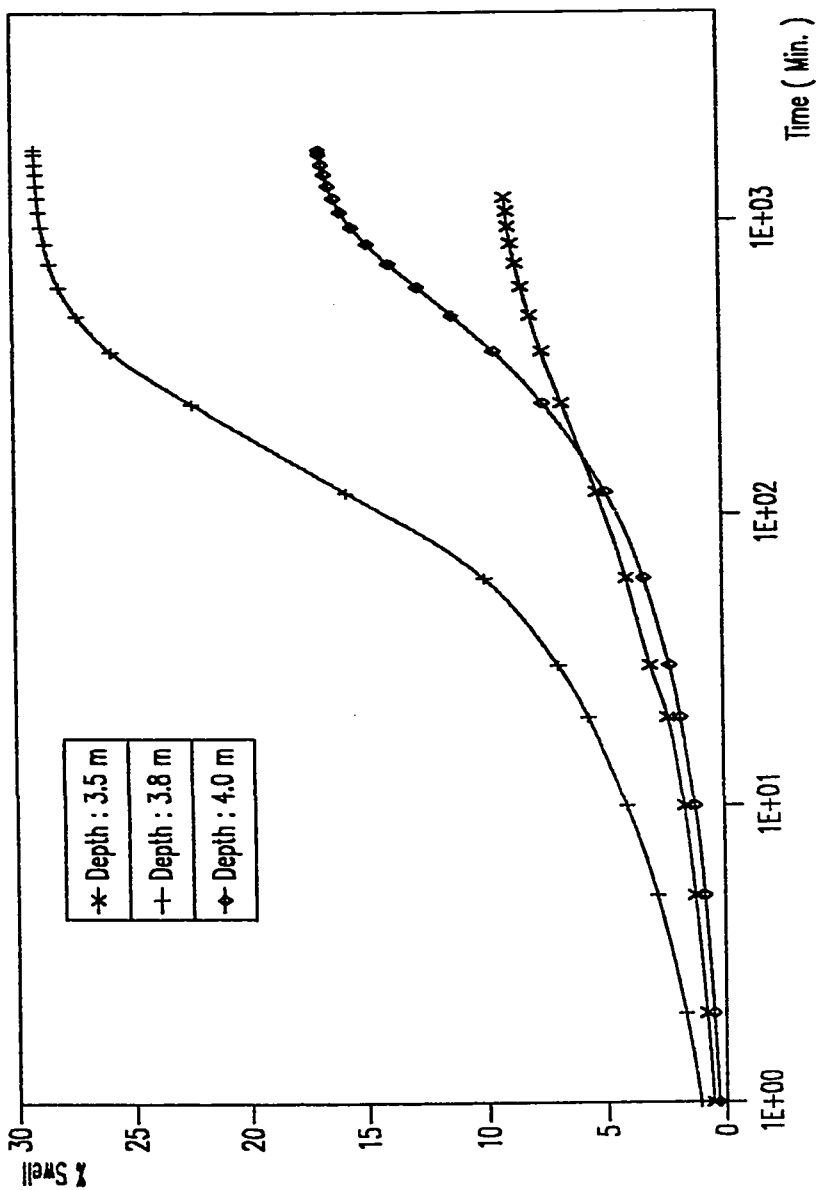


Figure (6.4), % Swell vs Time For B.H # 1

stages: initial, intermediate and final which may be simulated to instantaneous, primary and secondary consolidation. When water is added to the sample, swelling starts slowly till interaction between water and clay takes place after which a sudden increase in swelling occurs till the sample reaches its maximum swell. Figure 6.5 shows the swelling curves for three samples collected from BH#2. It is interesting to note that sample #1 (4.2 m) exhibited 19.56 % swell while sample #2 (4.3 m) exhibited only 0.61 % swell. This difference in the swell potential is a direct result of the difference in the plasticity and initial water content. Sample#1 has a higher plasticity than sample#2, and its initial water content is close to its plastic limit. The same behavior is also observed between Sample #1 (9.7-10 m) and Sample #2 (9.7-10) of B.H. #4 in Al-Jesh. In BH #3 (Fig. 6.6), the sample at depth 1.8-2.1 m, exhibits the maximum swelling. This sample as can be noted from table 5.2 has a higher plasticity and a lower initial water content than any other sample at different depth has. The mineralogical composition of this sample, presented in table 5.10 as well as table B.9 and Figure B.17, indicates that this sample is rich in montmorillonite (Ca-type) (25%) and contains dolomite, quartz, palygorskite, kaolinite and sepiolite. BH#6 was drilled in Umm Al-Sahek. Four samples were obtained from this bore hole, and their % swell vs. time curves are shown in Figure 6.9. Sample at depth 9.0-9.4 m was classified, based on its plasticity as a soil with a high expansivity, this was confirmed experimentally and the sample exhibited 18.75 %

swelling. On the other hand, the sample at depth 4.5-4.7 m was expected to have a small amount of swelling since it has low plasticity. The experimental results show that only 0.24 % swell was recorded by this sample. Umm Al-Sahek soil was observed visually to have a considerable amount of gypsum. The mineralogical composition for sample #10 (BH #6, 0.45-0.6 m) shows that the soil contains dolomite (48%), quartz, palygorskite, kaolinite, smectite (montmorillonite, Ca-type) (13%) as well as gypsum (11%). The presence of gypsum increases the cementation bonds and as a result reduces the amount of swelling. In general, Umm Al-Sahek samples recorded relatively low swell potential. By studying the results of Umm Al-Hamam, it is clear that only the samples with very high plasticity and low dry density exhibited a high percent of swelling. The sample at depth 5.6-5.75 m. exhibited the maximum swelling percentage (12.88%). This sample has a high plasticity (126.6%) and a very high percentage of smectite (39%) and illite (39%). This considerable amount of smectite indicates that percentage of swelling should be more than 12.88%, however, the swelling was limited to this value due to the high initial water content (73.6%). Figure 6.11 shows the swell behavior with time. This behavior is better noticed in figure 6.12 were the same curves were plotted on a semi-log scale. Again three stages can be identified during the swelling process. The variation of % swell with depth is shown in figure 6.49. Generally speaking, Al-Qatif area clay has a a very high swell potential. Al-Jesh, Al-Aujam,

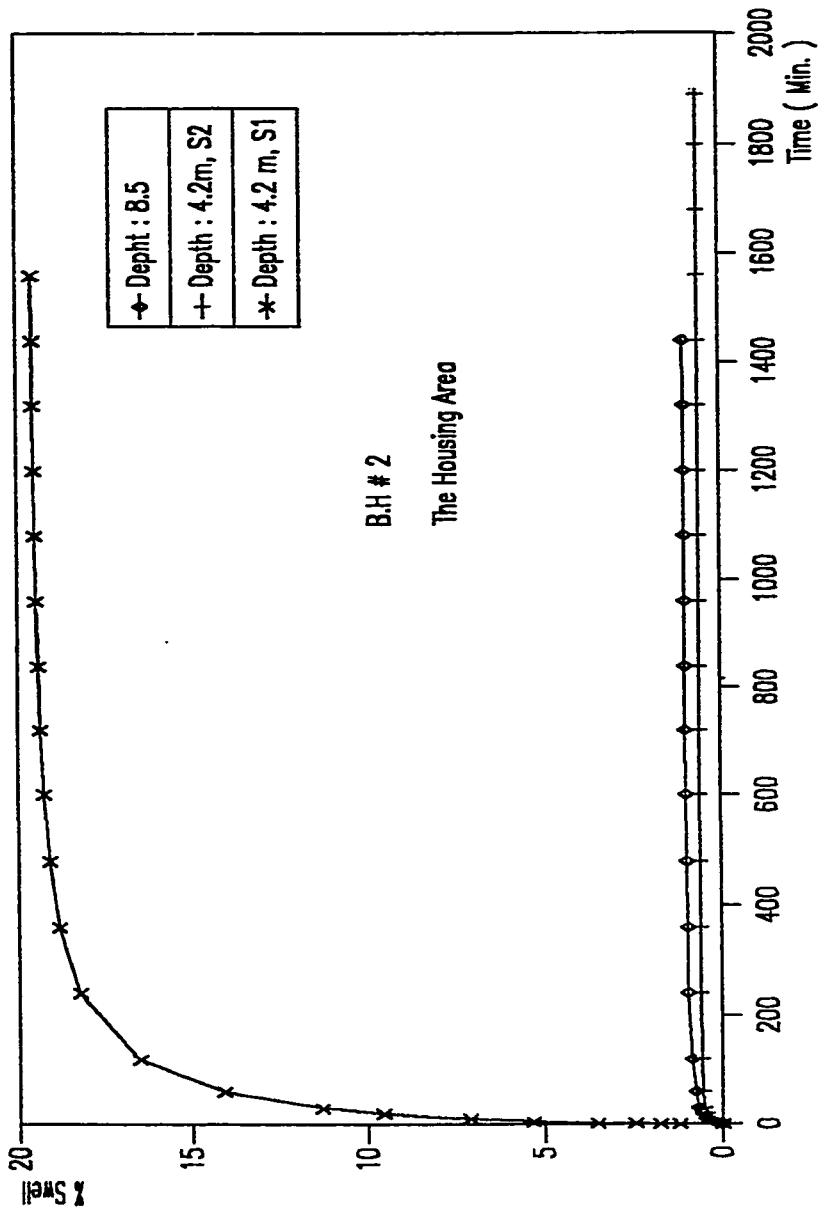


Figure (6.5) : % Swell vs Time

BH # 2, Al-Qatif Housing Area

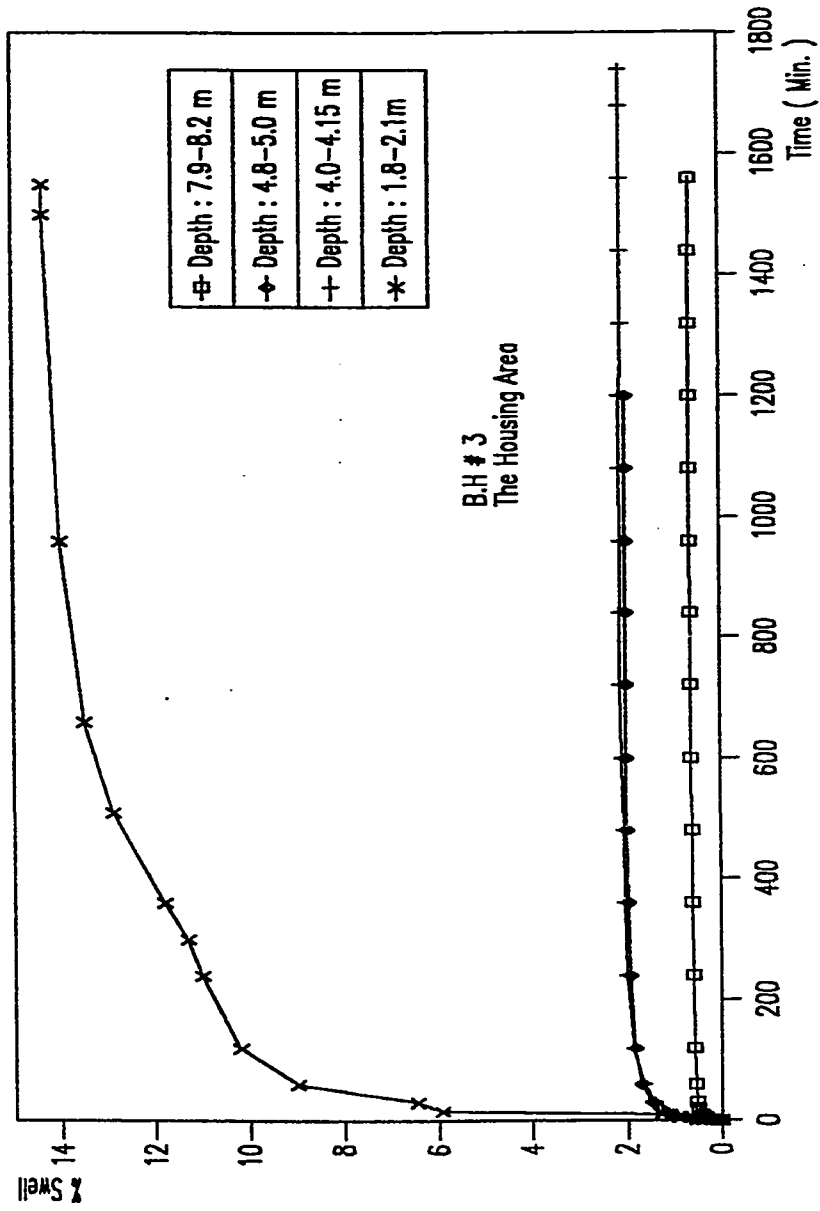


Figure (6.6) : % Swell vs Time

BH # 3, Al-Qatif Housing Area

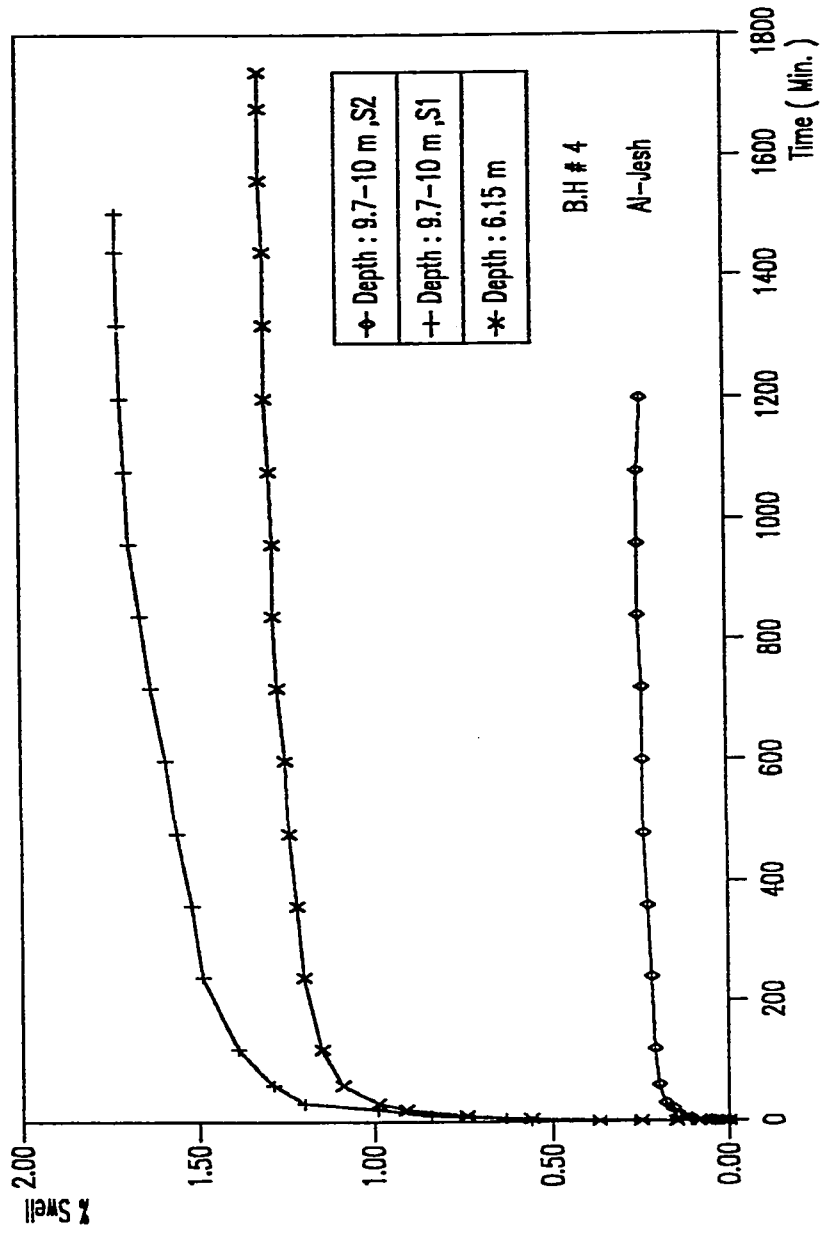


Figure (6.7) : % Swell vs Time

BH # 4, A1-Jesh

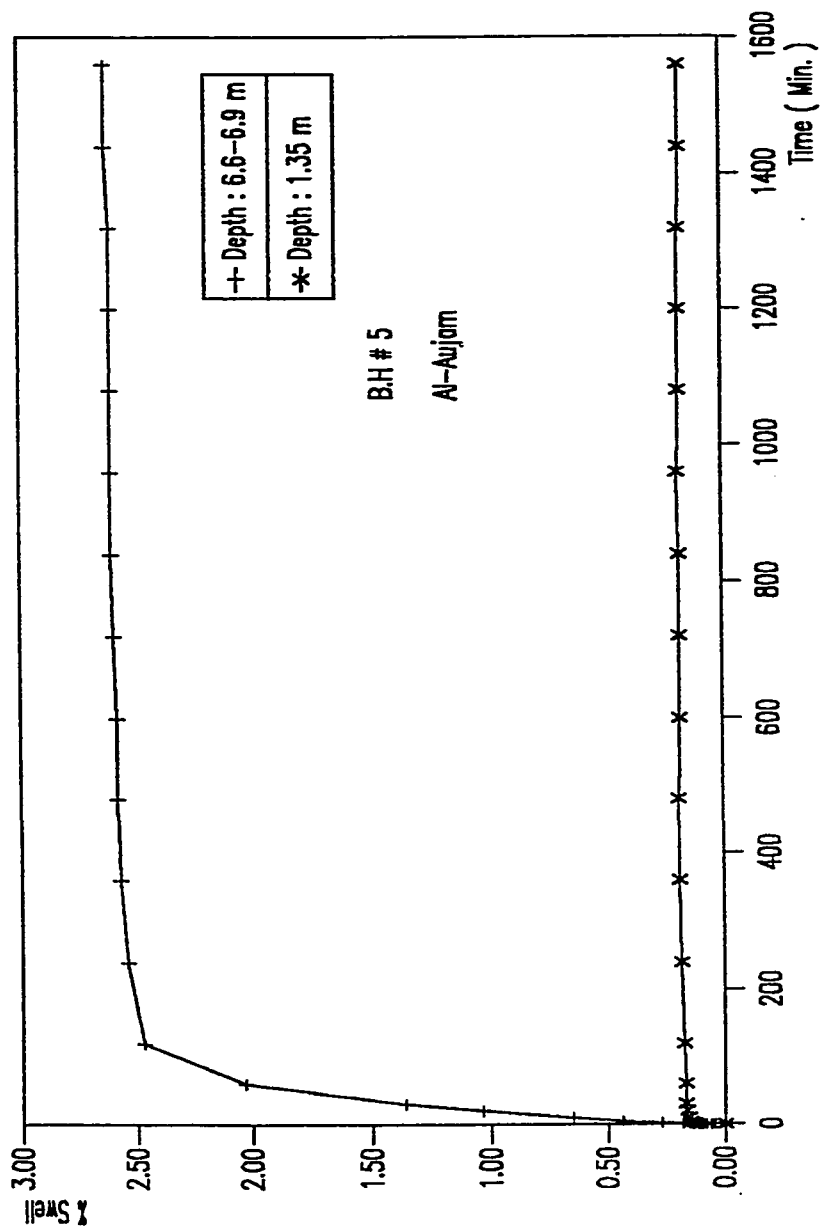


Figure (6.8) : % Swell vs Time

BH # 5, Al-Aujam

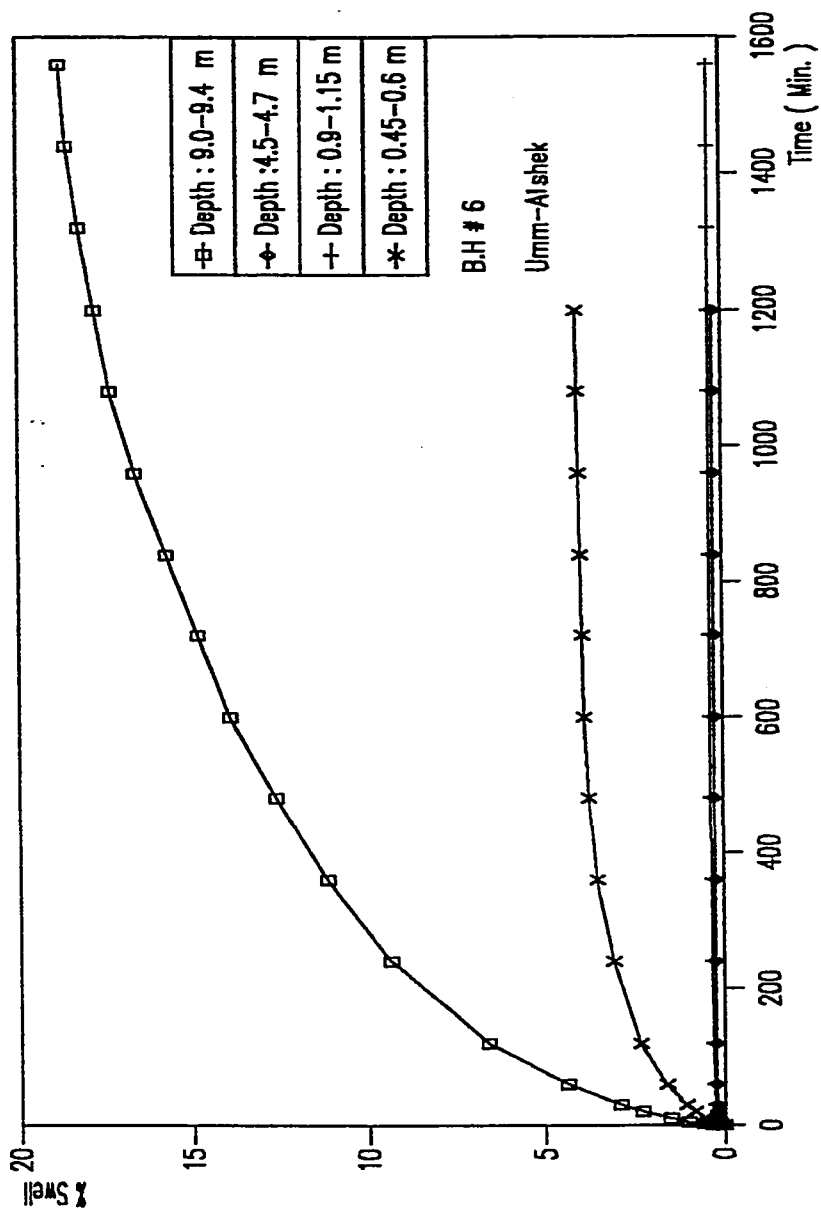


Figure (6.9) : % Swell vs Time

BH # 6, Umm Al-Sahek

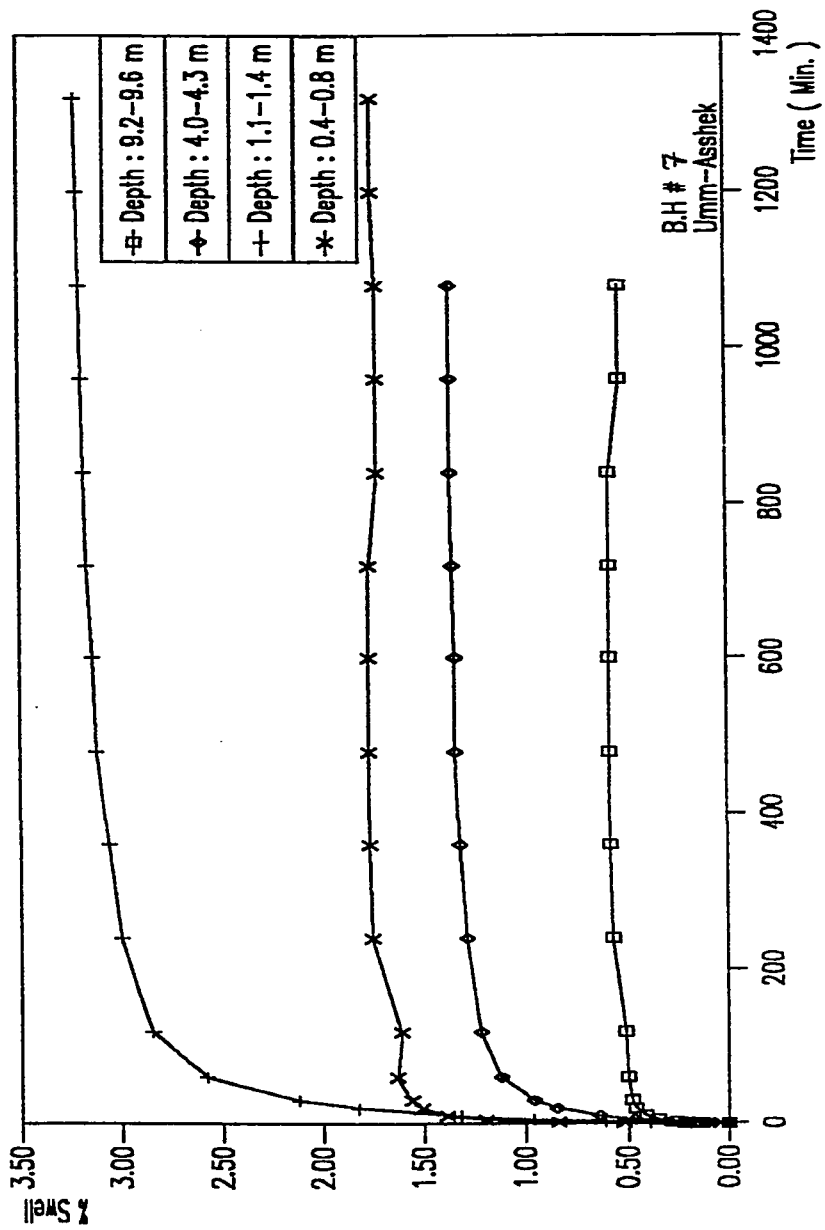


Figure (6.10) : % Swell vs Time

B.H # 7, Umm Al-Sahek

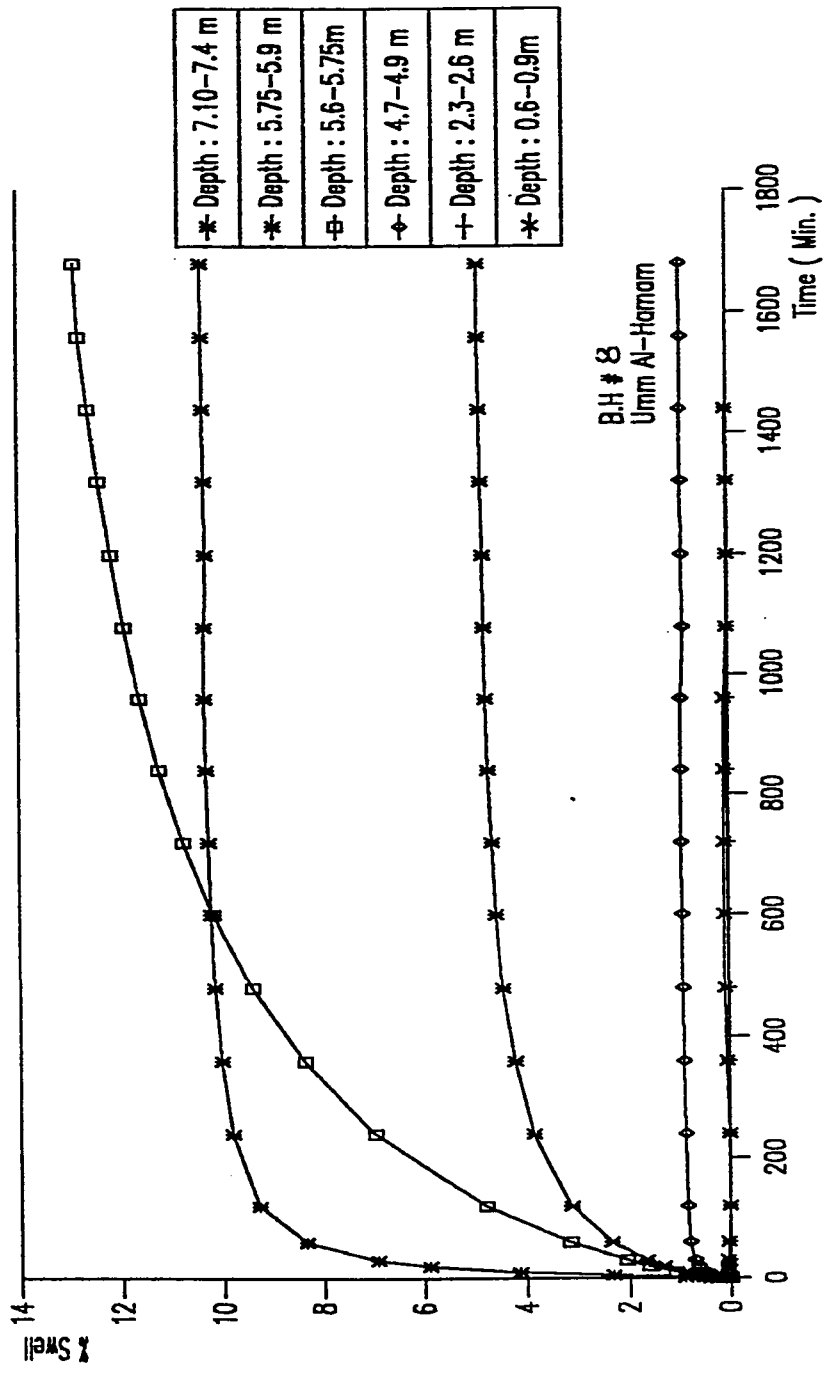


Figure (6.11) X Swell vs Time

BH # 8, Umm Al-Hamam

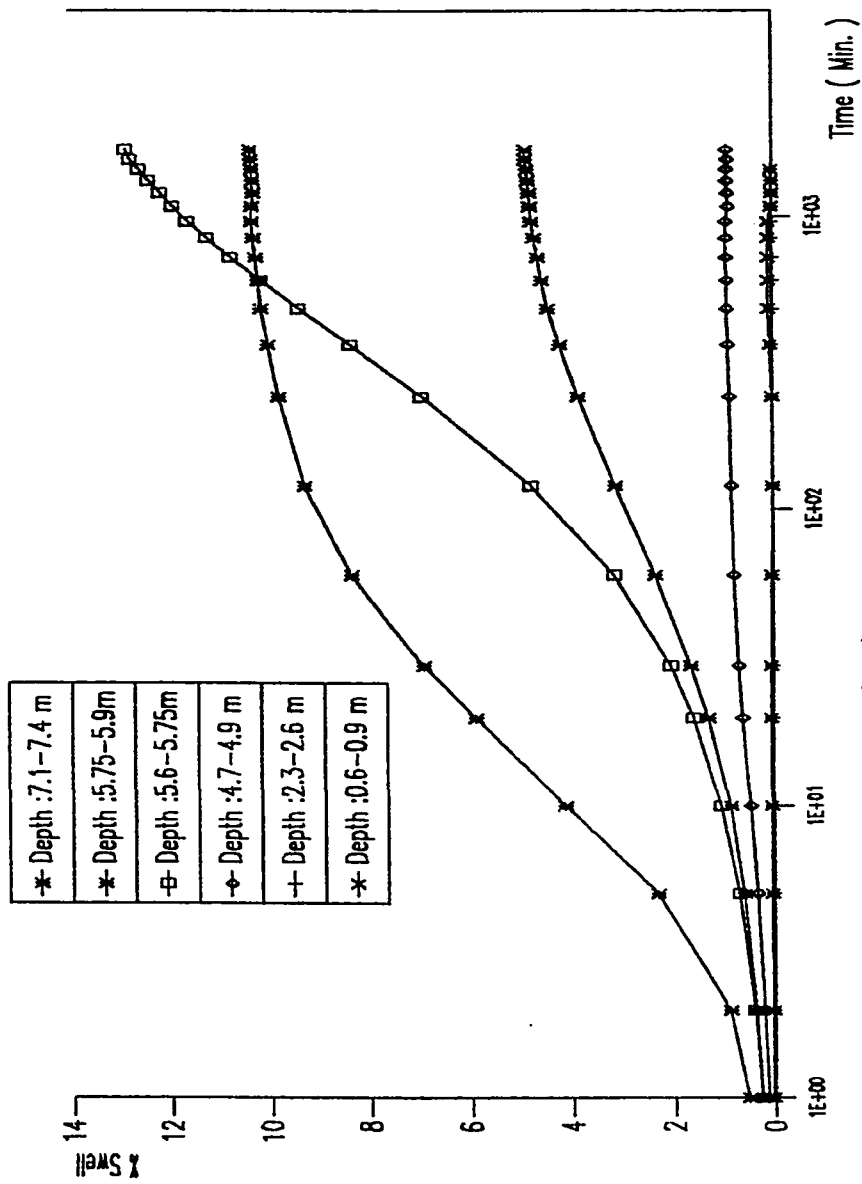


Figure (6.12), % Swell vs. Time For B.H # 8
Umm Al-Hamam

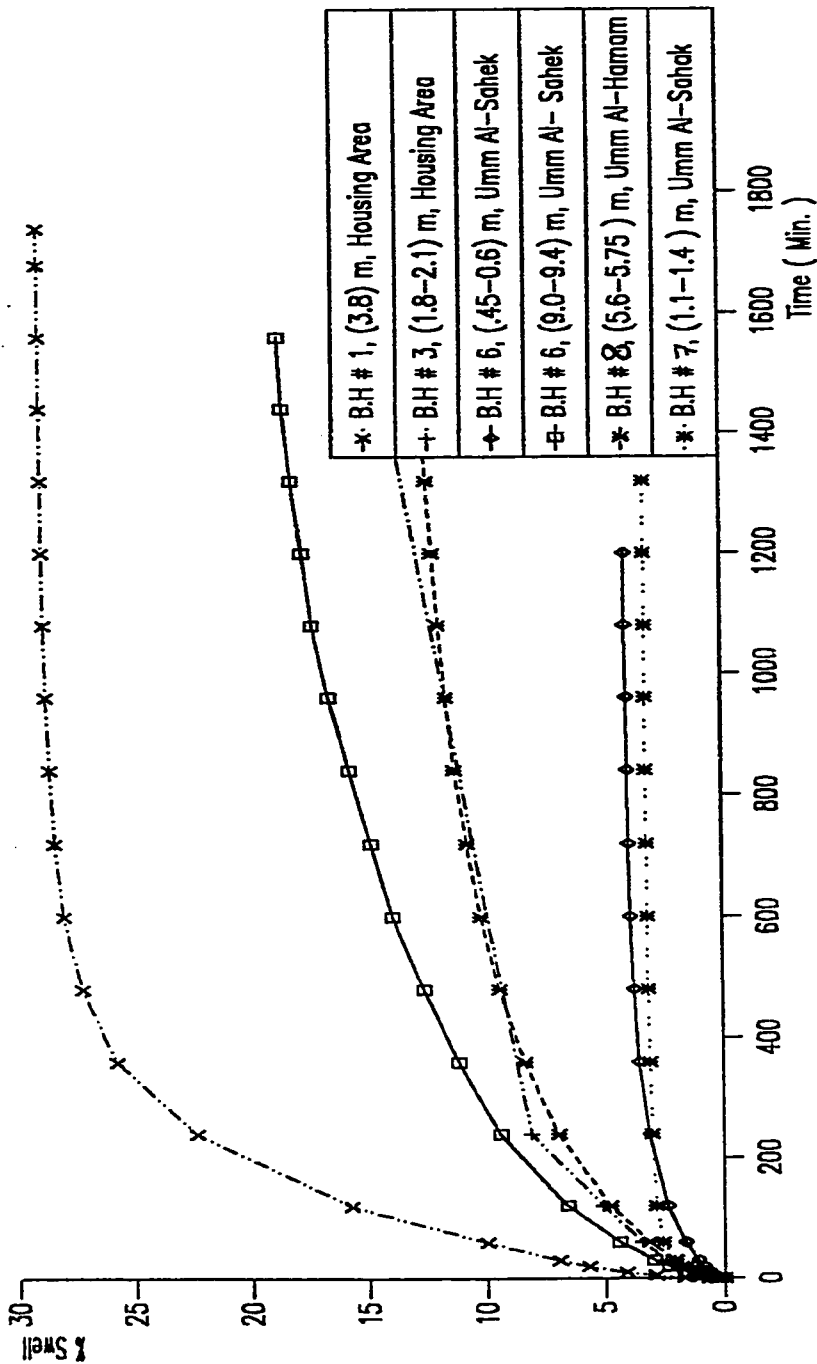


Figure (6.13) : % Swell vs. Time For Some Samples In Al-Qatif Area

Umm Al-Sahek and Umm Al-Hamam exhibited low to medium swell potential. Figure 6.13 presents a comparison of % swell for samples from different locations.

It is worth noting at this point to emphasize that the use of the plasticity index or liquid limit to predict the swell potential of the soil is reliable to a big degree. However, a quick skimming for Tables 5.1-5.4 show that the use of shrinkage limit to predict the swellability of a soil is misleading, at least for the soils in the study area.

Ten samples from five test pits in Al-Hasa area were tested. During the preparation of the samples they experienced different degrees of disturbance because the samples were dry and stiff. The results of these samples are presented in Table 5.3 and Figs. 6.14 - 6.18. Results show that the maximum swell potential of 16.33% and 14.17% were exhibited by samples from Al-Naathel area TP #9, at 1.1 & 2.2 m, respectively. Figure 6.16 shows % swell vs. time for these samples which were very dry and very stiff, and had a relatively high plasticity. The mineralogical composition of sample #6 (TP #9, 2.2 m) shows that the soil contains smectite (montmorillonite and saponite), palygorskite, kaolinite, calcite and quartz. Samples from TP #8 in Al-Hamadiya area had the same initial water content and dry unit weight, however, due to the higher plasticity of the sample at depth 0.2m, it exhibited a much larger degree of swell potential, Fig. 6.15. The

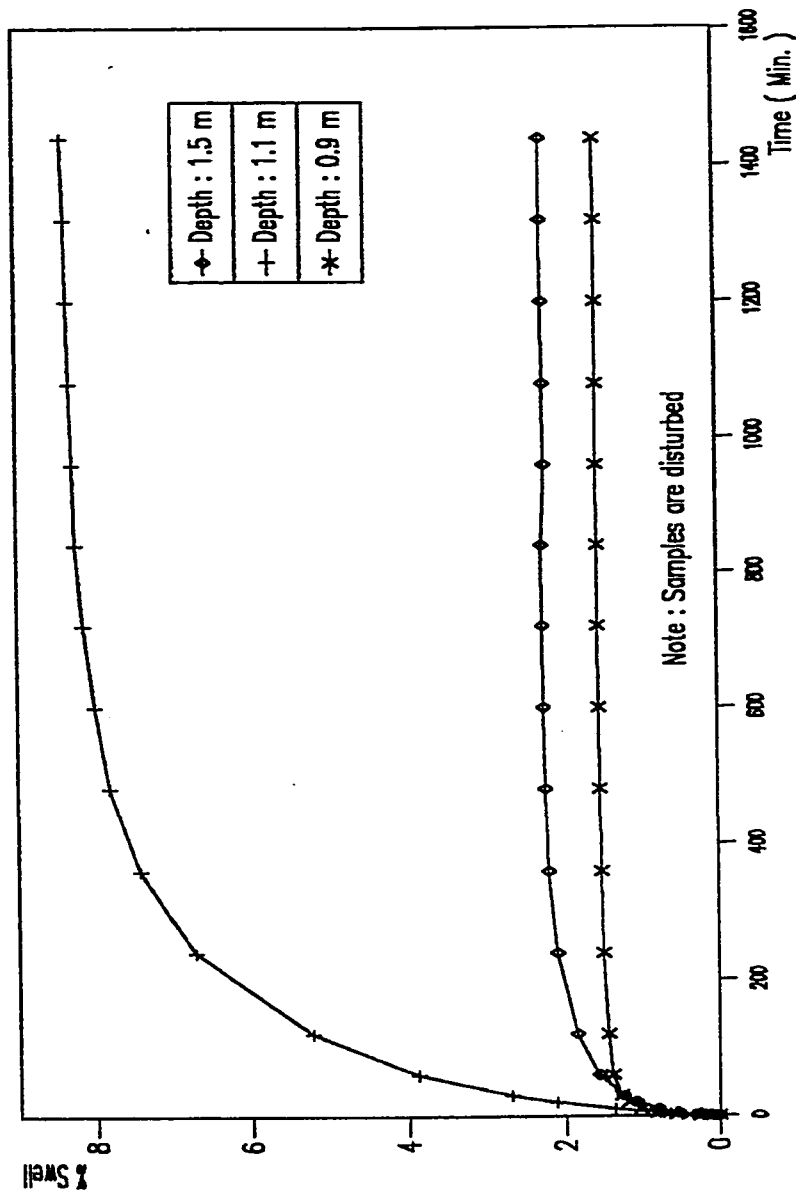
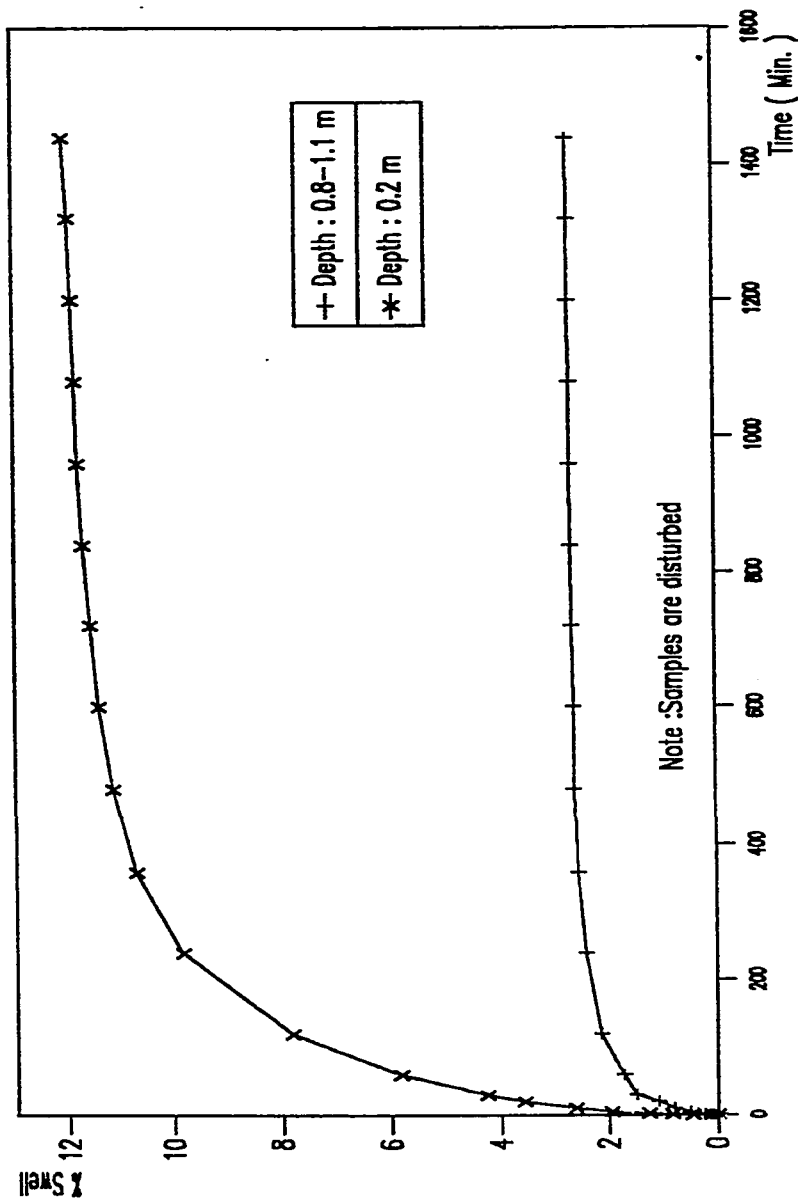


Figure (6.14) : % Swell vs Time
Test Pit # 7 A1-Haso



Note :Samples are disturbed

Figure (6.15) : % Swell vs Time
Test Pit # 8, Al-Haso

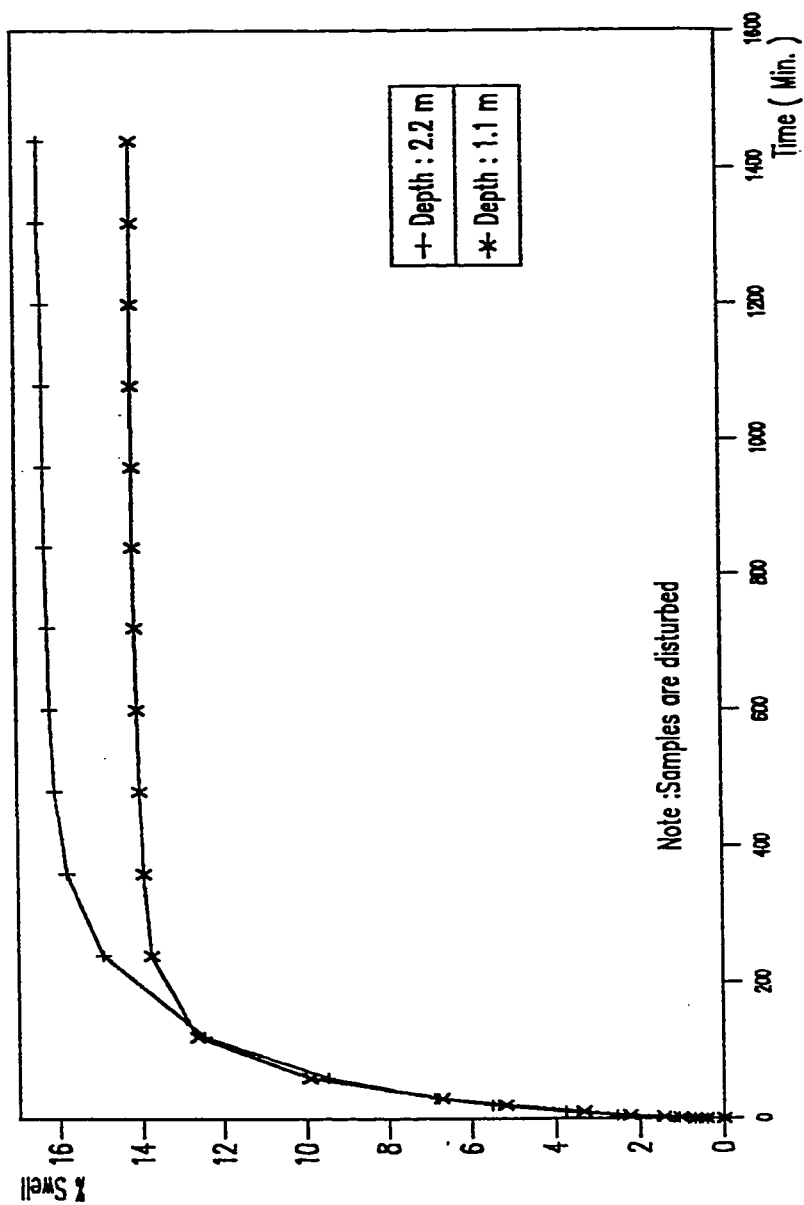


Figure (6.16) : % Swell vs Time
Test Pit # 9, Al-Hobo

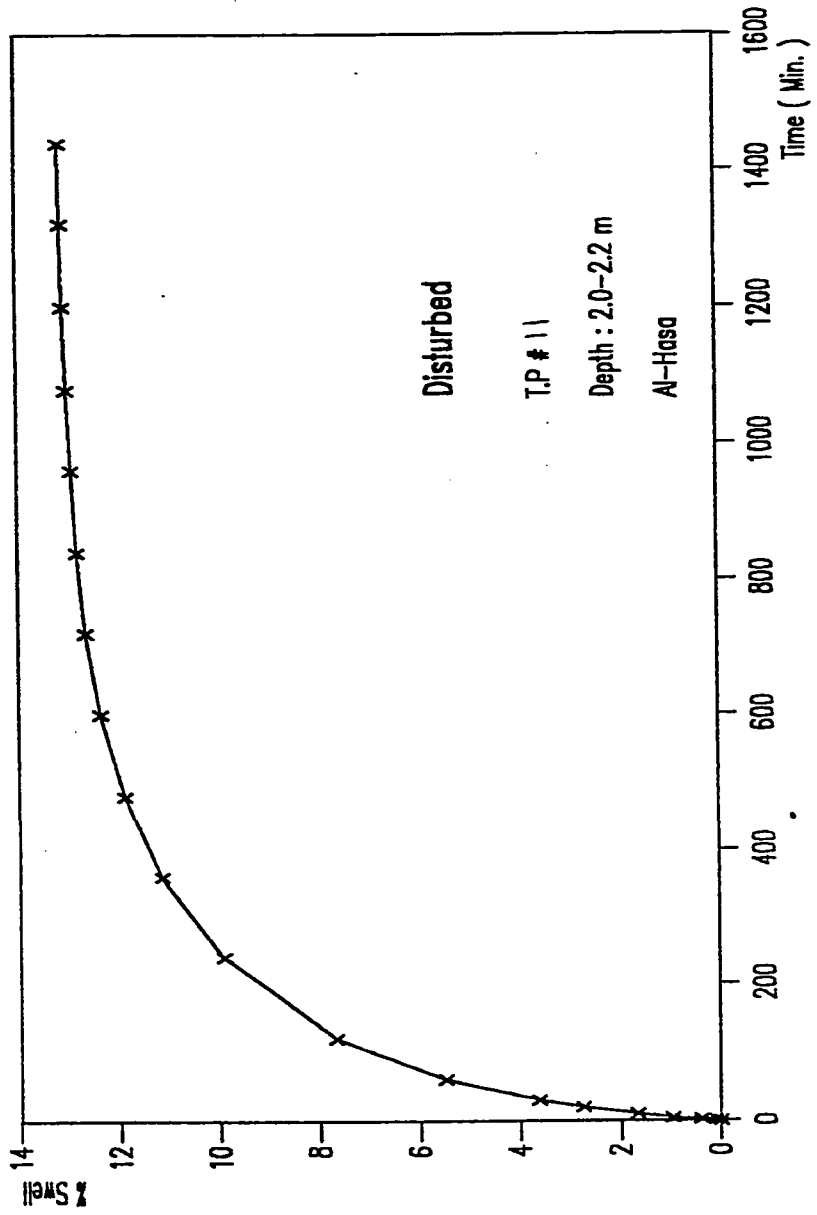


Figure (6.18) : % Swell vs Time

TP # 11, Al-Hasa

sample from test pit #11 (2.0-2.2 m) was very similar to that of TP #9 and also recorded a high swell potential, Figure 6.18. The mineralogical composition of this sample which was collected from near ARAMCO Hospital in Mahasen shows that it contains montmorillonite (both Na & Ca types) , kaolinite, sepiolite and palygorskite as well as quartz and calcite. Figure 5.28 shows the diffraction patterns for this sample.

In addition to the test pits samples, twenty three other samples from Al-Hasa bore holes were obtained. The results are shown in Table 5.4 and Figures 6.19-6.25. The classification of the swell potential of Al-Hasa samples based on their index properties, as shown in Table 5.8, indicates that they possess a high to a very high swell potential. However, the results show that the swell potential of Al-Hasa clays is not as high as that of Al-Qatif area. The maximum swell potential of 7.16% was recorded for a sample from BH. #11 (depth: 1.0-1.3m), as can be seen in figure 6.21. This sample has the highest plasticity. Other samples exhibited smaller percentages of swell. Figure 6.25 presents a comparison in % swell results between some samples from different locations. The mineralogical analysis of Al-Hasa samples shows that Al-Hasa clays contain smectite as well as palygorskite, kaolinite, illite, dolomite, quartz and calcite.

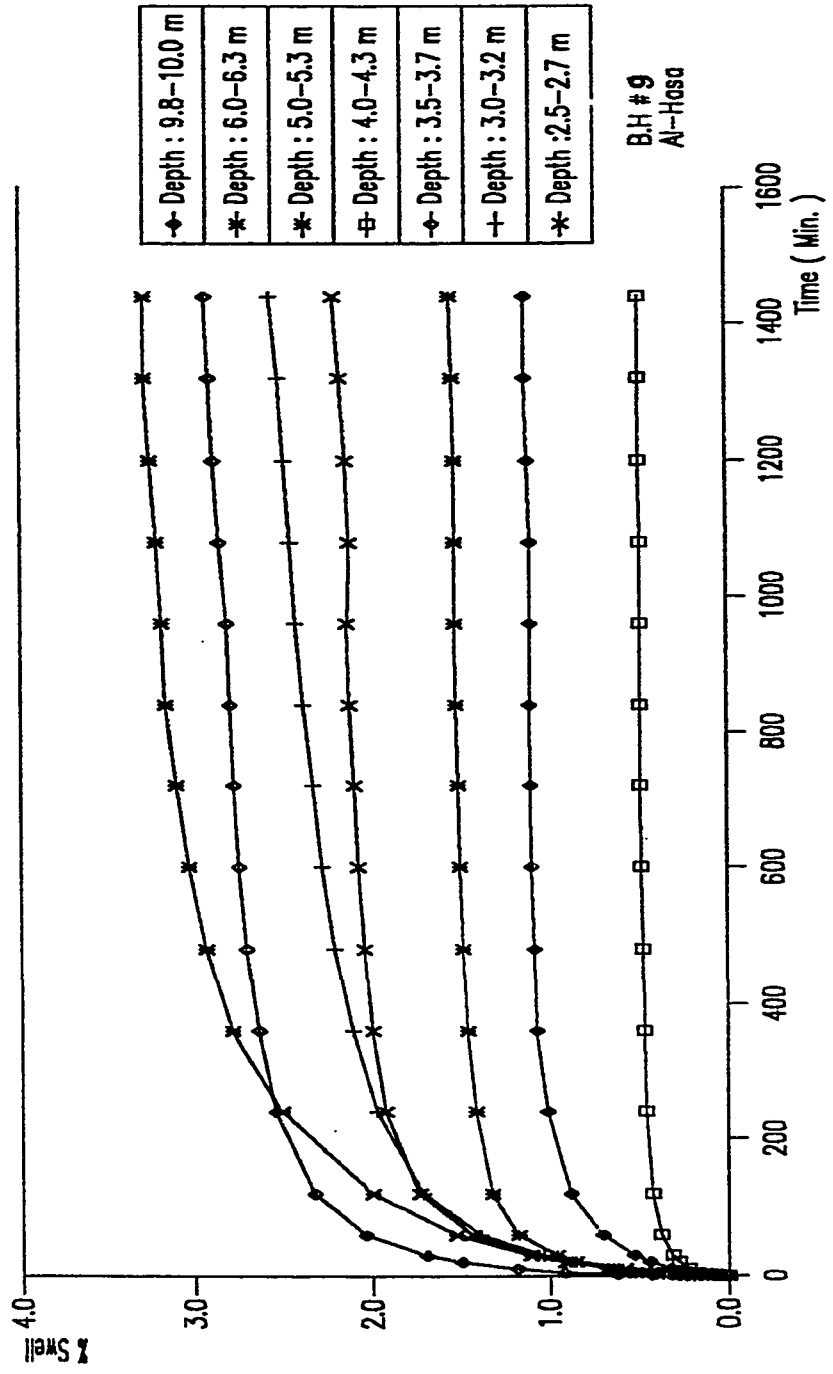


FIG. 6.19 : Swell vs Time
BH # 9, A1-Hasa

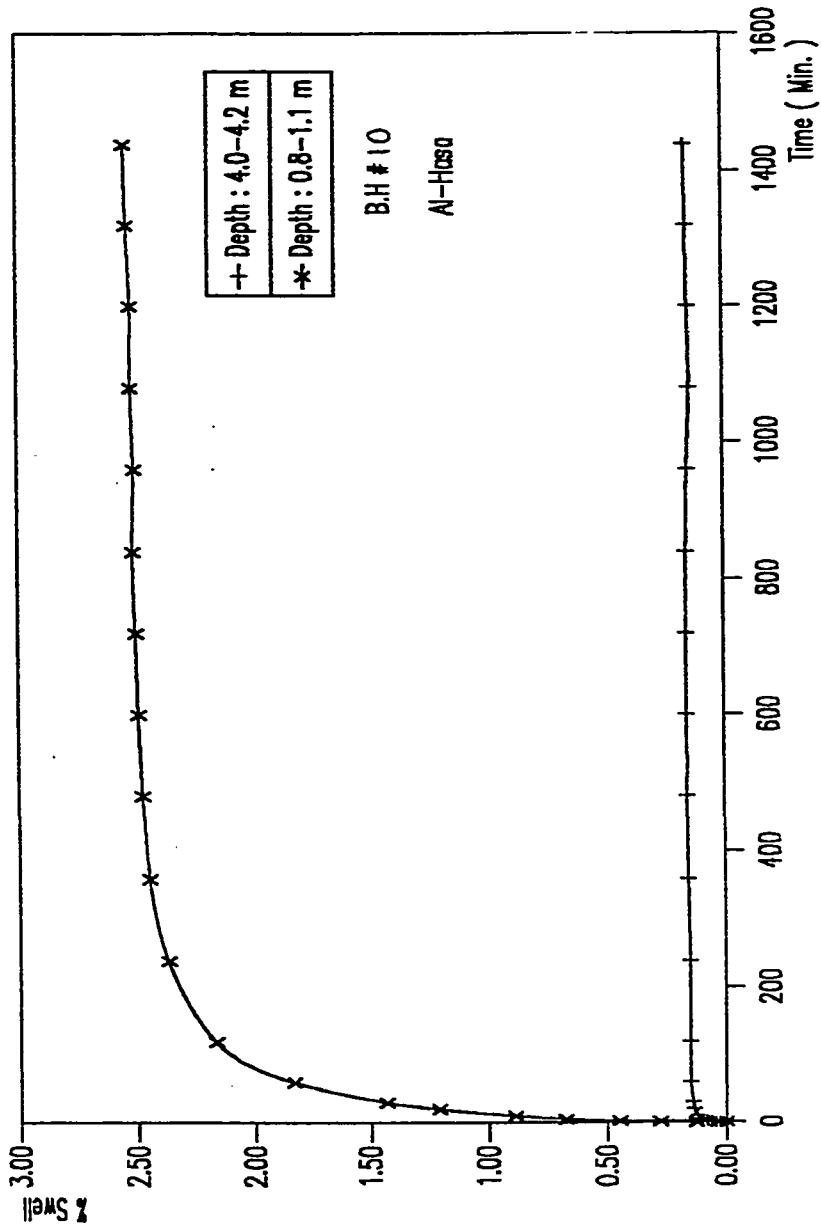


Figure (6.20) : % Swell vs Time

BH # 10, Al-Hasa

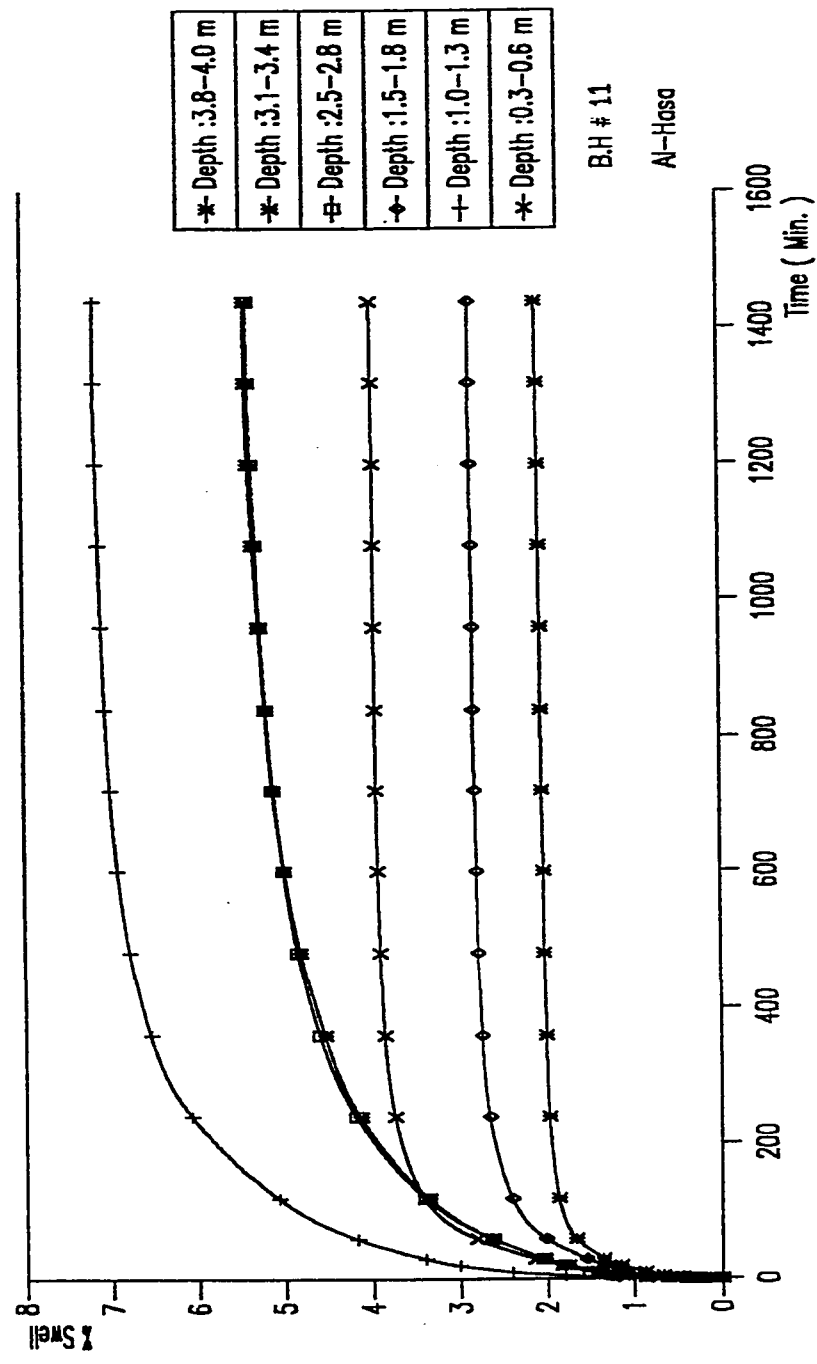


Figure (6.2) : % Swell vs Time
BH # 11, Al Hasa

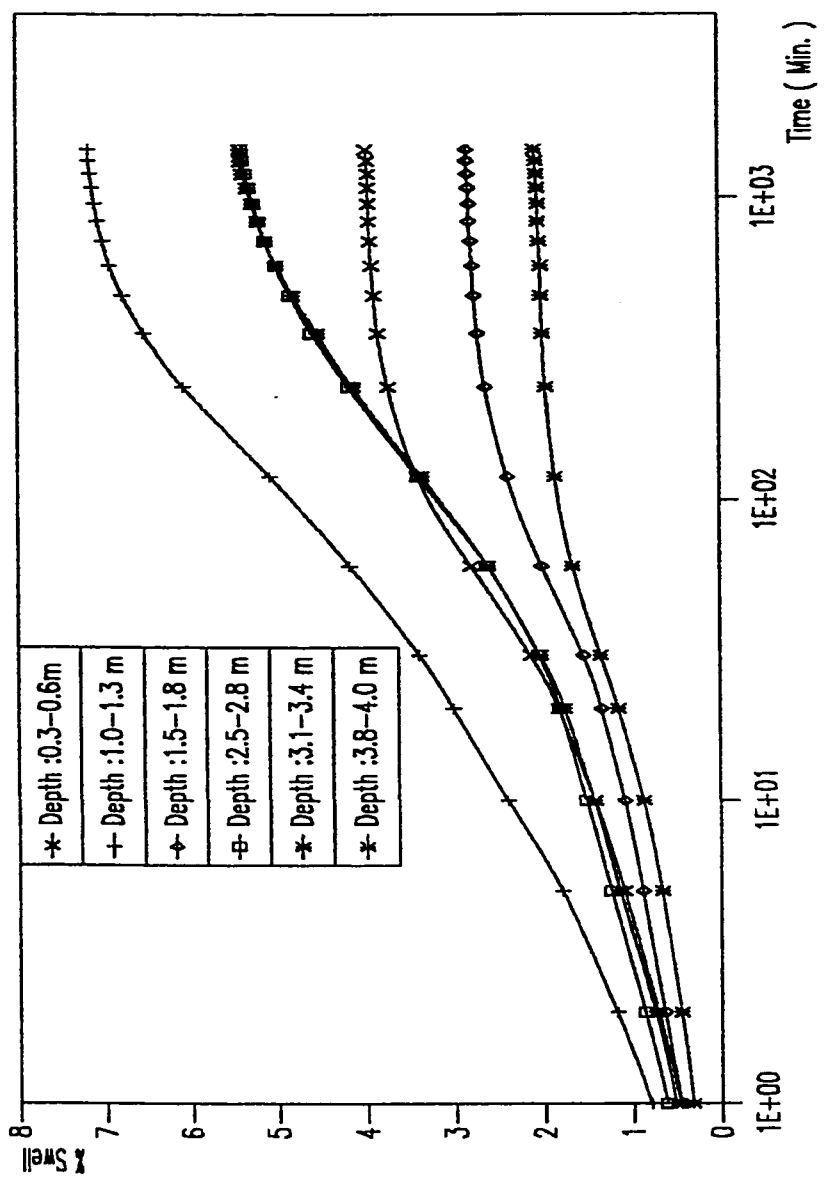


Figure (6.22), % Swell vs. Time for B.H # 11, Al-Hosho.

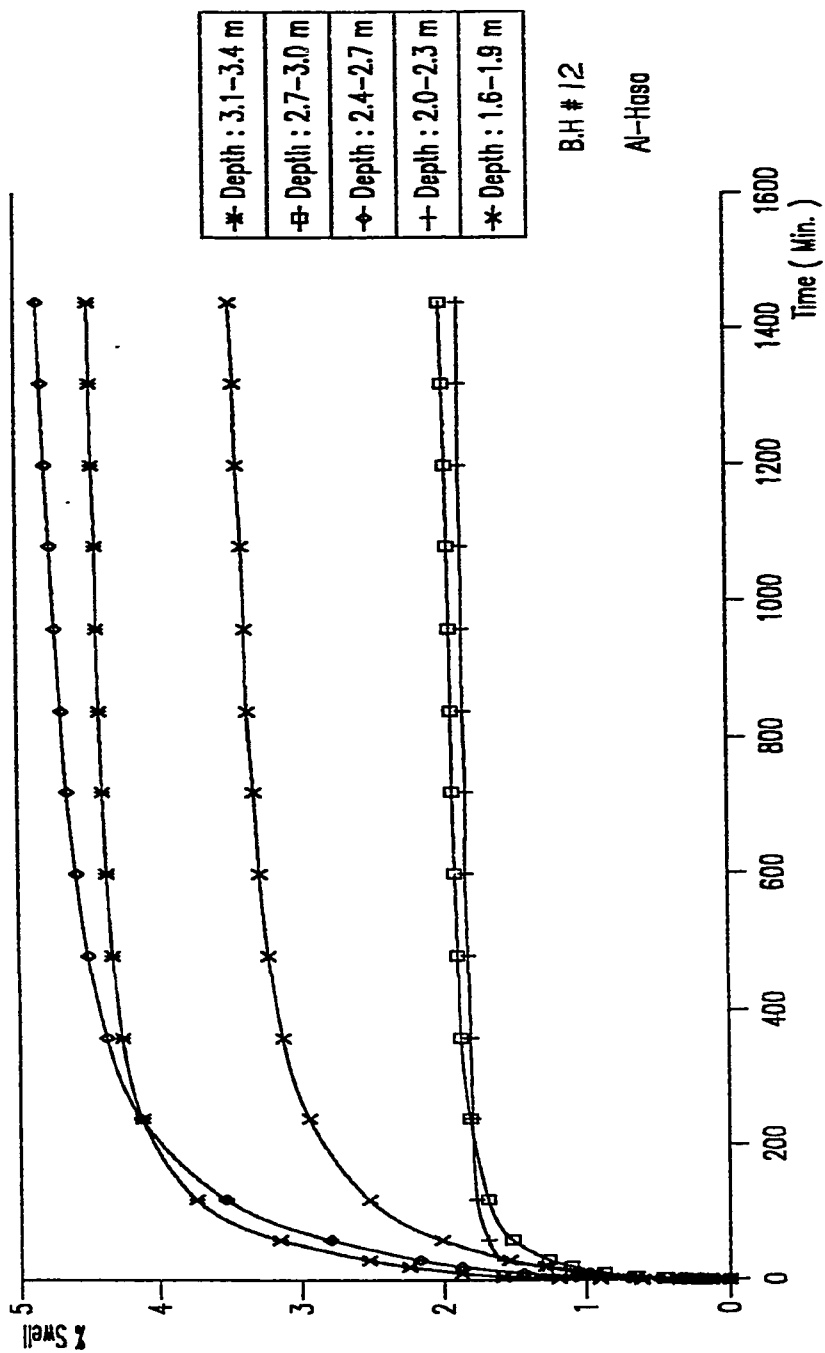


Figure (6.23) : % Swell vs Time

BH# 12, A1 Haso

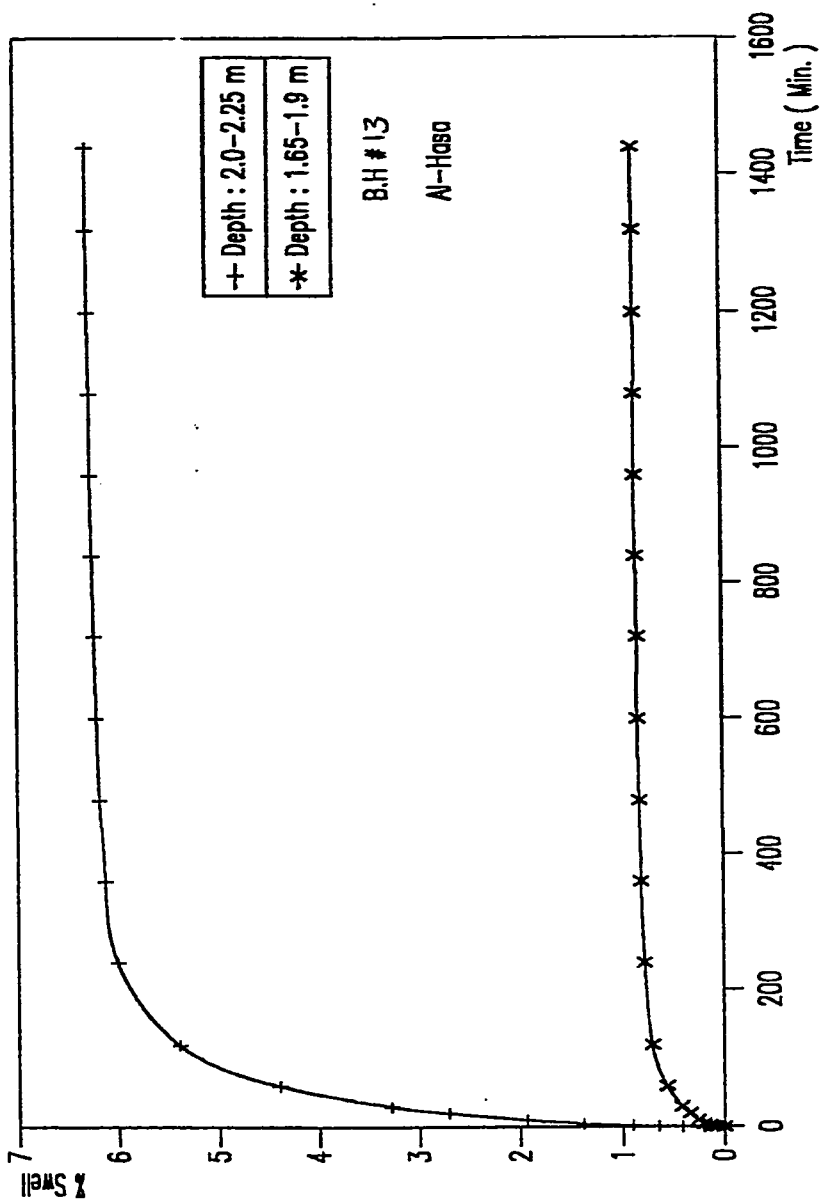


Figure (6.24) : % Swell vs Time

BH # 13, Al-Hasa

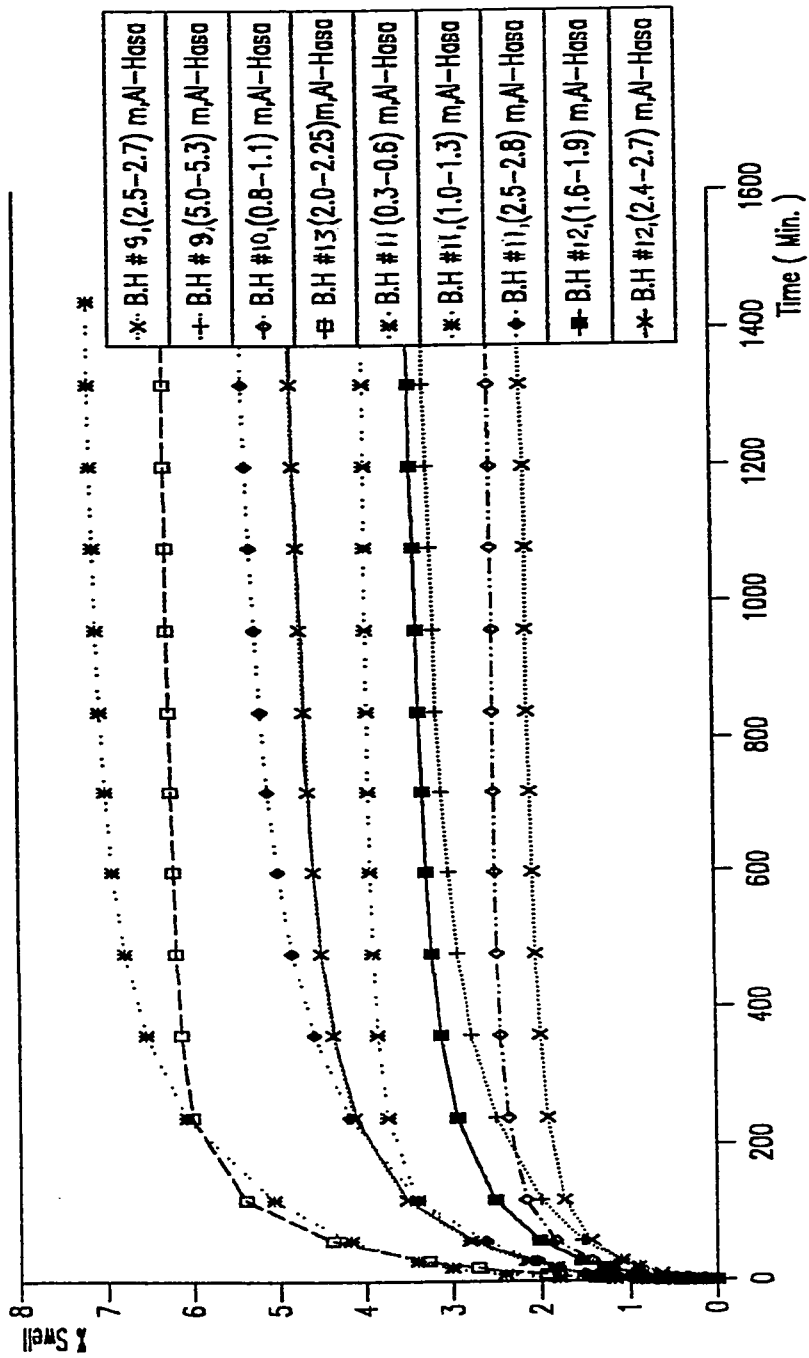


Figure (6.25) : % Swell vs. Time For Some Samples In Al-Hasa Area.

6.4 SWELL PRESSURE RESULTS

The swell pressure results for all samples are shown in tables 5.1- 5.4. For each sample % swell vs. swell pressure curve was plotted. The curves for Al-Qatif area are shown on Figures 6.26-6.35. Figures 6.36-6.46 show the swell percent vs. swell pressure for Al-Hasa samples.

The swell pressure results for the samples from Al-Qatif pits are shown in Table 5.1 and fig. 6.26. The maximum swelling pressure of 19.3 kg/cm^2 was exerted by Sample 2B (TP #2, 4.0 m depth). This high swelling pressure can be attributed to high plasticity index (PI = 150.2%) and high clay fraction as well as the presence of smectite.

Table 5.2 and Figs. 6.27-6.35 show the results of swell pressure for samples collected from the bore holes of Al-Qatif area. Results for each bore hole were plotted in figures 6.27-6.34, while figure 6.35 shows the results of certain samples from different bore holes. The maximum swelling pressure of 20.0 kg/cm^2 was exerted by sample #1 at depth of 4.2m (B.H. #2) in Al-Qatif Housing area. The plasticity of this sample is very high. Sample #2 (BH #2, 4.3 m) has a lower plasticity and has consequently a lower swelling pressure. The same talking is true for sample #1 and Sample #2 (BH #4, depth :9.7-10 m) in Al-Jesh village. Results show that no clear conclusion can be depicted about the

relation between swelling pressure and initial moisture content. In order to get a good idea about the effect of initial water content, a sample should be tested with different initial moisture contents while fixing the other variables (i.e, plasticity, initial dry density and sample state). The same talking applies to the relation between initial dry unit weight and swelling pressure as no obvious relation was noticed, based on the results of this study.

The swell pressures for the samples from Al-Hasa test pits are presented in Table 5.3 and figs. 6.36-6.40. A swell pressure as high as 24.0 kg/cm^2 was recorded for Al-Naathel Sample (BH #11, depth 2.2m) and Mahasen Sample (BH #13), depth 2.0-2.2m). The samples in these two areas are very dry, stiff , have a high plasticity and rich in smectite.

Table 5.4 and figs. 6.41-6.45 show the results of Al-Hasa bore holes samples. Fig. 6.46 shows the results of some samples from different bore holes.

In general, the swelling pressures of Al-Hasa clays are smaller than that of Al-Qatif area. The maximum swelling pressure noted in Al-Hasa samples is 4.0 kg/cm^2 exerted by the sample (BH #11, depth 1.0-1.3) which has the maximum plasticity index of 56.83%. Moreover, the results show that the plasticity of the sample plays an important role in the amount of swelling pressure. It can be clearly concluded that as the plasticity increases the

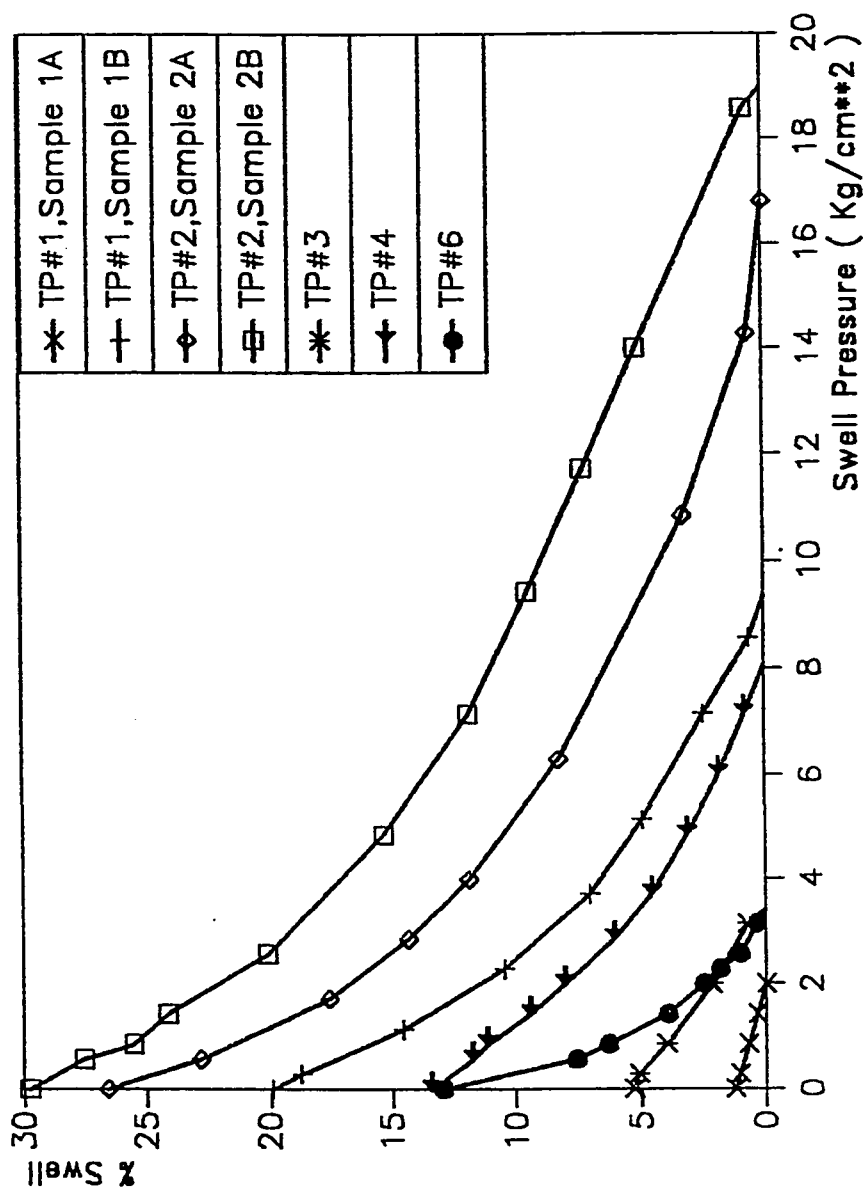


Figure (6.26), % Swell vs. Swell Pressure for Al-Qatif Area (Test Pits).

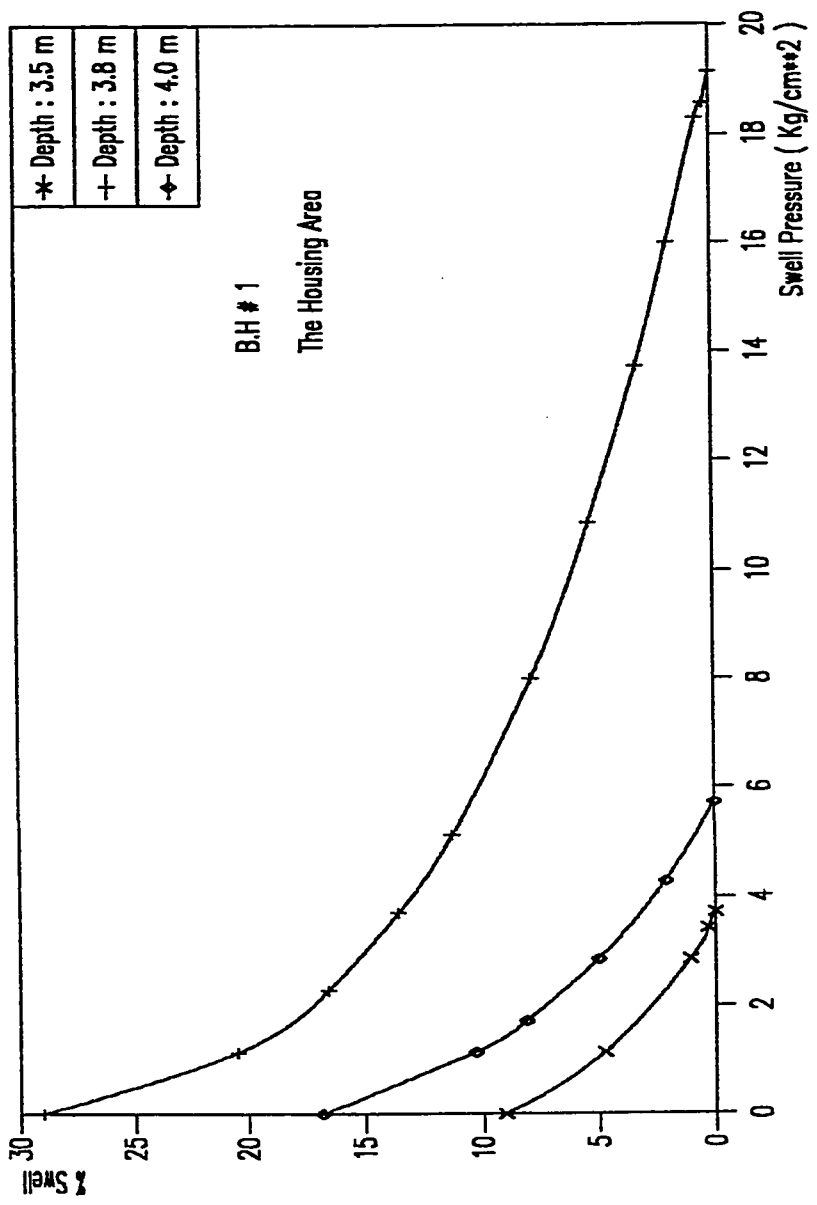


Figure (6.27) : % Swell vs Swell Pressure

BH # 1, Al Qat'if Housing Area

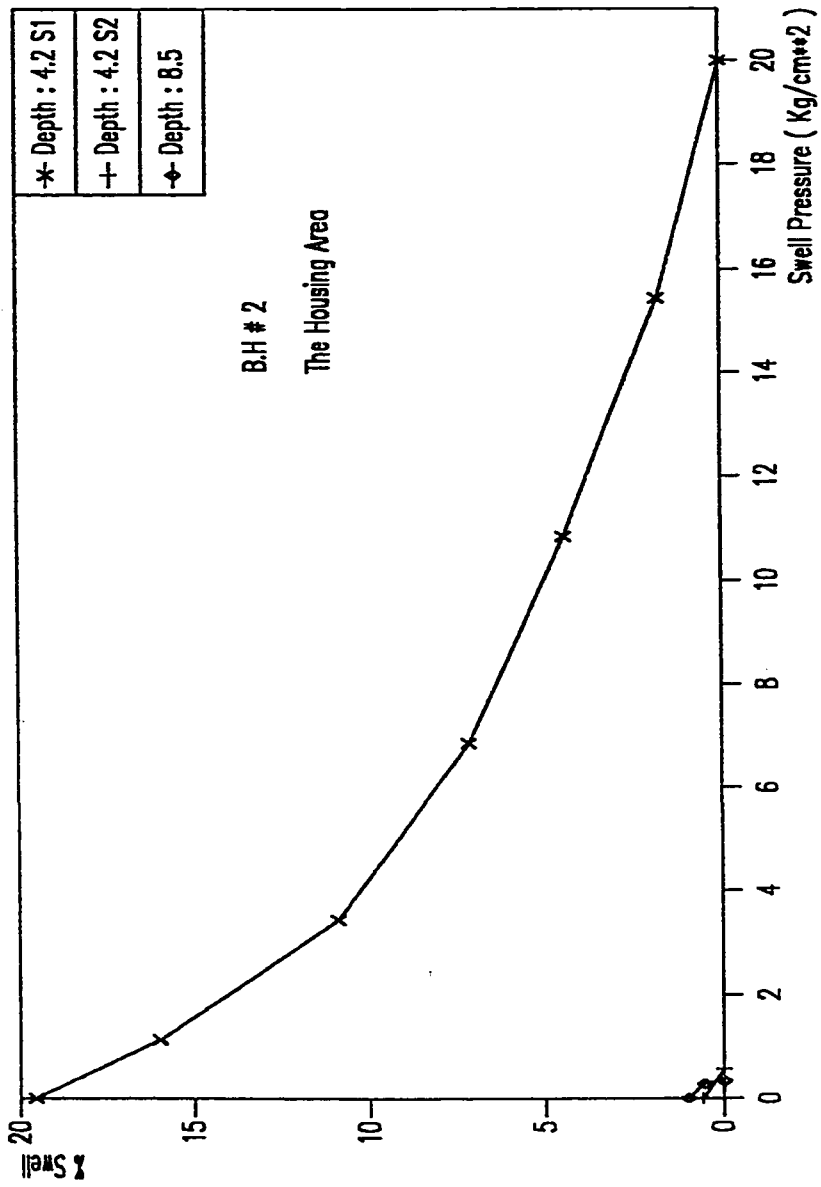


Figure (6.28) : % Swell vs Swell Pressure
BH # 2, Al-Qat'if Housing Area

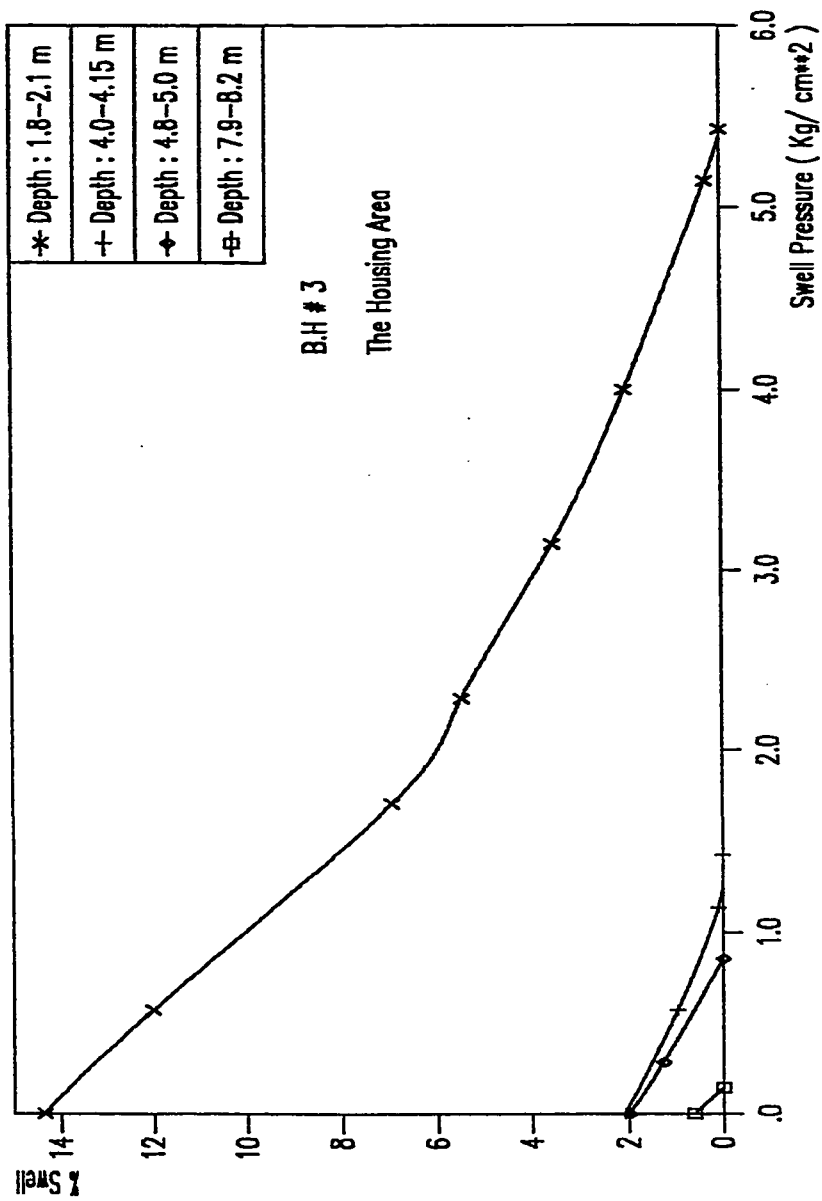


Figure (6.29) : % Swell vs Swell Pressure

BH # 3, Al-Qatif Housing Area

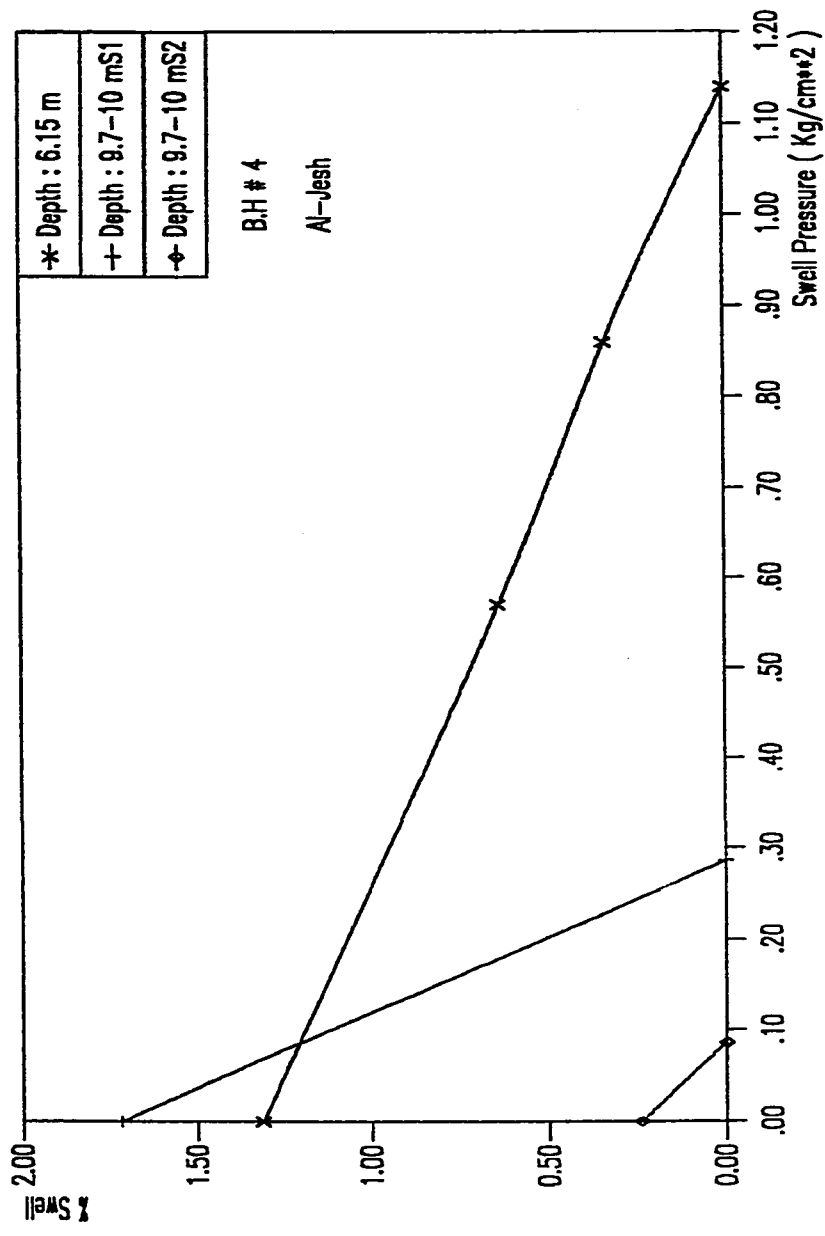


Figure (6.30) : Swell vs Swell Pressure
BH # 4, Al-Jesh

PLEASE NOTE

**Page(s) not included with original material
and unavailable from author or university.
Filmed as received.**

University Microfilms International

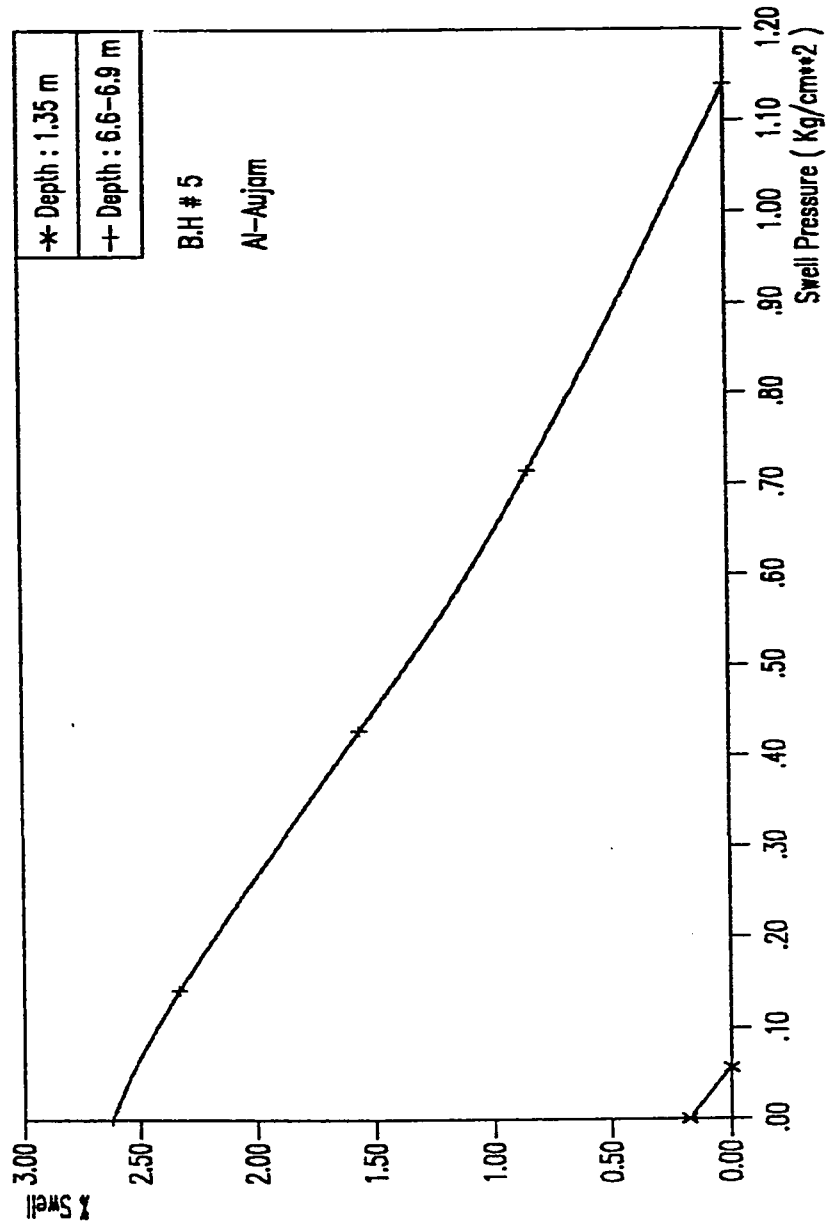


Figure (6.31) : % Swell vs Swell Pressure

BH # 5, Al-Aujam

PLEASE NOTE

**Page(s) not included with original material
and unavailable from author or university.
Filmed as received.**

University Microfilms International

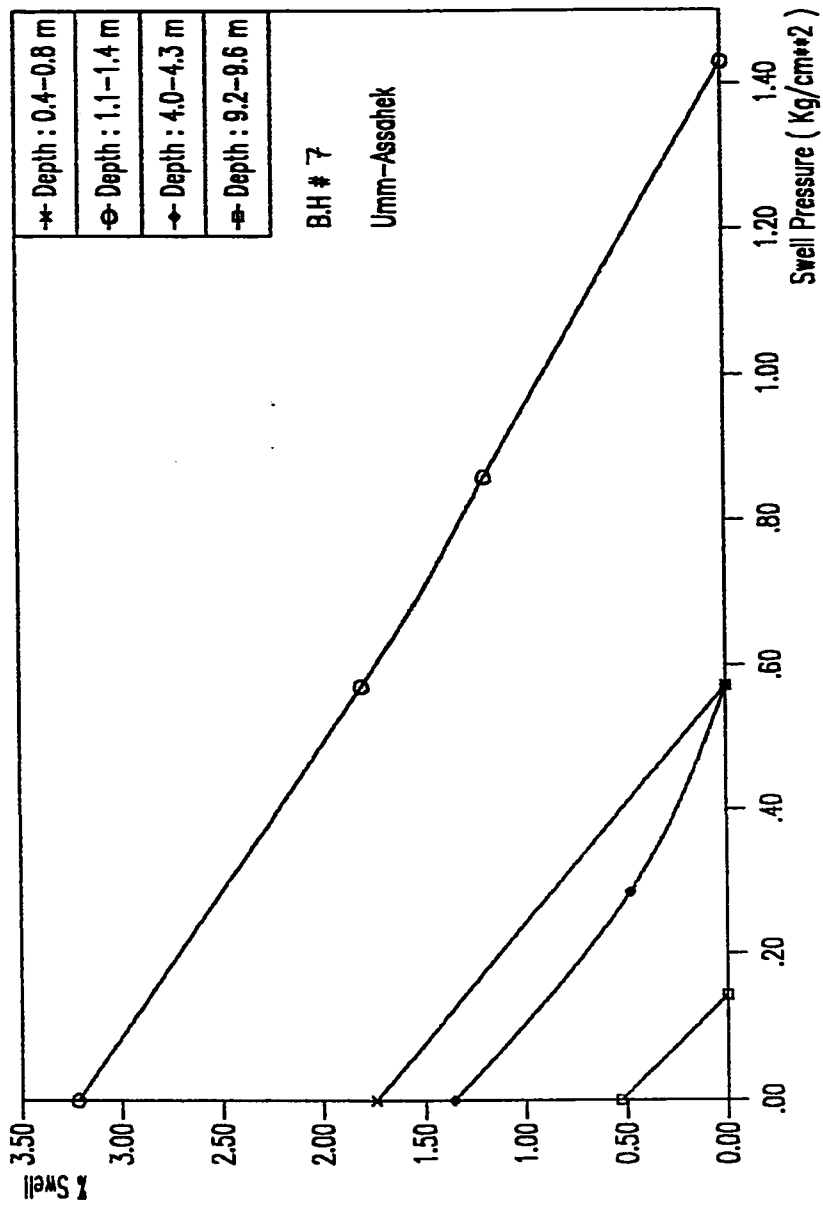


Figure (6.33) : % Swell vs Swell Pressure

BH # 7, Umm A1-Sahek

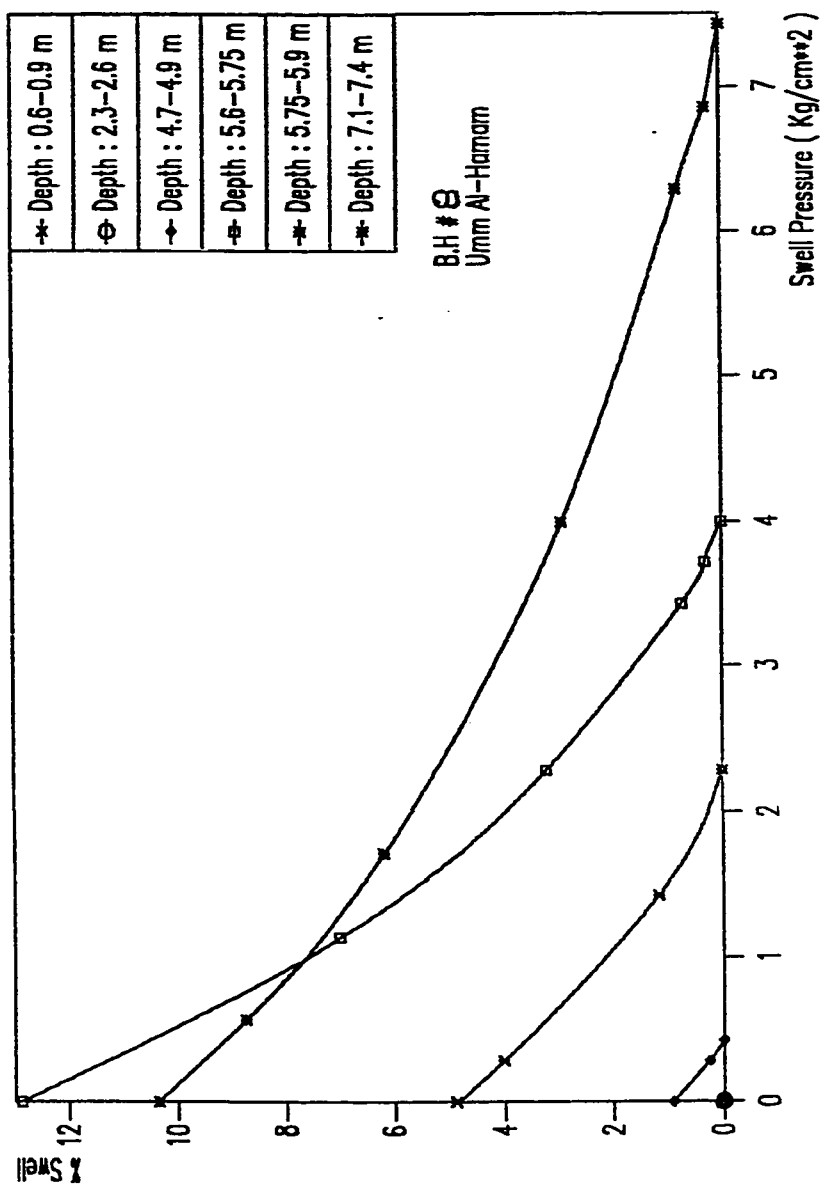


Figure (6.34) : % Swell vs Swell Pressure
BH # 8, Umm Al-Haram

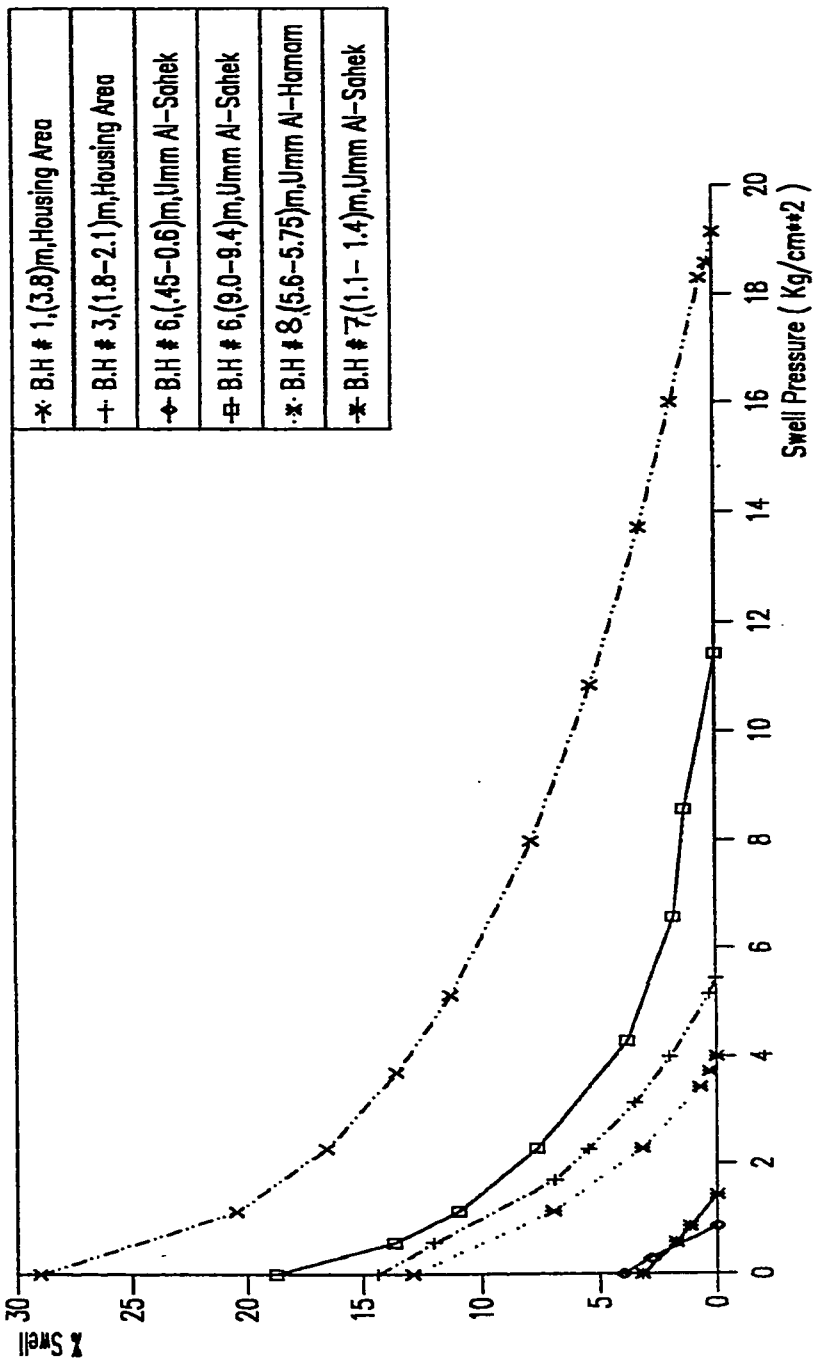


Figure (6.35) : % Swell vs. Swell Pressure For Some Samples In Al-Qatif Area

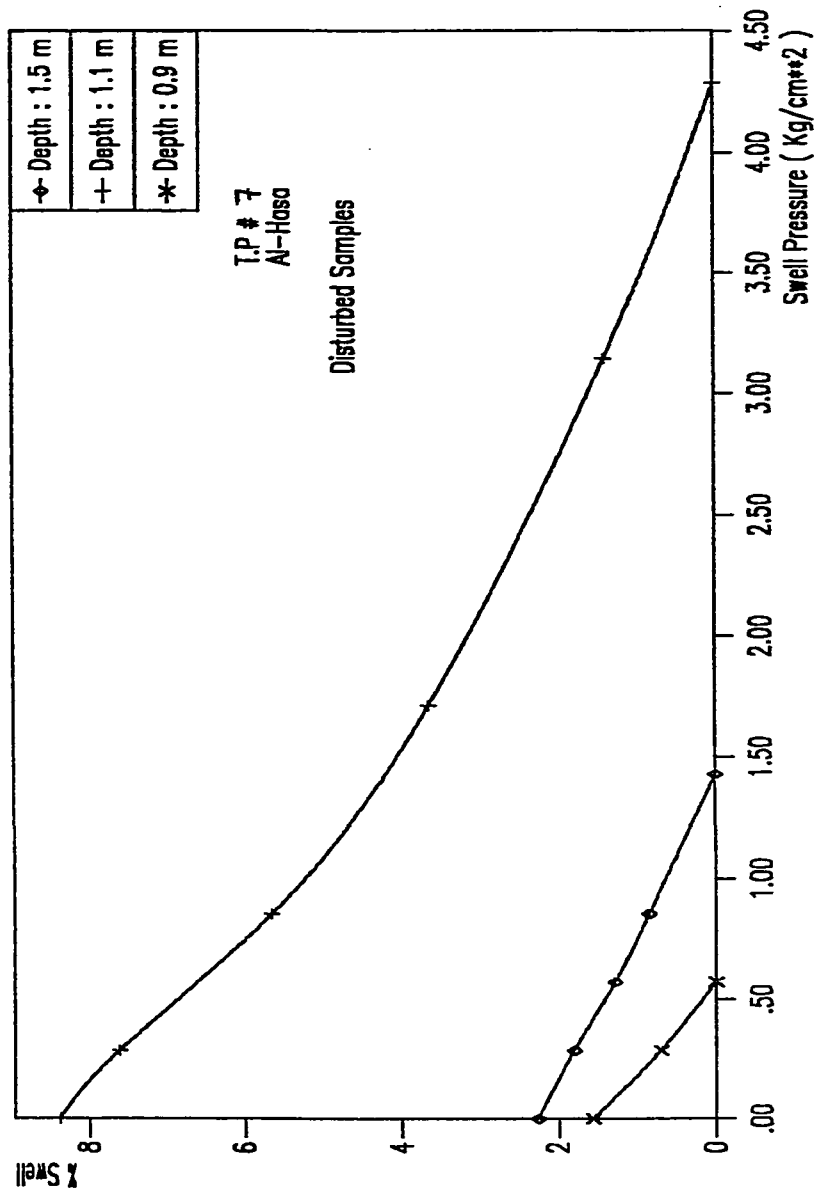


Figure (6.36) : % Swell vs Swell Pressure

T.P. # 7, Al-Hasa

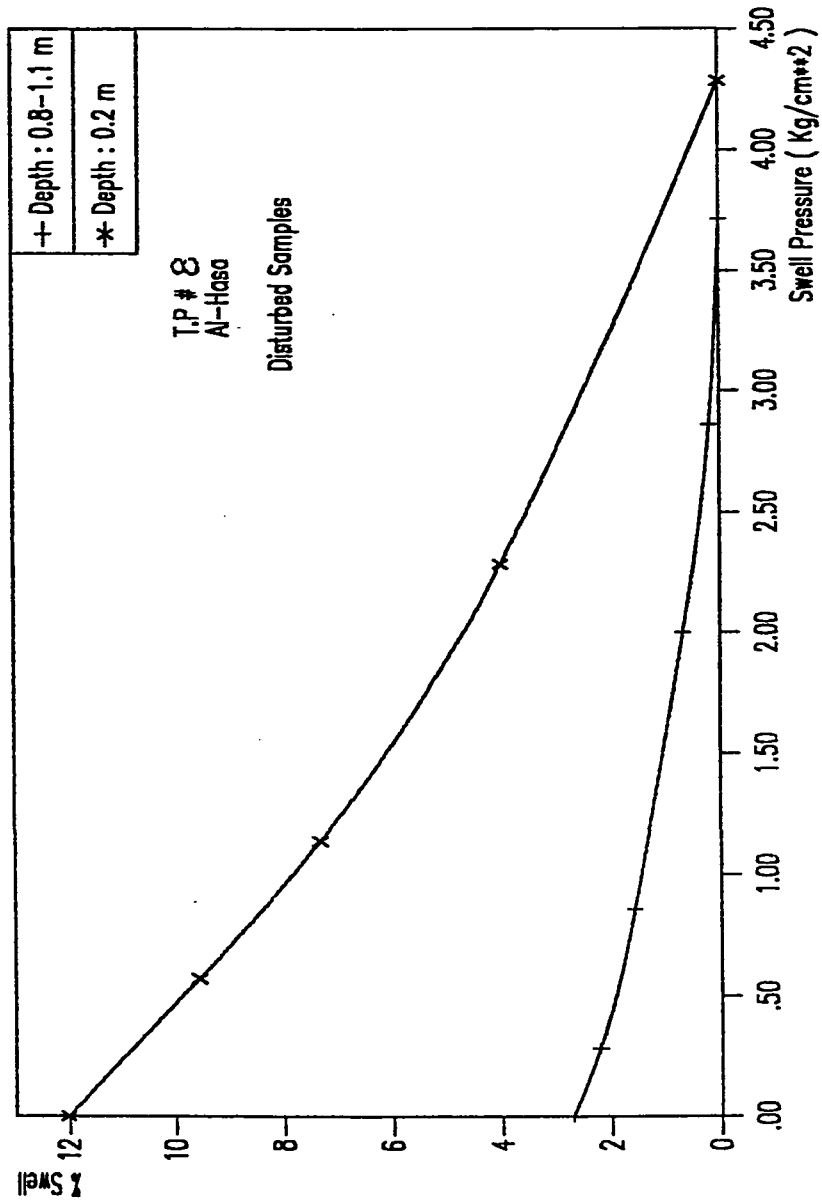


Figure (6.37) : % Swell vs Swell Pressure

T.P. # 8, Al-Hasa

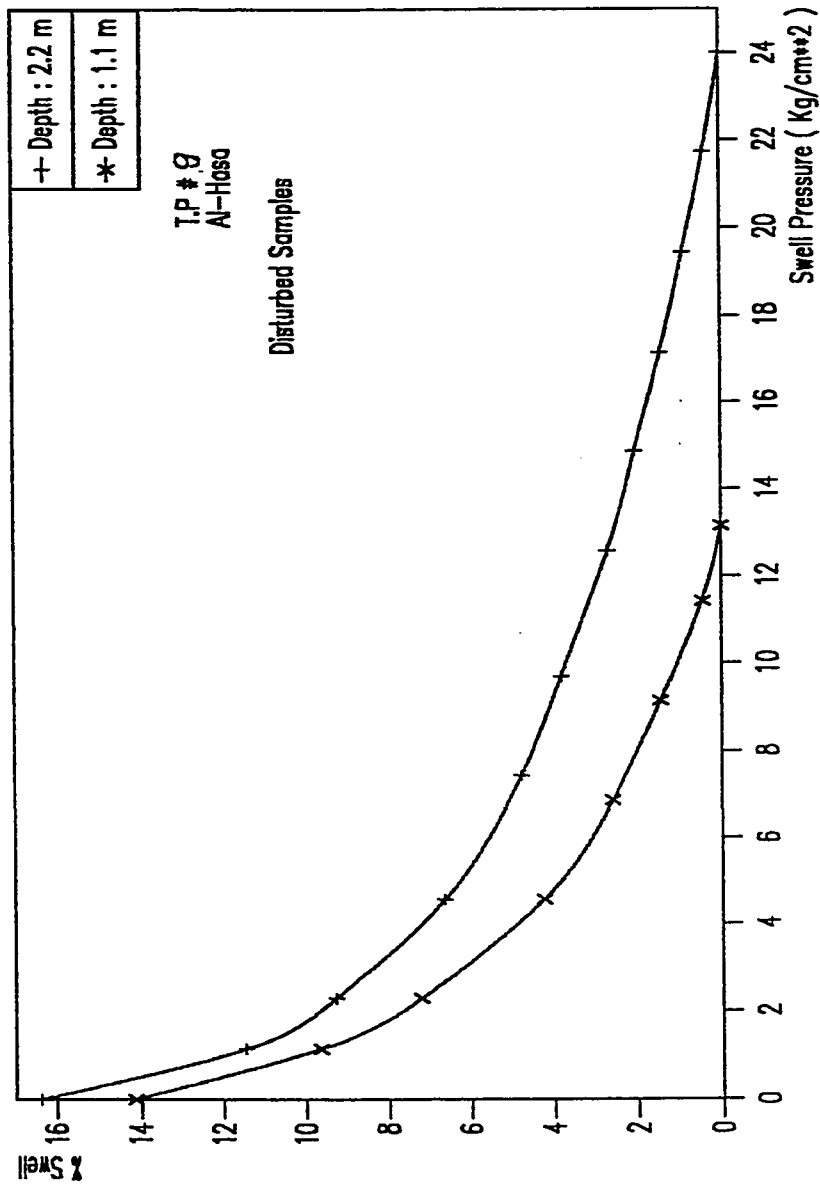


Figure (6.38) : % Swell vs Swell Pressure

TP # 9, Al-Hasa

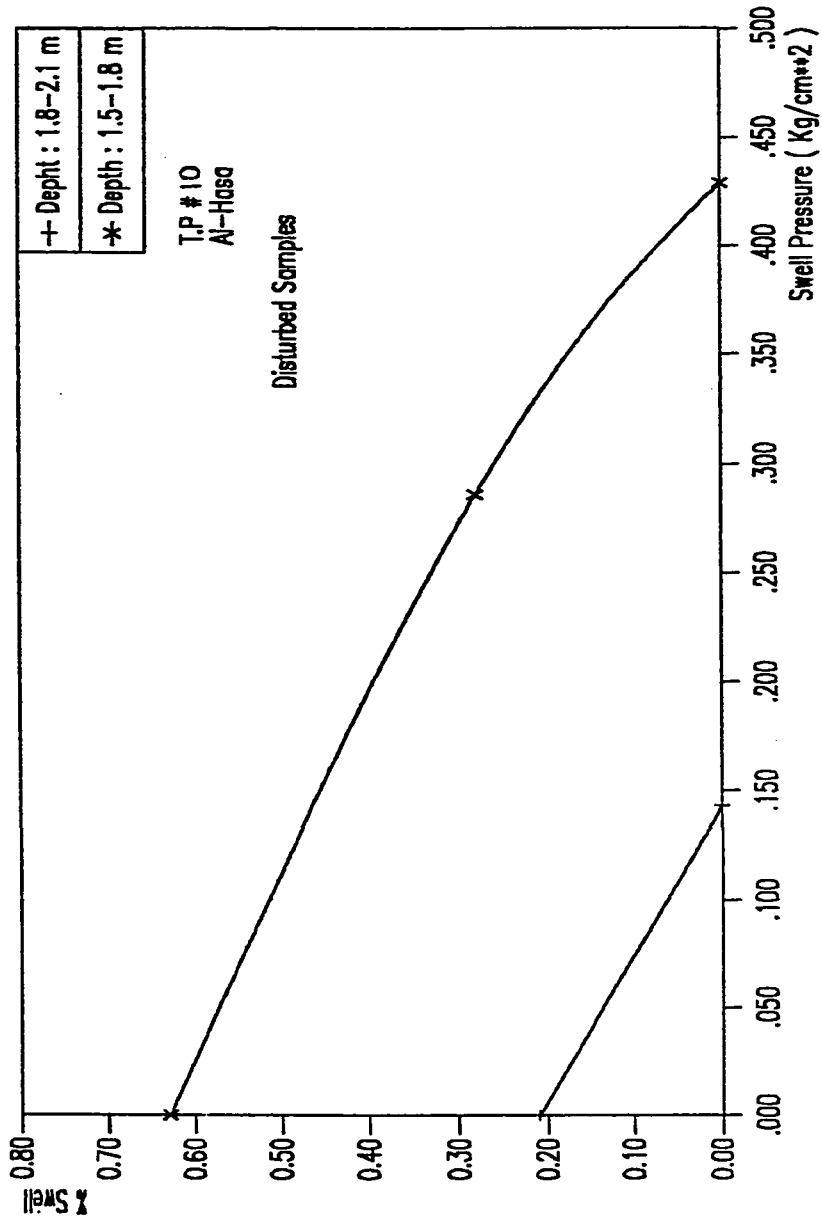


Figure (6.39) : % Swell vs Swell Pressure

TP # 10, AI-Hasa

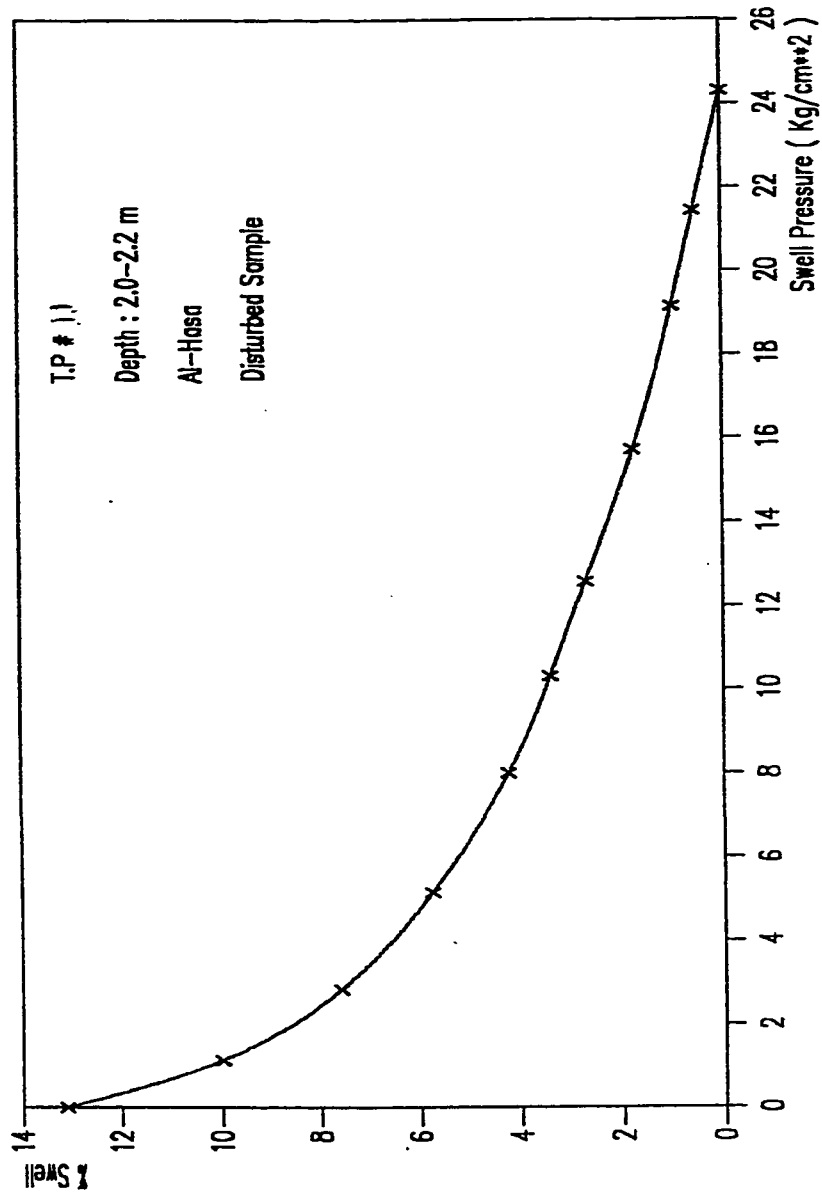


Figure (6.40) % Swell vs Swell Pressure

TP # 11, Al-Hasa

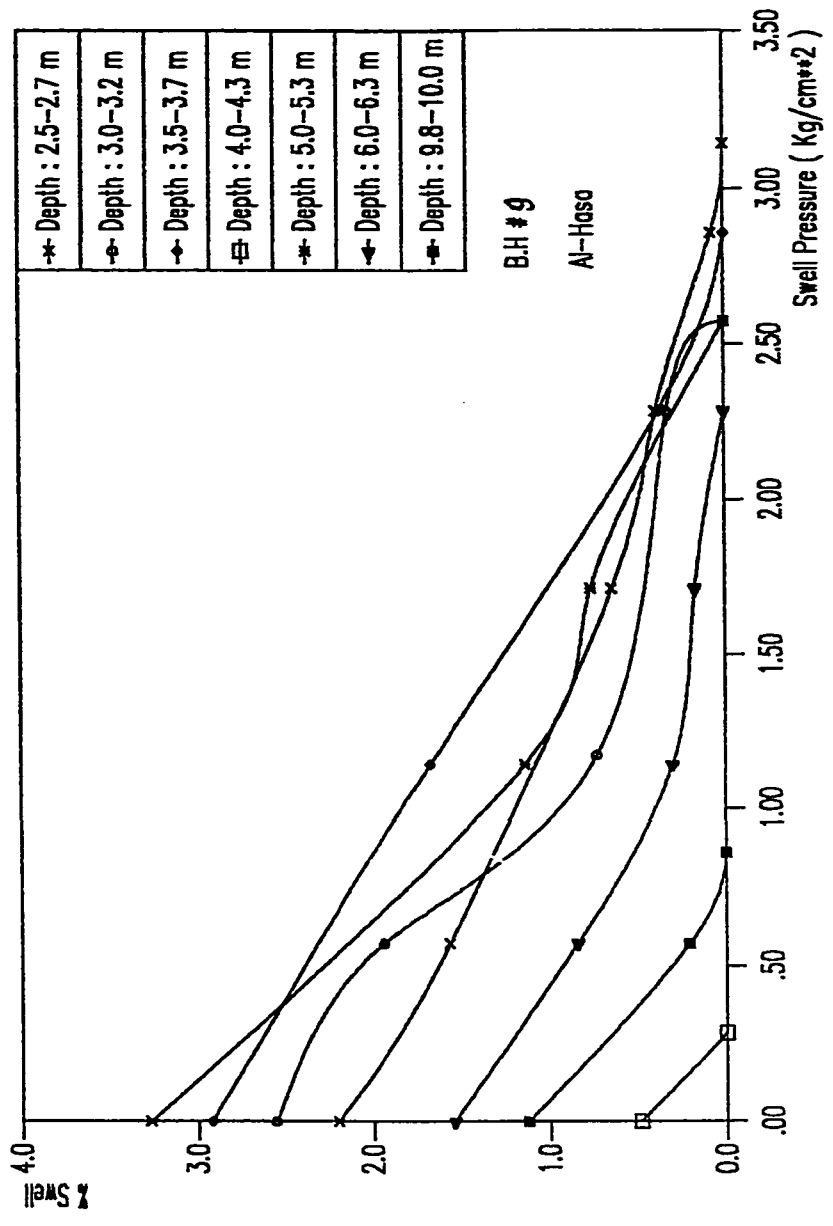


Figure (6.41): % Swell vs Swell Pressure

BH # 9, Al-Hasa

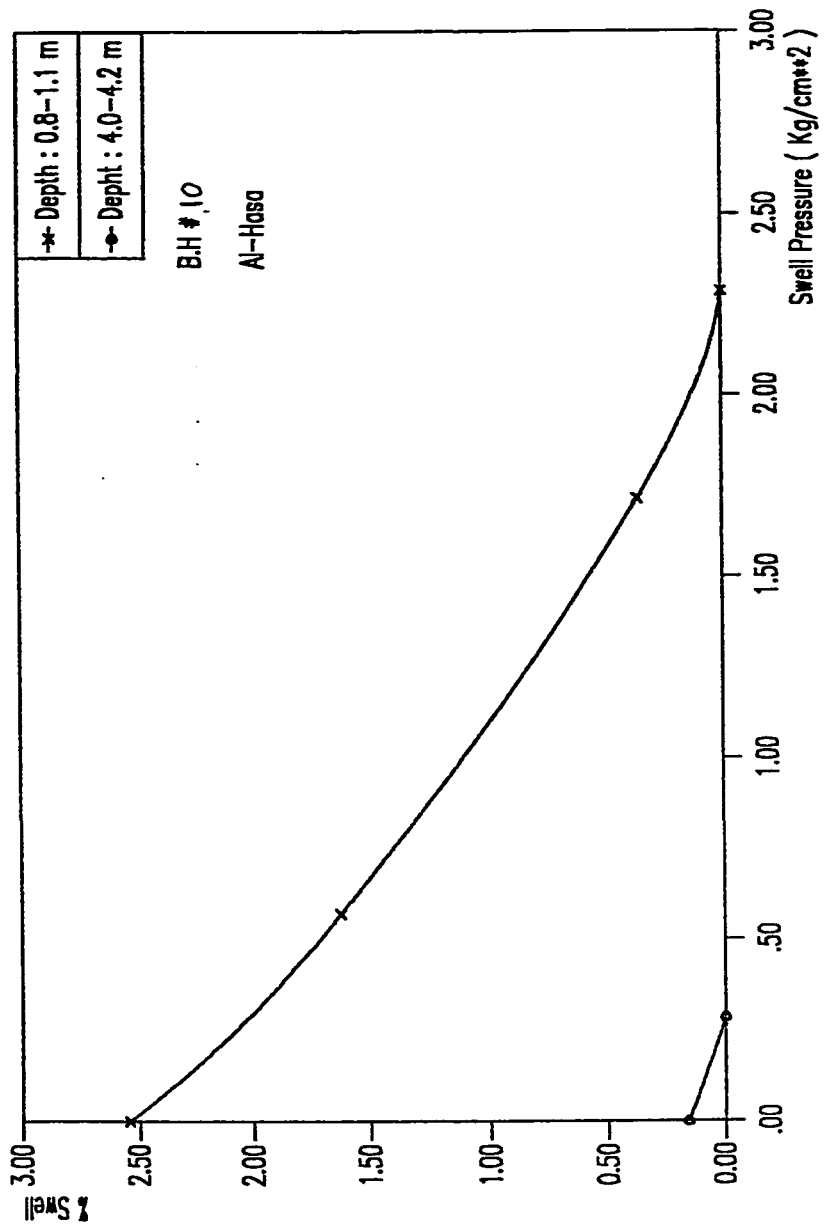


Figure (6.42) : % Swell vs Swell Pressure

BH # 10, Al-Hasa

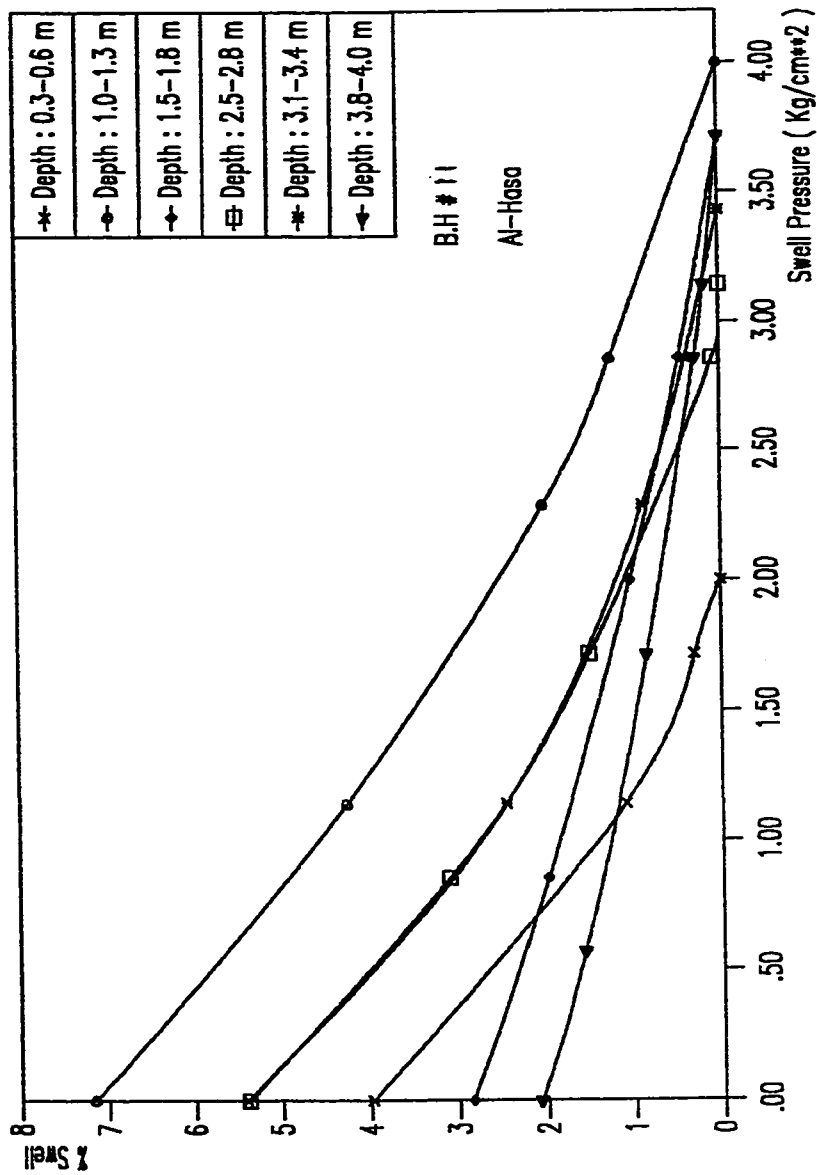


Figure (6.43) : % Swell vs Swell Pressure

BH # 11, Al-Hasa

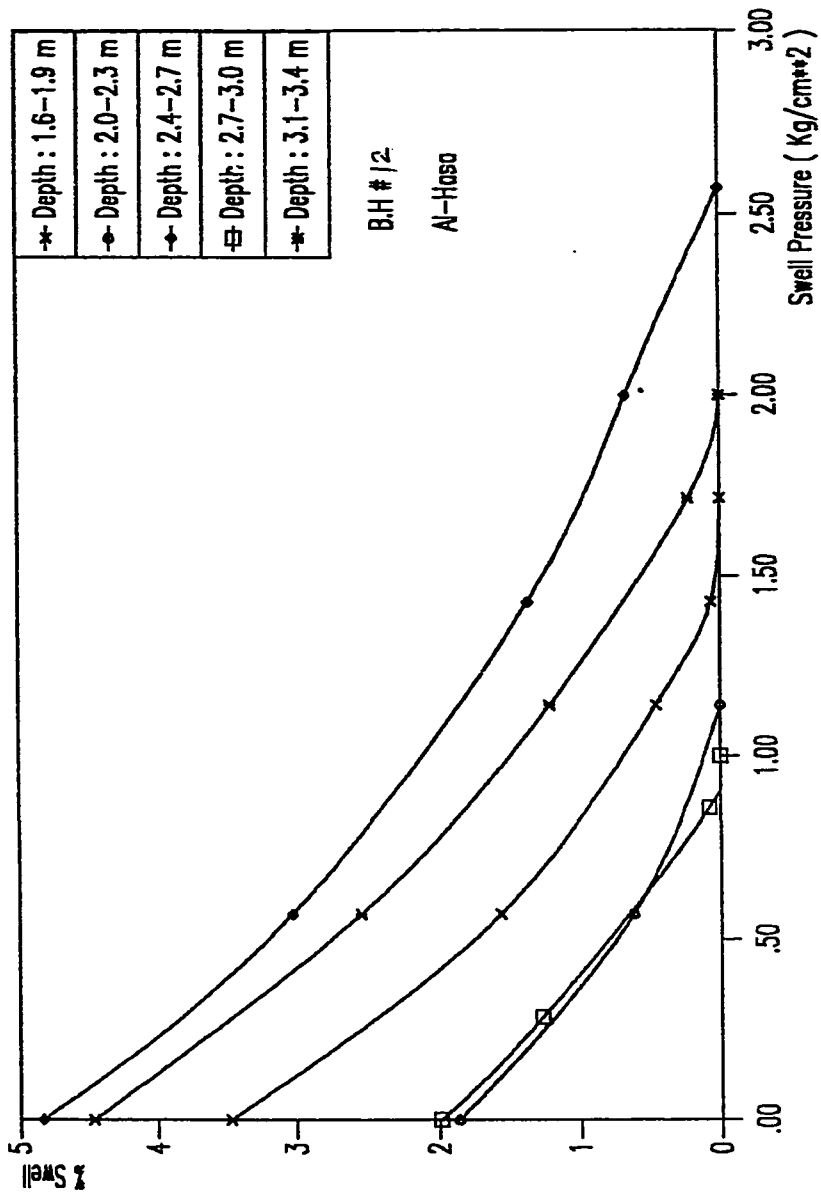


Figure (6.44) : % Swell vs Swell pressure
BH #12, Al-Hasa

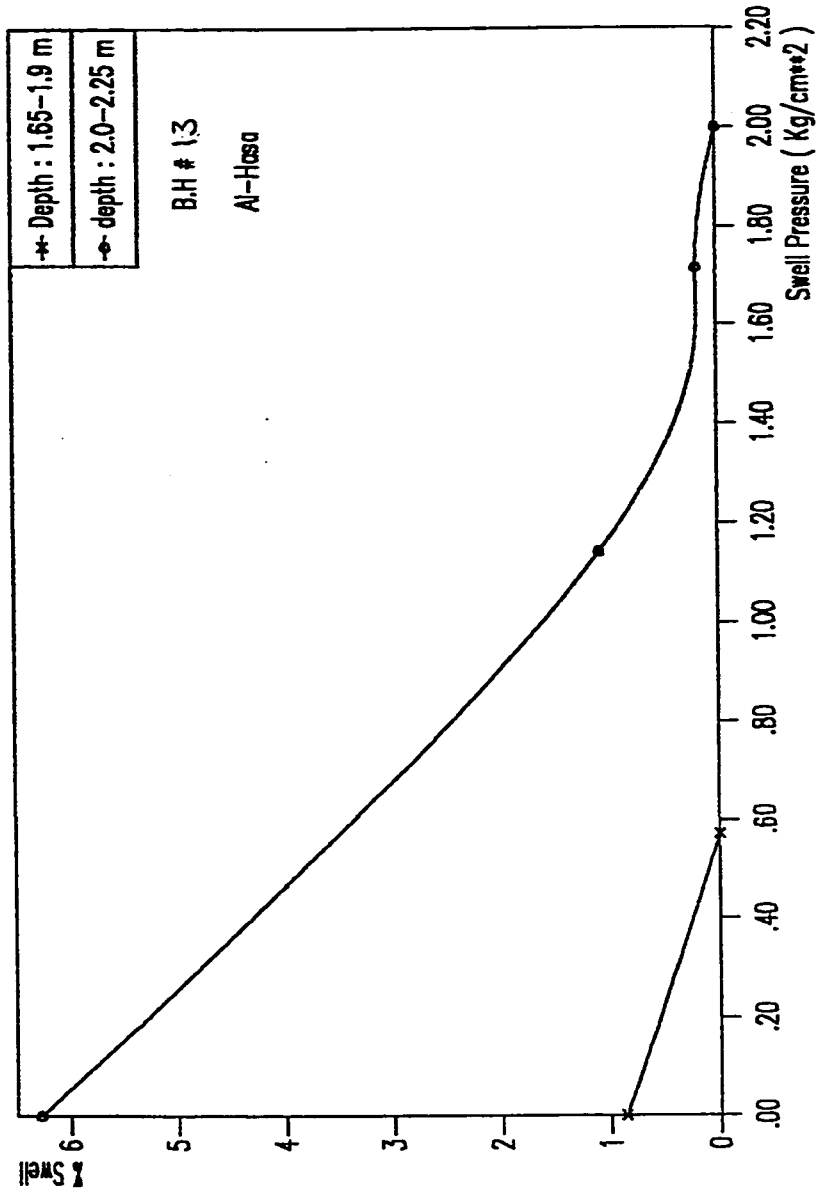


Figure (6.45) : * Swell vs Swell Pressure

BH #13, Al-Hasa

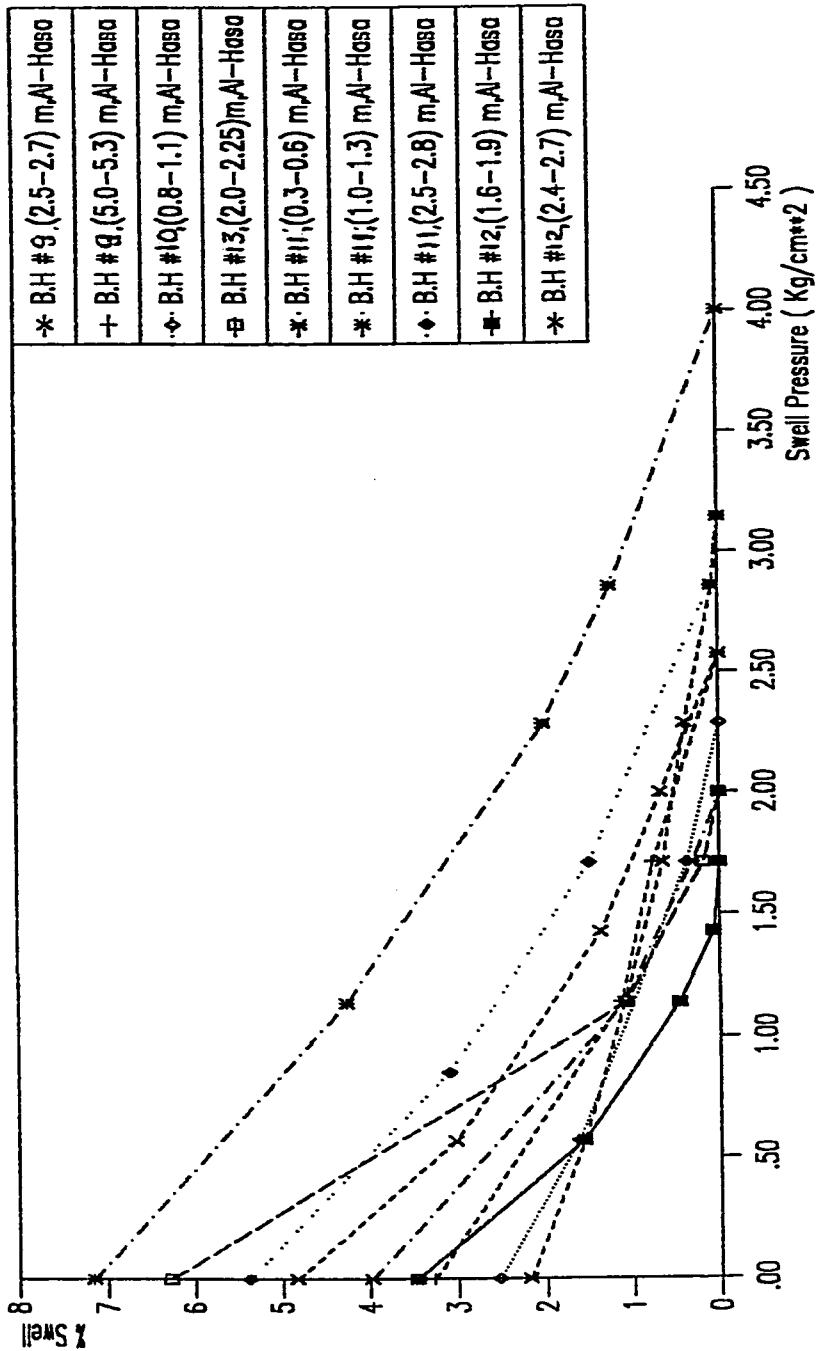


Figure (6.46) : % Swell vs Swell Pressure For Some Samples In Al-Hasa Area.

swelling pressure increases too.

6.5 EFFECT OF INITIAL SURCHARGE

Various investigators used different surcharge loads. A surcharge load of 1 psi has been used for swell tests by Holtz and Gibbs (1954), Seed, Woodward and Lundgren (1962), Kassif and Holland (1965), while Chen (1975) believes that since swell is very sensitive to changes in pressure, the use of low surcharge pressure may lead to erratic and erroneous results. Chen therefore recommended a surcharge load of about 7.2 psi simulating the pressure that most footing foundations are likely to exert on the soil (42). In this study the effect of initial surcharge on swell potential and swelling pressure was investigated. Two samples were used for this investigation namely: Sample #4 (TP #4, depth 1.7m) and Sample 2B (TP #2, depth 4.0m) both from Al-Qatif Housing Area. Sample #4 was subject to two different surcharges: 1 psi (0.086 Kg/cm^2) and 5.98 psi (0.51 Kg/cm^2) (simulating overburden pressure), while Sample #2B was subjected to three different surcharges, 1 psi, 5.9 psi (simulating overburden pressure) and 12.63 psi (1.086 Kg/cm^2) (simulating the pressure exerted by a footing). The results for Sample # 2B are shown in Fig. 6.47 and it is clearly seen that the smaller the initial surcharge, the higher the final swelling percentage. While at 1 psi surcharge the

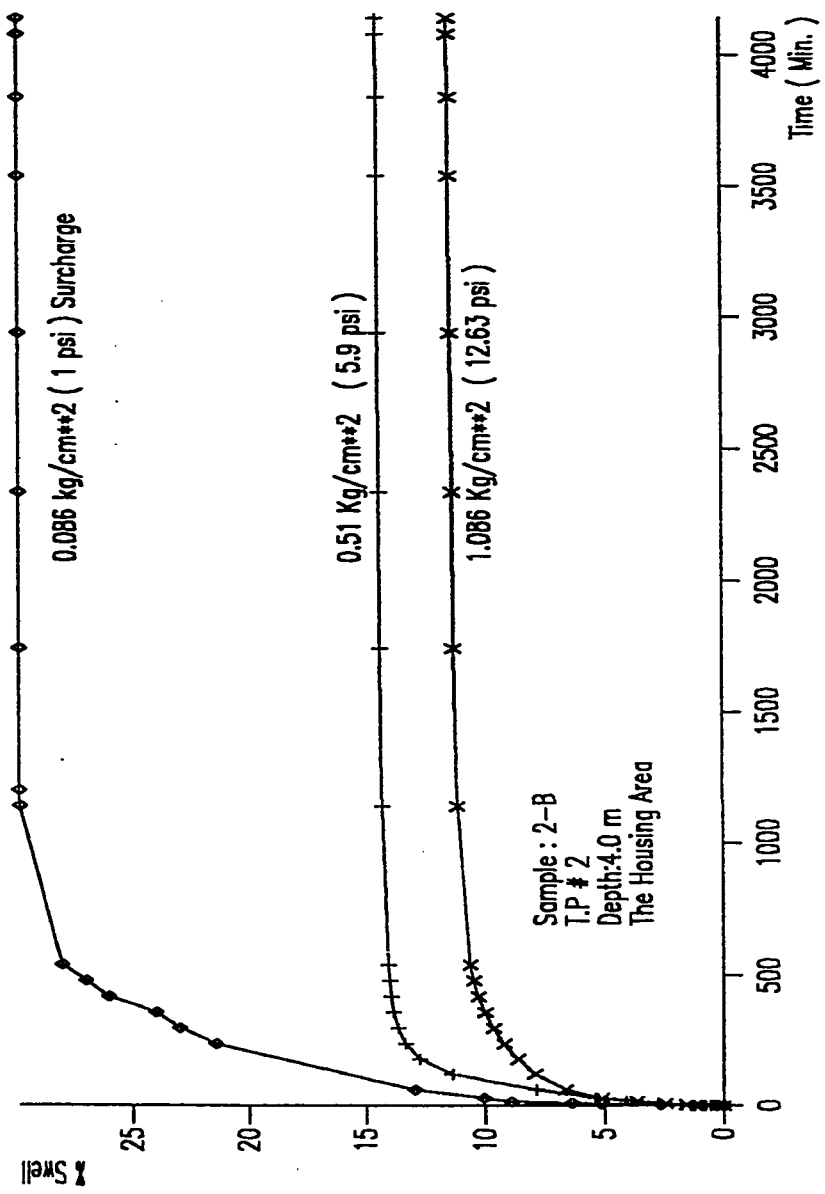


Figure 6.47: Swell vs. Time For sample 2B
 TP # 2, (4.0m.), Al Qat'if Housing Area

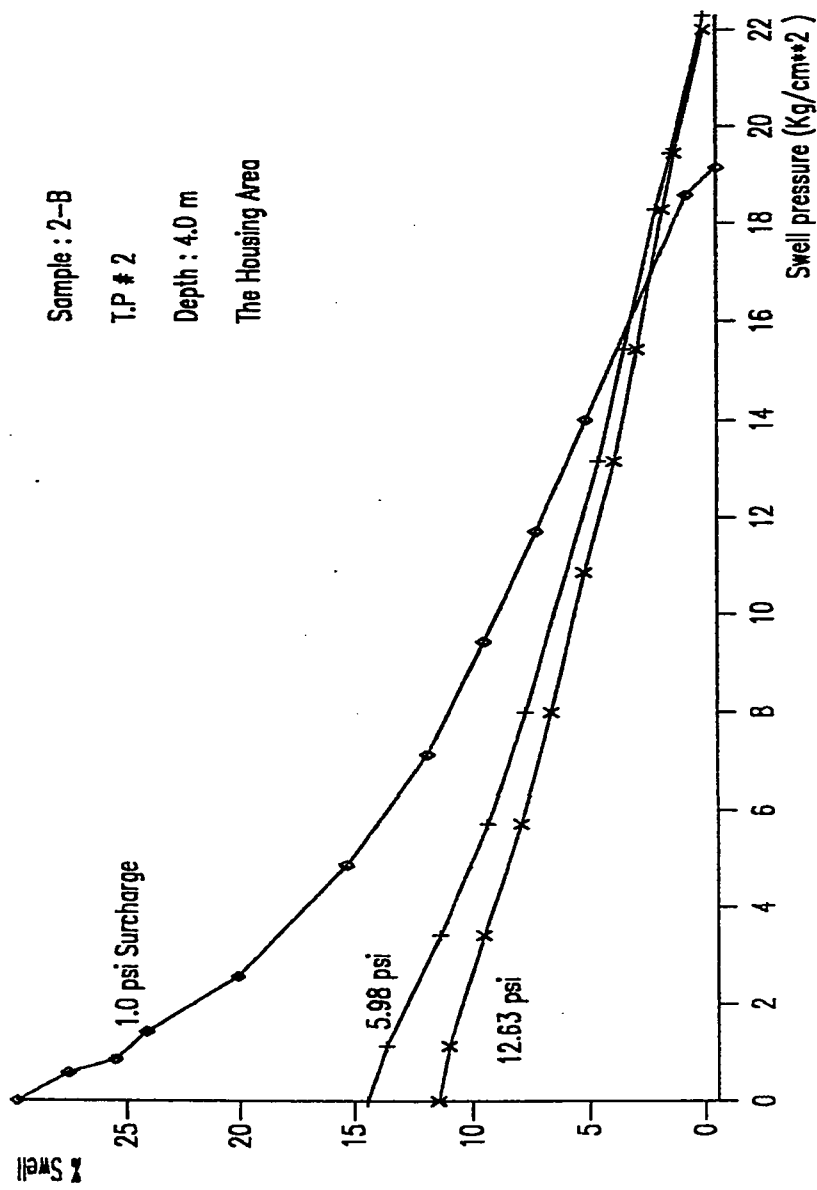


Figure 6.48: Swell vs. Swell Pressure -Effect of initial surcharge
Sample 2B, TP # 2, Depth (4.0).

sample exhibited about 29% swell, it exhibited only about 13% swell under 5.9 psi surcharge and only 10% swell under 12.63 initial surcharge.

The effect of the initial surcharge on the swelling pressure is shown in Figure 6.48 and as can be seen, no major change is observed in swelling pressures with the change of initial surcharge.

6.6 CORRELATION BETWEEN GEOTECHNICAL PROPERTIES AND SWELL POTENTIAL

Several attempts have been made in the past to establish meaningful correlations between swelling potential of expansive clays and simple physical and classification properties. A method based on a correlation of plasticity index and clay fraction with the total surface heave of a soil profile has been proposed by Van der Merwe. Another relationship between void ratio, water content, and plasticity index has been suggested by Brakly (37). Other examples of such early studies are those by Gizienski and Lee (1965), Ladd and Lambe (1961), and See et al. (1962). Liquidity index was suggested by Sowers and Kennedy (1967) as a measure of swelling potential. Komornik and David (1969) suggested a correlation between dry unit weight, liquid limit and swelling pressure. Ghazzaly (1970) proposed several single and multiple statistical correlations between swell pressure or percent swell, and

Table 6.1: Empirical Method for Predicting Heave

No.	Description	Reference
1.	$S_p = 0.00411 (LL_w)^{4.17} \sigma_v^{-3.86} w_o^{-2.33}$	Weston
2.	$\log S_p = \frac{1}{12} (0.44LL - w_o + 5.5)$	Vijayengiya et al
3.	$\log S_p = 0.0526 \gamma_d + 0.033LL - 6.8,$ (γ_d in lb/ft ³ units)	Vijayengiya et al
4.	$S_F = 0.925(0.43 LL - w_i)^{0.51} + 1.19 PI^{0.40} -$ $0.74(100-C)^{0.33}$	Dhowian et al
5.	$S_p = 0.00216 PI^{2.44}$	Seed et al
6.	$\Delta H = Fe^{-0.377D} (e^{-0.377H} - 1)$	Van der Merve
7.	$S_p = (0.00229 PI)(1.45C)/w_o + 6.38$	Nayak et al
8.	$P_s = (3.58 \times 10^{-2}) PI^{1.12} C^2/w_o^2 + 3.79,$ (P_s in psi)	Nayak et al
8.	$\log S_p = 0.9(PI/w_o) - 1.19$	Shneider et al
9.a	$S_p = 23.82 + 0.7346 PI - 0.1458 H - 1.7 w_o +$ $0.00225 PI w_o - 0.0088 PI H$	Johnson
9.b	$S_p = -9.18 + 1.5546 PI + 0.08224 H + 0.1 w_o -$ $0.0432 PI w_o - 0.0215 PI H$	
10.	$\log P_s = -2.132 + 0.0208 LL + 0.000665 \gamma_d - 0.0269 w_o$	Komornik et al

S_p	: percent swell, %.	LL	: Liquid limit
PI	: Plasticity index.	w_o	: Initial water content
ΔH	: Total heave	γ_d	: dry unit weight
F	: Correction factor for degree of expansiveness	C	: Clay percent
D	: Thickness of nonexpansive layer	σ_v	: Surcharge load
H	: Thickness of expansive layer	LLw	: Weighted liquid limit
		P_s	: Swell pressure

various classification properties of natural clays (60).

A comparative study of various empirical methods concluded that empirical relationships may yield unreliable predictions of swelling and additional geological and experimental information is necessary to validate any empirical relationship when it is used in an unfamiliar situation (37). Among the numerous methods published in current literature the most commonly referred correlations are summarized in Table 6.1

In the present study a linear regression analysis was carried out to develop a model equation relating percentage of swell to some easily determined soil properties. Preliminary analysis has shown that percentage of swell is strongly correlated with plasticity index (PI), liquid limit (LL), and in situ water content (Wn). The analysis of 42 test results revealed the following empirical relationship to predict the percentage of swell:

$$\% \text{ Swell} = 5.0 + 0.4 (\text{PI } \%) - 0.2 (\text{LL } \%) - 0.01 (\text{Wn } \%) \quad (6.3)$$

Fig. 6.49 shows a comparison between the calculated and measured % swell. The distribution of these points shows that the empirical equation predicts the percentage of swell with a good degree of accuracy. However, this relationship is useful only to soils within the study area. Table 6.2 presents a comparison between experimental percentage of swell, calculated (using eqn. 6.3), and calculated (using eqns. from literature). This table indicates that

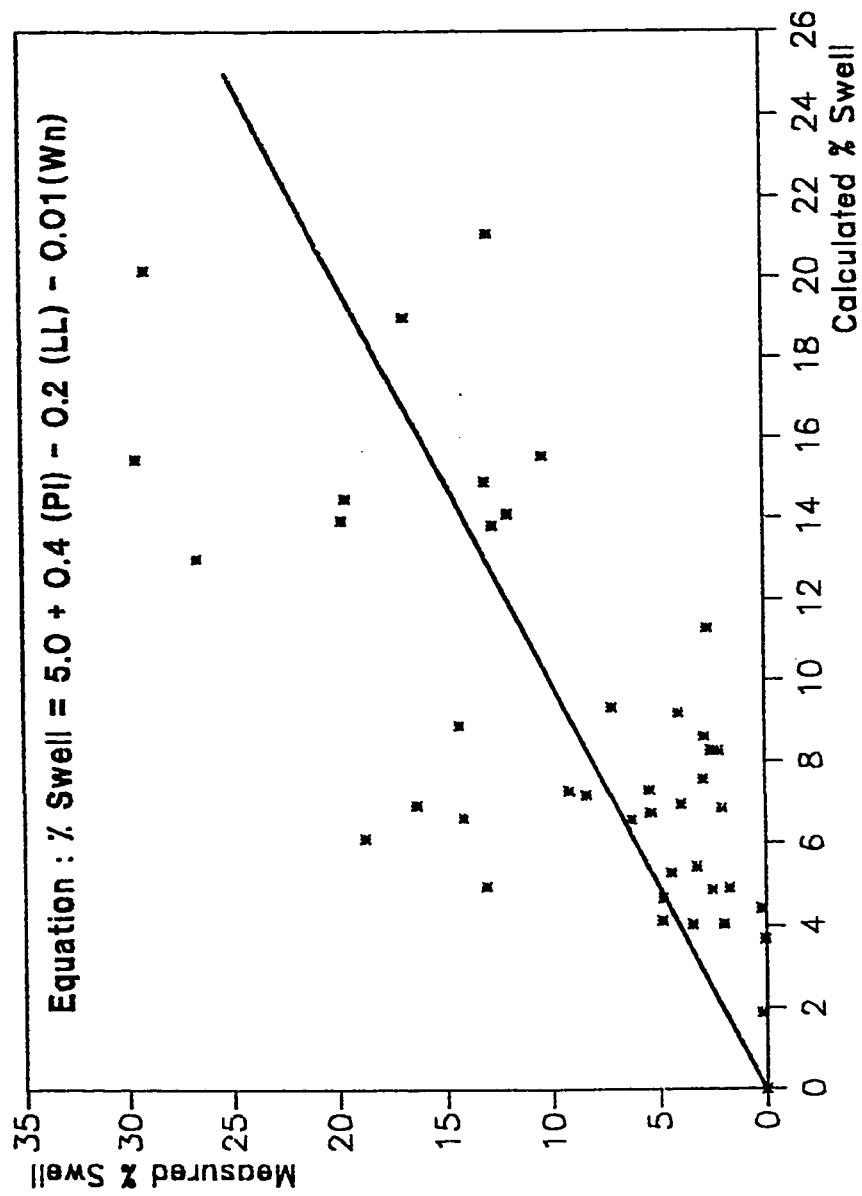


Figure 6.49: Comparison Between Measured and Calculated % Swell

Table(6.2): Comparasion Between Experimental & Calculated % Swell

BH/TP #	Depth (m)	% Swell Experimental	% Swell * Calculated from Eqn.	% Swell ** Calculated after Seed	% Swell *** Calculated after Rijayengia
TP # 1	4.0 - 4.5	19.76	13.96	166.3	2.5
TP # 2	3.8 - 4.0	26.60	13.03	93.6	7.2
TP # 2	3.2	29.49	15.48	174.4	50.9
TP # 4	1.7	13.08	14.92	131.3	10.5
TP # 6	1.5	12.74	13.84	138.6	5.33
BH # 1	3.5	9.02	7.29	21.7	0.8
BH # 1	3.8	29.02	20.18	161.5	1.02
BH # 1	4.0	16.81	19.02	214.6	21.2
BH # 2	4.2, S1	19.56	14.50	224.1	5.49
BH # 3	1.8 - 2.1	14.35	8.90	31.1	36.6
BH # 3	4.8 - 5.0	2.00	4.06	3.6	0.56
BH # 4	9.7 - 10, S1	1.72	4.93	5.8	0.009
BH # 4	9.7 - 10, S2	0.25	4.43	2.23	1.04
BH # 6	0.45 - 0.6	4.06	9.20	21.9	2.39
BH # 6	4.5 - 4.7	0.24	1.89	0.44	0.25
BH # 6	9.0 - 9.4	18.75	6.14	8.8	5.45
BH # 8	0.6 - 0.9	0.086	3.70	1.03	0.22
BH # 8	2.3 - 2.6	0.026	0	0.04	0.35
BH # 8	5.6 - 5.75	12.88	21.10	291.3	3.3
BH # 8	5.75 - 5.9	4.89	4.15	3.9	0.003
BH # 8	7.1 - 7.4	10.36	15.56	747.8	10000
TP # 7	1.1	8.40	7.18	19.3	23.8
TP # 8	0.2	12.03	14.12	144.0	143.4
TP # 8	0.8 - 1.1	2.70	11.30	91.4	24.7
TP # 9	1.1	14.17	6.63	19.5	26.3
TP # 9	2.2	16.38	6.94	25.3	36.8
TP # 11	2.0 - 2.2	13.11	4.97	9.4	9.23
BH # 9	2.6 - 2.7	2.20	8.28	25.2	39.1
BH # 9	3.0 - 3.2	2.56	8.27	22.0	29.3
BH # 9	3.5 - 3.7	2.93	7.56	32.1	4.8
BH # 9	5.0 - 5.3	3.27	5.43	14.3	5.98
BH # 10	0.8 - 1.1	2.54	4.88	8.8	14.5
BH # 13	2.0 - 2.25	6.28	6.57	15.3	21.5
BH # 11	0.3 - 0.6	3.98	6.96	21.9	80.8
BH # 11	1.0 - 1.3	7.16	9.34	41.3	20.7
BH # 11	1.5 - 1.8	2.86	8.62	25.9	26.9
BH # 11	2.5 - 2.8	5.39	6.74	14.7	6.19
BH # 11	3.1 - 3.4	5.41	7.30	15.5	10.2
BH # 11	3.8 - 4.0	2.08	6.85	15.5	16.6
BH # 12	1.6 - 1.9	3.47	4.05	2.6	1.17
BH # 12	2.4 - 2.7	4.84	4.68	6.9	3.56
BH # 12	3.1 - 3.4	4.47	5.29	14.2	6.84

* % Swell = $5.0 + 0.4 (PI) - 0.2 (LL) - 0.01 (Wn)$

** %Swell = $0.00216 PI$

*** $\log(\% Swell) = 1/12 (0.44 LL - Wn + 5.5)$

empirical equations are applicable only to soils within the study area.

Chapter 7

CONCLUSIONS AND RECOMMENDATIONS

7.1 CONCLUSIONS

This study can be considered an important reference for those interested in the geotechnical aspects in general and in expansive soils in Eastern Province of Saudi Arabia in particular, as it is one of the first studies that investigated in detail the problems of expansive soils in the area. Based on the data collected and the results obtained from the extensive investigations, the following conclusions are drawn:

- 1) Climatic conditions and geology of the area have a big influence on the formation and behavior of expansive clays. The formation of expansive soils in the area is a result of the weathering of dolimitic limestone and marls rich in magnesium. The formation of expansive soils is favoured by the alkaline environment and the absence of leaching due to the small amount of rain in the area.
- 2) Expansive soil formations were found in Al-Qatif, Al-Aujam, Umm Al-Hamam, Umm Al-Sahek, Al-Jesh and in Al-Hasa area including Al-Khars, Al-Mansoriyah, Al-Hamadiyah, Al-Naathel, Al-Salehiya and Mahasen.

- 3) The subsurface soil of Al-Qatif and the villages around it, such as Al-Aujam, Al-Jesh, Umm Al-Hamam and Umm Al-Sahek consists mainly of dense to very dense calcareous clay silt with limestone, while Al-Hasa subsurface soil consists mainly of stiff, hard, reddish brown and light green silty clay with limestone fragments and gypsum nodules.
- 4) Clays in Al-Qatif and the villages around it are highly plastic and possess very high swelling potential, while clays in Al-Hasa area including Al-Mubarraz and Al-Hofuf are plastic and possess moderate to high swelling potential.
- 5) There is a strong correlation between swell potential and the plasticity of the clay. An empirical equation was developed to present this correlation.
- 6) The study shows that shrinkage limit is not a good indicator for swelling potential of expansive soils.
- 7) An increase in surcharge load decreases the magnitude of percentage of swell while the swelling pressure remains almost constant.
- 8) The properties of Al-Qatif clays vary from one location to another even though the locations are very close

(heterogeneous). So, special precautions against differential swelling should be taken to safeguard structures which are going to be constructed in the area.

- 9) The clays of Al-Qatif and villages around it like Umm Al-Hamam, Al-Jesh, Umm Al-Sahek and Al-Aujam are rich in smectite, illite, dolomite and palygorskite, while Al-Hasa clay is rich in calcite, illite, palygorskite and kaolinite.

7.2 RECOMMENDATIONS

- 1) This study should be supplemented with other studies to have a comprehensive picture and data about expansive soils in the area.
- 2) Using other identification techniques such as chemical analysis, SEM, DTA, is very useful to confirm the results obtained and to have a better idea about the composition of the soil.
- 3) Field experimental study should be carried out and compared to the results obtained in the laboratory.

APPENDIX A

Sampler 76-mm thin-walled tube and
Types: BX core barrel

Location: Qatif Housing Area

241

Depth, m	Symbol	Samples	DESCRIPTION OF MATERIAL	Undisturbed Sample		COMMENTS
				No.	Depth m	
1			Light brown calcareous fine to medium sand with cemented nodules (1.5 m)			Samples are not required in sand
2			Interbedded light gray clayey silt and moderately strong limestone (3.5 m)	5A	3.5	Sample from clayey silt layer
4			Hard green clay with silt seams (4.0 m)	5B 5C	3.8 4.0	Two clay samples
5			Moderately strong light gray sandy limestone with clayey silt layers and clay seams			One sample from clay layer. The rock cores given to KFUPM.
6						
7						
8						
9						
10						

Final Penetration: 10.0 m

Depth to water

Date:

Date: June 4, 1990

Caved at: 5.0 m

Date: June 6, 1990

Fig. A.1 LOG OF BORING NO. 1
Al-Qatif Housing Area

Sampler 76-mm thin-walled tube and
Types: HX core-barrel

Location: Qatif Housing Area

242

Depth, m	Symbol	Samples	DESCRIPTION OF MATERIAL	Undisturbed Sample		COMMENTS
				No.	Depth m	
			Light gray silt with limestone fragments (1.0 m)			No sample
-1			Interbedded green clay and light gray clayey silt (1.5 m)			Not enough clay to obtain a sample.
-2			Light gray fine to medium sand (2.8 m)			Sample in sand not required
3			Green clay (3.0 m)			Not enough clay to sample
4			Interbedded green clay and moderately strong light gray limestone (5.0 m)	S-6	4.2	Clay layers thin to obtain many undisturbed samples
-5			Light gray silty clay (6.8 m)			
-6						
-7			Light gray moderately strong limestone with sandy silt layers (7.8 m)			No clay
-8			Light brown silt with clay seams (9.0 m)	11-A 11-B	8.0 8.5	
-9			Light gray limestone (9.5 m)			
-10			Light gray silt with clay layers			Not enough clay to sample

Final Penetration: 10.0 m

Depth to water

Date:

Date: June 7, 1990

Caved at:

Date:

Fig. A.2 LOG OF BORING NO. 2
Al-Qatif Housing Area

Sampler 76-mm thin-walled tube and
Types: EX core-barrel

Location: Qatif Housing Area

245

Depth, m	Symbol	Samples	DESCRIPTION OF MATERIAL	Undisturbed Sample		COMMENTS
				No.	Depth m	
1			Light gray silt with clay seams (1.8 m)			Not enough clay for sampling
2			Light gray clayey silt with limestone nodules - silty sand to 2.0 m (3.65 m)	S-5	2.1	
4			Light brown silty clay (4.6 m)	S-8 S-8A S-8B	3.8 4.15 4.6	
5			Interbedded light gray clayey silt and green clay - light gray limestone layers, 5.5 to 5.6 m (6.6 m)	S-9 S-9A	4.8 5.0	
7			Light brown sandy silt, clayey with limestone nodules (7.9 m)	S-11	S-9	
8			Interbedded light brown clayey silt and moderately strong light gray limestone (9.7 m)	S-13	8.2	
10						

Final Penetration: 9.7 m
Date: June 10, 1990

Depth to water 7.85 m
Caved at :
Date: June 17, 1990

Fig. A.3 LOG OF BORING NO. 3
Al-Qatif Housing Area

Sampler 76-mm thin-walled tube and
Types: HX core-barrel

Location: Al Qatif

244

Depth, m	Symbol	Samples	DESCRIPTION OF MATERIAL	Undisturbed Sample		COMMENTS
				No.	Depth m	
			Dark gray fine to medium sand - light brown below 0.3 m (0.8 m)			Not enough clay to obtain undisturbed samples
-1			Light gray sandy silt - clayey to 1.4 m - silty sand below 1.4 m (2.0 m)			Sample not required below water level
-2			Moderately strong gray sandy limestone			
-3			- sandstone, 3.5 to 4.0 m			
-4			- light brown, 4.0 to 6.0 m			
-5						
-6			- light gray below 6.0 m			
-7						
-8						
-9						
-10			(10.0 m)			

Final Penetration: 10.0 m

Depth to water 0.7 m

Date: June 20, 1990

Date: June 20, 1990

Caved at:

Date:

Fig. A.4 LOG OF BORING NO. 3A
Al-Qatif City

Sampler 76-mm thin-walled tube and
Types: HX core barrel

Location: Al Jesh Village

Depth, m	Symbol	Samples	DESCRIPTION OF MATERIAL	Undisturbed Sample		COMMENTS
				No.	Depth m	
1			Dark gray fine sand			No clay was encountered hence no undisturbed sample was taken
2						
3						
4						
			- fine to medium below 3.6 m			
			(4.6 m)			
5			Weak to moderately strong light gray limestone	S-13	6.15	
6			- clayey silt layer, 6.0 to 6.2 m			
7						
8						
9						
			(9.3 m)			
10			Light gray cemented sand			
			(10.0 m)			

Final Penetration: 10.0 m
Date: June 11, 1990

Depth to water
Caved at:

Date:
Date:

Fig. A.5 LOG OF BORING NO. 4
Al-Jesh

Sampler 76-mm thin-walled tube and
Types: FX core-barrel

Location: Al Aujam

246

Depth, m	Symbol	Samples	DESCRIPTION OF MATERIAL	Undisturbed Sample		COMMENTS
				No.	Depth m	
-1			Light gray fine sand with clayey silt layers - clayey silt, 1.05 to 1.35 - clayey silt, 1.65 to 1.8 m	S-4 S-6	1.35 1.8	
-2						
-3						
-4						
-5						
-6			Light gray silty clay Light gray fine sand	S-18	5.6	
-7						
-8						
-9			Light gray silty clay	S-25	10.0	
-10						

Final Penetration: _____ Date: _____
 Depth to water: _____ Caved at: _____ Date: _____

Fig. A.6 LOG OF BORING NO. 5
Al-Aujam

123

Sampler 76-mm thin-walled tube and
Types: HX core barrel

Location: Um Al Sahik near
Water Tower

247

Depth, m	Symbol	Samples	DESCRIPTION OF MATERIAL	Undisturbed Sample		COMMENTS
				No.	Depth m	
1			Pale brown silty clay - gypsum layer, 0.25 to 0.7 m (1.2 m)	S-1 S-2 S-3	0.6 0.9 1.15	
2			Moderately strong light gray limestone with silty sand seams (2.7 m)			
3			Interbedded light gray sandy silt and silty sand with cemented nodules (5.3 m)	S-9	4.7	
6			Moderately strong light gray sandy limestone with silt layers (6.6 m)			
7			Interbedded light gray sandy silt and silty clay - with limestone fragments and cemented sand nodules - limestone, 9.4 to 9.7 m (10.0 m)	S-17	9.4	
10						

Final Penetration: 10.0 m

Depth to water 1.0 m

Date: June 19, 1990

Date: June 13, 1990

Caved at:

Date:

Fig. A.7 LOG OF BORING NO. 6

Umm Al-Sahek

Sampler 76-mm thin-walled tube
 Types: 76-mm rock core-barrel

Location: Umm Al Sahik Village

Depth, m	Symbol	Samples	DESCRIPTION OF MATERIAL	Undisturbed Sample		COMMENTS
				No.	Depth m	
-1			Light brown silty clay with quartz - clayey silt to 0.5 m (2.1 m)	S-1	0.4	
				S-2	0.8	
				S-3	1.1	
				S-4	1.4	
				S-5	1.7	
				S-6	1.9	
-2			Moderately strong light gray sandy limestone with silty clay seams and pockets (3.45 m)	S-7	2.1	
-3						
-4			Interbedded light gray sandy lime- stone, silty clay and sandy silt (7.0 m)	S-9	3.8	
-5				S-10	4.3	
-6						
-7						
-8			Interbedded green clay and light brown silty clay with limestone nodules (10.0 m)	S-13	7.4	
-9				S-14	7.7	
				S-16	8.6	
				S-17	9.6	
-10				S-18	10.0	

Final Penetration: 10.0 m

Depth to water 3.7 m

Date: June 21, 1990

Date: June 21, 1990

Caved at :

Date:

Fig. A.7 LOG OF BORING NO. 7

Umm Al-Sahek

123

Sampler 76-mm thin-walled tube and
Types: HX core-barrel

Location: Umm Al Hamman

249

Depth, m	Symbol	Samples	DESCRIPTION OF MATERIAL	Undisturbed Sample		COMMENTS
				No.	Depth m	
-1			Light brown fine to medium sand - gray carbonate sandy silt with -- shell fragments and roots, 0.3 to 1.1 m (1.7 m)	S-1 S-2 S-3	0.6 0.9 1.2	
-2			Light gray carbonate sandy silt - with cemented nodules to 2.0 m (3.0 m)	S-7	2.3	
-3			Moderately strong light gray sandy limestone with iron oxide stains (4.5 m)			
-4						
-5			Interbedded light gray limestone with light brown silty clay - limestone layers, 4.5 to 4.7 m and 5.15 to 5.6 m (5.9 m)	S-11 S-12 S-13	4.9 5.15 5.9	
-6			Moderately strong limestone (7.1 m)			
-7						
-8			Light brown silty clay (8.0 m)	S-14	7.4	
-9			Light gray carbonate silt with green clay pockets and limestone layers (10.0 m)			
-10						

Final Penetration: 10.0 m

Depth to water 0.6 m

Date: June 18, 1990

Date: June 18, 1990

Caved at:

Date:

Fig. A.9 LOG OF BORING NO. 8

Umm Al-Hamam

Sampler 76-mm thin-walled tube and
Types: 76-mm inner split core barrel Location:

Depth, m	Symbol	Samples	DESCRIPTION OF MATERIAL	Undisturbed Sample		COMMENTS
				No.	Depth m	
- 1			Fill: Light brown silty fine to coarse sand with limestone fragments	1	1.2	Shelby
- 2			(2.3 m)			
- 3			Hard reddish brown and light gray silty clay	2	2.5	Shelby
			- with gypsum nodules to 3.0 m	3	2.7	"
			- light gray with sandy silt pockets and limestone fragments, 3.0 to 3.5 m	4	3.2	"
				5	3.7	"
				6	4.3	"
			- olive gray with light brown silty fine to coarse sand seams, pockets and limestone fragments below 3.5 m	7	4.3	"
				8	6.3	"
				9	6.9	"
				10	7.0 to 8.0	Coring
					8.0 to 9.5	Coring
				11	9.5	
- 10			(10.1 m)	12	10	Shelby

Final Penetration: 10.1 m

Depth to water

Date: December 6, 1990

Cored at: 3.2 m Date: December 13, 1990

Fig. A.10 LOG OF BORING NO. 9
Al-khars, Al-Mubarraz

Sampler 76-mm thin-walled tube and
Types: 76-mm inner split core barrel Location:

251

Depth, m	Symbol	Samples	DESCRIPTION OF MATERIAL	Undisturbed Sample		COMMENTS
				No.	Depth m	
-1			Dense dark gray sandy silt, clayey with limestone fragments (03. m)	1	1.10	Shelby
-2			Hard olive and light gray silty clay with limestone nodules and reddish brown silty sand layers	2	2.2 to 2.10	Core
-3				3	2.2 to 3.6	Core
-4			- olive gray with limestone layers and fragments below 4.0 m	4	4.2	Shelby
-5				5	4.5 to 6.0	Core
-6				6	6.0 to 7.5	Core
-7				7	7.5 to 8.7	Core
-8				8	7.5 to 10.0	Core
-9						
-10			(10.0 m)			

Final Penetration: 10.0 m
Date: December 8, 1990

Depth to water
Coved at: 2.5 m Date: December 13, 1990

Fig. A.11 LOG OF BORING NO. 10
Al-Mansoriyah, Al-Mubarraz

Sampler 76-mm thin-walled tube and
Types: 76-mm inner split core barrel Location:

Depth, m	Symbol	Samples	DESCRIPTION OF MATERIAL	Undisturbed Sample		COMMENTS
				No.	Depth m	
			Light brown fine to coarse sand with occasional fine gravel (0.3 m)	1	0.6	Shelby
- 1			Hard olive and reddish brown clay with light gray silty clay pockets and gypsum nodules to 3.5 m - with limestone fragments below 3.5 m	2	1.3	"
				3	1.8	"
- 2				4	2.3	"
				5	2.8	"
- 3				6	3.4	"
				7	4.0	"
- 4				8	4.0 to 5.5	Core
- 5			9	5.5 to 6.8	Core	
- 6			(7.0 m)			
- 7			Interbedded strong light gray dolomitic limestone and olive gray silty clay		6.8 to 8.2	Core
- 8				10	8.2	
				11	8.5	Shelby
- 9			(9.8 m)		8.5 to 9.8	Core
				12	9.8	
- 10						

Final Penetration: 9.8 m
Date: December 10, 1990

Depth to water
Caved at: 2.0 m Date: December 13, 1990

Fig. A.12 LOG OF BORING NO. 11

Al-Hamadiya, Al-Mubarrac

123

50-mm core-barrel

Sampler 76-mm thin-walled tube and
Types: 76-mm inner split barrel

Location: Near Soccer Stadium

Depth, m	Symbol	Samples	DESCRIPTION OF MATERIAL	Undisturbed Sample		COMMENTS
				No.	Depth m	
- 1			Fill: Dark gray and light gray silty sand with limestone fragments (1.6 m)			
- 2			Hard olive gray clay with silty sand layers and seams - gypsum layer, 2.4 to 2.7 m - with limestone fragments below 2.7 m (3.1 m)	1	1.9	Shelby
				2	2.3	"
				3	2.7	"
- 3				4	3.0	"
- 4			Light gray sandy silt clayey with clay seams (5.0 m)	5	3.4	Shelby
				6	3.6 to 5.0	Core
- 5			Hard olive gray silty clay with limestone nodules and iron oxide stains - light gray and pale brown with reddish brown sandy silt pockets below 7.5 m	7	5.0 to 6.0	Core
- 6				8	6.0 to 7.5	Core
- 7				9	7.5 to 9.0	Core no recovery
- 8				10	9-10	Shelby bent
- 9				11	9.10 to 9.6	Core
- 10			(10.0 m)	12	9.6 to 10.0	Core

Final Penetration: 10.0 m
Date: December 12, 1990

Depth to water
Cored at: 5.0 m Date: December 13, 1990

Fig. A.13 LOG OF BORING NO. 12
Al-Salchiya, Al-Hofuf

123

Sampler 76-mm thin-walled tube and
Types: 76-mm inner split tube

Location: Saudi Aramco Hospital

254

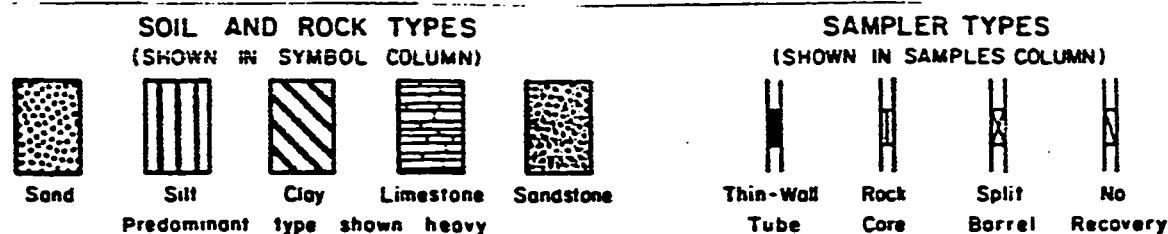
Depth, m	Symbol	Samples	DESCRIPTION OF MATERIAL	Undisturbed Sample		COMMENTS
				No.	Depth m	
			Dense reddish brown sandy silt (0.05 m)			
- 1			Hard olive gray light brown silty clay	1	0.15 to 1.65	Core
- 2			- with limestone fragments below 2.2 m (2.5 m)	2	1.9	Shelby
				3	2.25	Shelby
- 3			Hard olive gray clayey silty clay layers and sandy silt pockets			
- 4			(4.0 m)	4	2.5 to 4.0	Core
- 5			Interbedded hard light gray and pale brown silty clay and strong light gray limestone	5	4.0 to 5.5	Core
- 6				6	5.5 to 7.0	Core
- 7						
- 8				7	7.0 to 8.5	Core
- 9						
- 10			(10.0 m)	8	8.5 to 10.0	Core

Final Penetration: 10.0 m

Date: December 13, 1990

Fig. A.14 LOG OF BORING NO. 13
Mahasen, Al-Hofuf

123



TERMS DESCRIBING CONDITION OR CONSISTENCY

The condition of coarse grained soils may be obtained by performing sampler penetration tests or cone penetrometer tests. Approximate correlation between these tests and the condition are given below.

CONDITION	SPT VALUES, N	CONE TIP RESISTANCE, MPa
Very Loose	<4	<2
Loose	4 to 10	2 to 4
Medium Dense	10 to 30	4 to 12
Dense	30 to 50	12 to 20
Very Dense	>50	>20

Density versus SPT value relationship is after Terzaghi and Peck, 1968. See Lacroix and Horn, 1973 if non-standard samplers are used. Density versus cone tip resistance relationship given above, after Meyerhof 1965, is a function of depth also; see Schmertmann, 1978.

The consistencies of cohesive soils may be obtained by performing undrained shear strength tests. Degrees of consistency are given below.

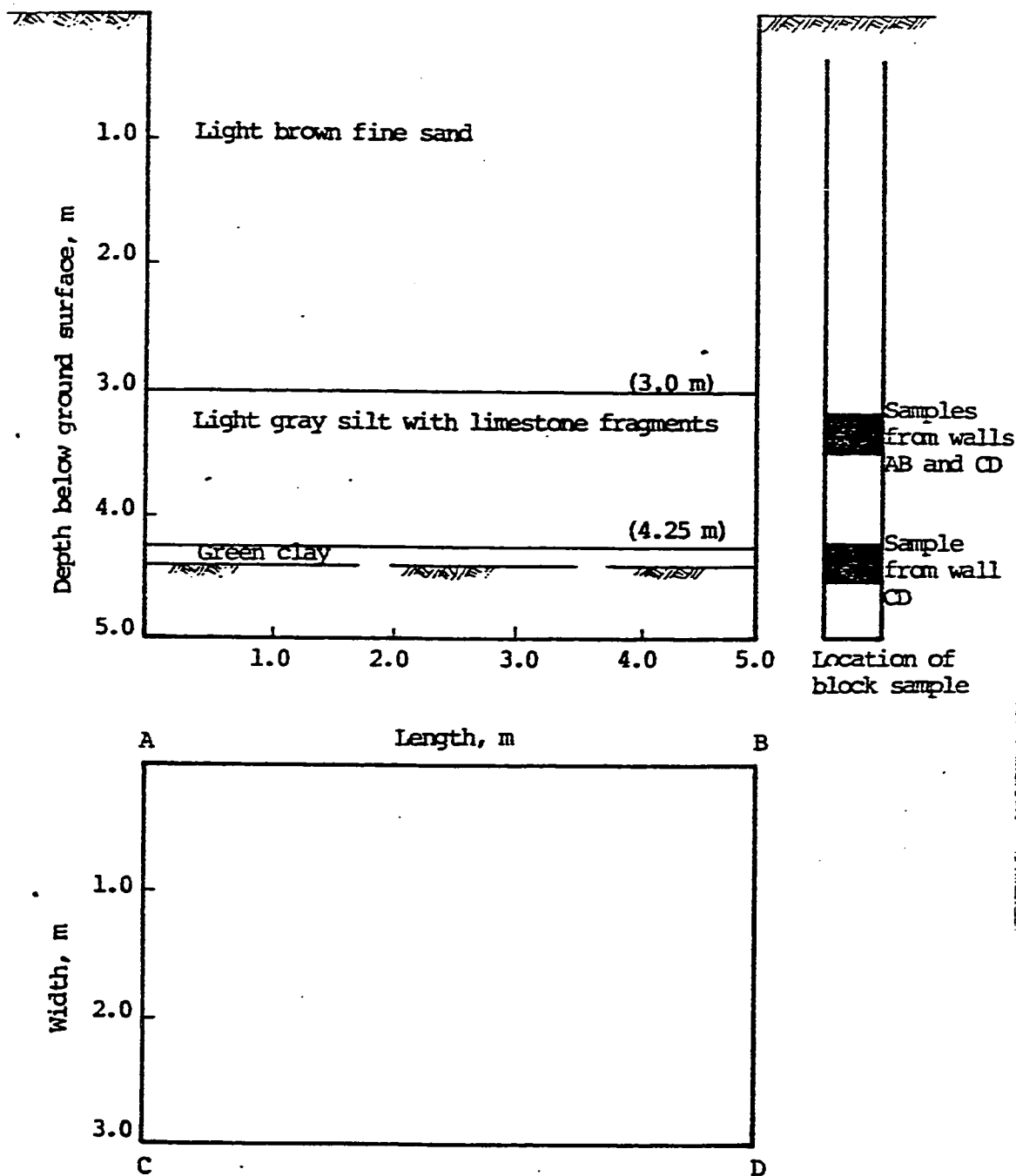
CONSISTENCY	UNDRAINED SHEAR STRENGTH, kPa
Very Soft	<12
Soft	12 to 25
Firm	25 to 50
Stiff	50 to 100
Very Stiff	100 to 200
Hard	>200

TERMS CHARACTERIZING SOIL STRUCTURE

Parting	- horizontal inclusion of different soil type less than 3-mm thick.
Seam	- horizontal inclusion of different soil type 3 to 75-mm thick.
Layer	- horizontal inclusion of different soil type greater than 75-mm thick.
Pocket	- inclusion of different soil type that is smaller than the diameter of the soil sample.
Fissured	- containing shrinkage cracks, frequently filled with fine sand or silt; usually more or less vertical.
Interbedded	- composed of alternate layers of different soil types.
Silty	- containing 12 to 50 percent silt size particles.
Calcareous	- containing 12 to 50 percent carbonates.
Carbonate	- containing more than 50 percent carbonates.

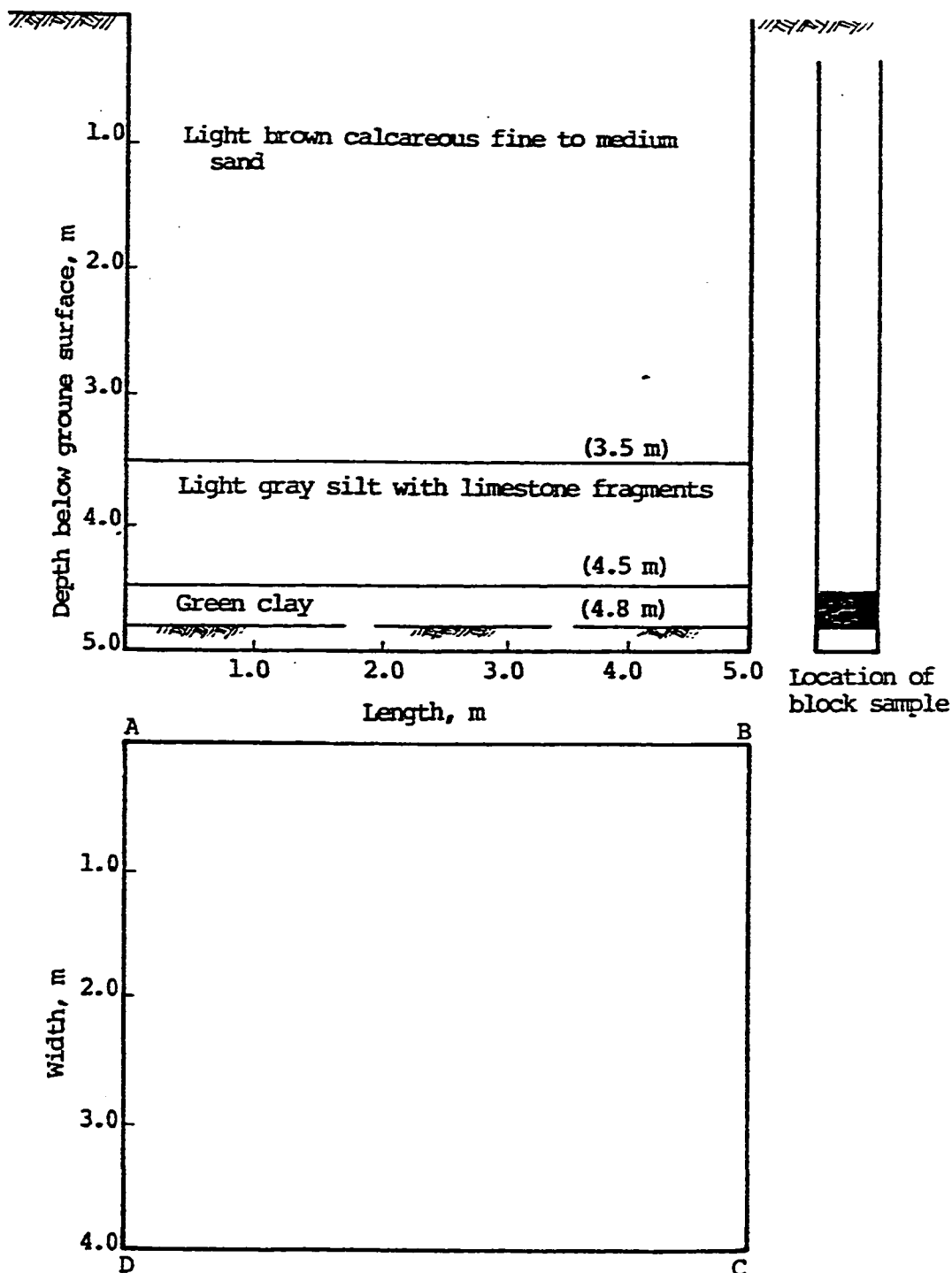
Terms used in this report for describing soils according to their texture or grain size distribution are in accordance with the UNIFIED SOIL CLASSIFICATION SYSTEM, as described in Technical Memorandum No. 3-357 Waterways Experiment Station, 3/53

Fig. A.16 SYMBOLS AND TERMS USED ON BORING LOGS



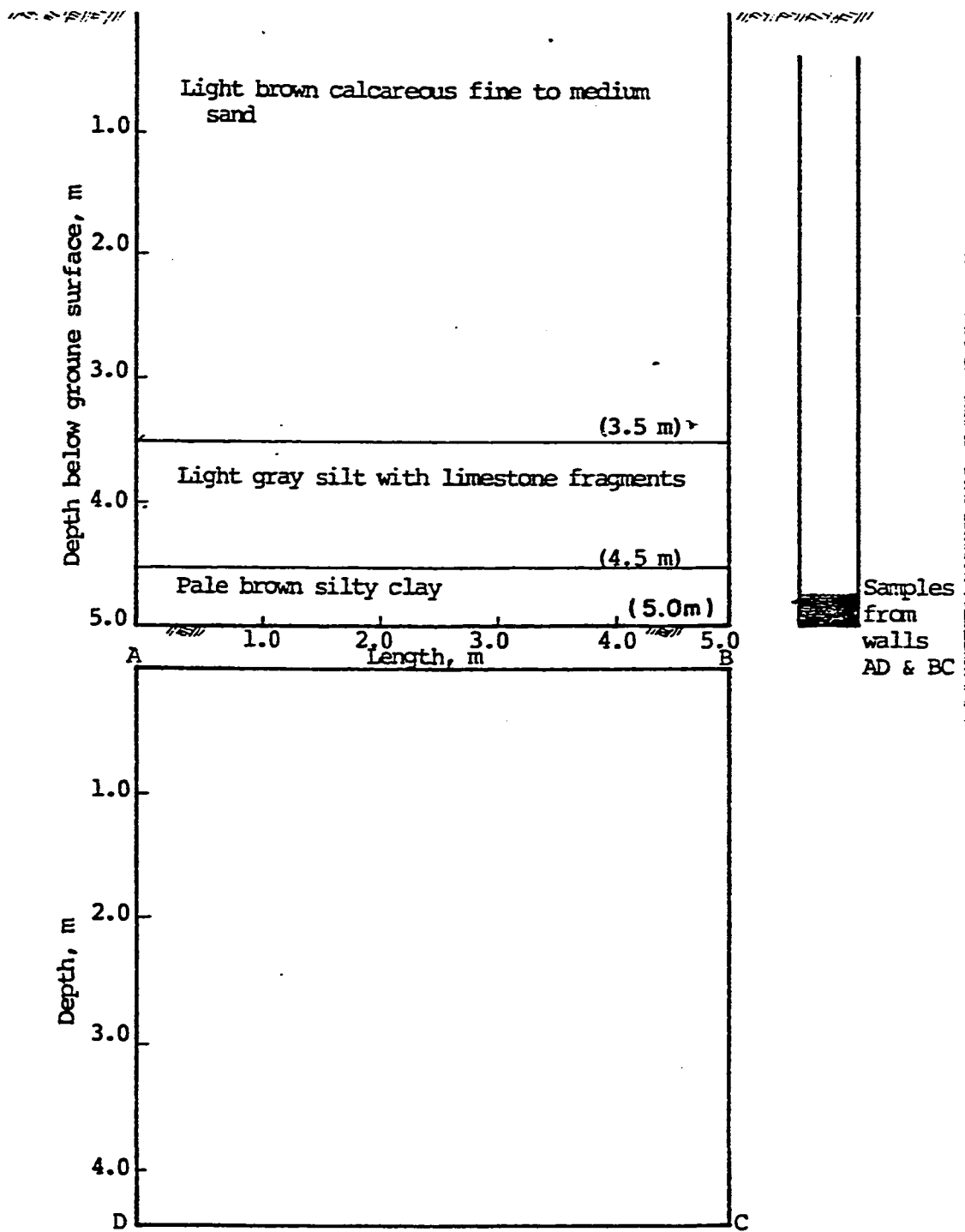
Location of Test Pit : Qatif Housing Project Water Depth: Dry
 Date of Excavation : June 5, 1990 Date of Meast.: June 5, 1990

Fig. A.17 **LOG OF TEST PIT No. 1**
 Al-Oatif Housing Area



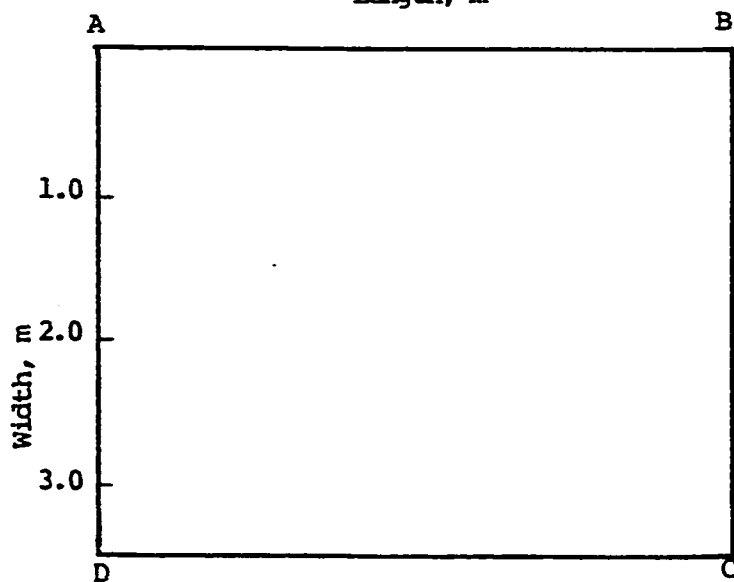
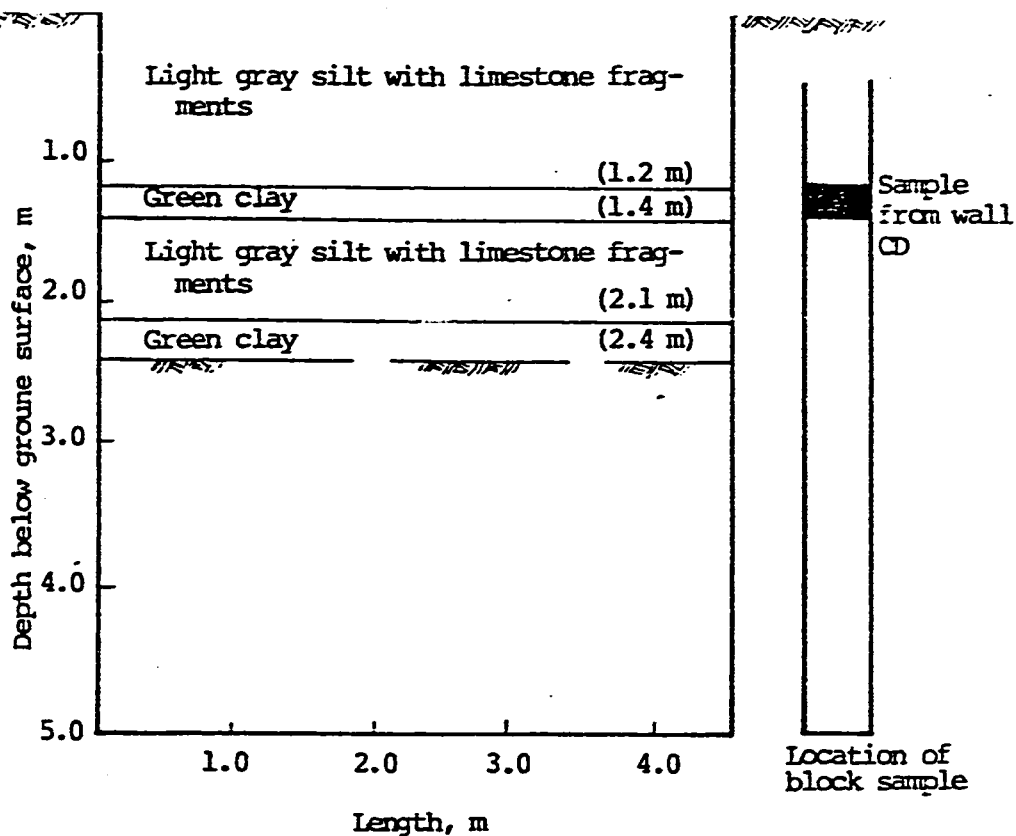
Location of Test Pit : Qatif Housing Project Water Depth: Dry
 Date of Excavation : June 9, 1990 Date of Meast.: June 9, 1990

Fig. A.18 **LOG OF TEST PIT No. 2**
 Al-Qatif Housing Area



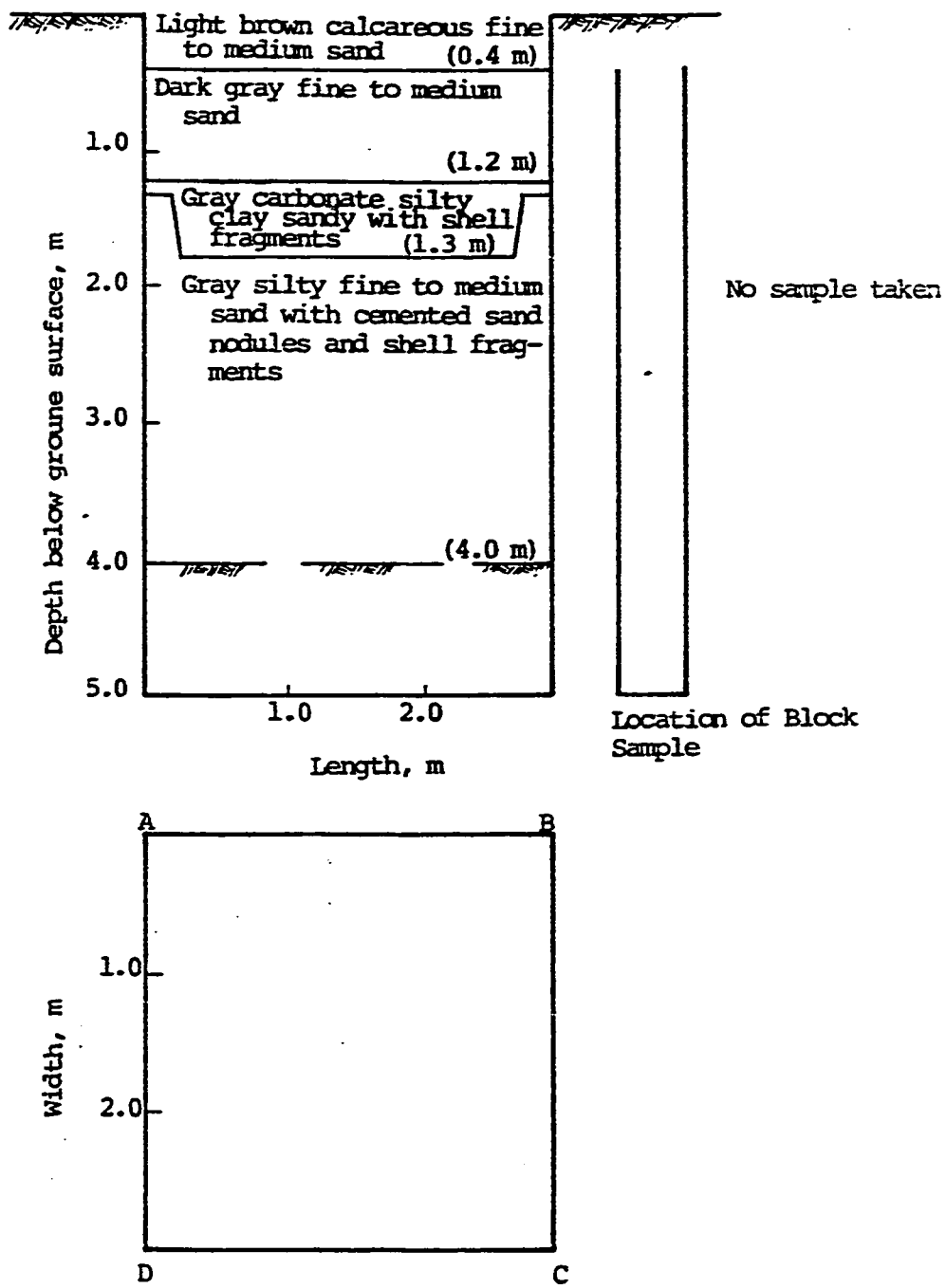
Location of Test Pit : Qatif Housing Project Water Depth: Dry
Date of Excavation : June 9, 1990 Date of Meast.: June 9, 1990

Fig. A.19 **LOG OF TEST PIT No.3**
Al-Qatif Housing Area



Location of Test Pit : Qatif Housing Project Water Depth: Dry
 Date of Excavation : June 9, 1990 Date of Meast.: June 9, 1990

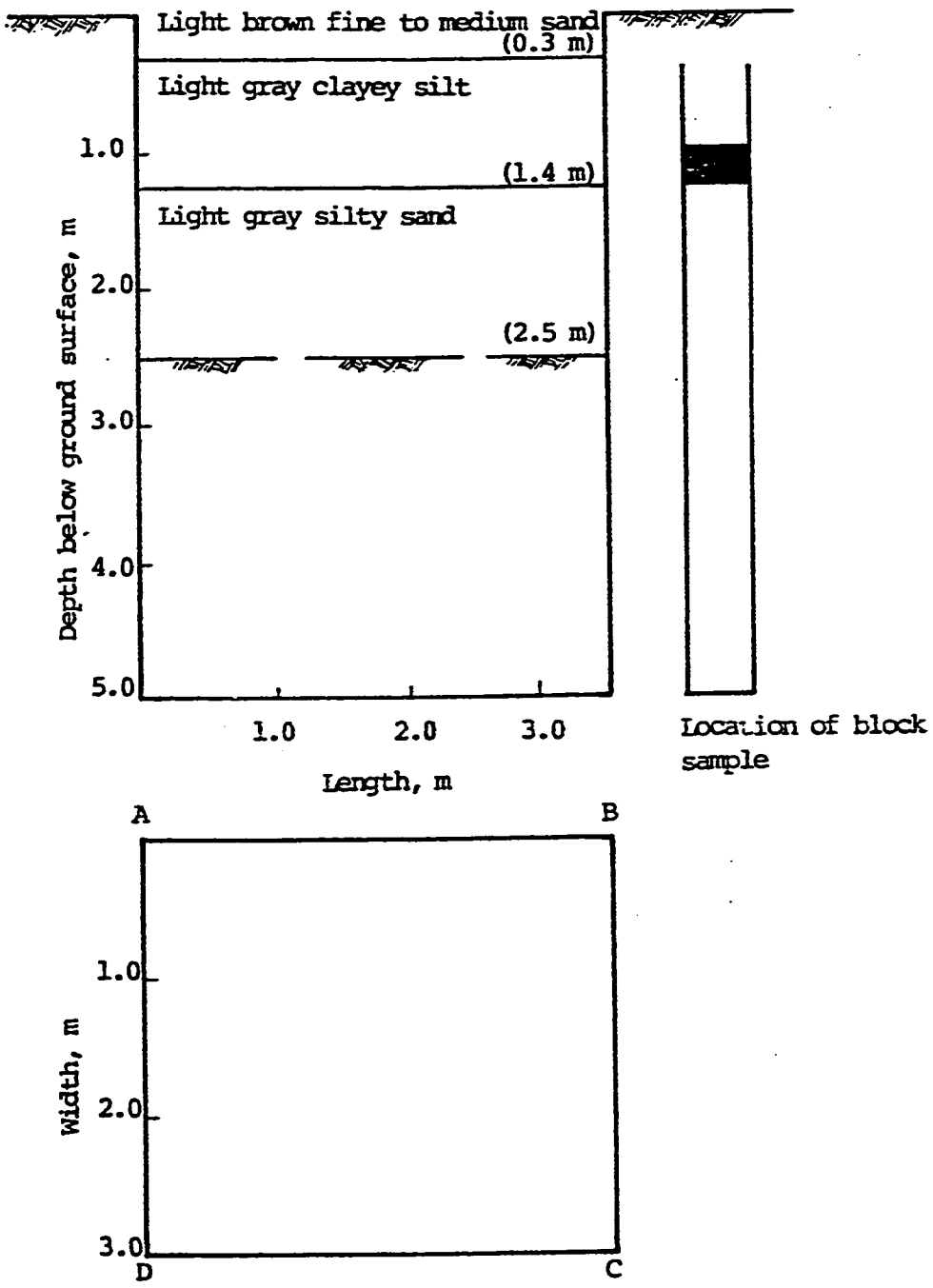
Fig. A.20 **LOG OF TEST PIT No. 4**
 Al-Qatif Housing Area



Location of Test Pit : Al Jesh
 Date of Excavation : June 10, 1990

Water Depth: 1.1 m
 Date of Meast.: June 10, 1990

Fig. A.21 LOG OF TEST PIT No.5A
 Al-Jesh

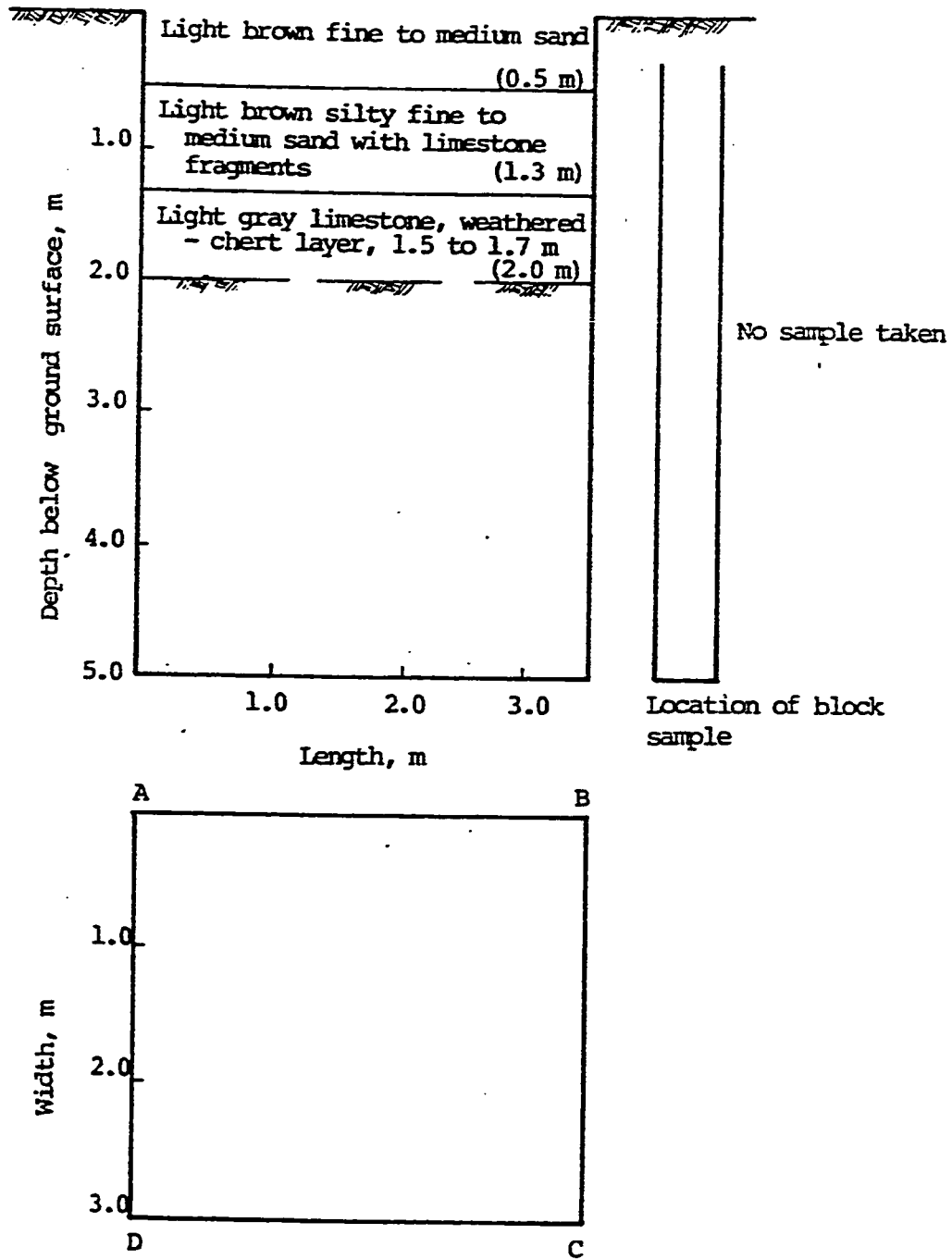


Location of Test Pit : Al Aujam
Date of Excavation : June 10, 1990

Water Depth: 1.0 m
Date of Meast.: June 10, 1990

Fig. A.22 LOG OF TEST PIT No.5
Al-Aujam

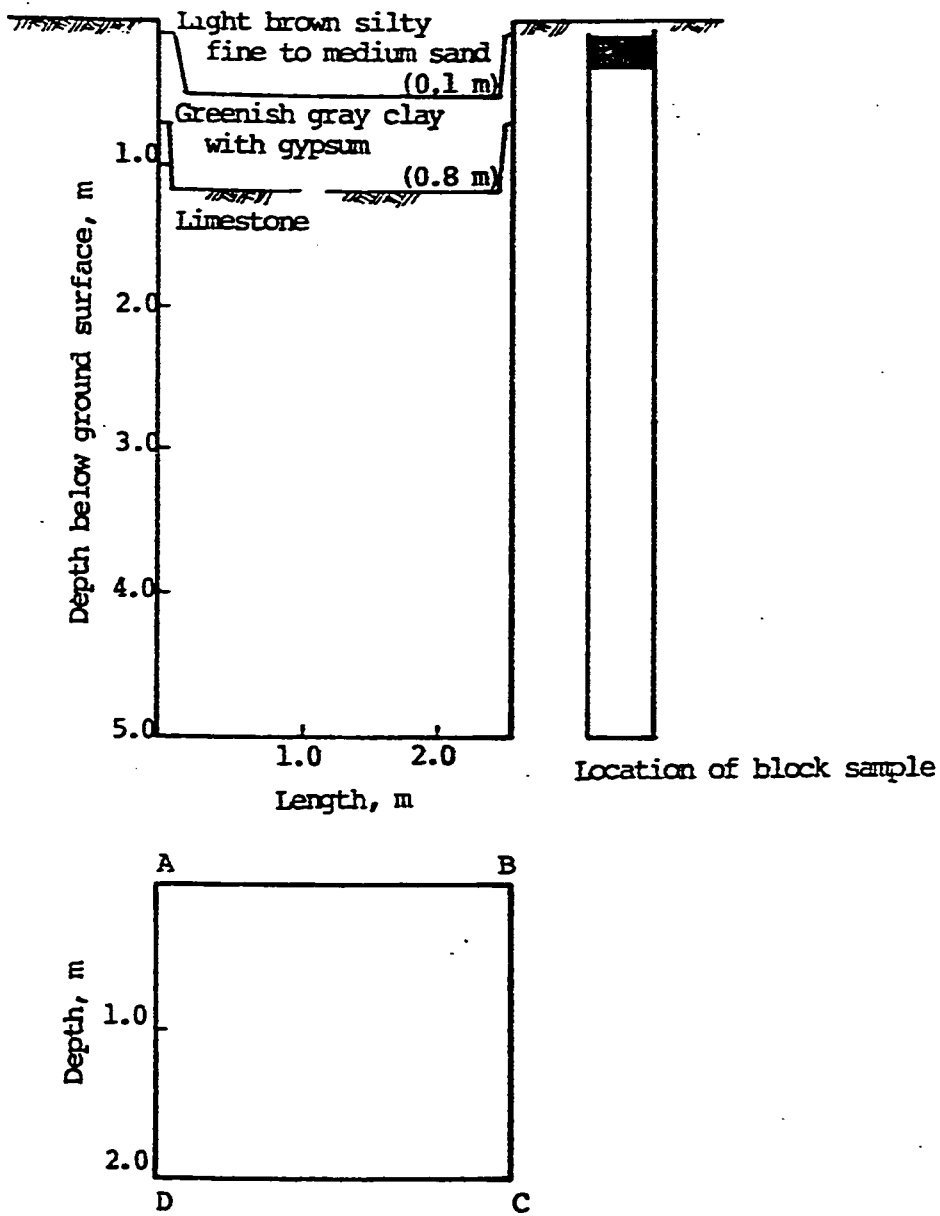
123



Location of Test Pit : Um Al Saik^h
 Date of Excavation : June 11, 1990

Water Depth: 1.55 m
 Date of Meast.: June 11, 1990

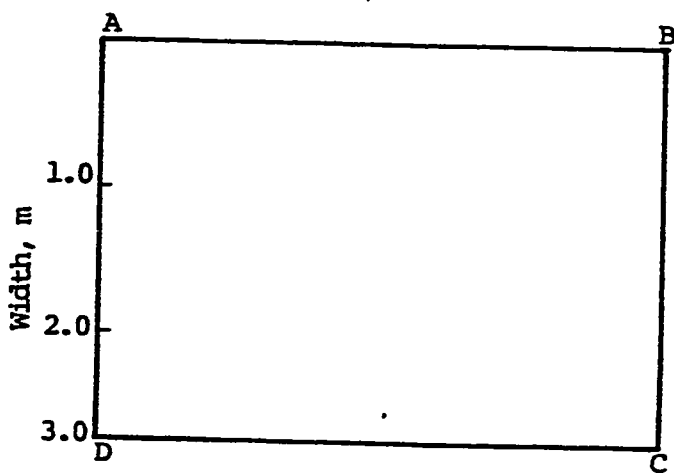
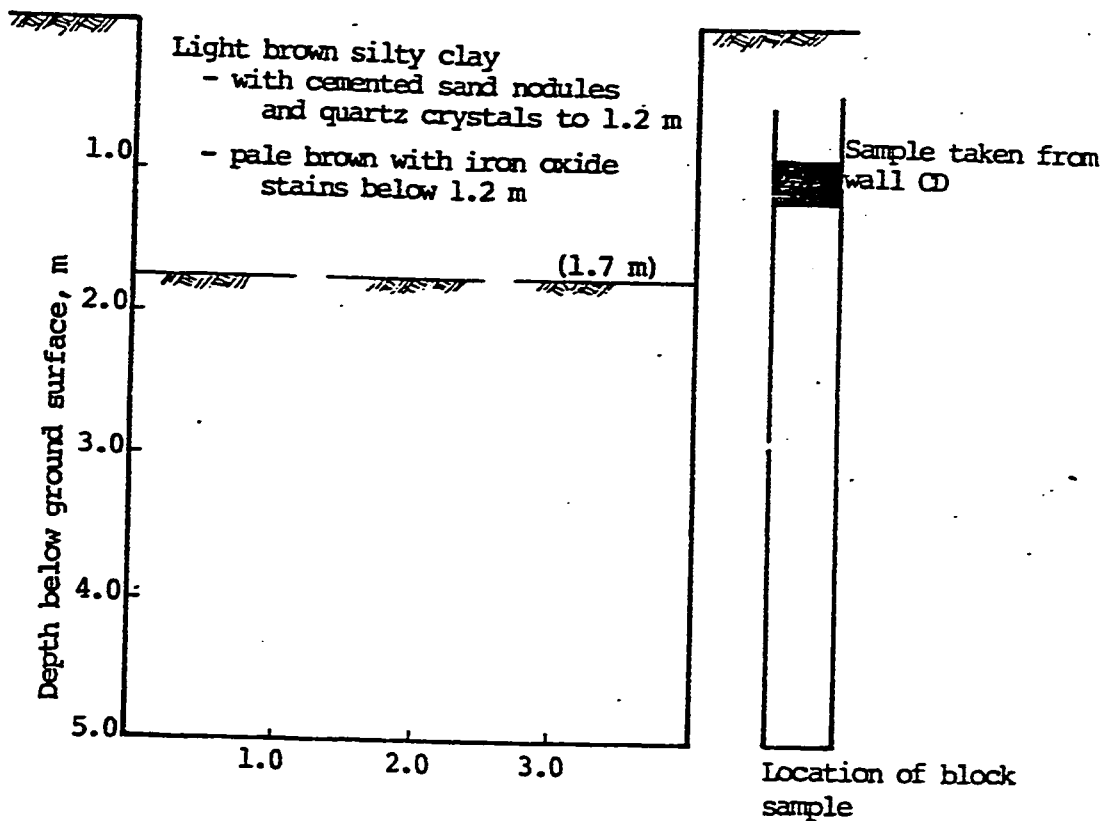
Fig. A.23 **LOG OF TEST PIT No. 6**
 Umm Al-Sahek



Location of Test Pit : Um Al Saik^h
 Date of Excavation : June 11, 1990

Water Depth: Dry
 Date of Meast.: June 11, 1990

Fig. A.24 LOG OF TEST PIT No. 6A
 Umm Al-Sahek



Location of Test Pit : Um Al Saik
 Date of Excavation : June 19, 1990

Water Depth: Dry
 Date of Meast.: June 19, 1990

Fig. A.25 LOG OF TEST PIT No. 6B
 Umm Al-Sahek

APPENDIX B

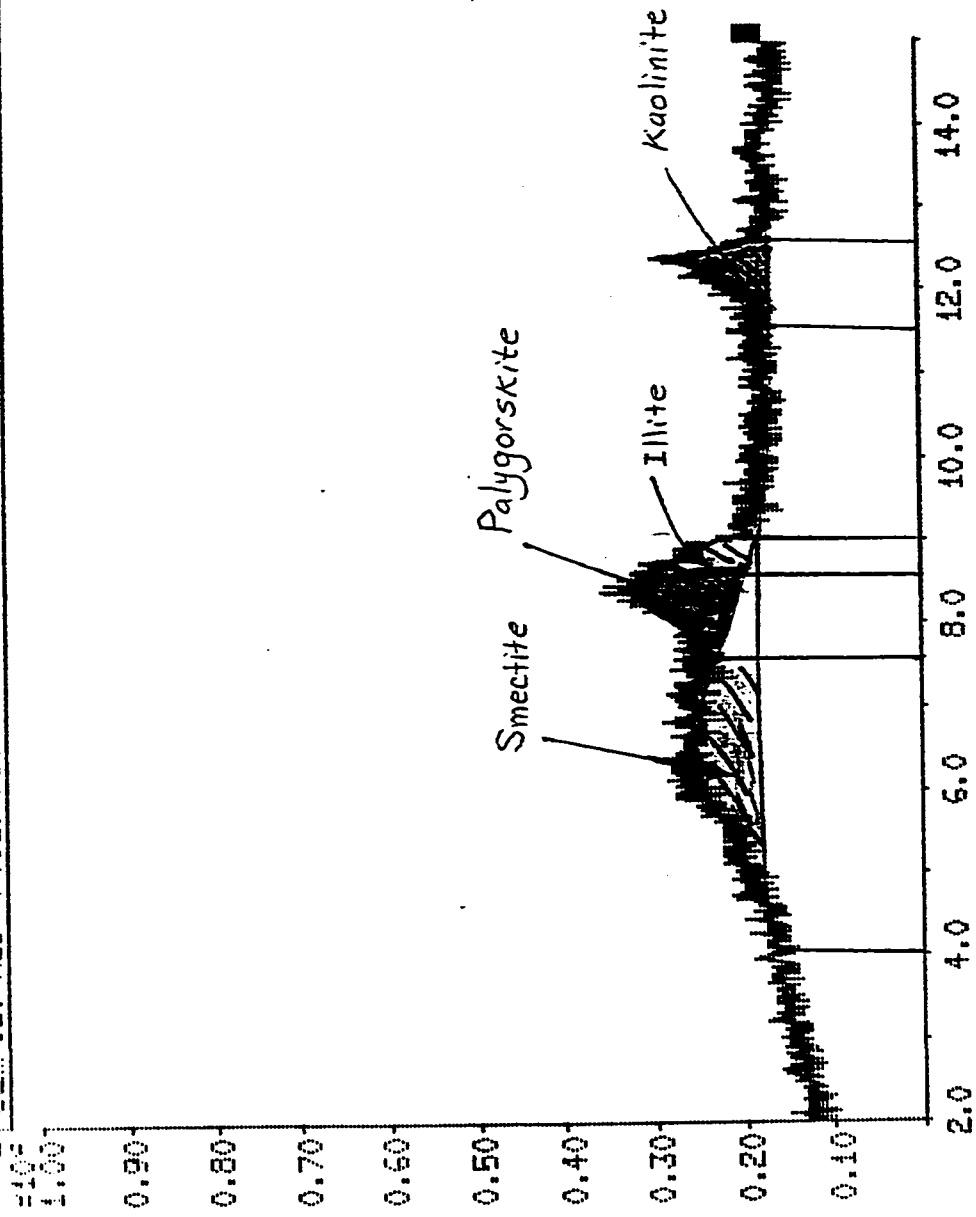


Fig. B.2 XR-Diffraction Pattern (enlarged scale) for Sample # 1, BH # 9 (2.5-2.7 m)

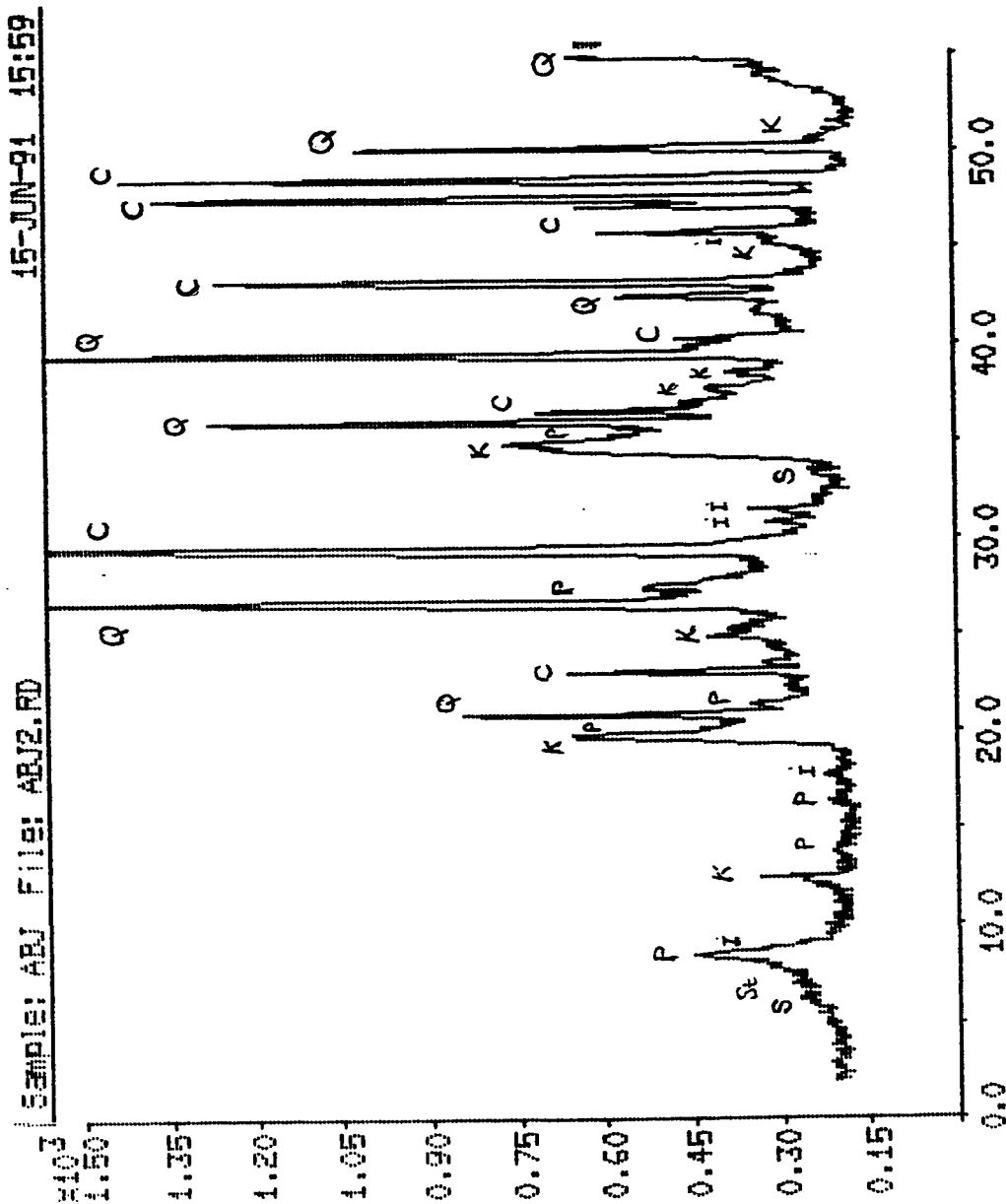


Fig. B.3 XR-Diffraction Pattern for Sample # 2, BH # 13
(2.0-2.25 m)

Sample: ABJ File: ABJ2.RD 15-JUN-91 16:00

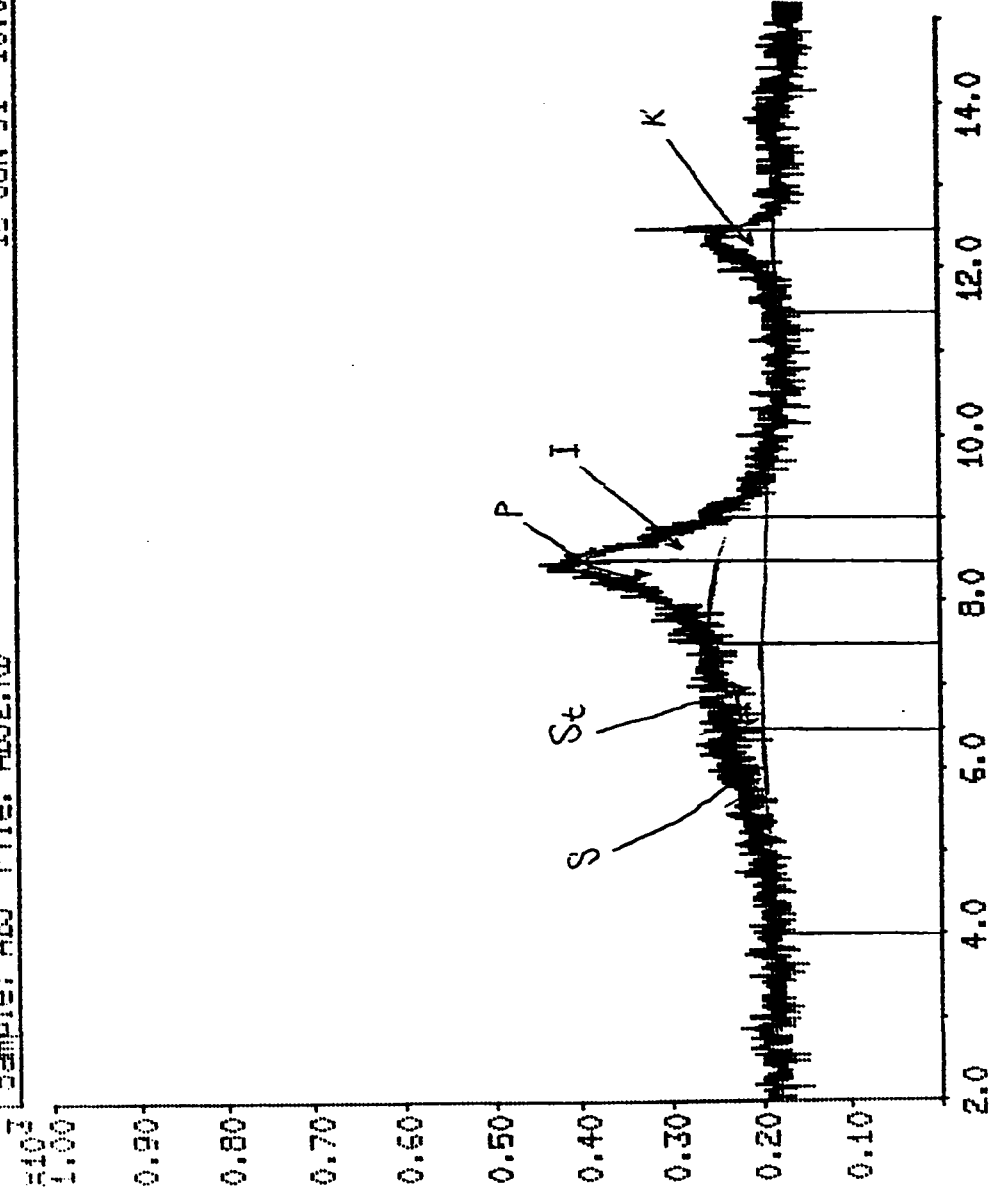


Fig. B.4 XR-Diffraction Pattern (enlarged scale) for Sample # 2, BH # 13 (2.0-2.25 m)

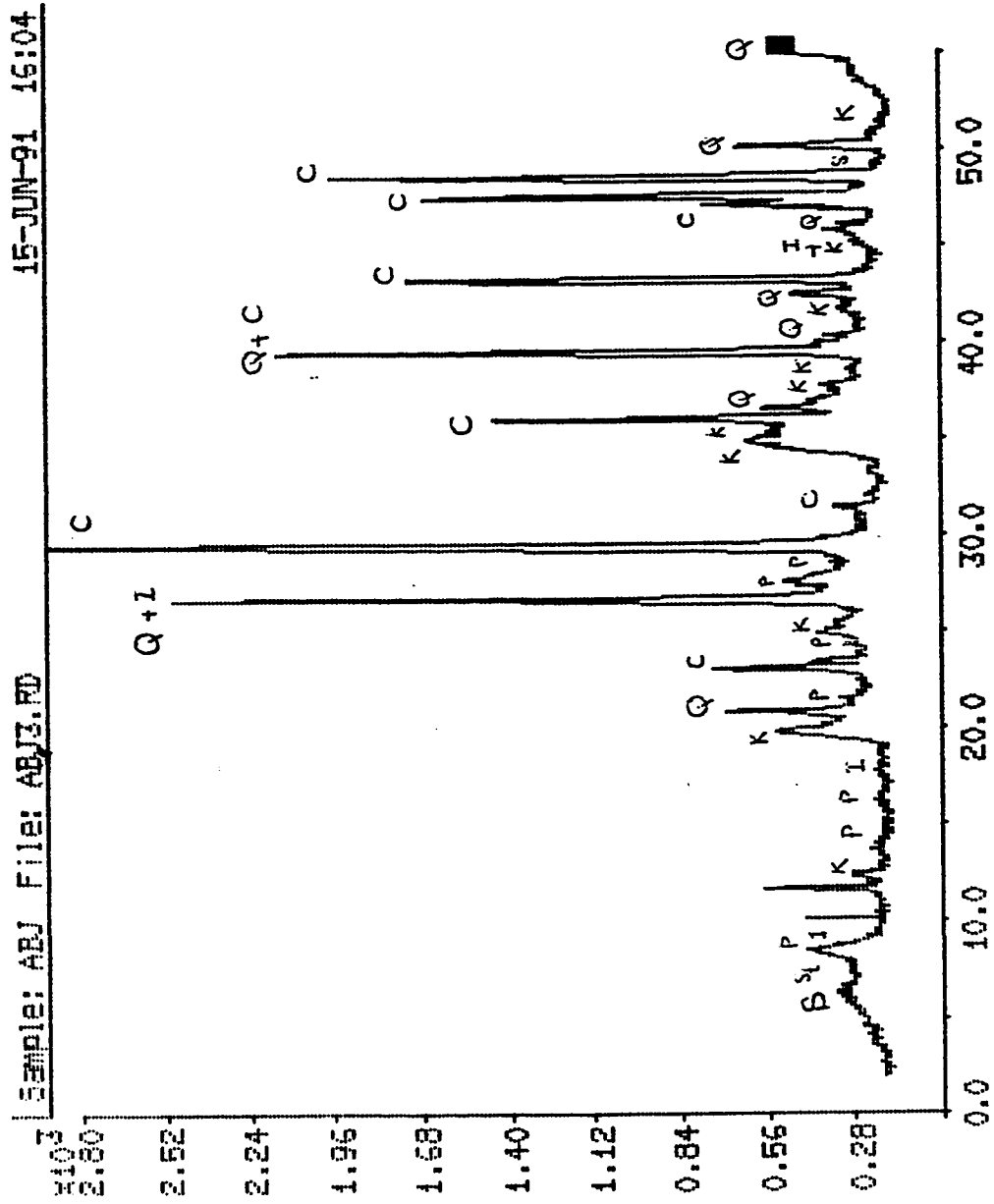


Fig. B.5 XR-Diffraction Pattern for Sample # 3, BH # 11 (1.0-1.3 m)

EMPIRE: ABJ FILE: ABJ3.PD 15-JUN-91 15:05

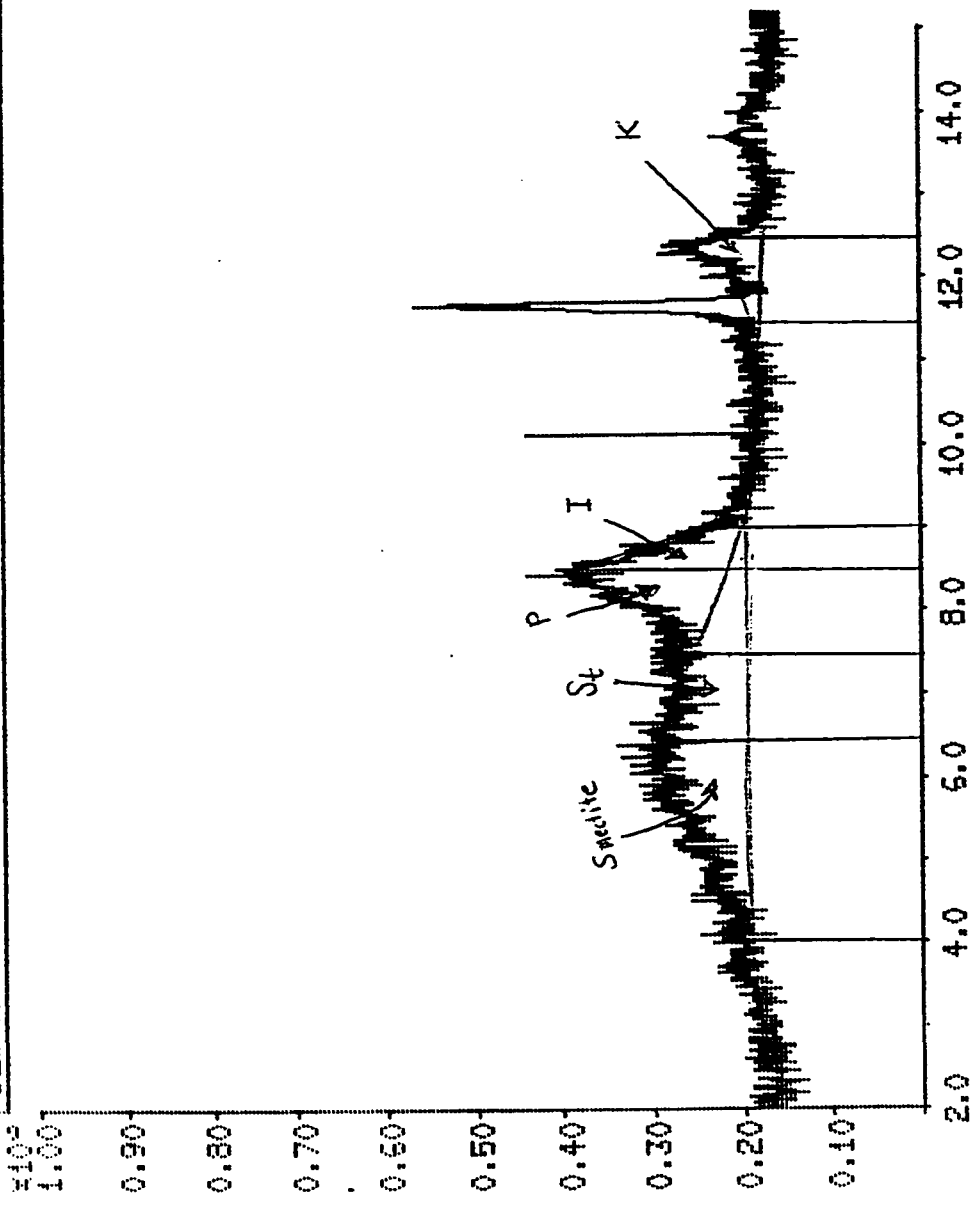


Fig. B.6 XR-Diffraction Pattern (enlarged scale) for Sample # 3, BH # 11 (1.0-1.3 m)

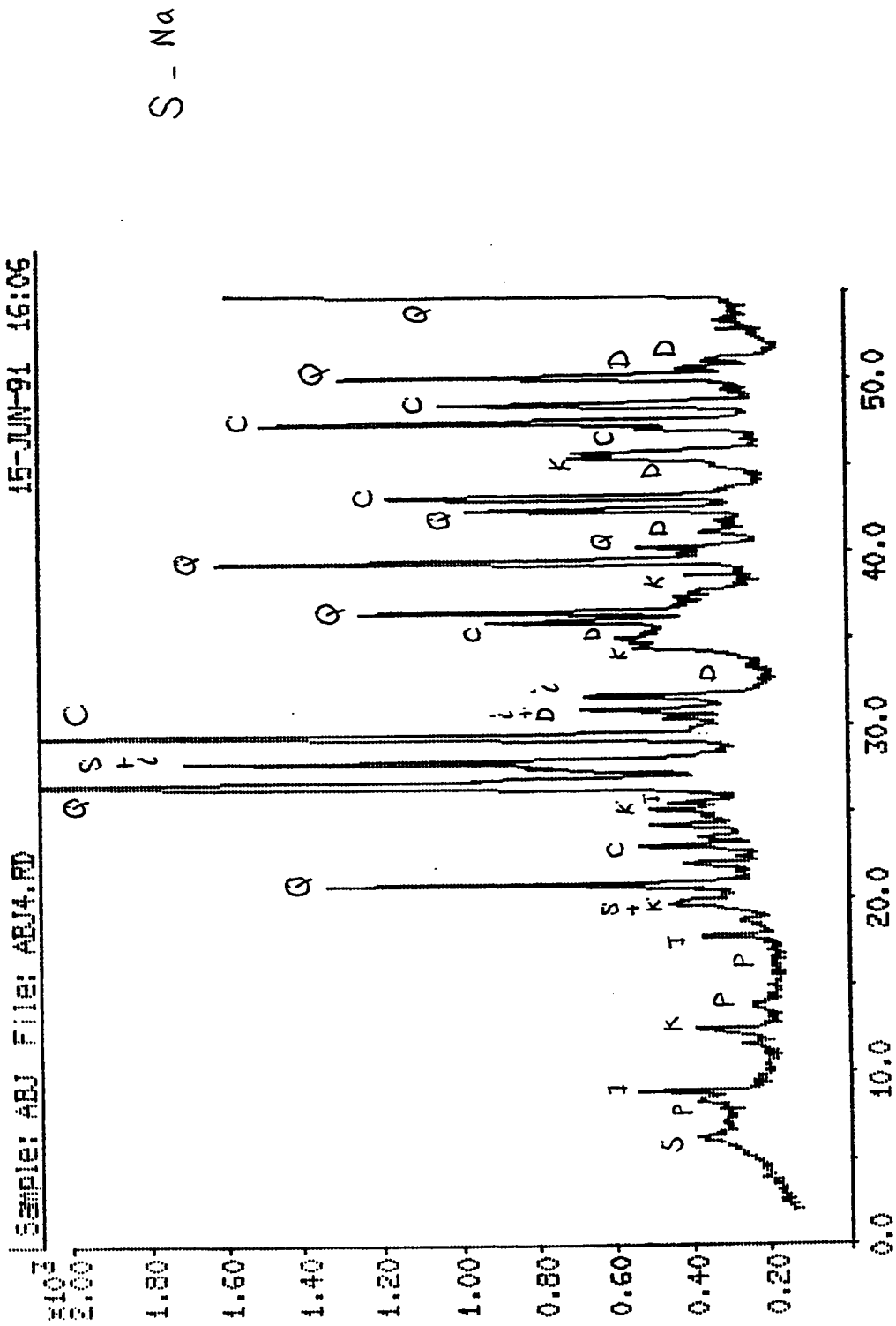


Fig. B.7 XR-Diffraction Pattern for Sample # 4, BH # 12 (2.4-2.7 m)

Sample: ABJ File: ABJ4.RD 15-JUN-91 15:15

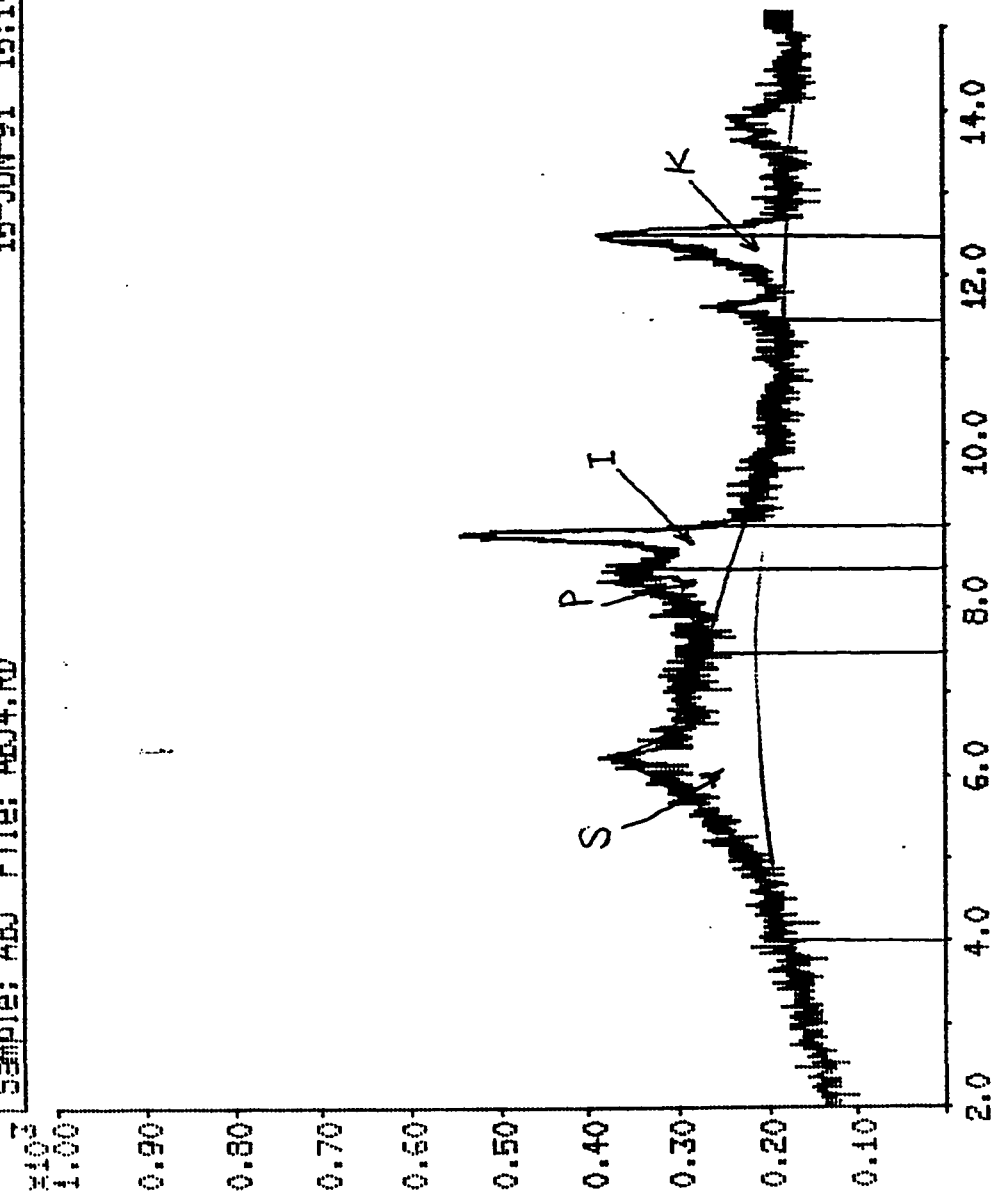


Fig. B.8 XR-Diffraction Pattern (enlarged scale) for Sample # 4, BH # 12 (2.4-2.7 m)

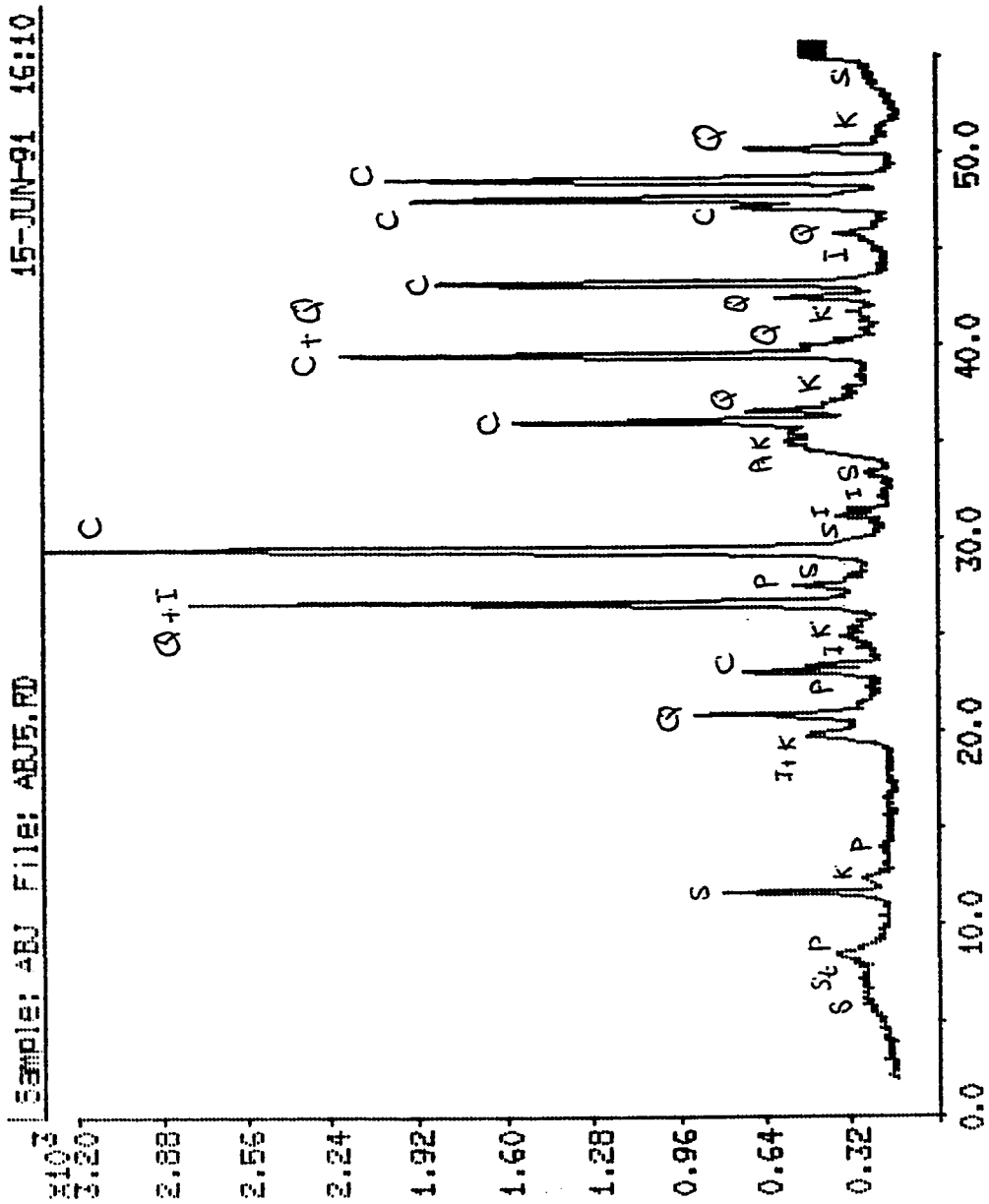


Fig. B.9 XR-Diffraction Pattern for Sample # 5, TP # 7 (1.1 m)

15-JUN-91 15:12

SAMPLE: ABJ FILE: ABJ5.FD

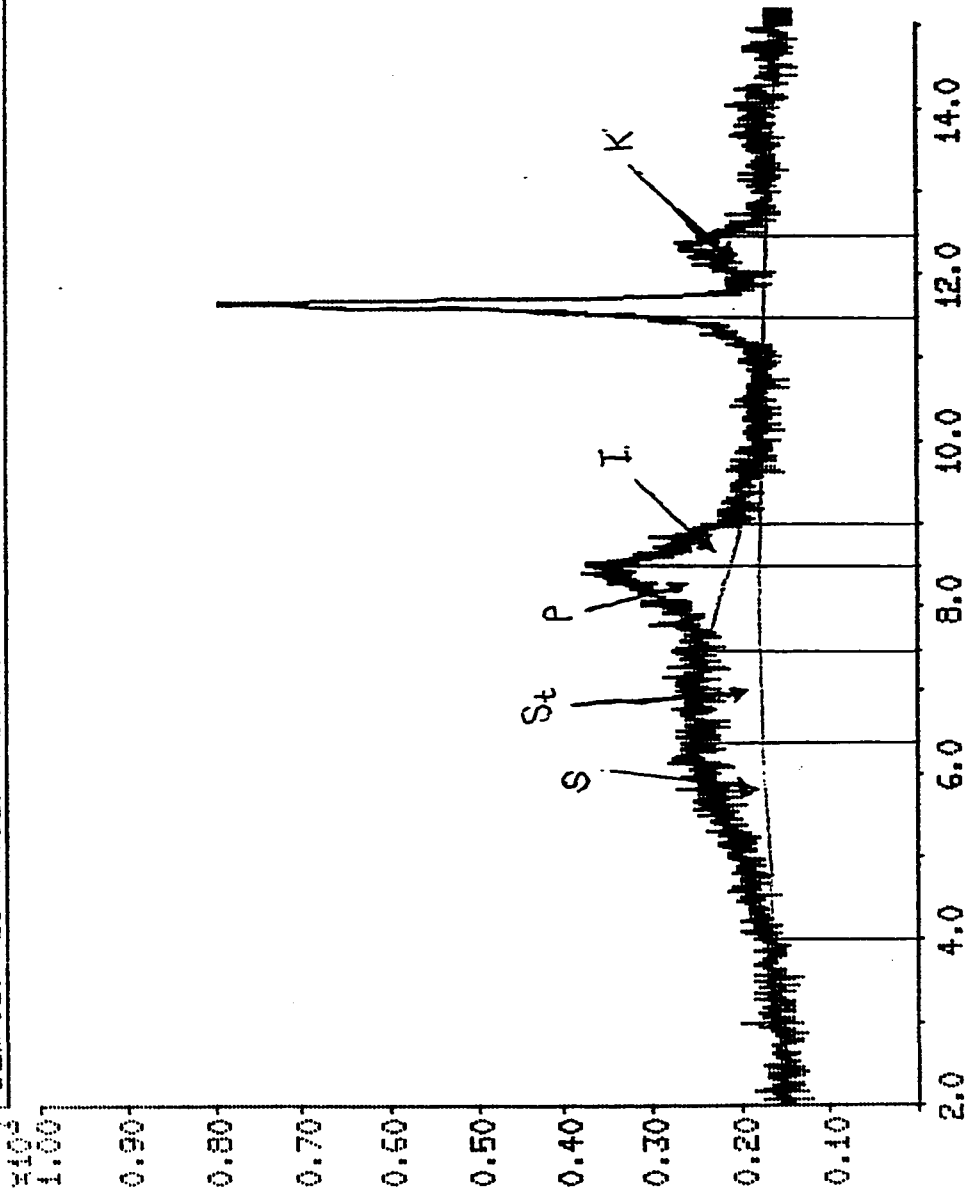


Fig. B.10 XR-Diffraction Pattern (enlarged scale) for Sample # 5, TP # 7 (1.1 m)

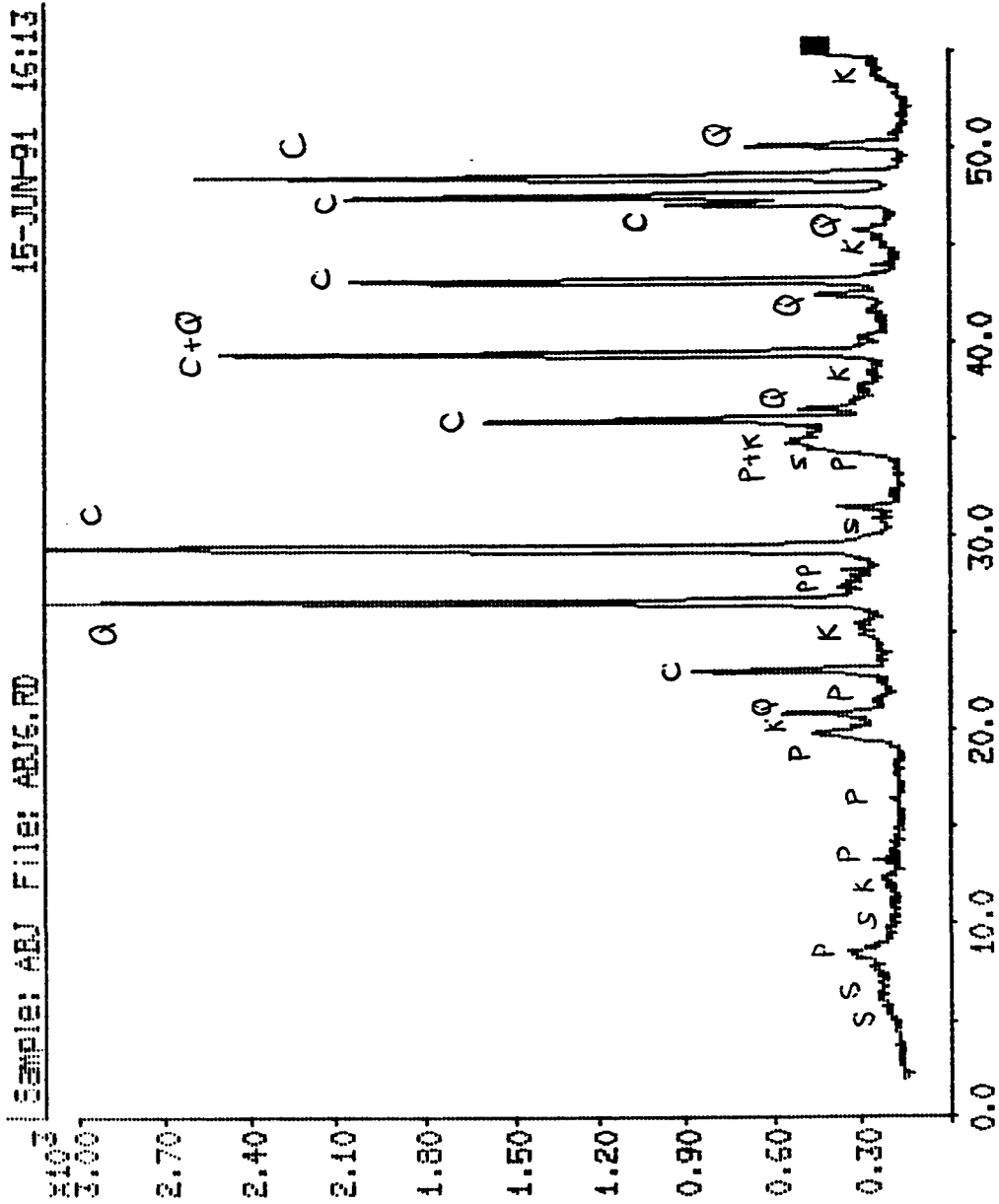


Fig. B.11 XR-Diffraction Pattern for Sample # 6, TRP # 9 (2.2 m)

SAMPLE: ABJ File: ABJ6.RD 15-JUN-91 16:14

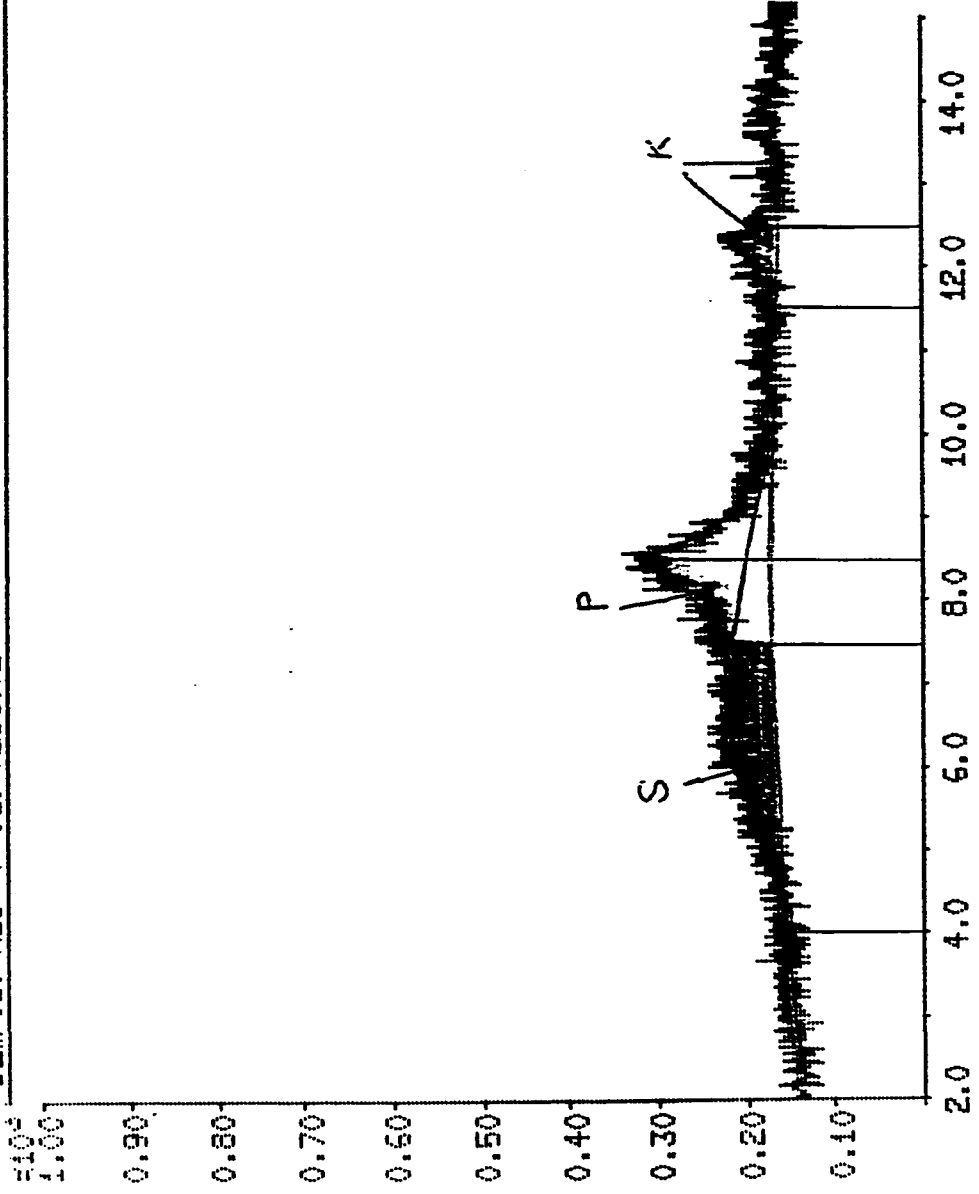


Fig. B.12 XR-Diffraction Pattern (enlarged scale) for Sample # 6, TP # 9 (2.2 m)

15-JUN-91 16:15

SAMPLE: ABJ FILE: ABJ7.RD

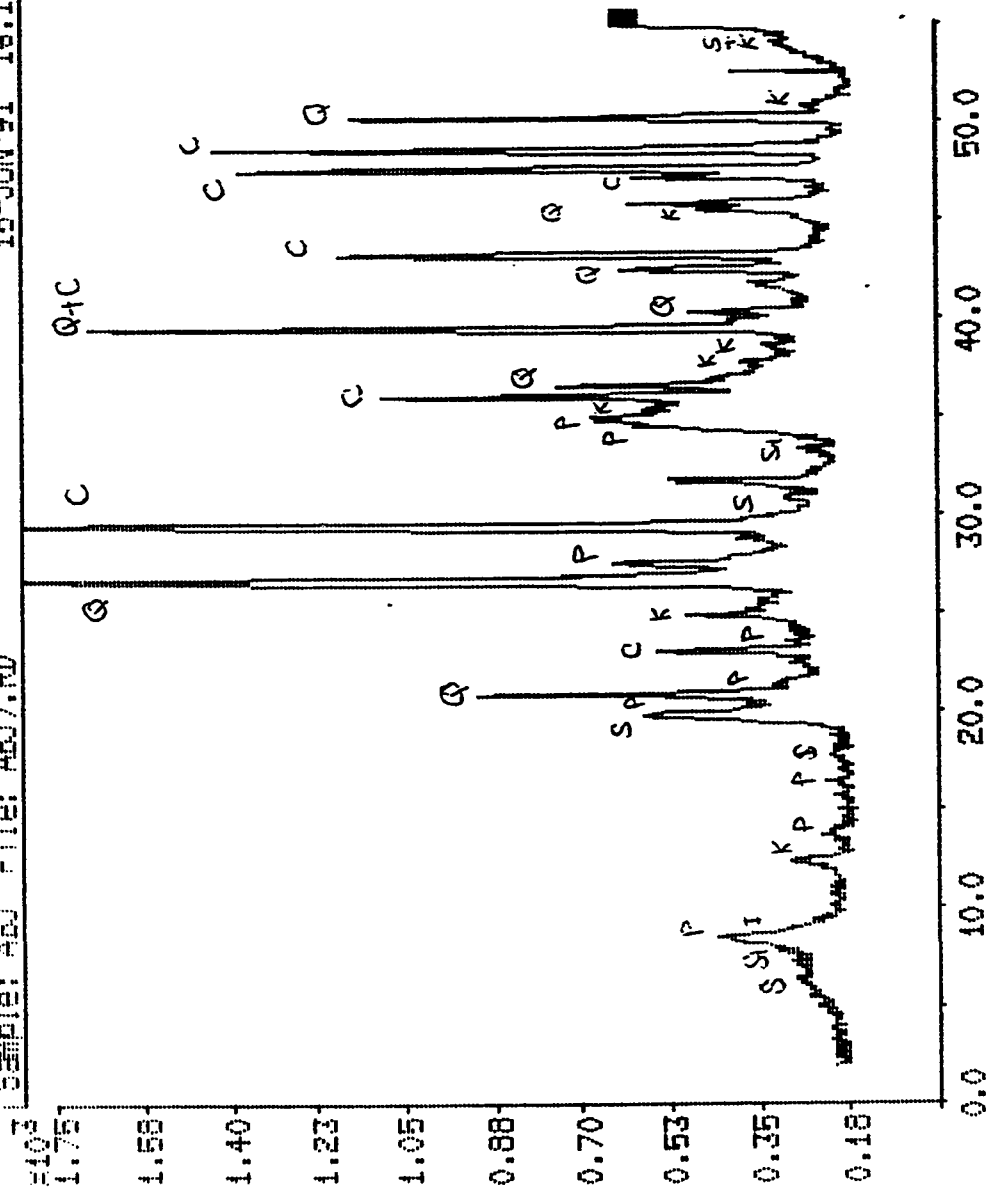


Fig. B.13 XR-Diffraction Pattern for Sample # 7, TP # 11 (2.0-2.2 m)

SAMPLE: ABJ FILE: ABJ7.RD 15-JUN-91 15:16

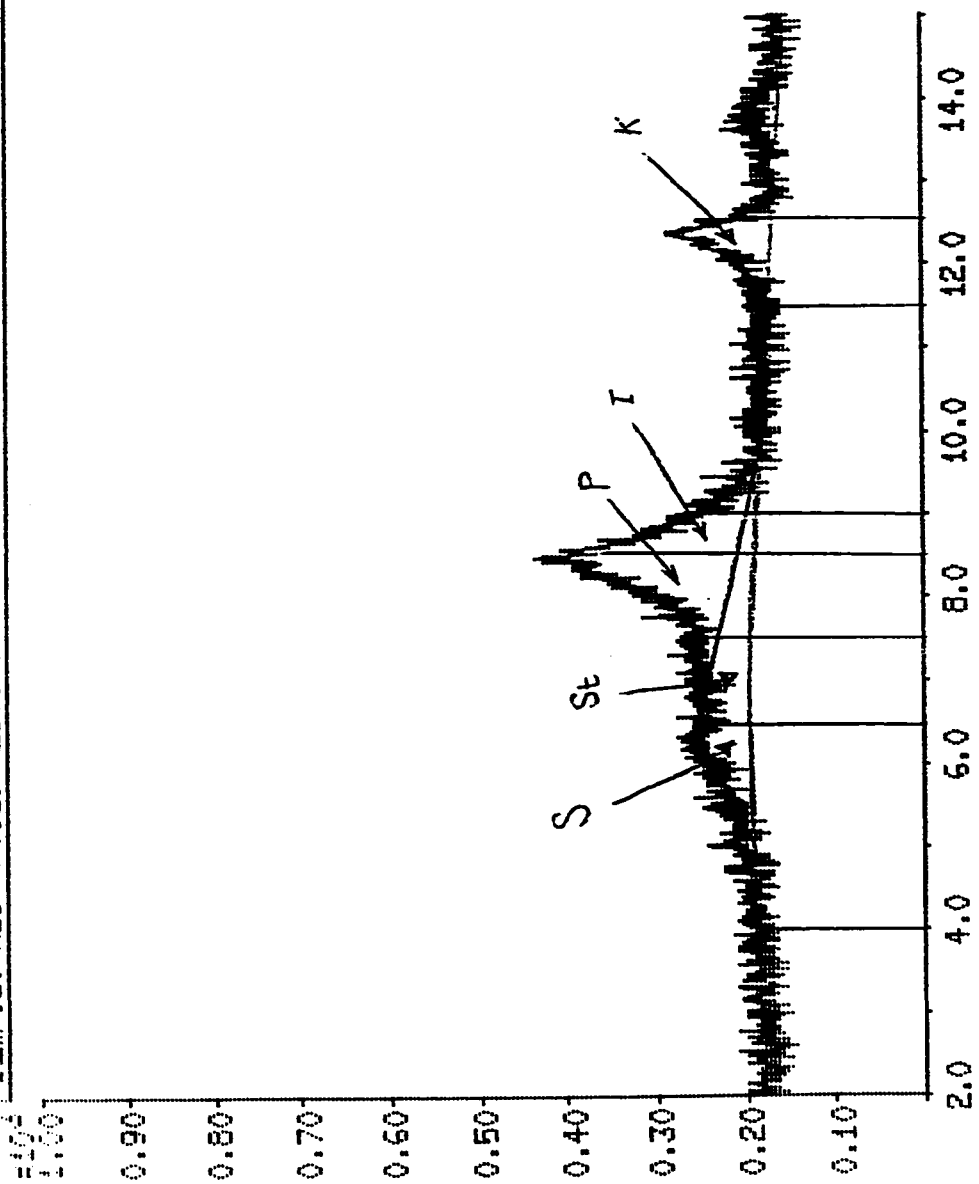


Fig. B.14 XR-Diffraction Pattern (enlarged scale) for Sample # 7, TP # 11 (2.0-2.2 m)

15-JUN-91 15:18
SAMPLE: ABJ FILE: ABJS.RD

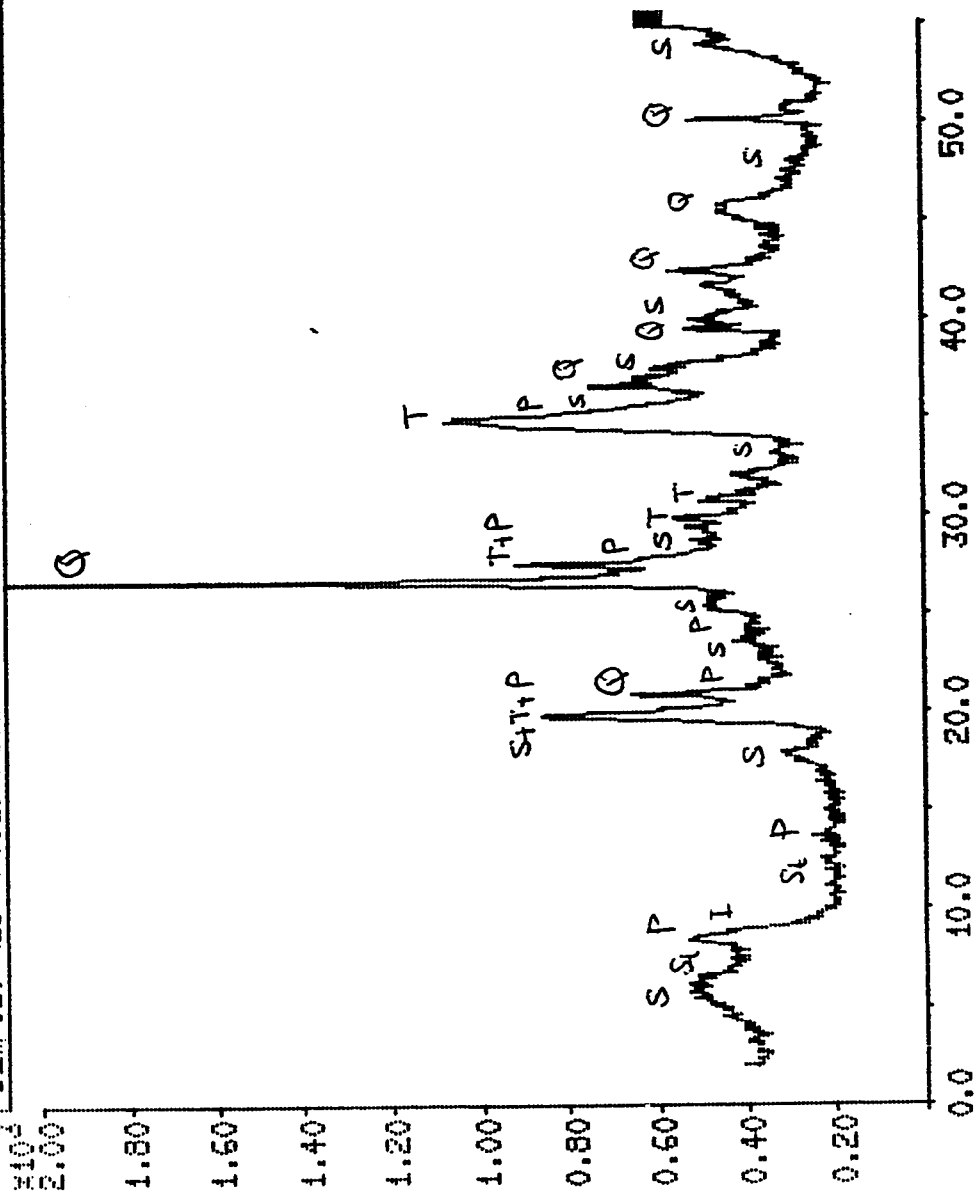


Fig. B.15 XR-Diffraction Pattern for Sample # 8, BH # 1 (3.8 m)

SEMPIS: ABJ FILE: ABJS.FD 15-JUN-91 15:19

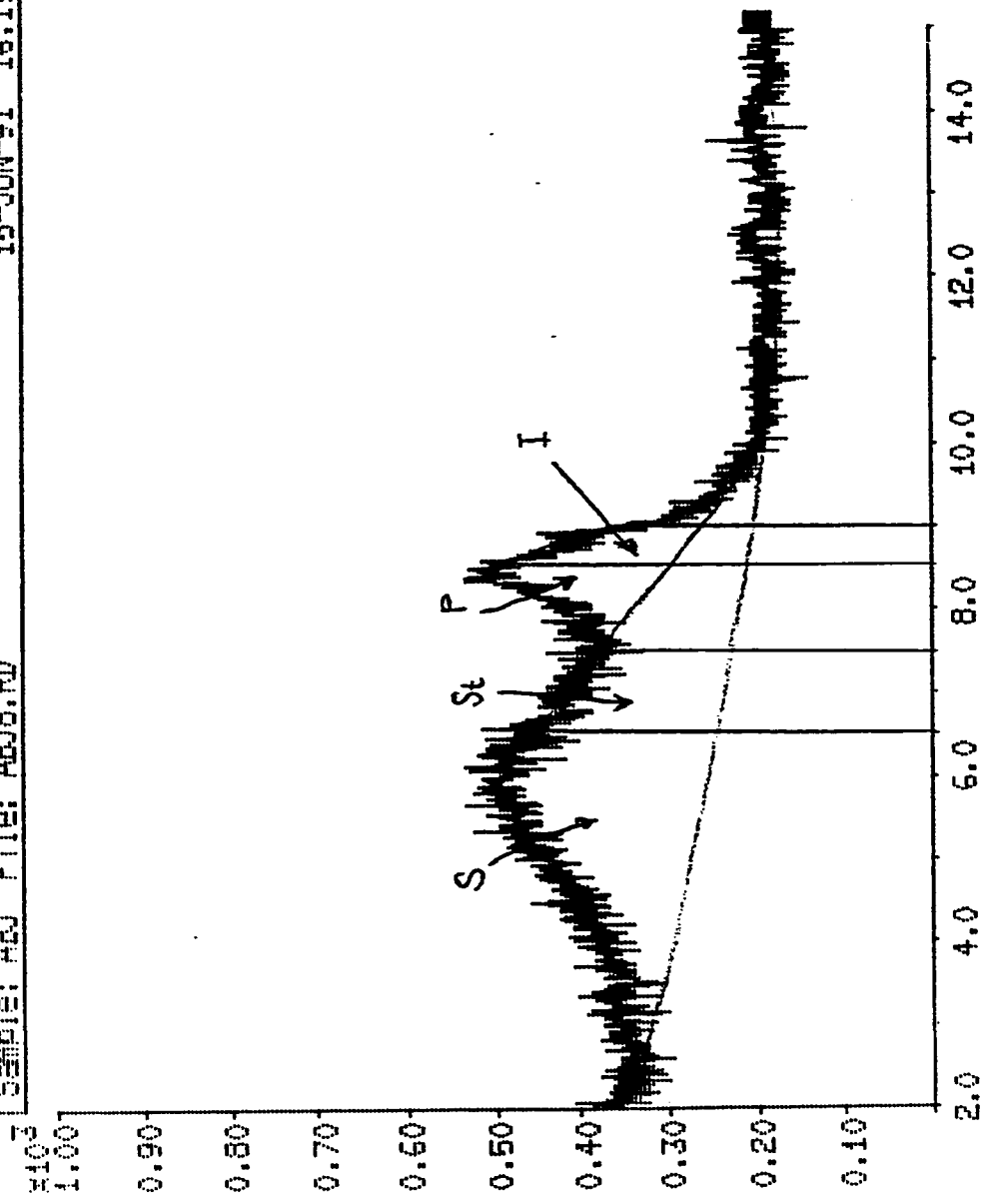


Fig. B.16 XR-Diffraction Pattern (enlarged scale) for Sample # 8, BH # 1 (3.8 m)

SAMPLE: ABJ FILE: ABJ9.RD 15-JUN-91 16:21

103

1.00
0.90
0.80
0.70
0.60
0.50
0.40
0.30
0.20
0.10

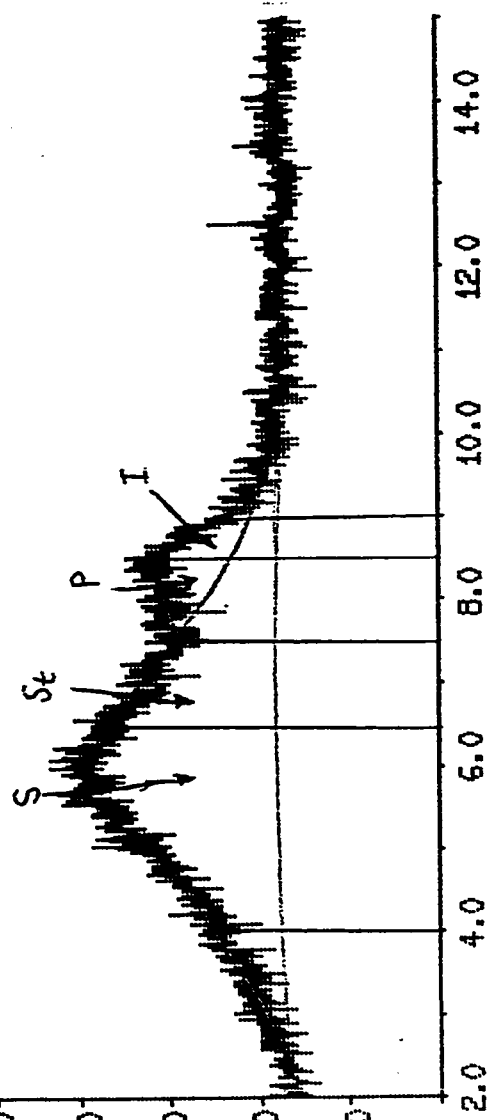


Fig. B.18 XR-Diffraction Pattern (enlarged scale) for Sample # 9, BH # 3 (1.8-2.1 m)

123

SAMPLE: ABJ1 FILE: ABJ10.RD 15-JUN-91 16:23

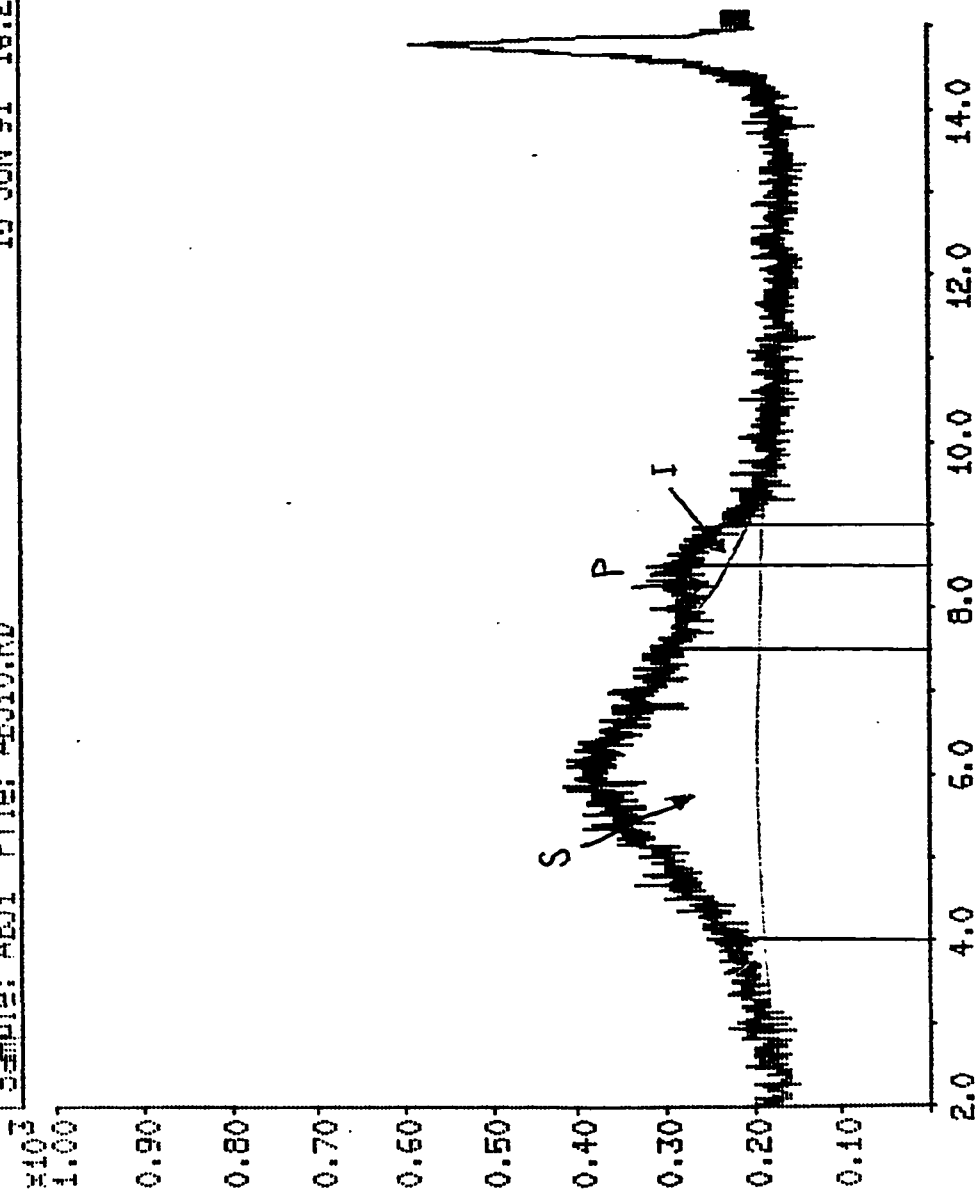


Fig. B.20 XR-Diffraction Pattern (enlarged scale) for Sample # 10,
BH # 6 (0.45-0.6 m)

123

SAMPLE: ABJ1 FILE: ABJ11.RD 15-JUN-91 16:26

1.00
0.90
0.80
0.70
0.60
0.50
0.40
0.30
0.20
0.10

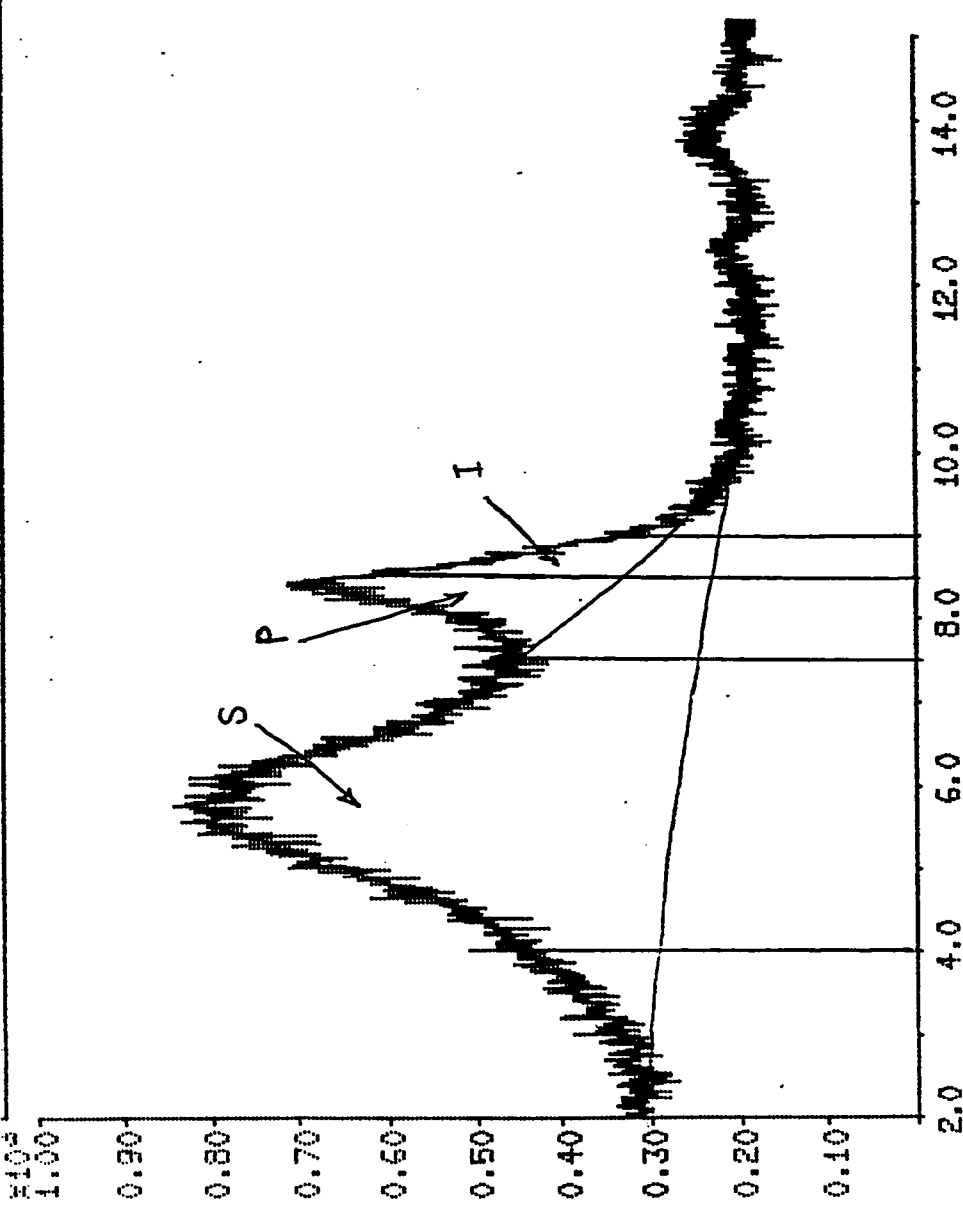


Fig. B.22 XR-Diffraction Pattern (enlarged scale) for Sample # 11,
BH # 8 (5.6-5.75 m)

Mineral	Line/Area 2	Standard Intensity	Unknown Intensity	%tage of Mineral	Normalized % of Mineral
Quartz	26.7	10935	1904	17.4	10
Calcite	29.4	8226	7000	85.1	50
Palygorskite	7.5 - 8.5 A	517	69.3	13.4	8
Illite	8.5 - 9.0 A	87.5	28	32	19
Kaolinite	11.5 - 12.5 A	570	50.7	8.89	5
Smectite	4 - 7.5 A	1210	146.67	12.12	7

Table(B.1): Mineralogical Composition of Sample #1

Mineral	Line/Area 2	Standard Intensity	Unknown Intensity	%tage of Mineral	Normalized % of Mineral
Quartz	26.7	10935	2917	26.7	16
Calcite	29.4	8226	4666.7	56.73	34
Palygorskite	7.5 - 8.5 A	517	70	13.54	8
Illite	8.5 - 9.0 A	87.5	44.5	50.86	31
Kaolinite	11.5 - 12.5 A	570	25	4.39	3
Smectite	4 - 7.5 A	1210	78	6.4	4
Sepiolite	6.5 - 7.5 A	820	47.3	5.77	4

Table(B.2): Mineralogical Composition of Sample #2

Mineral	Line/Area 2	Standard Intensity	Unknown Intensity	%tage of Mineral	Normalized % of Mineral
Quartz	26.7	10935	2333.3	21.34	10
Calcite	29.4	8226	6066.7	73.75	35
Palygorskite	7.5 - 8.5 A	517	83.48	16.15	8
Illite	8.5 - 9.0 A	87.5	55.65	63.6	30
Kaolinite	11.5 - 12.5 A	570	41.74	7.3	3
Smectite	4 - 7.5 A	1210	211.5	17.48	8
Sepiolite	6.5 - 7.5 A	820	86.26	10.52	5

Table(B.3): Mineralogical Composition of Sample #3

Mineral	Line/Area 2	Standard Intensity	Unknown Intensity	%tage of Mineral	Normalized % of Mineral
Quartz	26.7	10935	5833.3	53.35	19
Calcite	29.4	8226	4433.3	53.89	19
Dolomite	31	11694	466.67	3.99	1
Palygorskite	7.5 - 8.5 A	517	50.67	9.8	4
Illite	8.5 - 9.0 A	87.5	117.3	134	47
Kaolinite	11.5 - 12.5 A	570	69.33	12.16	4
Smectite	4 - 7.5 A	1210	194.67	16.09	6

Table(B.4): Mineralogical Composition of Sample #4

Mineral	Line/Area 2	Standard Intensity	Unknown Intensity	%tage of Mineral	Normalized % of Mineral
Quartz	26.7	10935	2566.67	23.47	11
Calcite	29.4	8226	6533.3	79.42	39
Palygorskite	7.5 - 8.5 A	517	101.33	19.6	10
Illite	8.5 - 9.0 A	87.5	34.667	39.62	19
Kaolinite	11.5 - 12.5 A	570	130.67	22.92	11
Smectite	4 - 7.5 A	1210	152	12.56	6
Sepiolite	6.5 - 7.5 A	820	69.3	8.45	4

Table(B.5): Mineralogical Composition of Sample #5

Mineral	Line/Area 2	Standard Intensity	Unknown Intensity	%tage of Mineral	Normalized % of Mineral
Quartz	26.7	10935	3966.67	36.27	24
Calcite	29.4	8226	7700	93.6	61
Palygorskite	7.5 - 8.5 A	517	48	9.3	6
Kaolinite	11.5 - 12.5 A	570	24	4.2	3
Smectite	4 - 7.5 A	1210	106.67	8.8	6

Table(B.6): Mineralogical Composition of Sample #6

Mineral	Line/Area 2	Standard Intensity	Unknown Intensity	%tage of Mineral	Normalized % of Mineral
Quartz	26.7	10935	4166.67	38.1	19
Calcite	29.4	8226	4500	54.7	27
Palygorskite	7.5 - 8.5 A	517	101.57	19.65	10
Illite	8.5 - 9.0 A	87.5	55.65	63.6	32
Kaolinite	11.5 - 12.5 A	570	52.87	9.3	5
Smectite	4 - 7.5 A	1210	108.52	8.97	4
Sepiolite	6.5 - 7.5 A	820	50.09	6.11	3

Table(B.7): Mineralogical Composition of Sample #7

Mineral	Line/Area 2	Standard Intensity	Unknown Intensity	%tage of Mineral	Normalized % of Mineral
Quartz	26.7	10935	2000	18.29	9
Palygorskite	7.5 - 8.5 A	517	89.04	17.22	9
Illite	8.5 - 9.0 A	87.5	66.78	76.32	40
Smectite	4 - 7.5 A	1210	687.3	56.8	30
Sepiolite	6.5 - 7.5 A	820	192	23.41	12

Table(B.8): Mineralogical Composition of Sample #8

Mineral	Line/Area 2	Standard Intensity	Unknown Intensity	%tage of Mineral	Normalized % of Mineral
Quartz	26.7	10935	1400	12.8	7
Dolomite	31	11694	6883.3	58.86	32
Palygorskite	7.5 - 8.5 A	517	41.74	8.07	4
Illite	8.5 - 9.0 A	87.5	33.39	38.16	21
Kaolinite	11.5 - 12.5 A	570			
Smectite	4 - 7.5 A	1210	559.3	46.2	25
Sepiolite	6.5 - 7.5 A	820	155.83	19	10

Table(B.9): Mineralogical Composition of Sample #9

Mineral	Line/Area 2	Standard Intensity	Unknown Intensity	%tage of Mineral	Normalized % of Mineral
Quartz	26.7	10935	1152	10.53	4
Dolomite	31	11694	15500	132.55	48
Gypsum	14.9	1452	420	28.93	11
Palygorskite	7.5 - 8.5 A	517	25.04	4.8	2
Illite	8.5 - 9.0 A	87.5	22.26	61.94	22
Kaolinite	11.5 - 12.5 A	570			
Smectite	4 - 7.5 A	1210	445.22	36.79	13

Table(B.10): Mineralogical Composition of Sample #10

Mineral	Line/Area 2	Standard Intenstity	Unknown Intensity	%tage of Mineral	Normalized % of Mineral
Quartz	26.7	10935	2833.3	25.91	10
Calcite	29.4	8226	57.6	0.7	0
Dolomite	31	11694	96	0.82	0
Palygorskite	7.5 - 8.5 A	517	141.91	27.45	11
Illite	8.5 - 9.0 A	87.5	89.04	101.76	39
Smectite	4 - 7.5 A	1210	1224.3	101.19	39

Table(B.11): Mineralogical Composition of Sample #11

REFERENCES

1. Abduljauwad, S. N. and A. Rafi, (1990), "Expansive Soil in Al-Qatif Area", *The Arabian Journal for Science and Engineering*, Vol. 15, No.2A.
2. Al-Najjar, Z., (1988), "Foundation Problems in Sabkha Deposits", In: Abduljauwad, S. (Coordinator), *Short Course on Foundation Engineering for Practicing Engineers*, KFUPM, Dhahran, April 9-13.
3. Al-Sayari, S. S. and J. G. Zotl, (1978), "Quarternary Period in Saudi Arabia", Vol. 1, Springer-Verlag/Wien, N. Y., U.S.A.
4. Al-Tamimi, M. H., (1985), "Stratigraphical and Microfacies Analysis of the Early Paleogene Succession in the Dammam Dome, Eastern Saudi Arabia", M.S. thesis, K.F.U.P.M., Dhahran, K.S.A.
5. Bowles, Joseph E.,(1982), "Foundation Analysis and Design", McGraw-Hill, Inc., Singapore.
6. Buchanan, S. J., (1980), "Key-note Address", *Proceedings of the 4th Int. Conf. on Expansive Soils*, Denver, Colorado, Vol. 2, pp. 661-669.
7. Butler, G. P.,(1969), "Modern Evaporite Deposition and Geochemistry of Coexisting Brines, The Sabkha, Trucial Coast, Arabian Gulf", *Journal of Sedimentary Petrology*, Vol. 39, No. 1.
8. Cagatay, M. N.,(1988), "Clay Mineralogy and Chemistry of Some Argillaceous Rocks in Central and Eastern Saudi Arabia", *The Arabian Journal for Science and Engineering*, Vol. 13, No. 1, pp. 47-63.
9. Cagatay, M. N.,(1990), "Polygorskite in the Eocene Rocks of the Dammam Dome, Saudi Arabia", *Clays and Clay Minerals*, Vol. 38, No. 3, pp. 299-307.
10. Carrillo-Gil, A., (1980), "Construction and Design of Light Structures in Peru", *Proceedings of the 4th Int. Conf. on Expansive Soils*, Denver, Colorado, Vol. 2, pp. 469-476.
11. Chen, F. H.,(1973), "The Basic Physical Property of Expansive Soils", *Proceedings of the Third International Conference on Expansive Soils*, Haifa, pp. 17-25.

12. Chen, F. H.,(1980), "Legal Aspect of Expansive Soils", Proceedings of the 4th Int. Conf. on Expansive Soils, Colorado, Vol. 1, pp. 639-645.
13. Chen, F. H., (1975, 1988), "Foundations on Expansive Soils", Elsevier Scientific Publishing Company, N. Y., U.S.A.
14. Collins, K., (1973), "Micro-Structural Features of Some Israeli Expansive Soils", Proceedings of the Third Int. Conf. on Expansive Soils, Haifa, pp. 27-33.
15. Corley, J. B., (1980), "Modelling Climatic Effects on Clay Beneath Slabs", Proceedings of the 4th Int. Conf. on Expansive Soils, Denver, Colorado, Vol. 1, pp. 533-550.
16. Dakshanamurthy, V. and V. Raman,(1973), "A Simple Method of Identifying An Expansive Soil", Soils and Foundations, Vol. 13, No. 1, March.
17. Das, B. M., (1984), "Principles of Foundation Engineering", PWS Engineering, Boston, 1984.
18. Dhowian, A., I. Ruwaih, A. Erol, and A. Youssef, (1985), "The Distribution of the Expansive Soils in Saudi Arabia", Second Saudi Engineering Conference, K.F.U.P.M., Dhahran, Saudi Arabia.
19. Dhowian, A. W. and O. Erol, (1989), "Heave Prediction of Expansive Shale Formations", Second Symposium on Geotechnical Problems in Saudi Arabia, Riyadh, Saudi Arabia.
20. El-Sayed, S. T.,(1980), A report about Cracked Buildings in Mubarraz Area, submitted to the Ministry of Public Works and Housing, Kingdom of Saudi Arabia.
21. El-Sayed, S. T., (1981), "Soils of Swelling and Collapsing Behavior, Mobaraz Town, Eastern Zone, K.S.A.", Symposium on Geotechnical Problems in Saudi Arabia, Vol. 1, Riyadh, Saudi Arabia.
22. El-Sohby, M. A., S. A. Rabba and O. Mazen, (1985), "Role of Mineralogical Composition in the Activity of Expansive Soils", Transportation Research Record 1032, pp. 28-33.
23. Erol,A.O.,& A. Dhowian, (1990), " Swell Behavior of Arid Climate Shales From Saudi Arabia ", Quaterly Journal of Engineering Geology, London, Vol.23, pp. 243-254.

24. Gromko, G. J., (1974), "Review of Expansive Soils", Journal of Geotechnical Engineering Division, Vol. 100, No. GT6, June.
25. Holland, J. E. and C. E. Lawrence, (1980), "Seasonal Heave of Australian Clay Soils", Proceedings of the 4th Int. Conf. on Expansive Soils, Denver, Colorado, Vol. 1, pp. 302-321.
26. Holtz, W. G. and H. J. Gibbs, (1954), "Engineering Properties of Expansive Clays", Papers in Geotechnical Engineering, ASCE, N. Y. U.S.A.
27. Holtz, W. G.,(1980), "Public Awareness of Homes Built on Shrink-Swell Soils", Proceedings of 4th Int. Conf. on Expansive Soils, Colorado, Vol. 1, pp. 617-638.
28. Irtem, O.,(1987), "Miocene Tidal Flat Stromatolites of the Dammam Formation, Saudi Arabia", The Arabian Journal for Science and Engineering, Vol. 12, No.2.
29. Krazynski, L. M. and L. J. Lee, "Identification and Testing of Expansive Soils", unknown source.
30. Krohn, J. P., and J. E. Slosson, (1980), "Assessment of Expansive Soils in the United States", Proceedings of the 4th Int. Conf. on Expansive Soils, Colorado, Vol. 1, pp. 596-608.
31. Krynine, D. P. and W. R. Judd, (1957). "Principles of Engineering Geology and Geotechnics", McGraw-Hill, Inc., N. Y., U.S.A.
32. Layton, R. L., (1980), "Creep Damage to Structures on Expansive Clay Slopes", Proceedings of the 4th Int. Conf. on Expansive Soils, Denver, Colorado, Vol. 1, pp. 284-301.
33. Millot, G.,(1970), "Geology of Clays", Springer-Verlag, N. Y., U.S.A.
34. Mitchell, James K., (1976), "Fundamentals of Soil Behavior", John Wiley & Sons, Inc., N. Y., U.S.A.
35. Mustafayev, A.A.O. and G. D. Chignier, (1980), "Rheology of Swelling Soils and Deformation Forecast", Proceedings of the 4th Int. Conf. on Expansive Soils, Denver, Colorado, Vol. 2, pp. 769-780.

36. - Nagaraj, T. S. and B. R. S. Murthy, (1985), "Rational Approach to Predict Swelling Soil Behavior", Transportation Research Record 1032, pp. 1-7.
37. Ofer, Z. and G. E. Blight, (1985), "Measurement of Swelling Pressure in the Laboratory and In Situ", Transportation Research Record 1032, pp. 15-22.
38. Okasha, T. M., (1988), "Mineralogical and Geotechnical Studies of Expansive Soils in Al-Madina and Al-Hofuf Cities, Saudi Arabia", M.S. thesis, K.F.U.P.M., Dhahran, K.S.A.
39. O'Neill, M. W., (1980), "Methodology for Foundations on Expansive Clays", Journal of the Geotechnical Engineering Division, Vol. 106, No. GT12, December.
40. Peck, R. B., et al., (1974), "Foundation Engineering", 2nd edition, John Wiley & Sons, Inc., N. Y., U.S.A.
41. Petry, T. M. and C. Armstrong, (1980), "Relationships and Variations of Properties of Clay", Proceedings of the 4th Int. Conf. on Expansive Soils, Denver, Colorado, Vol. 1, pp. 172-173.
42. Rafi, Ahmad, (1988), "Engineering Properties and Mineralogical Composition of Expansive Clays in Al-Qatif Area, K.S.A.", M.S. Thesis, K.F.U.P.M., Dhahran, Saudi Arabia.
43. Rao, R. R., H. Rahardjo and D. G. Fredlund, (1988), "Closed-Form Heave Solutions for Expansive Soils", Journal of Geotechnical Engineering, Vol. 114, No. 5, May.
44. Rasheeduddin M., (1988), "Numerical Modelling of Alat, Khobar and Umm Er Radhuma Aquifer System in Eastern Saudi Arabia", M.S. Thesis, KFUPM, Dhahran, K.S.A.
45. Ravina, I., (1973), "Swelling of Clays, Mineralogical Composition and Microstructure", Proceedings of the Third International Conference on Expansive Soils, Haifa, pp. 61-63.
46. Richards, D. P., (1980), "Construction on Expansive Rock Discussion", Proceedings of the 4th Int. Conf. on Expansive Soils, Denver, Colorado, Vol. 2, pp. 749-756.
47. Rocklin, R. C., (1980), "Water Conveyance Pipelines in Expansive Soil", Proceedings of the 4th Int. Conf. on

- Expansive Soils, Denver, Colorado, Vol. 1, pp. 477-495.
48. Ruwaih, I. A., (1984), "Case Studies on Swelling Soils in Saudi Arabia", 5th International Conference on Expansive Soils, Adelaide, South Australia, May.
 49. Shadfah, H., et al., (1985), "Polygorskite from Tertiary Formations of Eastern Saudi Arabia", Clays and Clay Minerals, Vol. 33, No. 5, pp. 451-457.
 50. Singer, A. and E. Galan, (1984), "Polygorskite-Sepiolite Occurrence, Genesis and Uses", Elsevier, N. Y., U.S.A.
 51. Slater, D. E., (1983), "Potential Expansive Soils in Arabian Peninsula", Journal of Geotechnical Engineering, Vol. 109, No. 5, May.
 52. Snethen, D. R., (1980), "Characterization of Expansive Soils Using Soil Suction Data", Proceedings of the 4th Int. Conf. on Expansive Soils, Denver, Colorado, Vol. 1, pp. 54-75.
 53. Snethen, D. R., (1984), "Evaluation of Expedient Methods for Identification and Classification of Potentially Expansive Soils", Proc. of the 5th Int. Conf. on Expansive Soils, Adelaide, South Australia, pp. 22-26.
 54. Sridharan, A. and S. M. Rao, (1988), "A Scientific Basis for the Use of Index Tests in Identification of Expansive Soils", Geotechnical Testing Journal, Vol. 11, No. 3, September.
 55. Steinberg, M. L., (1980), "Deep Vertical Fabric Moisture Seals", Proceedings of the 4th Int. Conf. on Expansive Soils, Denver, Colorado, Vol. 1, pp. 383-400.
 56. Steinberg, M. L., (1985), "Controlling Expansive Soil Destructiveness by Deep Vertical Geomembranes on Four Highways", Transportation Research Record 1032, pp. 48-53.
 57. Surrendra, M. and C. W. Lovell, (1984), "Estimation of Clay Minerals in Clay Shales by X-Ray Diffraction Technique", Proc. of the 5th Int. Conf. on Expansive Soils, Adelaide, South Australia, pp. 27-31.
 58. Tleel, J. W., (1972), "Surface Geology of Dammam Dome, Eastern Province, Saudi Arabia", M.S. Thesis, Texas Christian University, U.S.A.

59. Tschebotarioff, G. P.,(1973), "Foundations, Retaining and Earth Structures", McGraw-Hill, Inc., N. Y., U.S.A.
60. Vijayvergiya, V. N. and O. Ghazzaly, (1973), "Prediction of Swelling Potential for Natural Clays", Proceedings of the Third International Conference on Expansive Soils, Haifa, July-August, pp. 227-234.
61. Williams, A.A.B. and G. D. Donaldson, (1980), "Building on Expansive Soils in South Africa: 1973-1980", Proceedings of the 4th Int. Conf. on Expansive Soils, Denver, Colorado, Vol. 2, pp. 834-844.
62. Wiseman, G., A. Komornik and J. Greenstein, (1985), "Experience With Roads and Buildings on Expansive Clays", Transportation Research Record 1032, pp. 60-67.
63. Wray, W. K.,(1980), "Analysis of Stiffened Slabs-on-ground Over Expansive Soil", Proceedings of the 4th Int. Conf. on Expansive Soils, Denver, Colorado, Vol. 1, pp. 558-581.